Modelling Morphological and Physiological Responses of Tomato Introgression Lines to Drought Stress

Von der Naturwissenschaftlichen Fakultät der

Gottfried Wilhelm Leibniz Universität Hannover

zur Erlangung des Grades

Doktor der Gartenbauwissenschaften (Dr. rer. hort.)

genehmigte Dissertation

von

San Shwe Myint, Master of Science

2022

Referent: Prof. Dr. sc. agr. Hartmut Stützel

Korreferent: Prof. Dr. rer. nat. Thomas Debener

Tag der Promotion: 17. 12. 2020

Dedicated to my mother

Abstract

Tomato (*Solanum lycopersicum* L.) is a major vegetable crop grown in both outdoor fields and greenhouses. Water shortage is a significant problem in field-grown tomatoes. Genetic variation in the adaptation strategies to water shortage influences the differing water use and agronomic performances, in connection to varying climatic factors. Understanding the mechanisms of the adaptation to water deficit in the context of genetic implications is needed for better management and crop improvement. This work aims at investigating the adaptation mechanism of tomato to water deficit under a set of climatic condition, identifying the associated genome regions involved in the adaption, and predicting and evaluating the agronomic performances of virtual ILs in different climatic scenarios.

This study was conducted using 50 tomato introgression lines (ILs) and two parent lines *S. pennellii* and *S. lycopersicum* cv. M82, in greenhouse conditions. Terminal drought stress was given at seven 7th leaf stage. There was a high (R^2= 0.67 -0.75) causal relationships between unstressed and stressed performances for leaf areas increased, water transpired and shoot dry mass produced. The change in plasticity of shoot dry weight was mainly explained by that of leaf area while plasticity of cumulative transpiration was mainly attributed to that of specific transpiration. With the input of unstressed values and QTL-derived parameters from the response to water shortage of leaf expansion and stomatal conductance, stressed transpiration of all ILs was well predicted with high accuracy within the tested vapour pressure deficit ranges. With the implications of climatic factors, genotype-specific parameters (including drought reaction ones) were incorporated into an eco-physiological model, which consisted of three modules mainly for leaf growth, transpiration and dry matter production. With or without the inputs of leaf area and soil water, model performance was evaluated separately for target agronomic traits. The aggregated model could have well predicted the unstressed performances of leaf area, transpiration, shoot dry matter (accuracy = 0.69 - 0.84) and the fraction of transpirable soil water under stress (accuracy = 0.66). However, there was 20 to 30% of overestimation for the stressed performance (accuracy = 0.55 - 0.77). With the input of leaf area, the model performance was much improved for total water transpired and soil water. The genome-based eco-physiological model worked well as a tool to predict the stressed agronomic performances of tomato introgression lines.

Keywords: Introgression lines, *Solanum pennellii*, osmotic adjustment, QTL, eco-physiological model, transpiration, dry matter, leaf area, fraction of transpirable soil water

Kurzzusammenfassung

Die Tomate (*Solanum lycopersicum* L.) ist eine wichtige Gemüsepflanze, die sowohl im Freiland als auch in Gewächshäusern angebaut wird. Wasserknappheit ist ein bedeutendes Problem bei Freiland-Tomaten. Genetische Unterschiede in den Anpassungsstrategien an den Wassermangel beeinflussen den unterschiedlichen Wasserverbrauch und die agronomischen Leistungen in Verbindung mit unterschiedlichen klimatischen Faktoren. Das Verständnis der Mechanismen der Anpassung an Wassermangel im Zusammenhang mit den genetischen Implikationen ist für ein besseres Management und eine Verbesserung der Kulturpflanzen erforderlich. Diese Arbeit zielte darauf ab, den Anpassungsmechanismus von Tomaten an Wassermangel unter einer Reihe von klimatischen Bedingungen zu untersuchen, die damit verbundenen Genomregionen , die in die Anpassung einbezogen sind zu identifizieren, und die agronomischen Leistungen virtueller ILs in verschiedenen klimatischen Szenarien vorherzusagen und auszuwerten.

Verwendung von 50 Tomaten-Introgressionslinien (ILs) und zwei Elternlinien: *S. pennellii* und *S. lycopersicum* cv. M82, wurde diese Studie unter Gewächshausbedingungen durchgeführt, indem ein terminaler Trockenstress im siebten Blattstadium festgestellt wurde. Es bestand ein hoher (R^2 = 0,67 -0,75) kausaler Zusammenhang zwischen unbelasteten und belasteten Leistungen für erhöhte Blattflächen, transpirierte Wasser und produzierte Sprosstrockenmasse. Die Änderung der Plastizität des Trockengewichts der Triebe wurde hauptsächlich durch die Blattfläche erklärt, während die Plastizität der kumulativen Transpiration hauptsächlich der spezifischen Transpiration zugeschrieben wurde. Mit der Eingabe von unbelasteten Werten und QTL-abgeleiteten Parametern aus der Reaktion auf Wassermangel von Blattausdehnung und stomatärer Leitfähigkeit wurde die betonte Transpiration aller ILs mit hoher Genauigkeit innerhalb der getesteten Sättigungsdefizit-Bereiche gut vorhergesagt. Um die Auswirkungen der klimatischen Faktoren zu untersuchen, wurden genotypspezifische Parameter (einschließlich der Parameter für die Dürrereaktion) in ein ökophysiologisches Modell integriert, das aus drei Modulen bestand, die hauptsächlich für das Blattwachstum, die Trockenmasseproduktion und die Transpiration bestimmt waren. Mit oder ohne den Input von Blattfläche und Bodenwasser wurde die Modellleistung getrennt nach agronomischen Zielmerkmalen bewertet. Das Modell in aggregierter Form sagte für die bewässerte Pflanze die Blattfläche, die Transpiration und die Sprosstrockensubstanz (Genauigkeit = 0,69 - 0,84) und den transpirierbaren Bodenwasseranteil (Genauigkeit = 0,66) gut voraus. Allerdings gab es eine Überschätzung der gestressten Leistung um 20 bis 30% (Genauigkeit = 0,55 - 0,77). Mit der Eingabe der Blattfläche wurde die Modellleistung für das gesamte transpirierte Wasser und das Bodenwasser deutlich verbessert. Ein genombasiertes ökophysiologisches Modell kann als Werkzeug zur Vorhersage gestresster agronomischer Leistungen in Tomaten-Introgressionslinien verwendet werden.

Schlagworte: Introgressionslinien, *Solanum pennellii*, osmotischen Anpassung, QTL, ökophysiologisches Modell, Transpiration, Trockensubstanz, Blattfläche, transpirierbarer Bodenwasseranteil

Content

List of Tables

List of Figures

Chapter 1

General Introduction

Abiotic stresses such as high temperatures, low water availability, high salt levels and mineral deficiency, and toxicity are usually encountered by plants in both natural and agricultural systems (Jogaiah et al., 2013). On a global basis, losses in crop yield due to drought stress exceed losses in crop yield due to all other biotic and environmental factors combined (Lambers and Oliveira, 2019). The timing, intensity and duration of stress episodes are pivotal to determine the drought effects. Understanding the mechanisms underlying those different responses can support the design of new management tools and genotypes for modern precision agriculture (Chaves and Oliveira, 2004).

Drought effects and drought adaptations

Water stress impedes the plant processes throughout the ontogeny. Water stress directly affects rates of photosynthesis due to the decreased availability of CO_2 through the stomatal closure (Flexas et al., 2006; Chaves et al., 2009), and/or from changes in photosynthetic metabolism (Lawlor, 2002). Reduction in expansive growth can reduce the water loss, but also diminish the photosynthesis areas, leading to a net reduction of dry matter production.

The plant performance under water-limited environment has two dimensions for evaluation. Firstly, it is concerned with the processes in favour of sustained productivity, and secondly with survival. These two responses are not always compatible, and plants have to get a balance between them for successful drought adaptation. Water use efficiency (WUE) or transpiration efficiency (TE) known as the economic production per unit water consumption, was widely used as a breeding target in water-saving agriculture (Condon et al., 2004). However, the relationship between WUE and drought resistance is still unknown. Drought adaptation of plants for survival can be broadly categorized into drought escape and drought resistance (dehydration avoidance and dehydration tolerance) (Levitt, 1980; Ludlow and Much, 1990). According to Blum (1999), drought recovery is also one strategy of drought resistance.

Drought resistance can be defined as the crop survival ability and production capacity under drought conditions (Blum, 2011). Firstly, crops under drought conditions need to maintain a high plant water status by water uptake or a reduction of water loss (dehydration avoidance

DA). DA can be achieved through the development of a broad and deep root system to capture the water from the soil as well as through the reduction of leaf area increase and stomatal closure or a non-permeable leaf cuticle to reduce transpiration (Claeys and Inzé, 2013). Secondly, crops need to endure severe dehydration and maintain their physiological functions under lower leaf water status (dehydration tolerance DT), which can be achieved through the active accumulation of compatible proteins and solutes such as proline, soluble sugars and removal of harmful substances (e.g. ROS) accumulated in plants and anti-oxidation via osmotic adjustment (OA) and osmoprotectants (Luo, 2010). Both avoidance and tolerance responses are mainly orchestrated by abscisic acid (ABA) (Claeys and Inzé, 2013). Thirdly, the crop can recover water status and function after severe drought stress which causes the complete session of growth, a complete loss of turgor, and leaf desiccation (drought recovery DR) (Blum, 1999). These mechanisms are usually involved together in the plant function (even in one genotype). DA is the primary factor in drought-resistant performance, but the DT is seen as the second line of defence after DA (Blum, 2005).

From the phenotypic standpoint, an adaptive trait can be defined as an alteration in plant structure or function which improves the stressed performance of a considered genotype (e.g. reduction in transpiration rate through reduced leaf expansion and/or stomatal conductance, allowing the plants to conserve water). Conversely, a constitutive trait is either unaffected by environmental conditions or is affected by similar amounts in all studied genotypes (no G x E interaction) (Reymond et al., 2004). A constitutive trait does not respond to water stress. However, it can lead in a comparative advantage (e.g. transpiration efficiency under well-watered conditions, deep root system, or early vigour) (Richards et al., 2002).

In connection to coping strategies, the interesting questions are to what extent the structural and functional (especially water relation) traits show the plasticity (adaptive or passive) after drought stress and which trait components exhibit the genetic variations for plasticity, and which genome regions are associated to these responses. Since some of the consequences of OA promote DA, and some reduce it (Ludlow et al., 1983), whether OA ameliorates the drought effects should be clarified.

The role of leaf expansion and stomatal conductance

As an integral response to soil drying, many plants regulate the growth mainly through limiting the expansive growth and thereby the evaporation surface. Reduction in leaf expansion is a fast and actively regulated response, not merely a consequence of altered

hydraulics even before the leaf water potential is affected. Expansive growth is also much more sensitive to water limitation than photosynthesis (Muller et al., 2011). Not only the growth rate but also the duration of leaf expansion can be affected by drought stress (Claeys and Inzé, 2013). Inhibition of shoot growth (i.e. mainly leaf area), both directly through an active response (i.e. reduction in the expansion) and indirectly by stomatal closure can improve the water balance and stress tolerance, which can lead to more prolonged plant survival by reducing the water loss. However, growth limitation and continued growth should be balanced depending on the episodes of stress scenarios. Therefore, the balance between growth and survival is tightly regulated, and specific adaptations have evolved to allow growth under drought conditions.

Shoot growth and the physiology of plants in drying soil can be modified as a function of soil drying, even when shoot water relations are not perturbed (Turner et al., 1985). In responses of soil water status, stomatal conductance, photosynthesis and leaf expansion rate are in the significant part independent of leaf water status. Variables such as leaf conductance and extension (expansion) rate may be more useful indicators of plant stress than the more commonly used variables of leaf water relations (Davies et al., 1991). In cases where leaf water status does change, variation in shoot physiology can often be linked more closely to changes in soil water status than to changes in leaf water status (Turner et al., 1985). Wang and Bughrara (2008) concluded that leaf elongation under drought stress was a reliable selection criterion for drought resistance in Atlas fescue, perennial ryegrass, and their progeny. It seems that leaf elongation is a right integrator of overall plant capacity to cope with drought stress, as supported by detailed research in maize (Chenu et al., 2008).

Therefore, using leaf expansion and stomatal conductance as a function of soil drying could help to explore the genetic determinism in drought adaptation and model the genome-based plant performances. However, it needs repeated measurements of leaf length on the same standard leaf in each studied genotype, which could be a challenge to work with multiple genotypes. Using the sufficient dataset, one can investigate the drought responses in leaf expansion, stomatal conductance and transpiration, what are the genome regions (or QTL) controlling the parameters of drought responses, and what are their role in predicting stressed performance for transpiration.

Wild genetic resource - Interspecific tomato introgression lines

Solanum pennellii is a wild green-fruited tomato species endemic to Andean regions in South American, where it was evolved to thrive in arid habitats. *S. pennellii* exhibits beneficial traits such as abiotic stress resistances (Lippman et al., 2007; Koenig et al., 2013). Because of its stress tolerance and unusual morphology, it is a primary donor of germplasm for the cultivated tomato *Solanum lycopersicum* (Bolger et al., 2014a).

Solanum pennellii and *S. lycopersicum* are highly divergent species in the family Solanaceae. However, they are still related enough to produce viable progeny that expose the variation that has driven evolutionary change and provided the raw material for crop domestication and breeding. The genome size of *S. pennellii* is similar to domesticated tomato (1.2×10^9 vs 1×10^9 bp), and highly syntenic with potato, eggplant, pepper and other Solanaceae (Zamir, 2007). Crosses between distantly related plants can lead to substantial improvements in performance. Notably, *S. pennellii* × *S. lycopersicum* ILs have been used to define numerous quantitative trait loci (QTLs) for superior yield, chemical composition, morphology, abiotic stress. *S. pennellii* is a resource to identify, manipulate, and incorporate genes controlling plant growth and biomass production, and responses to drought and salt stress.

S. pennellii ILs were the founding members of the first introgression line population (Eshed and Zamir, 1994), and have been adopted as the standard for exploring and utilizing the hidden breeding potential of wild species to improve biomass and yield as well as product quality, and performance also in drought stress environments (Eshed and Zamir, 1995). Moreover, *S. pennellii* has been used to generate a panel of introgression (Eshed and Zamir, 1995) and backcrossed introgression (Ofner et al., 2016) lines that have been used to identify many interesting quantitative trait loci (Alseekh et al., 2015; Fernandez-Moreno et al., 2017). *S. pennellii* ILs are a set of nearly isogenic lines (NILs), representing the whole-genome coverage of *S. pennellii* in overlapping segments in the genetic background of *S. lycopersicum* cv. M82. In the first IL population phenotyped in 1993 consisted of 50 genotypes (Eshed and Zamir, 1994; Eshed et al., 1992), and presently this library consists of 76 genotypes.

ILs were developed through a succession of backcrosses, where each line carries a single genetically defined chromosome segment from a divergent genome. Therefore the resulting lines generally resemble the cultivated parent, thus allowing the reproducible mapping of QTL for the most complex integrated traits in plants - yield and biomass production. Over the years, the ILs have been phenotyped for hundreds of traits including repeated measurements

of the same traits, thus allowing for the identification of 2795 QTL (Zamir, 2007; Zamir, 2001). In 2014, the genome of *S. pennellii* was successfully sequenced, and over 100 of drought stress-related genes were identified as well (Bolger et al., 2014a).

In many cases, QTL mapping studies involve the whole genome segregating populations. However, from a practical plant breeding perspective, epistatic interactions in segregating populations, whether hybrid (F2) or recombinant inbred lines (RILs), make it difficult to define and characterize individual loci that control complex phenotypes fully. However, ILs are mostly devoid of epistasis, because unlinked QTL from other regions of the genome are absent. A complete IL population has enough members to reconstitute the donor parent in overlapping chromosomal segments and is immortal since it can be maintained by self-pollination. Consequently, these populations are very useful in identifying QTL, because any phenotypic difference between an IL and the recurrent parent is attributed solely to one or more donor parent genes within the introgressed chromosomal segment (Zamir, 2007).

Each IL contains on average an introgression of 33 cM. The size and identity of the introgressed segments were determined based on Random Fragment Length Polymorphism (RFLP) analysis of 350 markers (Eshed and Zamir, 1995; Eshed et al., 1992; Eshed and Zamir, 1994). Through the use of the data on stressed and unstressed performances, detection of wild chromosome segments harbouring the putative QTLs can be performed by using the Dunnett test through the multiple comparisons of all ILs with the recurrent line M82.

Use of genome-based crop modelling

By using the segmented plateau regression model, one can estimate the parameters of drought responses (i.e. thresholds and slope) for both stomatal conductance and leaf expansion as the stable characteristics which can be used as genotype-specific parameters (GSPs) for drought reaction. Moreover, the influence of evaporative demand can be evaluated on the responses of QTL-derived parameters. After evaluation of model performance, QTL information could be incorporated into a crop model which takes account of the climatic factors. Similarly to environmental factors, QTL information was additional input to the model. Therefore, the new (QTL- or) gene-based eco-physiological model implicitly includes the genotype x environment interaction (G x E) for the upper integration level traits such as both unstressed and stressed performances of leaf expansion, transpiration and dry matter production.

Most of the parameters used in the crop model (e.g. leaf growth module) are stable characteristics (e.g. maximum leaf expansion rate) of the considered genotype, encapsulate the environmental effects and can be related to QTL, independent of the environment (Reymond et al., 2003; Welcker et al., 2007). Use of these traits enables avoidance of complex QTL x environment interactions that are commonly observed for more complex traits such as leaf area or biomass accumulation (Yin et al., 1999; Reymond et al., 2004). The traits such as the duration of the vegetative phase (Yin et al., 1999), leaf width (Reymond et al., 2004), and the maximum elongation rate, and their responses to temperature, soil water status and evaporative demand (Reymond et al., 2003; Welcker et al., 2007) are some examples of stable traits. This type of study opens the way for modelling genetic variability at the whole-plant scale under fluctuating conditions. Hence, it should help in the evaluation of the contribution to the yield of QTL for individual traits components.

Because crop models represent causality between component processes and yield, they can predict crop performance beyond the environments for which the model parameters (primarily as GSPs) were estimated. This property allows the models potentially to resolve G x E into underlying processes daily and predict crop performance in any environment (Kropff and Struik, 2002). The structure of the model is essentially the same, except that the genetic factor like environmental factor is added for targeted traits. Based on the assumption that GSPs are controlled by genes that vary among genotypes, several crop modelling groups have used the empirically derived GSPs to enable simulation of differences in responses among genotypes (White and Hoogenboom, 1996; 2003; Hammer et al., 1996; Cooper et al., 2002; Yin et al., 2002; Messina et al., 2014). Through the incorporation of functions describing the linear relationship between GSPs and QTLs, a dynamic genome-based model can be developed.

This model-based approach comprises the following steps: (i) Create a crop model that predicts complex traits based on relations between elementary processes and environmental variable, (ii) Evaluate the capability of the model to predict the complex trait across a wide range of G x E combinations, (iii) Identify QTL for model-input traits using a genetic QTL approach, (iv) Develop a QTL-based model whereby QTL-based inputs replace the original values of model input. (v) Validate the QTL-based model across environments (Yin et al., 2004).

QTL-based modelling was first used to predict the complex trait in barley (*Hordeum vulgare*) grain yield (Yin et al., 1999; Yin et al., 2000), and it turned out that current crop models need to be improved to predict yield differences among relatively similar RILs. Again, a similar

analysis was conducted for simpler traits: leaf elongation rates in maize (*Zea mays*) (Reymond et al., 2003) and flowering time in barley (Yin et al., unpublished), demonstrating the potential of this approach. The question is, what is the role of drought reaction parameters in the connection to more complex canopy traits such as plant transpiration in a genome-based crop model under varying environments. Depending on the model performances, improvement in the lower level module can be made for better predictability and more understanding of the genetic and environmental effect on these drought responses.

Objectives

This study was conducted aiming at understanding the drought adaptation mechanisms of the tomatoes introgression lines in order to predict the performance of this later under various environmental conditions. The following general objectives were accomplished:

1) understanding the adaptive drought responses, and identifying the genome regions associated with morphological, dry matter and physiological traits under well-watered and drought-stressed conditions (Chapter 2);

2) investigating the drought reactions of leaf expansion, stomatal conductance and transpiration, identifying the QTLs and predicting the responses of stressed transpiration by dissecting it into the specific rate and leaf area with the use of QTL-based approaches while taking account of the environmental variation (Chapter 3), and

3) predicting the genome-wide performances of canopy level performance traits (e.g. shoot dry matter production, transpiration) in both well-watered and drought-stressed conditions over different climatic scenarios using a gene-based crop model (called TILSIM, **T**omato **I**ntrogression **L**ine **SIM**ulator) (Chapter 4).

Chapter 2

Genetic variation in adaptive responses explains the growth performances of tomato introgression lines under drought

San Shwe Myint[1,2], Dany Moualeu-Ngangue[1], Hartmut Stützel[1]

[1]Institute of Horticultural Production Systems, Leibniz Unversität Hannover, Hannover, Germany; [2] Department of Horticulture, Yezin Agricultural University, Naypyitaw, Myanmar

Abstract

The sensitivity and adaptation of plants to water deficits vary with the ontogeny, genotype and environment. With the use of introgression lines, drought stress responses were evaluated to evaluate the adaptation strategy and identify favourable genome regions holding putative QTLs for drought adaptation. Terminal drought stress was imposed by withholding water until the transpiration of the stressed plants reached <10% of the well-watered plants. There was a strong genotypic variation and drought effects for most trait values. Significant interaction between genotype and drought treatment was found for leaf area and cumulative tranpiration. The variation of phenotypic plasticity among traits ranged from 23 to 118%. The heritability of dry matter traits was high ($H^2 > 0.75$) while that of phenotypic plasticity for all studied traits was low ($H^2 < 0.4$). The phenotypic plasticity of shoot dry weight increase was mainly attributed to plasticity of leaf area growth while that of cumulative transpiration was mainly explained by that of specific transpiration. The genotypes of longer survival showed less reduction of growth and water relation traits, improved specific trsnapiration. There was a weak positive relationship between osmotic adjustment and dry matter traits. Among 60 detected genomic regions for trait values, 78.3% showed constitutive allelic effects and the remaining 21.7% were adaptive. Introgressions from chromosomes 3, 6 and 7 revealed high line-trait associations. Among the five stringent regions associated with osmotic adjustment, three genome regions were co-localized for osmotic adjustment and improved specific transpiration. This study quantified the role of genotypic variation in plasticity of drought adaptive traits on maintaining dry matter productivity and the relation between drought survival and responses of water relation, and determined underlying genomic regions holding the favourable QTLs in tomatoes.

Keywords: Drought, Plasticity, Adaptation, Heritability, Survival**,** *Solanum pennellii*

Introduction

Drought problems in arid and semiarid regions are forecasted to be the inevitable threat for global food security due to climate change (Godfray et al., 2010; Elliott et al., 2014). Plants are thought to cope with drought stress through escape, avoidance and tolerance strategies (Levitt, 1980; Ludlow, 1989; Levitt, 1972). Drought escape is often related to a short life cycle or plastic shifts in phenology. The avoidance strategy includes adaptive responses that maintain plant–water status via stomatal closure, leaf area reduction and diversion of carbon allocation to non-photosynthetic organs such as roots and stems (Chaves et al., 2002; Juenger, 2013). This strategy also includes increasing water uptake ability through extensive root systems and enhancing water use efficiency through high leaf mass ratio (Schulze, 1986; Jackson et al., 2000). The tolerance strategy is an adaptation to protect plant cells and tissues from water deficits (Juenger, 2013), through osmotic adjustment (OA), enhancing the antioxidant capacity, and desiccation tolerance (Zhang, 2007). The adaptation strategies are not mutually exclusive and presumably play differing roles across species and stress of varying duration, intensity, and timing (Juenger, 2013).

Turgor maintenance via OA under water stress is a key mechanism (Hsiao et al., 1976) consisting of the net (active) accumulation of compatible organic and inorganic solutes within cells (Jones, 2013) and lowering the cell's osmotic potential. Among others, potassium and nitrate ions were also reported to accumulate (Itoh et al., 1986; Itoh et al., 1987; Morgan, 1992; Tschaplinski and Tuskan, 1994; Premachandra et al., 1995; Aroca, 2012) under drought stress provided there is sufficient supply. Moreover, OA enables sustained growth and photosynthesis at lower soil and leaf water potentials (Turner, 2017), possibly through the maintenance of specific transpiration and delayed stomata closure. OA is designated as a prime drought stress adaptive engine in support of plant production (Blum, 2017), complemented by the fact that volume maintenance in chloroplasts by OA may preserve photosynthetic capacity (Santakumari and Berkowitz, 1991). To what degree OA can contribute to drought tolerance and prolonged survival as the interplay between plant and environment is still unclear (Aroca, 2012).

Phenotypic plasticity is defined as the ability of a single genotype to produce multiple phenotypes in response to the environment (Nicotra and Davidson, 2010). Natural variation in plasticity is commonly measured as gene-by-environment interaction, and its occurrence in response to drought was frequently reported (Juenger, 2013). From a crop physiological view,

adaptive responses of plants include leaf area development, dry matter production and partitioning (allocation), osmotic adjustment (OA) and transpiration (Masinde et al., 2005; 2006).

Despite the great efforts in crop breeding for tolerance to drought, the development of tolerant varieties is slow and is greatly restricted by narrow genetic variation and by the complex and multi-genic nature of the traits of drought tolerance (Hill et al., 2013; Langridge and Reynolds, 2015). For developing genotypes with enhanced tolerance and growth performance under drought stress, it is essential to combine the understanding of the relationships between structural and physiological trait components with the underlying genome regions relevant for drought stress tolerance (Zhu et al., 2016). Despite the economic importance of tomato (FAOSTAT, 2017), the mechanisms that govern responses to drought stress in this horticultural species are not well characterized (Iovieno et al., 2016; Arms et al., 2017). *Solanum pennellii* (Sp), a drought-adapted wild species, constitutes an ideal experimental model to advance our understanding of drought adaptation and tolerance mechanisms in tomato (Atarés et al., 2011). The Sp genome library, a permanent mapping source for QTL analysis, is composed of a series of introgression lines, in which defined genomic segments of the Sp genome replace homologous regions in *S. lycopersicum* (cv. M82) background.

This study raised three questions: (i) Are physiological traits more plastic than morphological and dry matter traits under drought stress? (ii) Can plasticity of plant dry matter production in response to drought be explained by the plasticity of adaptation mechanisms? (iii) What are the favourable genome regions holding the QTLs associated with plant productivity and plasticity under drought stress? Therefore, this work aimed at:

(1) evaluating the drought sensitivity of trait components and their environmental variation,

(2) assessing the relationship between the plasticity of plant performance and drought adapted responses and

(3) identifying the favourable genome regions holding the putative QTLs associated with the growth traits and their plasticity under drought stress.

Materials and Methods

Plant materials

A genotype panel consisting of 50 introgression lines (ILs) and two parent lines (*S. pennellii* (LA0716) and *S. lycopersicum* cv. M82 (LA3475)) of tomato obtained from C.M. Rick Tomato Genetics Resource Center (University of California, Davis, USA) were used in this study. Each IL contains single introgression from donor *S. pennellii* (Sp) in the genetic background of the drought-sensitive cultivar M82. This library provides complete coverage of the wild species genome. The lines contain on average an introgression of 33 cM from a total genome size of 1200 cM. The size and identity of the introgressed segments were determined based on Random Fragment Length Polymorphism (RFLP) analysis of 350 markers (Eshed and Zamir, 1995; Eshed et al., 1992; Eshed and Zamir, 1994).

The experimental set-up, plant cultivation and management

Pot experiments were conducted in a greenhouse of the Institute for Horticultural Production Systems, Leibniz Universität Hannover (52.5° N, 9.7° E). 10 L plastic pots (25 cm height and 24 cm diameter) and 2 L pots were filled with loamy sand with a bulk density of $\approx$ 1.25 g cm^{-3}. The soil had a water content of 28 % (w/w) at full water holding capacity (WHC). The experiment was laid out in a randomized complete block design with replications at four different times in 2016 (June - November) and 2017 (March - May). For each replication, eight seeds of each IL and 16 seeds each of parent lines were sown in separate cells (50 cm^3) of plastic trays using peat-based growing media (>90% organic matter, pH 5.5–6.5, EC 0.7–1.2, bulk density 330–430 kg/m^3, Potgrond H, Klasmann-Deilmann, Germany). Emergence started in most lines about four days after sowing (DAS). When two leaves were fully unfolded at $\approx$ 10 DAS at 25°C, the four most uniform seedlings of each line were transplanted, two to 10 L pots and two to 2 L pots. Greenhouse temperatures were set to 28±2°C during the day and 20±2°C during the night. Fertilizer (Ferty® 2 Special, Planta, GMBH, Germany) was applied with the irrigation water before treatment start at a rate corresponding to 160 kg N ha^{-1}, 60 kg P$_2$O$_5$ ha^{-1} and 260 kg K$_2$O ha^{-1}.

During the first 2–3 weeks (until 6–8 leaves emerged) all pots were watered daily. At the seven[th] leaf initiation stage of most lines, initial data on morphological and dry matter traits were recorded by harvesting the plants from the 2 L pots and the drought stress was imposed

in the 10 L pots. The well-watered pots were re-watered daily to 90% of the WHC (control) and the water-limited pots were subjected to water withholding until the transpiration rate of the stressed plants dropped to less than 10% of the corresponding control. Each pot surface was covered to a depth of ≈ 4 cm with quartz gravel as an evaporation barrier. Moreover, two pots without plants were used to measure evaporative loss. The pots were re-arranged every day to have a random distribution of genotypes and drought treatments. After stress imposition, all pots were weighed daily around the same time to calculate the daily transpiration rate and soil water content. When necessary, supplementary light with 400 W high-pressure sodium lamps was provided to ensure 14 hours of daylight with the approximated PPFD of 200 μmol m^{-2} s^{-1} in the morning and evening. Throughout the experiment, the plants were kept single stem by removing the side shoots.

Determination of morphological and dry matter traits

Net phenotypic values produced during the stress period were estimated as the differences between the values at the imposition of stress and values at harvest. Stem length (SL) was measured from the point of cotyledon to the base of the shoot tip using a meter ruler. Leaf number (LN) was recorded counting from the base of the stem to the newest leaves with at least 2 cm in length. Average internode length was estimated as the ratio of SL to LN. Total leaf area LA_t was measured destructively using the leaf area meter (model 3100; LICOR, Lincoln, NE, USA). Dry matter of above ground components (leaf, petiole and stem) was measured after drying the materials in an oven (min. 72 h at 70 °C). In order to minimize the age and temperature effects on harvested data, the calculated values were shown for a treatment period of 14 equivalent days at 25°C (14 d$_{25°C}$), for which base temperature (7.7°C) obtained from a preliminary test with M82 was used. It was, therefore, possible to quantify and compare phenotypic values of different genotypes at similar physiological ages for both stressed and unstressed conditions. Moreover, specific leaf area (SLA, the ratio of LA_t to leaf dry weight (DW_{le})) and transpiration efficiency (TE, ratio of DW_{le} to cumulative water transpired (CT)) were calculated to evaluate the efficiency and partitioning aspect of traits.

Determination of water relation traits

Transpiration was determined by daily pot weight measurements using an electronic balance (QS 64B; Sartorius, Göttingen, Germany). The differences in weights between two consecutive days were considered as the water lost through transpiration. The specific

transpiration rate ST was calculated as the ratio of the CT and integral of the LA_t for the stressed period.

Water relation traits were determined as described in Masinde et al. (2006). Measurements were carried out on the youngest fully expanded leaves between 11.00 and 15.00 h. Leaf water potential (WP) was determined by using a Scholander-Hammel type pressure bomb (Soil Moisture Equipment Corp., Santa Barbara, CA, USA) according to Scholander et al. (1965). For leaf relative water content (RWC) determination, each leaflet was placed in distilled deionized water and left at 20 ± 2 °C in dim illumination for 24 h. After blotting, the turgid weight (TW) was determined; after that, the leaflets were oven-dried at 80°C to a constant weight to obtain the dry weight (DW). Fresh weight (FW), TW and DW were used to determine the RWC.

$$RWC = \frac{FW - DW}{TW - DW} \qquad \text{(Eqn 2-1)}$$

Leaf osmotic potential (OP) was measured from leaf discs of 1 cm diameter (0.78 cm^2), excised from the same leaf and immediately wrapped in aluminium foil and frozen by first immersing in liquid nitrogen, and subsequently stored at -18°C until required. OP was measured at 22 ± 1°C with a psychrometer (C-52-chamber, Wescor Corp., Logan, Utah, USA). The product between RWC and OP was then taken as OP at full turgor (OP_{100}). For quantification of osmotic adjustment (OA), Ludlow's full-turgor adjustment method was used (Ludlow et al., 1983) as the difference between OP_{100} at WW and DS conditions.

Determination of total nitrogen, nitrate nitrogen and potassium

Total nitrogen (TN) of shoots was measured by tube digestion procedures of the Kjeldahl method (Nelson and Sommers, 1973). Nitrate nitrogen (NN) was determined by nitration of salicylic acid, according to Cataldo et al. (1975). Potassium content was measured with an Atomic Absorption Spectrometer 1100 B (Bodenseewerk Perkin-Elmer GmbH, USA) using the flame emission technique.

Data processing and statistical analysis

Parent line M82 was replicated three times in each block. The variation observed in a phenotypic trait of harvested data was partitioned to the source of variation in line (*L*), treatment (*T*), and their interaction (*L x T*). ANOVA was performed by using a mixed linear

model for each phenotypic trait using *lmer* function of *lme4* package in R-3.6.0 (R Foundation for Statistical Computing) defined by

$$Y_{ijk} = \mu + L_i + T_j + (L \times T)_{ij} + r_{k(j)} + \varepsilon_{k(ij)},$$ (Eqn 2-2)

where Y_{ijk} is the measured trait value, μ the vector of general mean, L_i the effect of ith line, T_j the fixed effect of jth treatment, *(L x T)*$_{ij}$ the interaction effects of the ith line and j^{th} treatment, $r_{k(j)}$ the effect of replication (block) k within j^{th} treatment and $\varepsilon_{k(ij)}$ the random error of y_{ijk}. Line and treatment were considered as fixed factors with their interaction (*L x T*) term in the model, and replication was treated as a random factor. Significant main effects of each L and T indicate the genotypic variation and plasticity, respectively. *L x T* designates the genotypic variability of the plasticity of a particular trait.

Phenotypic plasticity (*pX*), an index of drought response, of a given genotype for a particular trait *X* was calculated as the relative change in stressed values compared with the controlled ones as (Kadam et al., 2017; Sandhu et al., 2016):

$$pX = \frac{Y_d - Y_w}{Y_w} \times 100,$$ (Eqn 2-3)

where *Y* indicates the phenotypic values of each trait, while the subscripts *d* and *w* designate the droughted (water-limited) and well-watered treatments, respectively. All symbols for plasticity start with the lowercase letter *p* (**Table 2-1**).

Table 2-1. List of 20 morphological, dry matter and physiological traits evaluated for 50 ILs and two parent lines in the experiments

Trait	Trait acronym	Unit	Phenotypic plasticity acronym	Method of quantification
(A) Morphological traits				
Stem length	SL	cm plant^{-1}	pSL	Length from the point of epicotyl to tip of main stem
Leaf number	LN	nr. plant^{-1}	pLN	Number of unfolded (~2 cm) leaf on main stem
Internode length	INL	cm	pINL	SL/ LN
Total leaf area	LA_t	cm^2 plant^{-1}	pLA_t	Leaf area of all leaves on main stem
Specific leaf area	SLA_t	cm^2 g^{-1}	$pSLA_t$	LA_t/ DW_{le}
(B) Dry matter traits				
Leaf dry weight	DW_{le}	g plant^{-1}	pDW_{le}	Dry weight of leaves on main stem
Stem dry weight	DW_{st}	g plant^{-1}	pDW_{st}	Dry weight of main stem
Shoot dry weight	DW_{sh}	g plant^{-1}	pDW_{sh}	DW_{le} + DW_{st}
(C) Physiological traits				
Cumulative transpiration	CT	kg plant^{-1}	pCT	Total water transpired during stress period
Transpiration efficiency	TE	g kg^{-1}	pTE	DW_{sh} /CT
Specific transpiration	ST	kg m^{-2}day^{-1}	pST	Ratio of CT and integral of LA_t for the stressed period
Leaf water potential	WP	MPa	pWP	Scholander *et al.* (1965)
Osmotic potential	OP	MPa	pOP	Psychrometer (C52 chamber)
Relative leaf water content	RWC	-	pRWC	FW-DW/TW-DW
Turgid osmotic potential	OP_{100}	MPa	pOP_{100}	OP x RWC
Total nitrogen	TN	mg g^{-1}	pTN	Nelson & Sommers (1980)
Nitrate nitrogen	NN	mg g^{-1}	pNN	Cataldo *et al.* (1975)
Potassium	K	mg g^{-1}	pK	AAS
Osmotic adjustment	OA	MPa	-	Difference of OP_{100} between well-watered and drought stressed condition
Drought survival	SUR	dpi	-	Days to reaching transpiration ratio < 0.1

The variability of phenotype traits due to genetic factors was evaluated using the broad-sense heritability (H^2) for each treatment (WW and DS) and also for pX:

$$H^2 = \frac{\sigma_g^2}{(\sigma_g^2 + \frac{\sigma_\varepsilon^2}{(r)})} \qquad \text{(Eqn 2-4)}$$

where σ_g^2 is the genotypic variance, σ_ε^2 the residual variance, and r the number of replications (n=4).

For determining H^2 across water supply environments, the variance component for the interaction was added:

$$H^2 = \frac{\sigma_g^2}{(\sigma_g^2 + \frac{\sigma_{ge}^2}{m} + \frac{\sigma_\varepsilon^2}{(rm)})} \qquad \text{(Eqn 2-5)}$$

where σ_{ge}^2 is the genotype x environment interaction variance, m is the number of environments (n=2) and r the number of replications (n=4) according to Holland et al. (2010).

Pearson correlation coefficients were computed using trait means, and plasticity using the *corrplot* package in R. Shapiro-wilk normality tests and regression analyses were performed in SIGMAPLOT 11.0 (Systat Software Inc., San Jose, CA, USA). The P values of the correlation coefficients were calculated by two-sided Student's t-test using the correlation function of the *agricolae* package. Heat maps were generated for increased or decreased relative effects of the introgressed segments as compared to the reference M82 by using JMP Pro. 13 (SAS Institute Inc., Cary, NC, USA).

For detection of line x trait associations, the model was modified by assigning line as the fixed factor and the rest as random factors according to Schmalenbach et al. (2009). When the ANOVA revealed significant line main effects (*L*), or line x treatment interaction effects (*L x T*), the *post hoc* two-sided Dunnett's test was applied for comparing the individual ILs with the recurrent parent M82 (Dunnett, 1955). The presence of a chromosome region in an introgression for phenotypic values or plasticity was assumed if the values of particular IL showed a significant difference at FDR ≤ 0.05 from M82. The regions showing main effects across the treatments or showing line effects in both treatments (*L + I*) were regarded as constitutive regions. At the same time, those associated in only one condition (I, stress or

control) were considered as adaptive (interactive) regions. Those regions exclusively associated with plasticity (pX) were assumed novel regions. The relative effect of a wild allele was quantified by calculating the relative difference (RD in %) of a particular IL holding the putative genome region as compared to the recurrent parent M82 according to Naz et al. (2014).

$$RD(IL) = \frac{Lsmeans(IL) - Lsmeans\,(M82)}{Lsmeans\,(M82)} \times 100 \qquad \text{(Eqn 2-6)}$$

Results

Variations of phenotypic traits values and plasticity

A total of 20 phenotypic traits of tomato lines were categorized into three trait classes: morphology, dry matter, physiology. Analysis of variance showed that genotypic effects were significant for most trait values, except RWC (**Fig. 2-1, S1; Table 2-S1**). The main effect of water limitation was highly significant for each studied trait. There were significant interactions between genotype and water supply environment for leaf area and cumulative transpiration (CT). There were genotypic differences for phenotypic plasticity of specific transpiration, osmotic potential and for osmotic adjustment and survival **(Table 2-S2)**. The grand mean of plasticity (*pX*) ranged from 23% for relative water content to 118% for water potential, regardless of positive or negative signs (**Fig. 2-1, S1**). Upon drought imposition, *pX* of most physiological traits were positive while that of morphological and dry matter traits were negative. Among the traits relevant for water relations, the highest drought responses were revealed in water potential (pWP = 118%), and among the studied minerals, nitrate nitrogen showed the highest plasticity (pNN = 110%) (**Fig. 2-S1**). Under drought stress, leaf area was more reduced than leaf weight DW_{le} (pLA$_t$= -61% vs pDW$_t$=-49%), leading to a considerable decrease of specific leaf area (pSLA$_t$ = -24%) (**Fig. 2-1D, E, F**). Moreover, there was a 22% higher reduction of total water uptake (CT) than shoot dry weight (DW_{sh}) (pCT = -68% vs pDW$_{sh}$=-46%) upon drought stress, which could be visualized by the relative increase of transpiration efficiency upon drought stress (pTE = 68%) (**Fig. 2-1H, I, J).** Over all, the magnitude of the phenotypic plasticity was higher in the physiological class (61±30.58%) than the other two classes (dry matter (43±14.52%); morphology (35±6.02%)).
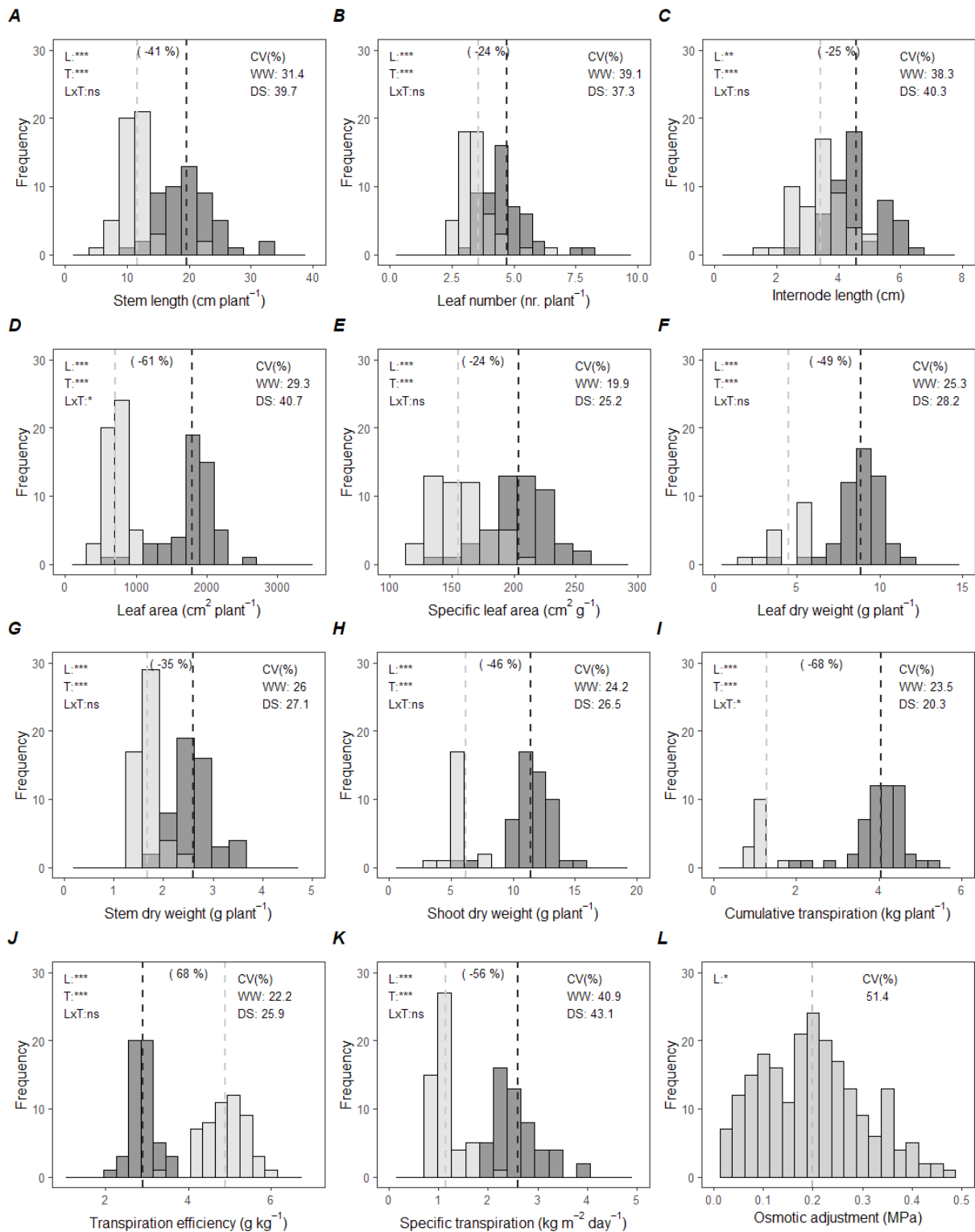
Fig. 2-1. Frequency distribution of morphological (A - E), dry matter (F - H), and some physiological (I – L) traits under well-watered (WW, dark grey) and drought-stressed (DS, light grey) conditions. Dashed lines indicate the trait means for each of WW and DS environments. Mean phenotypic plasticity (*pX*) is described in parentheses as the relative change (percent increase (+) or decrease (-)) upon stress. F-tests show line (*L*), treatment (*T*) and interaction (*L x T*) effects. CV (%) are given for both WW and DS conditions. * and *** denote significance at p < 0.05 and 0.001, respectively. ns denotes non-significance.

Environmental variation and heritability

In most traits studied, coefficients of variation (CV%) were larger across-environments than within environments (**Table 2-S3**). Within-environment variations were smaller in most water relation traits than in the other traits, especially under drought stress condition. Except mineral matters, most physiological traits of introgression lines showed smaller CV% under DS than WW. The broad-sense heritability revealed a large variability ranging from 0.24 to 0.71, 0.0 to 0.73 and 0.29 to 0.83 for drought-stressed, well-watered and across water supply treatments, respectively (**Fig. 2-2**). The difference in heritability between WW and DS was the least for K (0.003) and the highest for RWC (0.36). Average heritability across environments was higher for dry matter (0.74 ± 0.04, n = 3) and morphological traits (0.72 ± 0.14, n = 5) than for physiological traits (0.59 ± 0.16, n = 10). Under DS, the average heritability for water relation traits (WP, OP, RWC, OP_{100}) was higher than in the well-watered treatment. Average heritability of phenotypic plasticity *pX* (0.11 ± 0.12) was lower than heritability of trait values per se across environments (0.65 ± 0.15). Heritability of *pX* was higher for most physiological traits, except WP and minerals than for both morphological and dry matter traits. Osmotic adjustment and drought survival exhibited medium (0.36) and high (0.69) level heritabilities, respectively.
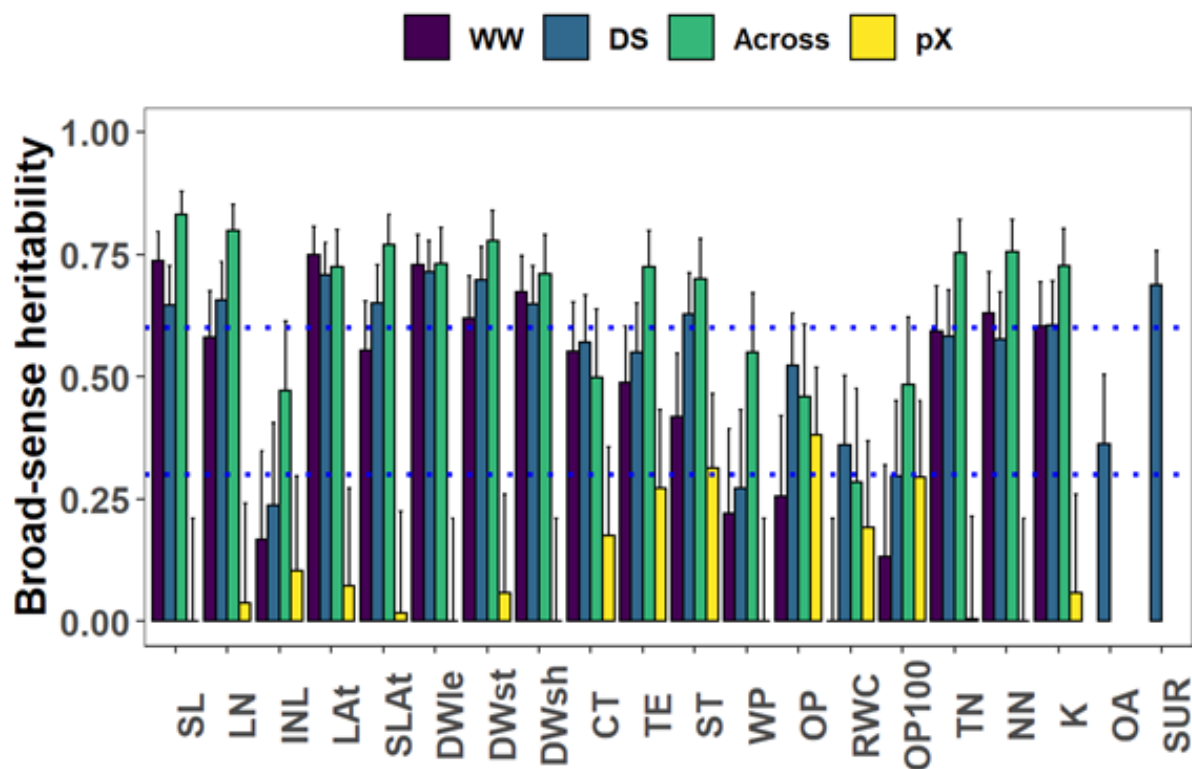
Fig. 2-2. Broad-sense heritability (H^2 with SE) of morphological, dry matter and physiological traits evaluated at each (WW and DS) and across the water supply environments, and for phenotypic plasticity (*pX*). Dotted blue lines signify low ($H^2 < 0.3$), medium ($H^2 = 0.3 - 0.6$) and high ($H^2 > 0.6$) heritability according to Robinson et al. (1949). Acronyms are described in **Table 2-1**. WW, well-watered, DS, drought-stressed, SUR, drought survival.

Relationships between trait values and between their plasticity

In both treatments, major growth-related traits such as CT, LA_t, DW_{le} and DW_{sh} showed strong inter-correlations (**Fig. 2-3A, B**). Stem length revealed a wide range of positive correlations with other growth-related traits (i.e. LN, INL, DW_{st}). In both treatments, TE exhibited a noticeable negative correlation with CT but a strong positive correlation with most dry matter traits. Under DS, a significant negative correlation was observed between major growth traits (e.g DW_{sh}) including CT and most water relation traits (i.e OP, RWC, OP_{100}). Mineral contents (e.g. TN) were negatively correlated with SLA_t and LA_t in both water supply conditions and with SL and LN under DS (**Fig. 2-3A, B**). The plasticities of dry matter traits showed positive correlations with most adaptive traits such as pLA_t, pCT, pTE, pST, pOP_{100} and OA in varying degrees of coefficients (**Fig. 2-3C**). Moreover, pLA_t, $pSLA_t$ and pRWC were negatively correlated with plasticities of mineral contents pTN and pK while pTE was negatively correlated with pCT and pST.
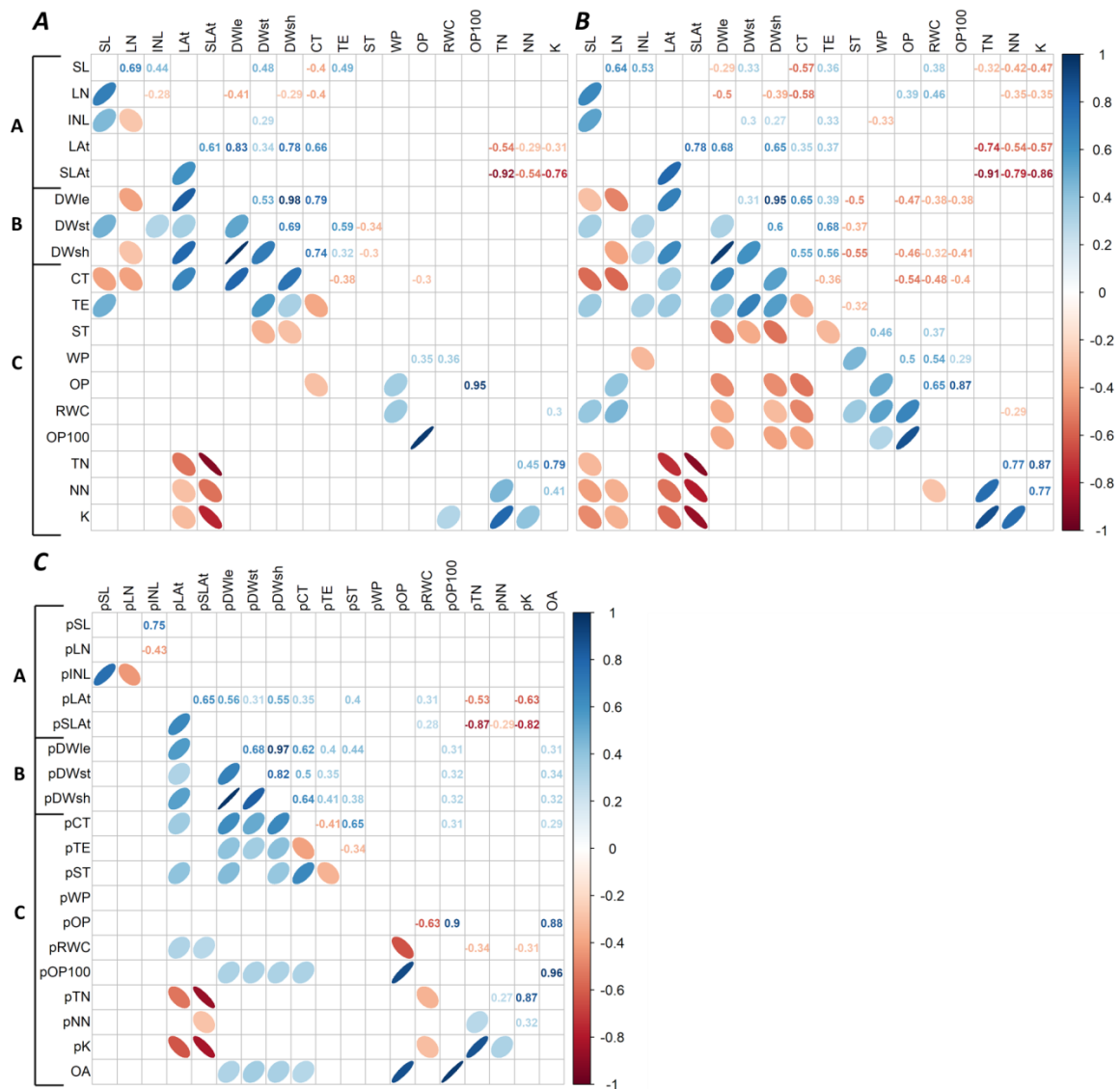
Fig. 2-3. Correlations among phenotypic trait values under well-watered (A) and drought stressed (B) conditions, and their phenotypic plasticity (and OA) (C). Pearson correlation coefficients are shown in the upper panel. Blue (right oblique) and orange (left oblique) colours show positive and negative correlations, respectively. Colour intensity and slimness of ellipses indicates the strength of correlation coefficients between pairs of traits. Correlations were calculated from LSMEANS of individual lines. Uppercase letters on the left panels of the figures correspond with trait classification; for trait acronyms, trait classes and units see the **Table 2-1**.

Influence of drought survival on growth and water relation performances

Drought survival, days to reaching transpiration ratio < 0.1, was observed to vary among genotypes ranging from 10 to 17 days **(Fig. 2-4)**. Genotypes showing the longer survival were those of lower magnitudes in growth traits such as leaf area and shoot dry weight and lower total water transpired. Under drought stress, the longer the survival the less in reduction of growth performance and water transpired **(Fig. 2-4A, B, C)**. In both water supply treatments, the genotypes showing the longer survival were higher in specific transpiration compared to those of shorter survival **(Fig. 2-4D)**. For water relation traits, there was no apparent relation between survival and trait values under well- watered condition **(Fig. 2-4E, F, G, H)**. Under drought stress, reduction of WP, RWC, OP and OP_{100} was less in genotypes showing the prolong survival than in genotypes of shorter survival. Amelioration in reduction of trait value under drought stress was most explained for RWC ($R^2 = 0.45$) and least explained for OP_{100} ($R^2 = 0.14$) by genotypic variation in drought survival.
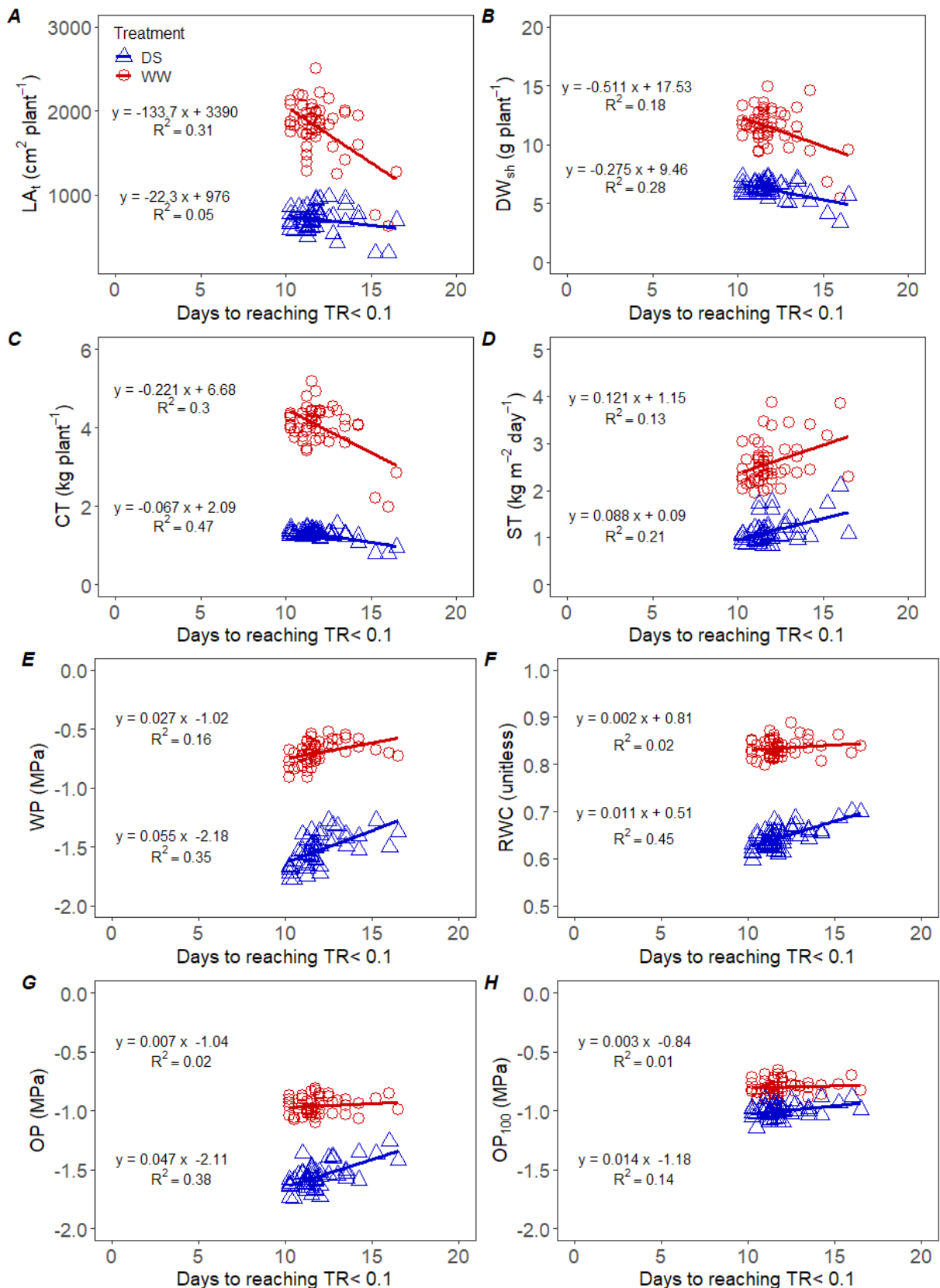
Fig. 2-4. Agronomic and water relation performances of tomato introgression lines against days to reaching TR < 0.1. DS, drought-stressed; WW, well-watered; TR, transpiration ratio between DS and WW plants.

Influence of plasticity in adaptive traits on dry matter production

Genotypic variation in drought effects on shoot dry weight (pDW_{sh}) was more explained by the variation in plasticity of leaf area (pLA_t) than in specific transpiration (pST) (**Fig. 2-5A, B**). The magnitude of variation in pDW_{sh} was 0.35 and 0.55 for each unit variation of pST and pLA_t, respectively. The potential pDW_{sh} was 25% when there was no pST and 11% when there was no pLA_t. Thirty percent of genotypic variation for pDW_{sh} could be explained by that of pLA_t. For the variation in plasticity of cumulative transpiration (pCT), pST was more attributable than pLA_t (**Fig. 2-5C, D**). The potential pCT was already around 47% and 54% when there was no plasticity of ST and LA_t respectively. The change of pCT was 0.36 and 0.22 for each unit change of pST and pLA_t. The variation in pST could explain the 42% of that in pCT. Influences of the plasticity of turgid osmotic potential (pOP_{100}) and osmotic adjustment (OA) on pDW_{sh} and pCT were rather weak in comparison to pST and pLA_t (**Fig. 2-S3**). Only 10 and 11% of variation in pDW_{sh} could separately be explained by the variations in pOP_{100} and OA and their attributions for pCT were 10 and 8%, respectively. For every 1 MPa increase of OA among genotypes, there was a possible reduction of plasticity (less drought effect) of DW_{sh} and CT by 32% and 17%, respectively (**Fig. 2-S3C, D**).
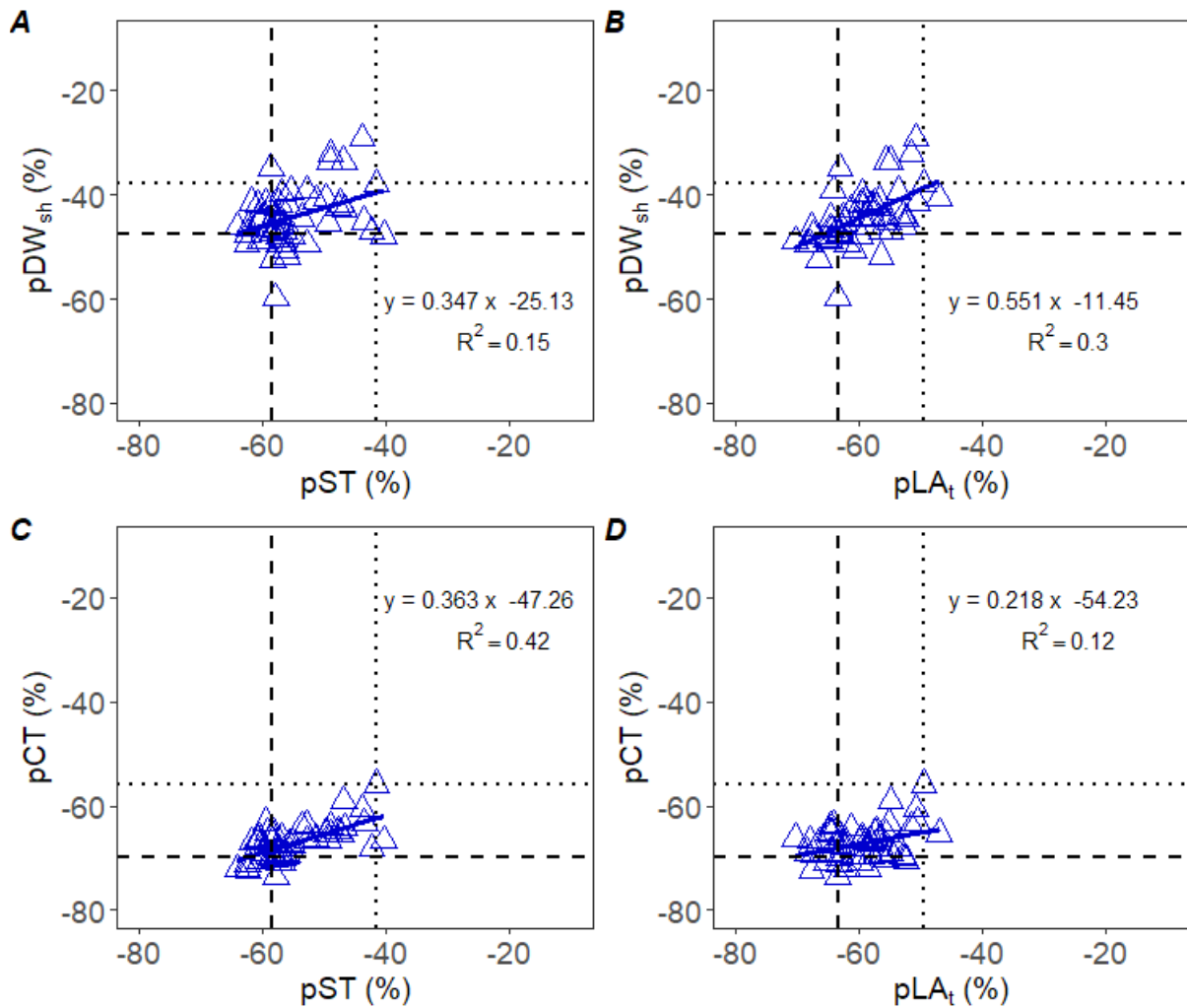
Fig. 2-5. Phenotypic plasticity of shoot dry weight (pDW$_{sh}$) and cumulative transpiration (pCT) of 50 introgression lines and two parent lines as dependent on phenotypic plasticity of specific transpiration (pST, A, C) and leaf area (pLA$_t$, B, D). Dashed and dotted lines indicate the plasticity of M82 and Sp, respectively. Regressions are based on means of individual lines. For trait acronyms, trait and classes see the **Table 2-1**.

Line-trait associations for trait values and plasticity

We identified 146 genome regions (including 16 regions for OA and 4 regions for drought survival (SUR)) for all studied traits. When duplications of detections on the same segments and detections for OA and SUR solely under drought stress condition were not considered, 74 exclusive regions, 60 for trait values and 14 for plasticity, favourably holding the QTLs were identified (**Fig. 2-6**; **Table 2-S4**). In each and across water supply treatments, regardless of the association for OA, SUR and *pX*, 78.3% of total detections for trait values showed line main effects and 21.7% exclusive interaction, revealing the constitutive and adaptive responses, respectively. Detected QTLs for OA and *pX* could be considered adaptive. Under WW and across treatments, morphological traits showed the highest proportion of detected regions per trait (7.2, 6.8%) compared to the dry matter (4.6, 6.0%) and physiological (2.4, 4.2%) traits. For DS condition, dry matter trait class revealed the highest proportion of associated genome region compared to morphological and physiological trait classes (4.0, 2.4, and 3.2%, respectively).

Most traits (SL, LN, INL, DW_{st}, TE, ST, RWC, OP_{100}, TN and K) showed more genome regions being associated with increased than with decreased relative performance under drought, while some (LA_t, SLA_t, DW_{le}, CT and WP) had higher numbers of regions with decreased trait values (**Fig. 2-7**). There were 14 favourable regions (5 for OP and 9 for OP_{100}) holding QTLs for higher plasticity (more negative direction). OA, an indicator of adaptive stress response, showed a high variation of wild allele effects, ranging from -1.69 to 223% differences from M82 (**Fig. 2-8; Table 2-S3**). Among 16 (32%) regions significantly different from the recurrent parent M82 (OA = 0.10±0.055), five detections from Chr. 1, 4, 5, 8 and 9 were stringent (p< 0.01) (**Fig. 2-8**). Out of the 60 detected regions, those from Chr. 3, 6 and 7 revealed the most frequent mappings (26.7%, 16.7% and 15%), being associated with 44%, 56% and 44% respectively of total traits studied under each and/or across water supply environments **(Table 2-S3)**.

Regardless of the water supply environment, six chromosome regions showed the possible presence of QTLs associated with higher values of DW_{st} (**Table 2-S3**). Among them, IL7-3 was co-localized for increased values of SL, LN, RWC, TE and drought survival (SUR), and decreased values of LA_t, DW_{le} and CT. IL6-2 was found to hold QTLs associated with the decrease of DW_{sh}, DW_{le}, LA_t, SLA_t and CT, and increase of ST, TN and K. IL4-3 was commonly mapped for increased values of LN and SUR. Increase of DW_{st}, TE and SUR were associated with one region from Chr. 11 (IL11-1). Five regions were detected for increased

ST especially upon the stressed condition of which three regions were also associated to higher OP, OP_{100} and OA. Moreover, four regions exhibited the co-localization for OP and OA. Most regions associated with OA were also observed to hold QTLs for OP_{100}. Among the regions associated for OA, only one (IL1-1) showed the co-localization for increased value of DW_{st}.
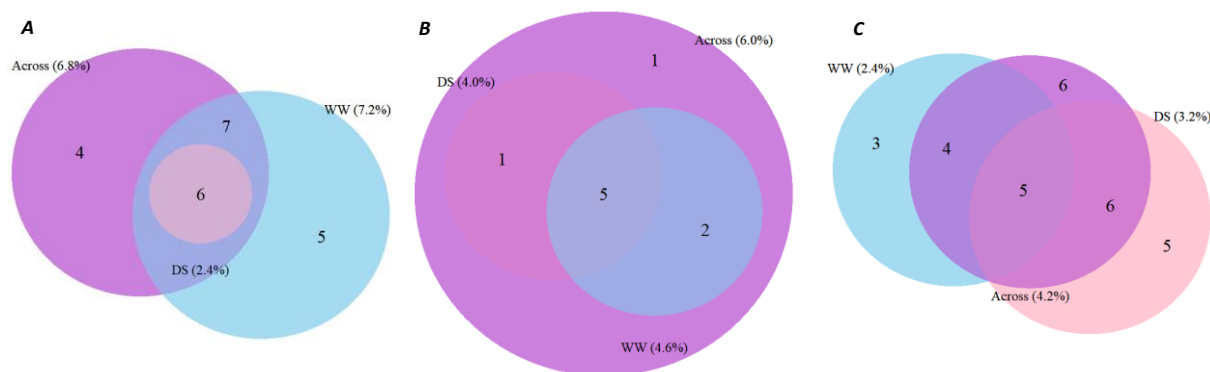
Fig. 2-6. Venn diagrams of the number of associated genome regions in each (well-watered (WW, blue) and drought-stressed (DS, pink)) and across (purple) water supply environments for genotypic values of morphological (A), dry matter (B), physiological (C) traits. Percent values in parentheses are proportions of QTLs detected for trait values in each and across treatments. Shared areas (36 regions) denote the line main effects and interaction effects (L + I), non-shared parts of WW and DS conditions (13 regions) show the exclusive interaction effect (I), and non-shared parts across treatments (11 regions) denote the exclusive line main effect (L), representing 60.0, 21.7 and 18.3% respectively of mutually exclusive detected 60 regions. Classes A, B and C consisted of five, three and ten trait components, respectively. The detailed information of means, relative difference, introgression regions and mode of effect for each trait component are described in **Table 2-S3**.
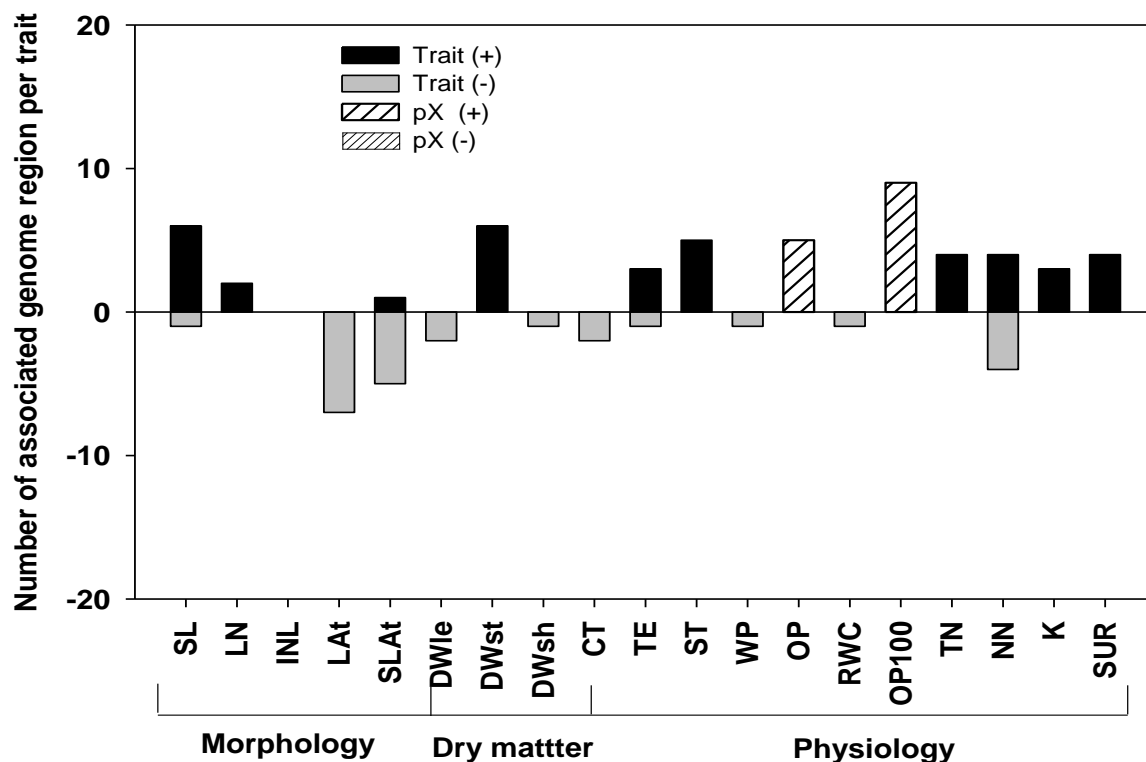
Fig. 2-7. Number of genome regions associated with trait values and phenotypic plasticity for three classes (morphology, dry matter, physiology). Stacked bars above and below the zero line constitute the number of regions with increased (+) and decreased (-) relative performances of trait values (Trait) or phenotypic plasticity (pX) compared to recurrent M82 according to Dunnett's test (FDR ≤ 0.05).
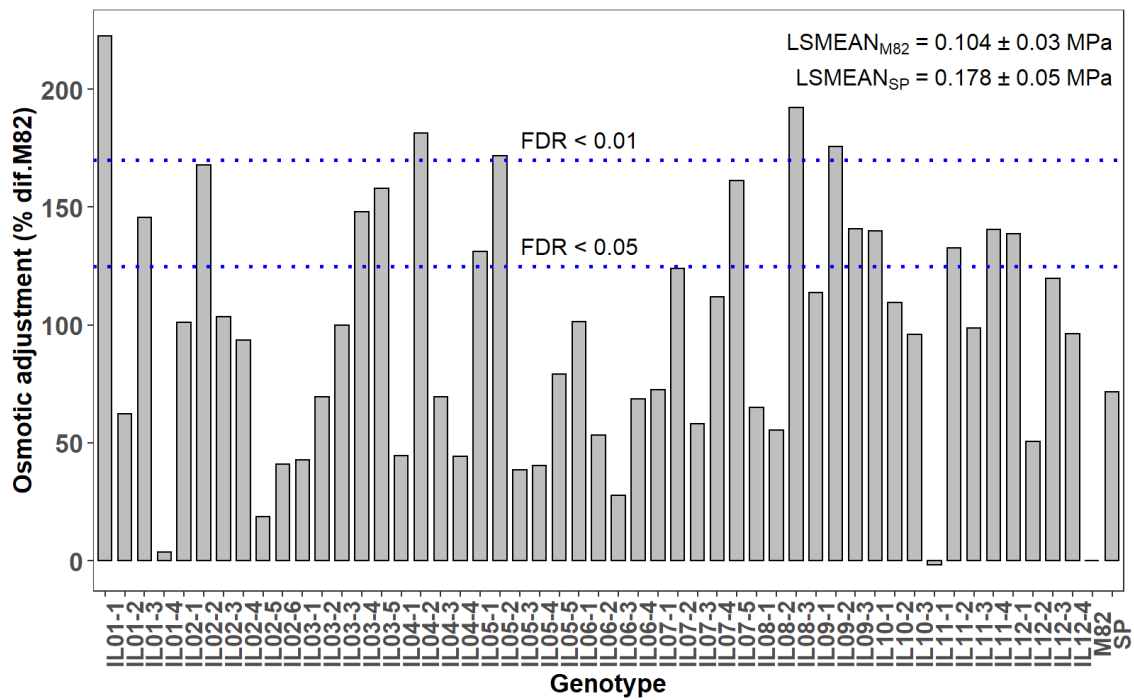
Fig. 2-8. Relative wild allelic effects of ILs compared to recurrent parent M82 for OA. The ILs with the values above the limits (dotted blue lines) are those holding associated chromosome segments mapped according to Dunnett test at FDR < 0.05 and 0.01, respectively. LSMEANS ± SE of parent lines is given at the upper right panel.

Discussion

The study was carried out to better understand the variation of the components of growth and physiological traits relevant for drought responses, to quantify their interrelationship and to detect the underlying genomic regions holding the putative QTLs associated with the growth traits and their phenotypic plasticity (*pX*) by using a complete set of tomato introgression lines.

Phenotypic variation depends on trait class and underlying genetic factors

In this study, the traits relevant for plant adaptation such as LA_t and CT showed the dependence of drought effects or plasticity on genotype **(Table 2-S1)**. The highest plasticity of physiological traits under DS indicates the different sensitivities between functional and structural traits (**Fig. 2-1, S1**). Plasticity of physiological traits is important as physiological responses generally occur short-term, are reversible under mild and medium level stress, and have lower energy costs compared to changes in morphological or dry matter traits (Meier and Leuschner, 2008). Without a significant genetic variation, the highest plasticity of WP implied that leaf water deficit was generally a direct reflection of soil water status, demonstrating the anisohydric behaviour of tomatoes (Sobeih et al., 2004; Jones, 2007). In two-way ANOVA, the plastic variance is the sum of environmental and genotype x environment variance (Scheiner and Lyman, 1989; Brown et al., 2014). Here, plasticity taken as the drought response was found to be a significant source of variation for most phenotypes. Genotypic variation in plasticity of key physiological traits such as transpiration efficiency, specific transpiration, osmotic potential and turgid osmotic potential, and that of osmotic adjustment and drought survival underlined the noticeable attribution of genetic factors **(Table 2-S2, 2)**. CV% has been used as an environmental variance in a range of growth and morphology traits in Arabidopsis, barley, corn, tomato, oak and poplar under favourable and stress conditions (Volis et al., 1998; Valladares et al., 2002; Pliura et al., 2007; Dong et al., 2008; Gaudin et al., 2011; Kooke et al., 2015). CV% was higher in WW than in DS condition for most traits (**Fig. 2-1, S1**). Under DS, most morphological and dry matter traits showed higher CV% than most physiological traits (see also **Table 2-S2**). The reason could be that the performance of morphological and dry matter traits was determined by the multitudes of variations in physiological mechanisms at the lower level, which represented more sources of errors. Differences in heritability indicated that variation of most water relation traits (WP, OP, RWC, OP_{100}, OA) was mostly environmental and that of agronomic traits and

minerals (TN, NN, K) was mainly genetic (**Fig. 2-2**). Under DS, the dependence of variation in some water relation traits such as RWC and OP on genetic factors increased ($H^2 > 0.3$), suggesting the specific genetic control depending on signals of soil water status. The phenotypic plasticity was an index of relative change calculated from the ratio of trait values. Therefore, the heritability of plasticity was lower than that of the traits per se for most components of growth performance.

Cell turgor maintenance through OA hardly improves dry matter productivity

The role of genotypic variation for OP, RWC and OP_{100} in the regulation of growth responses became appreciable under DS (**Fig. 2-3A, B**). Some evidence of sustained growth performances under DS underlined the turgor maintenance through OA (**Fig. 2-3C**). Not all ILs with higher OA led to improved fitness at harvest, suggesting the possible existence of genotypic variability in the plasticity of water relation traits (**Fig. 2-S3B, D**). Statistical analysis using a linear mixed model did not show significant interaction effects for either of OP, RWC or OP_{100} (**Fig. 2-S1B, D; Table 2-S1**). However, the strong relationships among different phenotypes (e.g. OP and dry matter traits) under DS suggests that there could be pleiotropic or tightly linked genetic loci or gene clusters associated with them (Kadam et al., 2017) (**Fig. 2-3B**). Plasticity of physiological traits is a prerequisite for plant adaptation to adverse environments, compared to that of other macro levels traits such as morphological and anatomical traits (Gratani, 2014). In this study, the plasticity of OP, RWC and OP_{100} led to improved OA and adaptive responses of some lines under DS (**Fig. 2-3C**). The magnitude of pOP_{100} was mainly attributed to that of pOP, since pRWC was relatively modest. This can also be seen in the relationships of their trait values under DS (**Fig. 2-3B**). Higher pOP_{100} usually leads to higher OA because OA was calculated as the difference between the absolute values of OP_{100} under WW and DS conditions. Maintenance of RWC at the high range was reported as a tolerant index which can be seen in Sp (**Table 2-S3**). Genotypes of good OA usually have high RWC (Bunce, 1986). Moreover, RWC was reported to be a more stable trait than leaf WP (Sade et al., 2012). We also found no significant line effect on RWC and there was relatively low plasticity of RWC compared to other components of water relation trait (**Fig. 2-S1C**). However, because of some variation of times when taking the plant samples, RWC in this experiment was primarily used to calculate OP_{100}. It was reported for tomatoes that there was a positive correlation between OA and dry matter accumulation (Smith et al., 1989). In our results, we found a slight positive influence of OA on plasticity of dry matter traits (e.g. pDW_{sh}) regardless of genetic variation for trait values (**Fig. 2-S3**). OA

does not always favour yield improvement, possibly because of some costs for the active accumulation of solutes, including compatible organic compounds (Turner and Jones, 1980). For low molecular weight compatible inorganic solutes, such as K, the energy cost of accumulation will be less. However, not all ILs with higher OA showed the superiority to M82 for growth traits (**Fig. 2-8; Table 2-S4**). There were also some lines showing better performances but not significantly higher OA than M82.

Drought adaptation highlights the role of adaptive plasticity

A reduction of leaf expansion (LA_t) is an avoidance strategy which can reduce the plant water consumption, but at the same time reduces canopy photosynthesis. In the present study, the reduction in LA_t was characterized by high negative plasticity (61%). With the decrease of SLA_t, the leaves became thicker and proteins more concentrated on area basis (Marchiori et al., 2017). This response could improve the photosynthesis under a given light condition because a large fraction of leaf proteins is involved in the photosynthetic apparatus (Makino et al., 2003). However, SLA_t was not significantly correlated with dry matter traits, may be because the overall plasticity of SLA_t was relatively small (24%) compared to other growth traits. The morpho-physiological responses of plants to their environment are dependent on the their ability to perceive environmental change (Valladares et al., 2006). It was suggested that the plasticity of some functional traits could benefit plant growth in adverse environmental conditions (Matesanz et al., 2010). In general, the physiological responses, including plasticity, to drought conditions are already known and described in recent papers (Blum, 2017; Egea et al., 2018; Viger et al., 2016; Turner, 2017). For instance, sustained transpiration and assimilation were associated with the OA in the moderate to severe water deficits, and such responses were genotype-dependent. Our study showed that tomato sensitivity to drought in terms of expansive growth and canopy biomass production was affected by the plasticity of the morphological and physiological variables under consideration implicated by varying levels of leaf water deficits. High plasticity of LA_t and ST did not lead to the same intensity of reduction in dry matter traits but less drought effect (**Fig. 2-5**). Differing regression coefficients of pDW_{sh} and pCT upon each unit change of pLA_t indicate that dry matter was produced with less cost of transpiration. The possible mechanisms would be reduced expansion of leaf areas, delayed production of new leaves, or improved transpiration efficiency (TE), as an adaptive strategy for water-saving and/or assimilate allocation. Tomato is believed to have a predominant unisohydric nature, by which the value of WP can be used as a proxy of soil water status. However, the water

relation traits were determined at the endpoint of transpiration. Leaf water potential (WP) at turgor loss point is theoretically -1.5 MPa for most plants. The observed WP values for stressed plants ranged from -1.1 to – 1.95 MPa, with an average of around -1.53 MPa. The high range of WP might indicate some artefacts at the time of measurements. However, it was found that varying levels of WP among lines had a positive covariation with osmotic potential (OP) in both WW and DS (**Fig. 2-3**). Through the active accumulation of compatible solutes (i.e. OA), plants try to maintain the turgor pressure in response to reduction of leaf WP, leading to more reduction (plasticity) of OP (**Fig. 2-3C**). It was also evident that the trait values and plasticity of water productivity of the lines had proper negative relation to that of CT (**Fig. 2-3**). Plasticity of TE can reflect the extent of water-saving strategy while reducing the drought effect on dry matter production (**Fig. 2-3C**). This indicates that drought adaptations of tomato lines included both of water saving and water spending means. Whether or how the same particular line can shift between the strategies was not clear.

Genotypic variation in drought survival links to growth and water relation

Drought survival was characterized by days to reaching the soil water status when stress transpiration was less than 10% of the control (i.e. TR< 0.1) (**Fig. 2-4**). Genotypes with lower magnitude of leaf area and shoot dry weight showed the less reduction of growth traits and the longer survival under drought stress compared to bigger genotypes (**Fig. 2-4A, B**). There could possibly be early drought reaction of adaptive traits such as leaf expansion and transpiration when soil water status was still high, as an avoidance strategy in those of smaller genotypes. This mechanism is plausible because higher specific transpiration and less reduction of total water transpired in genotypes of longer survival (**Fig. 2-4C, D**). Avoidance of cell water deficits resulted in maintenance of high water potential and relative leaf water content (**Fig. 2-4E, F**). However, maintenance of high osmotic potential helped with the turgor maintenance leading to tolerance strategy. Keeping the high turgid osmotic potential (low negative value) was comparable among genotypes and OA was slighly lower in the genotypes of longer survival, indicating the less favour of tolerance strategy (**Fig. 2-4G, H**).

Genetic control on trait values and drought adaptation

Genome regions detection depends on many factors including population size, marker density of the linkage map, the accuracy and precision of phenotypic characterization, environment, and the method and threshold of detection (Godfray et al., 2010). In our study, an IL was considered to harbour a genome region when the trait means for the line showed significant differences as compared to M82. A certain threshold level, for example, 30% or greater, can also be used for identification of major loci (Rousseaux et al., 2005; Frary et al., 2010; Frary et al., 2011). The thresholds allow using mean values directly for mapping. However, the intensities of phenotypic variation and responses are different among traits in plants or replications, which needs to adjust the significance thresholds for good statistical power. We used Dunnett's post hoc test with FDR adjustment method in order to reduce both positive and negative discovery rates. Under WW and across treatments, morphological traits showed the highest proportion of associated chrosome regions holding favourable QTLs while dry matter traits exhibited the highest proportion of QTL mappings under DS condition **(Fig. 2-6)**. QTLs associated with mophological traits such as LA_t and SLA_t were negative while that with stem dry weight were positive. Considerable proportion of chromosome regions was associated with OP, OP_{100}, OA and drought survival **(Fig. 2-7, 8)**. Broad sense heritability data also supported the genome trait association **(Fig. 2-2)**. Chromosome 3 was found to harbour the highest proportion of chromosome regions being associated with 44% of traits studied **(Table 2-S4)**. According to the overlay heat map of genome trait association, plasticity of most water relation and mineral traits revealed the noticeable wild allelic effects **(Fig. 2-S2)**. Knowledge on the overlapping and non-overlapping regions of introgression segments on the same chromosome and the bins responsible for relevant traits can further be used for fine-tuning of QTL detection.

Conclusion

Responses of tomato introgression lines were investigated for some agronomic and water relation traits upon soil drying. Our data indicate that plasticity of morphological traits such as leaf area conferred a compelling advantage for maintaining plant growth under water deficit. When the changes of physiological and agronomic traits were considered for effectiveness in maintaining plant growth, the present data suggested that the drought adaptive plasticity of traits, such as pLA_t and pST can ameliorate the drought effects especially on dry mass production of tomatoes. Genotypes of smaller leaf area maintained the longer survival by

favourably using the avoidance strategy with early reactions of drought relevant processes. The *S. pennellii* introgression lines are an extremely useful tool for QTL analysis and associated regions can be pinpointed without concern for interaction with other introgressions within or between chromosomes. Moreover, the favourable constitutive and adaptive regions for phenotypic values of growth traits, and novel regions for plasticity were identified. This information can bring insight into exploring the sources of genetic and non-genetic variations regarding drought responses and will be supportive for crop improvement programs.

Chapter 3

QTL-based modelling of water use in drought-stressed tomato introgression lines

San Shwe Myint[1,2], Dany Moualeu-Ngangue[1], Hartmut Stützel[1]

[1]*Institute of Horticultural Production Systems, Leibniz Unversität, Hannover, Germany;* [2]*Department of Horticulture, Yezin Agricultural University, Naypyitaw, Myanmar*

Abstract

Drought stress has significant impact on agronomic performance, including yield and produces quality. Exploration of genetic variation for relevant traits and incorporation in crop models are fundamental to identifying trait components relevant for better performance under a given drought scenarios. Using *Solanum pennellii* introgression lines, soil water thresholds for leaf expansion (c_L), stomatal conductance (c_g), specific transpiration (c_ε) and canopy transpiration (c_T) were quantified. QTLs controlling these thresholds and their response parameters to vapour pressure deficit (δe) were identified. We developed and evaluated a QTL-based model for stressed transpiration specific to a prevailing environment by using the parameters of drought reactions. Sixteen QTLs associated with tested traits were detected. Among the thresholds, the c_g showed the highest heritability and c_T the lowest. There was a good correspondence between simulated and observed data for leaf growth and transpiration for vapour pressure deficits (δe) between 1.4 and 2.3 kPa. Usage of both c_L and c_g gave similar predictions as c_T usage alone. The integration of the δe effect did not change the model output much. However, the inclusion of c_g together with δe improved the prediction accuracy compared to usage of c_T alone, taking account of the δe conditions between 1.4 to 2.3 kPa. Model outputs for canopy transpiration using QTL derived and genotype-specific parameters exhibited similar goodness of fit and were highly related to each other. Using the soil water thresholds for leaf expansion and stomatal conductance, the QTL-based model gave a prediction of transpiration with over 80% accuracy, sufficient for integration in the ecophysiological tomato model for further evaluations and model improvement.

Keywords: Thresholds, introgression lines, QTL, vapour pressure deficit, fraction of transpirable soil water, genetic variation, heritability, leaf expansion, transpiration, *Solanum pennellii,* modelling

Introduction

Soil water deficit is a major constraint to crop production with the most significant impact on agronomic performance including yield and produce quality (Denmead and Shaw, 1962; Porporato et al., 2001; Sadras and Milroy, 1996; Stagnari et al., 2016).

Water deficit occurs when there is an insufficient supply of soil water in relation to transpiration demand (Welcker et al., 2011). When soil water content drops below a critical point, plant growth and productivity are significantly reduced (Blum, 1996; Sadras and Milroy, 1996; Ray et al., 2002; Novák, 2009; Streck, 2004; Gholipoor et al., 2012; Ramadas and Govindaraju, 2015; Esmaeilzade-Moridani et al., 2015; Jefferies, 1993b; Ray and Sinclair, 1997). Several regression models have been used to estimate the critical soil moisture thresholds below which plant growth processes decline. These approaches included logistic (Soltani et al., 2000; Toms and Villard, 2015), negative exponential (Sadras and Milroy, 1996; Milroy and Goyne, 1995; Muchow and Sinclair, 1991; Schmidt et al., 2011), quadratic polynomial (Xu et al., 2010; Ma et al., 2018), linear spline (Soltani et al., 2000) and linear regression plateau (LRP) (Nable et al., 1999; Wang et al., 2008; Yan et al., 2010; Wu et al., 2011b; Meir et al., 2015; Masinde et al., 2005; 2006; Casadebaig et al., 2008)) models.

For the assessment of genotypic variation in physiological responses to drought, many authors used LRP models (Ray and Sinclair, 1997; Jefferies, 1993b; Liu and Stützel, 2002; Masinde et al., 2005; 2006; Casadebaig et al., 2008). These models allow the determination of thresholds c_x concerning the fraction of transpirable soil water, W_{ts}. When W_{ts} is lower than c_x, a relative trait starts to decline linearly relative to the well-watered situation. The use of W_{ts} is simple and reflects apparent physiological mechanisms (Sadras and Milroy, 1996), while avoiding complex equations to determining the water transfer in the plant and soil (Tardieu and Davies, 1992; Caldeira et al., 2014; Janott et al., 2011). Parameters of LRP model can be used as genotype specific parameters (GSPs) which describes the variability in drought reaction of a particular plant process (e.g leaf expansion rate) among genotypes. Analysis of quantitative trait loci (QTLs) is widely used to get more insight of gene-trait association and genotype-environment interactions. Provided that QTL based parameters or GSPs are available, incorporation of genetic information in a process-based model will make it possible to predict the performance of multiple genotypes under a defined set of environments and find out the optimum combination of genetic and environmental components for a desirable trait performance. This approach is known as gene-based or genome-based crop modelling.

However, robustness of the parameters of LRP models in a genomic crop model is not well studied.

Plants respond to limiting water availability through a complex series of adaptive changes (Chaves et al., 2002) occurring in all plant organs (Klamkowski and Treder, 2006). Different physiological processes have different sensitivities to soil water deficit (Hsiao, 1973; Hsiao et al., 1976; Andersen et al., 2002; Wu et al., 2011b; Wu et al., 2011a). Plant processes that depend on increases in cell volume are particularly sensitive to water deficits. At the plant level, reduction in leaf expansion is the most sensitive response to water stress (Boyer, 1970; Hsiao et al., 1985; Lecoeur and Sinclair, 1996). It is an adaptive process for more prolonged survival restricting water loss (partly or mainly) through decreased growth of canopy leaf area (Welcker et al., 2011; Jones, 1992; Sinclair and Muchow, 2001). In some crops, leaf expansion is reduced even before a noticeable decrease of leaf water status (Saab and Sharp, 1989; Dodd et al., 2002), attributed to a non-hydraulic signal (mainly ABA) primarily produced in roots even with only small changes in soil water potential (Davies et al., 1994; Davies et al., 1991; Davies et al., 2002). Genotypes with delayed wilting during a soil drying cycle had a large c_x (Devi et al., 2009). However, an allele conferring a high sensitivity of leaf elongation or expansion to water deficit resulted in either a positive or negative effect on yield depending on drought scenario, soil type, and plant management (Welcker et al., 2011). High evaporative demand (mainly air vapour pressure deficit δe) negatively affects the rate of expansive growth in leaves, even in well-watered plants (Shackel et al., 1987; Sadok et al., 2007).

In a drying soil, the soil hydraulic conductivity declines when the volumetric water content decreases, and the rate of root water uptake may not meet the potential rate of shoot water loss, resulting in a decline of stomatal conductance and specific transpiration (Sinclair and Ludlow, 1986). Although stomatal closure is directly sensitive to soil dehydration, even before any significant reduction in leaf mesophyll turgor pressure (Mahajan and Tuteja, 2005), it is considered less responsive to water deficit than tissue expansion (Sadras et al., 1993; Hsiao et al., 1976; Passioura, 1988). Stomata close in response to high vapour pressure deficit. However, the mechanism of δe induced stomatal closure is still unclear, and the debate about the role of ABA in stomatal δe response continues (Merilo et al., 2018).

Sadras and Milroy (1996) showed that the sensitivity of thresholds of stomatal conductance to drought increased under high δe in sunflower. Therefore, it appears necessary to account for

δe when determining the soil water thresholds of stomatal conductance in addition to that of leaf expansion and transpiration under different environments.

Modelling of plant responses to water deficit requires a quantitative understanding of the effects of water deficits on leaf expansion and gas exchange traits (Sadras and Milroy, 1996). By incorporating genetic information such as QTLs into an appropriate ecophysiological model, a better understanding of the genotype x environment interactions can be expected.

Tomato (*Solanum lycopersicum*) is sensitive to drought stress throughout the ontogeny. Water limitation reduces the agronomic performance of field-grown tomatoes. The genetic diversity of wild *Solanum* populations allows the investigation and dissection of drought tolerance components without interference from artificial selection (Easlon and Richards, 2009). The tomato *Solanum pennellii* (LA 0716) introgression population, originally composed of 50 introgression lines (ILs), each carrying just a single defined chromosome segment from the wild species (*S. pennellii*), which replaced homologous regions in *S. lycopersicum* cv. M82 background (Eshed and Zamir, 1995), is a permanent mapping source for QTLs analysis. This library is useful for QTL analysis as any phenotypic difference between an IL and the recurrent M82 is solely brought about by donor parent genes within the introgressed chromosomal segment (Eshed and Zamir, 1995). In several studies, e.g. maize, more than half of the genome is involved in tolerance to water deficit (Tuberosa et al., 2002; Sawkins et al., 2006). Bolger et al. (2014b) described the genome assembly of the lines *S. pennellii and S. lycopersicum* and found over 100 genes from four chromosomes involved in the drought and salt tolerance.

For the optimization of water management and crop improvement, it is necessary to understand the quantitative relationships between traits relevant for drought adaptation and productivity in connection with the prevailing environments as well as their underlying genetic control.

The objectives of this study were

1) to quantify the reaction variability of the drought relevant plant processes to soil water decline,

2) to identify the QTLs for drought reaction parameters and their dependence on δe and

3) to evaluate the applicability of QTL-based model for canopy transpiration under drought stress in place of GSP-based approach.

Materials and Methods

Models for plant transpiration under drought stress using genotype specific parameters

Plant transpiration of a drought-stressed tomato line T_d (kg per plant d^{-1}) was modelled either through soil water limitation of its components leaf area growth and specific transpiration using the genotype specific parameters (GSPs) for drought reactions of relative plant processes (**Fig. 3-1**).
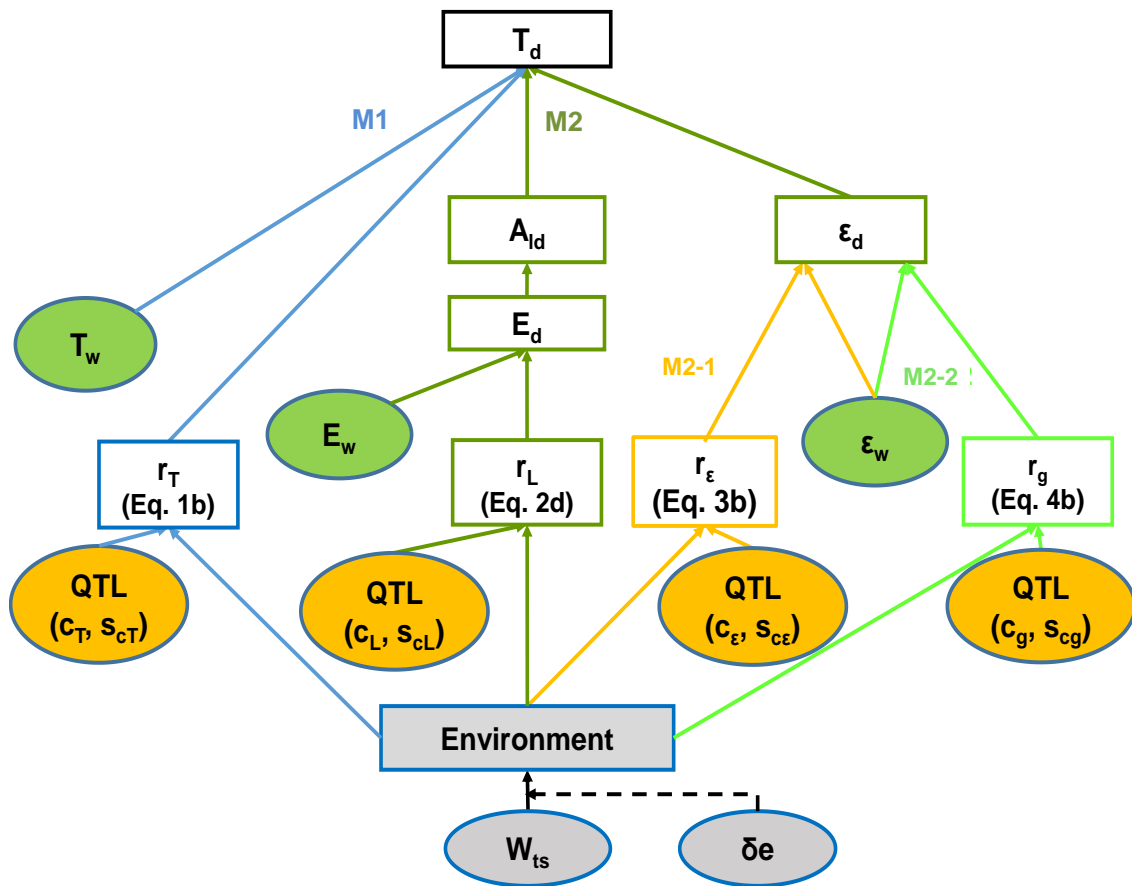
Fig. 3-1. Description of a model for canopy transpiration of tomato introgression lines under drought stress using QTL controlled parameters. Canopy transpiration rate of droughted plants, T_d, was simulated in two modelling approaches: 1) In M1, T_d is the product of the transpiration rate of well-watered plants, T_w and transpiration ratio r_T; 2) In M2, T_d is the product of leaf area A_{ld} and specific transpiration rate ε_d where QTL controlled parameters (orange) for environmental responses are involved. The relative performance of ε_d is controlled either through c_ε (M2-1) or c_g (M2-2). Environmental factors (grey) are declining soil water (W_{ts}) and average daytime vapour pressure deficit (δe). There are three inputs of plant variables (green) T_w, E_w and ε_w measured for unstressed conditions. The intermediate and final outputs (open) include relative traits (r_T, r_L, r_ε, and r_g) and absolute traits (E_d, A_{ld}, ε_d, T_d). The performance of each relative trait under three δe conditions (1.4, 1.9, 2.3 kPa) is controlled via two QTL parameters. The drought stress started at ca. 7th leaf stage and lasted till 9 to 20 days depending on different harvest dates. Abbreviations are described in **Table 3-1**.

Plant transpiration limited by transpiration ratio: model 1 (M1)

T_d is the product of unstressed transpiration T_w (kg per plant d^{-1}) and the transpiration ratio r_T (dimensionless):

$$T_d = T_w \times r_T(W_{ts}, \delta e) \qquad \text{(Eqn 3-1a)}$$

where T_w is an input which takes account of the prevailing environmental factors and r_T is a function of the fraction of transpirable soil water W_{ts} (dimensionless) and average air vapour pressure deficit δe (KPa) controlled with a biphasic relationship (**Fig. 3-S3,S4, S8**):

$$r_T = \begin{cases} s_T \times (W_{ts} - c_T) + 1, & W_{ts} < c_T \\ 1, & W_{ts} \geq c_T \end{cases} \qquad \text{(Eqn 3-1b)}$$

where s_T (dimensionless) and c_T (dimensionless) are intensity of decline and threshold of r_T, respectively. W_{ts} decribes the current soil water status as afraction of the total soil water available for transpiration.

The threshold c_T is assumed to be dependent on the vapour pressure deficit of the atmosphere, δe:

$$c_T = s_{cT} \times \delta e + a_{cT} \qquad \text{(Eqn 3-1c)}$$

where s_{cT} and a_{cT} are parameters of δe response curve of c_T.

Transpiration limited by leaf area and specific transpiration: model 2 (M2)

Alternatively, T_d is defined as the product of plant leaf area A_{ld} (m^2 per plant) and specific transpiration rate ε_d (kg H$_2$O m^{-2} leaf d^{-1}):

$$T_d = A_{ld} \times \varepsilon_d \qquad \text{(Eqn 3-2a)}$$

where A_{ld} is the integral of leaf expansion rate E_d (cm^2 per plant d^{-1}) in the drought treatment for the treatment period between drought imposition t_1 and endpoint t_f when the T_d reaches <10% T_w, plus the initial leaf area $A_{l,0}$ at the onset of drought:

$$A_{ld} = A_{l,0} + \int_{t_1}^{t_f} E_d(t)\, dt \qquad \text{(Eqn 3-2b)}$$

E_d is the product of E_w and r_L:

$$E_d = E_w \times r_L(W_{ts}, \delta e) \tag{Eqn 3-2c}$$

where E_w is leaf expansion rate of unstressed plant, and r_L is a function of W_{ts} and δe, analogous to r_T in Eq. 3-1b-1c:

$$r_L = \begin{cases} s_L \times (W_{ts} - c_L) + 1, & W_{ts} < c_L \\ 1, & W_{ts} \geq c_L \end{cases} \tag{Eqn 3-2d}$$

$$c_L = s_{cL} \times \delta e + a_{cL} \tag{Eqn 3-2e}$$

where r_L, s_L *and* c_L are relative leaf expansion rate, intensity of decline of r_L, and soil water thresholds of r_L; s_{cL} and a_{cL} are slope and intercept of δe response curve of c_L.

Specific transpiration ε_d can be calculated either as the product of specific transpiration rate of unstressed plants, ε_w (kg H_2O m^{-2} d^{-1}) and specific transpiration ratio r_ε (dimensionless) (M2-1), or as the product of ε_w and relative stomatal conductance r_g (dimensionless) (M2-2). Model M2-1 can be written:

$$\varepsilon_d = \varepsilon_w \times r_\varepsilon(W_{ts}, \delta e) \tag{Eqn 3-3a}$$

$$r_\varepsilon = \begin{cases} s_\varepsilon \times (W_{ts} - c_\varepsilon) + 1, & W_{ts} < c_\varepsilon \\ 1, & W_{ts} \geq c_\varepsilon \end{cases} \tag{Eqn 3-3b}$$

$$c_\varepsilon = s_{c\varepsilon} \times \delta e + a_{c\varepsilon} \tag{Eqn 3-3c}$$

where s_ε (dimensionless) and c_ε (dimensionless) are intensity of decline of r_ε and soil water thresholds of r_ε; $s_{c\varepsilon}$ and $a_{c\varepsilon}$ are parameter slope and intercept of the δe response curve of c_ε.

With M2-2, the stress response of stomatal conductance is assumed to be the same as canopy conductance (proxied to daily specific transpiration) in relative terms, and therefore r_ε is replaced by r_g:

$$\varepsilon_d = \varepsilon_w \times r_g(W_{ts}, \delta e) \tag{Eqn 3-4a}$$

$$r_g = \begin{cases} s_g \times (W_{ts} - c_g) + 1, & W_{ts} < c_g \\ 1, & W_{ts} \geq c_g \end{cases} \tag{Eqn 3-4b}$$

$$c_g = s_{cg} \times \delta e + a_{cg} \tag{Eqn 3-4c}$$

where r_g, s_g, and c_g are relative stomatal conductance, intensity of decline of r_g and soil water thresholds of r_g.; s_{cg} and a_{cg} are parameter slope and intercept of δe response curve of c_g.

QTL based stressed transpiration of each introgression line

In QTL based approach, the same models (M1, M2) were integrated with the genetic module on the soil water thresholds, c_x (i.e c_T, c_L, c_ε, c_g) and slope of the δe response curve, s_{cx} of c_x (i.e s_{cT}, s_{cL}, $s_{c\varepsilon}$, c_{cg}) for a given relative trait (i.e r_T, r_L, r_ε, r_g). In the first step, original c_x of those ILs showing significant wild allelic effect were taken unchanged and the rest were replaced with the c_x of recurrent M82. Later, the resulted c_x was subjected to δe dependent as described in GSP based model (Eqn 3-2e, 3-3c, 3-4c) where the parameter slope s_{cx} was computed based on the critical magnitude of wild allelic effect ($|R_{scx}| = 30\%$):

$$c_x = s_{cx} \times \delta e + a_{cx} \qquad \text{(Eqn 3-5a)}$$

$$s_{cx} = \begin{cases} s_{cx,M82} \times (1 + R_{scx}/100), & R_{scx} > 50 \\ s_{cx,M82}, & R_{scx} \le 50 \end{cases} \qquad \text{(Eqn 3-5b)}$$

where s_{cx} and a_{cx} are parameter slope and intercept of the δe response curve of threshold c_x for a given relative trait; $s_{cx,\ M82}$ and R_{scx} are s_{cx} of recurrent line M82 and relative wild allelic effects on a given IL holding QTL for s_{cx}, respectively.

Simulation and model evaluation

We run the simulations using the inputs parameters and variables of the independent Expt. (5), (6) and (7) (May - October 2017) which were generally characterized by the averaged daytime δe of 2.3 (± 0.24), 1.9 (± 0.22) and 1.4 (± 0.07) kPa, respectively. As the dynamic outputs, measured and simulated values of daily leaf expansion rate, leaf area, specific transpiration rate, and plant transpiration rate over the stressed period were drawn in 1:1 line regressions. As the static data, we evaluated the simulated final leaf area and total transpiration. Statistics of the evaluation of model outputs were root mean square error (RMSE), bias, and accuracy (Kahlen and Stützel, 2011; Kobayashi and Salam, 2000).

Plant materials

The tomato genome library of *Solanum pennellii* (Sp) comprising 50 introgression lines (ILs)) in the genetic background of the recurrent parent (*Solanum lycopersicum* cv. M82) was used in this experiment. The seeds were supplied by C.M. Rick Tomato Genetics Resource Center (TGRC), University of California, Davis, USA. Each of the ILs contains a single RFLP

marker defined chromosome segment of Sp. The introgression lines contain an average of 33 cM from a total genome size of 1200 cM (2.75%) with overlapping regions between neighbouring lines, covering the complete wild species genome (Eshed and Zamir, 1995).

Plant cultivation and experimental setup

Pot experiments were conducted in a greenhouse of the Institute for Horticultural Production Systems, Leibniz Universität Hannover (52.5° N, 9.7° E). The 10L plastic pots (25 cm height and 24 cm diameter) were filled with 12 kg loamy sand to 21 cm height with a bulk density of 1.25 g cm^{-3}. The soil had a water content of 28 % (w/w) (35% (v/v)) at full water holding capacity (WHC). The pots were filled with water until ca. 100% of WHC and allowed to drain, and the whole block was covered with plastic sheets to prevent evaporative loss before the onset of the experiment. The experiment was laid out in a RCBD using seven different periods from June 2016 and October 2017, from which the first five trials were used as blocks for parameterization, and the last two for evaluation. Temperature sum (GDD) and air vapour pressure deficits (δe, kPa) were calculated by using temperature and humidity. Mean *δe* for the first five trials ranged from 1.2 to 2.6 kPa and that for the last two trials was 1.4 and 1.9 kPa.

For establishment, eight seeds of each introgression line and 16 seeds of each parent line were sown in separate cells (50 cm^3) of plastic trays using peat-based growing media (>90% organic matter, pH 5.5-6.5, EC 0.7-1.2, bulk density 330-430 kg m^{-3}, Potgrond H, Klasmann-Delimann, Germany). Emergence started in most lines about four days after sowing (DAS). When two true leaves were fully unfolded (153°Cd, ca.10 DAS at 25°C), the four most uniform seedlings were transplanted, two to the 10L main experimental pots, and two to 2L pots to take initial data. During the experimental period, the average daily temperature was 25.0°C (17.0–37.7 °C), and relative humidity in the glasshouse was 63.4% (50.6–87.8%). Fertilizers (Ferty® 2 Special, Planta, GMBH, Germany) were applied with the irrigation water before the drying cycle at a rate corresponding to 160 kg N ha^{-1}, 60 kg P$_2$O$_5$ ha^{-1} and 260 kg K$_2$O ha^{-1}.

During the first 2-3 weeks (until 6–8 leaves emerged) all pots were irrigated daily. At drought stress imposition (7th leaf initiation stage of most lines, ca. 350°Cd), initial data on morphological and dry matter traits were recorded from plants grown in the 2L pots. Then half of the rest of the pots were irrigated daily to replenish the water lost, and the remaining

half were subjected to drought stress by the withholding water until the transpiration rate of the stressed plants reached below 10% of the control. The soil surface was covered to a depth of ca. 4 cm with quartz gravels to minimize soil evaporation. Moreover, to take account of any evaporation, two pots without plants were allocated with similar conditions as treated pots. The pots were moved and rearranged every measurement day to have a random distribution in each set of the greenhouse. When necessary particularly in the morning and evening, we provided the supplementary light (250 W High-Pressure Sodium Lamp (HPS)) to ensure 12 hours of daylight with the required PPFD (average ca. 200 μmol m^2 s^{-1}). Throughout the experiment, the plants were kept single stand by removing the side shoots.

Measurements

The fraction of transpirable soil water and plant transpiration

We performed daily measurements of soil water by taking the pot weight at approximately 16:00 h using an electronic balance (capacity 64 kg $\pm$ 5 g, QS 64B; Sartorius, Göttingen, Germany). The total transpirable soil water W_{tts} was defined as the difference between the soil water content at 100% WHC and the soil water content when the transpiration rate of the stressed plants decreased to < 10% of the control plants. The daily fraction of transpirable soil water W_{ts} was calculated as the ratio between the amount of transpirable soil water remaining in the pot and W_{tts}:

$$W_{ts} = \frac{WT_n - WT_f}{W_{tts}}$$ (Eqn 3-5)

where WT_n is the pot weight (kg per pot) on a given date and WT_f (kg per pot) the final weight of pot when the daily transpiration rate T (kg H$_2$O per plant d^{-1}) of stressed plants decreased to <10% of the well-watered plants (Sinclair and Ludlow, 1986). The difference in weights between two consecutive days was defined as the water lost through plant transpiration.

Leaf growth

From the onset of drought, measurements of maximum leaf length were made every other day on each genotype using a meter rule. All leaves with length > 1 cm from the base of the stem were counted. Measurements of leaf length from the insertion point of the petiole at the stem to the tip of the terminal leaf leaflet were taken on all growing leaves. We stopped the leaf length measurements when there was no more increase in length after two consecutive

measurements. The base temperature for plant growth was estimated to be 7.7 °C by our preliminary test with M82 and used to calculate the thermal time for all lines. For each line, the slope of the linear regression of leaf number plotted against temperature sum (TS) was taken as the leaf appearance rate (leaf °Cd^{-1}). The dynamics leaf length growth over time was estimated by fitting simple logistic functions to measured data points (**Fig. 3-S1**). Based on the phyllochron (°Cd per leaf), TS at the appearance of a given leaf was calculated and used as initial time in logistic fittings. At harvest, all leaf areas were measured destructively using a leaf area meter (LI3100; LICOR, Lincoln, NE, USA).

A genotype specific allometric relationship between leaf length L_i (cm) and leaf area A_i (cm^2) for a given leaf i was developed as:

$$A_i = a_{Ai} L_l{}^g \qquad \text{(Eqn 3-6)}$$

where a_{Ai} and g are empirical parameters. The relation was then transformed into linear functions using natural logarithms of both variables to enhance the linearity of relationships ($r^2 = 0.96$) (**Fig. 3-S2**). The change in whole-plant leaf area A_l (cm^2 per plant) between two consecutive days was taken as a daily leaf expansion rate (E, cm^2 per plant d^{-1}).

Stomatal conductance and specific transpiration

After the imposition of drought stress, stomatal conductance g_s (mmolH$_2$O m^{-2}leaf s^{-1}) was measured daily on one fully expanded upper leaf per plant between 10:00– 13:00 h with a steady-state porometer (LAI-1600, LI-COR Inc., Lincoln, NE, USA). Stomatal conductance was measured in the first four trials. Canopy specific transpiration ε (kg H$_2$O m^{-2} leaf d^{-1}) was calculated as T divided by A_l.

Relative performances under drought stress

For quantifying the performance of E and g_s under drought stress, relative leaf expansion rate r_L and relative stomatal conductance r_g were calculated as the ratio between stressed and controlled values. For T, the transpiration ratio was firstly calculated as the daily transpiration of stressed plants relative to the average transpiration of well-watered plants. Secondly, the daily transpiration ratio of each pot was divided by a mean transpiration ratio calculated for the period when soil moisture was high ($W_{ts} > 0.55$), giving a daily normalized transpiration ratio r_T (Masinde et al., 2006; Ray and Sinclair, 1998). A similar procedure was used to calculate specific transpiration ratio r_ε.

Harvest data on agronomic performance and drought reaction

Agronomic performance was quantified on final canopy leaf area A_l (cm^2 per plant), shoot dry weight W_{sh} (g per plant) and leaf dry weight W_{le} (g per plant). Plant specific leaf area (cm^2 g^{-1}) was calculated as the A_l divided by W_{le}. Transpiration efficiency (g kg^{-1}) was determined as W_{sh} (g per plant) produced divided by total water transired T_t (kg per plant). Osmotic adjustment OA (MPa) was calculated as described in Masinde et al. (2006).

Parameterization

Soil water thresholds and intensities of decline for GSP based model

For each of the measured relative traits (r_L, r_g, r_T, r_ε), parameters of the drought response curves were determined as a function of W_{ts} by using linear-plateau regression models in the nonlinear function PROC NLIN of SAS (SAS Institute Inc., Cary, NC, USA):

$$r_x = \begin{cases} s_x \cdot (W_{ts} - c_x) + 1, & W_{ts} < c_x \\ 1, & W_{ts} \geq c_x \end{cases} \qquad \text{(Eqn 3-7)}$$

where r_x is the magnitude of the relative trait in question, s_x the slope or drought stress intensity of decline, and c_x the soil water threshold at which the relative trait began to decline.

QTL for thresholds and intensity of decline

For the response parameters of each relative trait, one-way ANOVA was performed using a linear mixed model in R-3.6.0 (R Foundation for Statistical Computing, Vienna, Austria):

$$x_{jk} = \mu + \alpha_j + \beta_k + e_{jk} \qquad \text{(Eqn 3-8)}$$

where x_{jk} is the measured value of the jth line in the kth block, μ the overall mean, α_j the effect of jth line, β_k the effect of the kth block, e_{jk} a random error. The line was defined as a fixed factor and block as a random factor. When the ANOVA revealed a significant main effect, a two-sided Dunnett test for comparisons between each of the lines and the recurrent parent M82 was performed (Dunnett, 1955). According to Eshed and Zamir (1995), the minimum number of significant QTL affecting the trait was estimated based on three assumptions: 1) each IL affecting the trait carries only a single QTL, 2) two overlapping introgressions with a significant effect on the trait (in the same direction relative to the control) carry the same QTL

and 3) a QTL is counted only if the IL is significantly different from the control M82 at p< 0.05 (Schmalenbach et al., 2009).

For broad-sense heritability (H^2), variances components were first calculated using *mmer* (mixed model equations in R) function of the *sommer* package in R. Both of the genotype and block (replication) were assigned as random variables and covariance of residuals error variances:

$$H^2 = \frac{\sigma_g^2}{\sigma_g^2 + \sigma_\varepsilon^2/r}$$

(Eqn 3-9)

where σ_g^2 is the genotypic variance, σ_ε^2 the residual variance, r the number of replications (n=5) (Holland et al., 2010).

The relative QTL effect R_c on the threshold of any relative trait c_x was quantified as the relative difference of the least squared mean of a given introgression line from that of recurrent M82 according to Naz et al. (2014) as follow:

$$R_c = \frac{c_{x,j} - c_{x,M82}}{c_{x,M82}} \times 100$$

(Eqn 3-10)

where R_c is the relative QTL effect on threshold, $c_{x,j}$ the least squared means of the threshold of jth line and $c_{x,\,M82}$ that of the recurrent parent M82.

QTL for parameter slope of vapour pressure deficit response curve

The first four trials used in parameterization were characterized by arrays of daytime vapour pressure deficit δe, averaged over the stressed period, ranging from 1.2 to 2.62 kPa.

For each relative trait, the line-specific response of c_x to the δe was determined by linear regression:

$$c_x (\delta e) = s_{cx}\delta e + a_{cx},$$

(Eqn 3-11a)

where s_{cx} and $a_{cx,}$ are the slope and intercept of the δe response curve for c_x.

The intercept a_{cx} was defined as a function of s_{cx} across lines:

$$a_{cx} = d_{a \times} s_{cx} + e_{ax}, \tag{Eqn 3-11b}$$

where d_{ax} and e_{ax} are regression constants **(Fig. 3-S9)**.

The IL showing the coefficient of determination greater than 0.10 was assumed to be δe-responsive for a given c_x and the slope of the response curve s_{cx}, was taken as a genotypic coefficient.

Since each IL yielded only one slope (i.e one data point for each δe condition), the Dunnett's test was not applicable for QTL detection. Therefore, the IL with 50% relative change of s_{cx}, (i.e R_{sc}= 50 or -50) from the control line M82 were holding a putative QTL associated with the parameter.

Relative QTL effect R_{sc} for parameter slope s_{cx} was computed similarly to that mentioned in Eqn. (3-11a) for c_x.

$$R_{sc} = \frac{s_{c,j} - s_{c,M82}}{s_{c,M82}} \times 100. \tag{Eqn 3-12}$$

Parameter relationships and distribution

Pearson correlation coefficients (r) were computed by using trait mean values in R using the *corrplot* package. The p-values of the correlation coefficients were calculated by two-sided Student's t-test using the function of the *agricolae* package.

As heritability of s_x was generally low for most of the relative traits (**Fig. 3-4**), s_x was determined as a function of c_x:

$$s_x = a_s c_x{}^h, \tag{Eqn 3-13}$$

where, a_s and h are the regression parameters (**Fig. 3-S7**).

Shapiro-wilk normality test and regression analysis were done in SIGMAPLOT 11.0 (Systat Software Inc., San Jose, CA, USA). The distribution of the c_x and s_{cx} were described by using JMP Pro 13 (**Fig. 3-2, 3**).

Table 3-1. Variables and parameters used in the model and elsewhere

Description	Symbol	Unit
Broad-sense heritability	H^2	-
Cumulative transpiration	CT	kg H_2O per plant
Drought duration	D	Days
Daytime air vapour pressure deficit	δe	kPa
Drought-stressed condition	X_d	-
Intensity of decline in relative traits	$s_T, s_\epsilon, s_g, s_L$	-
Shoot dry weight	DW_{sh}	g per plant
Leaf dry weight	DW_{le}	g per plant
Fraction of transpirable soil water	W_{ts}	-
Leaf expansion rate	E	cm^2 per plant d^{-1}
Linear regression plateau	LRP	-
Normalized specific transpiration ratio	r_ϵ	-
Normalized transpiration ratio	r_T	-
Osmotic adjustment	OA	MPa
Plant leaf area	A_l	cm^2 per plant
Plant transpiration rate	T	kg H_2O per plant d^{-1}
Parameter intercepts of δe response curve of soil water thresholds	$a_{cT}, a_{c\epsilon}, a_{cg}, a_{cL}$	-
Parameter slopes of δe response curve of soil water thresholds	$s_{cT}, s_{c\epsilon}, s_{cg}, s_{cL}$	-
Relative allelic effect	R	%
Relative leaf expansion rate	r_L	-
Relative stomatal conductance	r_g	-
Plant specific leaf area	SLA_t	cm^2 g^{-1}
Specific transpiration rate	ϵ	kg H_2O m^{-2} leaf d^{-1}
Total plant leaf area	LA_t	cm^2 per plant
Transpiration efficiency	TE	g DW kg^{-1} H_2O
Soil water thresholds of LRP model	$c_T, c_\epsilon, c_g, c_L$	-
Stomatal conductance	g_s	mmol H_2O m^{-2} leaf s^{-1}
Well-watered condition	X_w	-

Results

Variation in soil water thresholds and their responses to vapour pressure deficit

The grand mean of the soil water threshold for leaf expansion rate, c_L, was higher than mean stomatal conductance, c_g, canopy transpiration, c_T, and specific transpiration, c_ε (**Fig. 3-2**). The average threshold values of the whole genome library revealed a similarity to the recurrent parent M82 and a moderate relative difference (5 to 27%) to the donor parent *Solanum pennellii* (Sp). The Sp parent was characterized by earlier drought responses than M82 for most plant processes except leaf expansion rate. Specific transpiration c_ε showed the highest coefficient of variation, followed by c_T, c_g, and c_L. Between-line variation (distribution of mean values) was largest in c_g (0.35 - 0.7) and smallest in c_T (0.41 - 0.60), where 50% (in terms of number of IL) of the whole genome library showed threshold values within the ranges of 0.45 - 0.57 and 0.47 - 0.52, respectively.

Similarly to soil water thresholds, the slope parameter s_{cg} of the response curves of c_g to δe revealed the widest distribution (-0.20 to 0.26) and s_{cT} of c_T the narrowest (-0.35 to -0.06) (**Fig. 3-3**). Most lines (51- 96%) exhibited the coefficients of determination (r^2) > 0.15. Parameters s_{cL} and s_{cg} revealed both positive and negative response directions while s_{cT} and $s_{c\varepsilon}$ were only the negative. In comparison to M82, the wild type Sp showed the higher sensitivity of c_L and c_ε, and lower sensitivity of c_T and c_ε to δe.

The thresholds c_g determined for parent lines M82 and Sp were larger under high than under low vapour pressure deficit (**Fig. 3-S3, S4**). In both lines, thresholds of the other traits (c_L, c_T, c_ε) were somewhat larger than c_g particularly under low vapour pressure deficit. Under high vapour pressure deficit condition, Sp showed higher drought sensitivities (higher c_x) for all the traits than M82.
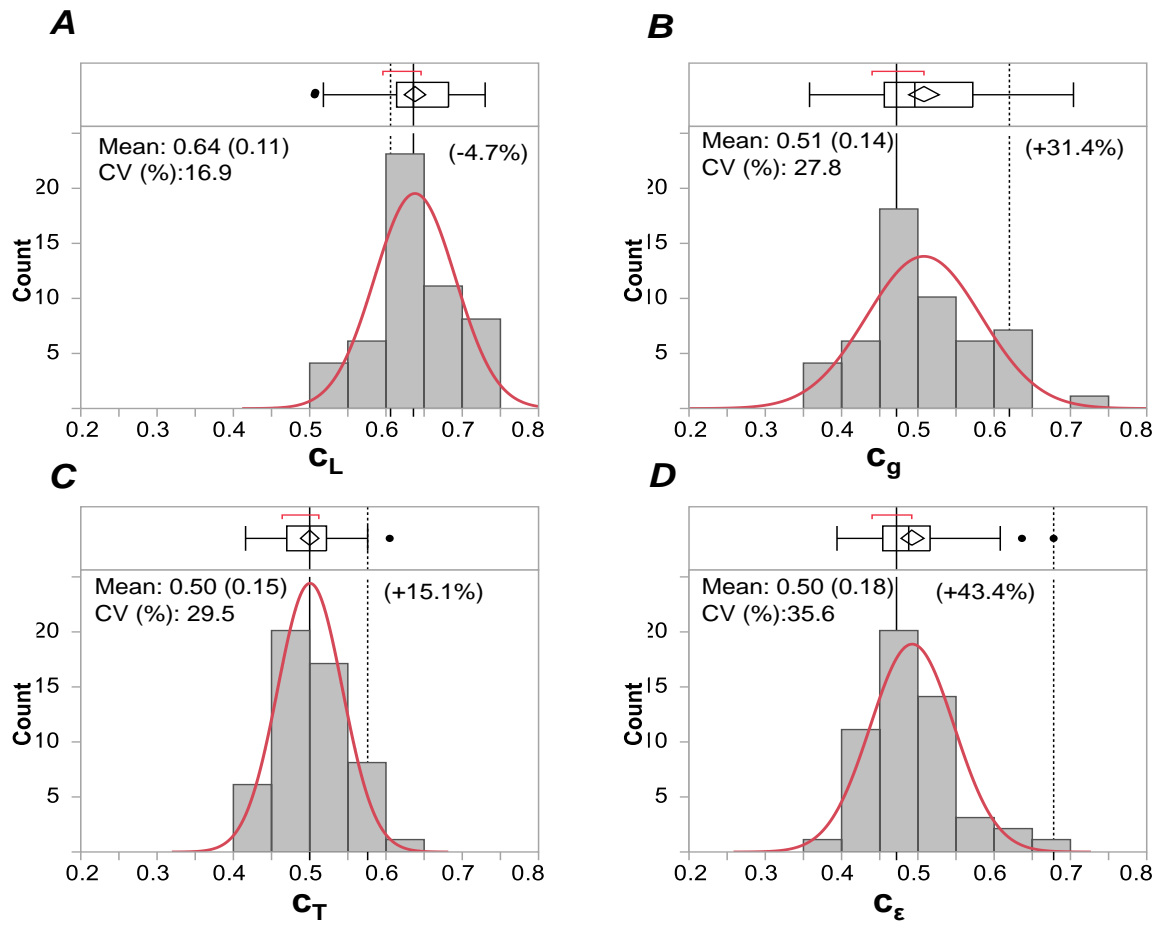
Fig. 3-2. Distribution of soil water thresholds: (A) c_L, (B) c_g, (C) c_T, and (D) c_ε of tomato lines estimated by using a linear plateau model (n = 52). Boxplots indicate a summary of the phenotypic variation. Solid and dashed vertical lines are the thresholds of parent lines M82 and Sp, respectively. The relative differences of Sp (% M82) are described in parentheses. Mean (SD) and CV (%) are calculated from the whole dataset (n=216). Red curves, normal distribution; red brackets, 95% confidence interval.
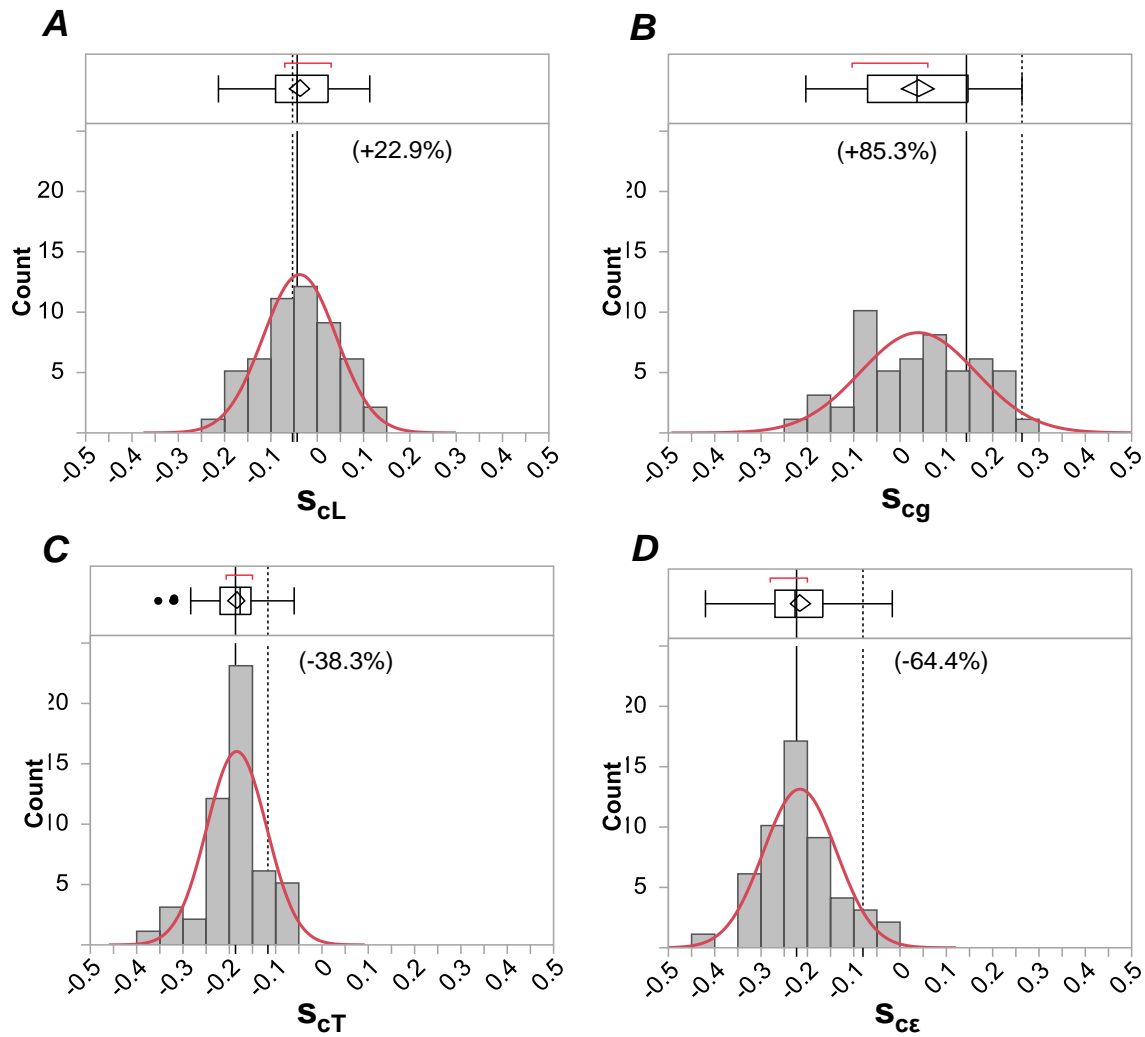
Fig. 3-3. Distribution of the slope parameters of δe response curves for soil water thresholds: (A) s_{cL}, (B) s_{cg}, (C) $s_{cT,}$ and (D) $s_{c\varepsilon}$ of tomato lines estimated by linear regression. Boxplot with whisker plot is described at the top. Solid and dashed lines describe the slopes of parent lines M82 and Sp, respectively. The relative difference of Sp (%M82) is described in parentheses. Lines distributed in negative and positive regions indicate the directions of responses to prevailing δe conditions. n= 52, red curves, normal distribution; red brackets, 95% confidence interval.

Trait relationships and the contribution of genetic factors for thresholds

For all traits studied, regressions between s_x and c_x were almost linear for r_g while the rate of change in s_x was increased by the powers of 1.297 to 1.412 for each unit change of c_x in other traits (**Fig. 3-S7**).

The threshold c_g was positively correlated with all the other thresholds (**Fig. 3-S6**). The c_T showed stronger correlation with c_ε than with c_L. However, there was no significant correlation between c_L and c_ε. Among slopes of the response curves to soil moisture, only the correlation between s_ε and s_T (r = 0.66) was significant. The s_g showed a good correlation with all other thresholds while s_L showed a correlation only with c_g (r = -0.32). Correlations of s_ε with c_g (r = -0.25) and with c_T (r = -0.62) were significant, but there was no correlation between s_ε and c_L. There was a negative correlation between thresholds and most agronomic traits. OA showed a positive correlation with the total water transpired (T_t), and thresholds of stomatal conductance and leaf expansion rate were positively correlated with the duration of the stress phase D (i.e. the time to reaching transpiration ratio <0.1).

The proportion of phenotypic variation due to the genetic values (H^2) of tested relative traits was generally higher for thresholds c_x ($H^2 = 0.09 - 0.39$) than for intensities of decline s_x ($H^2 = 0.04 - 0.27$) (**Fig. 3-4**). H^2 of c_g was the highest (0.39), which was followed by c_ε (0.29), c_L (0.26), and c_T (0.09). The c_T was largely environmental, and s_T showed higher heritability than c_T ($H^2 = 0.09$ vs 0.21).
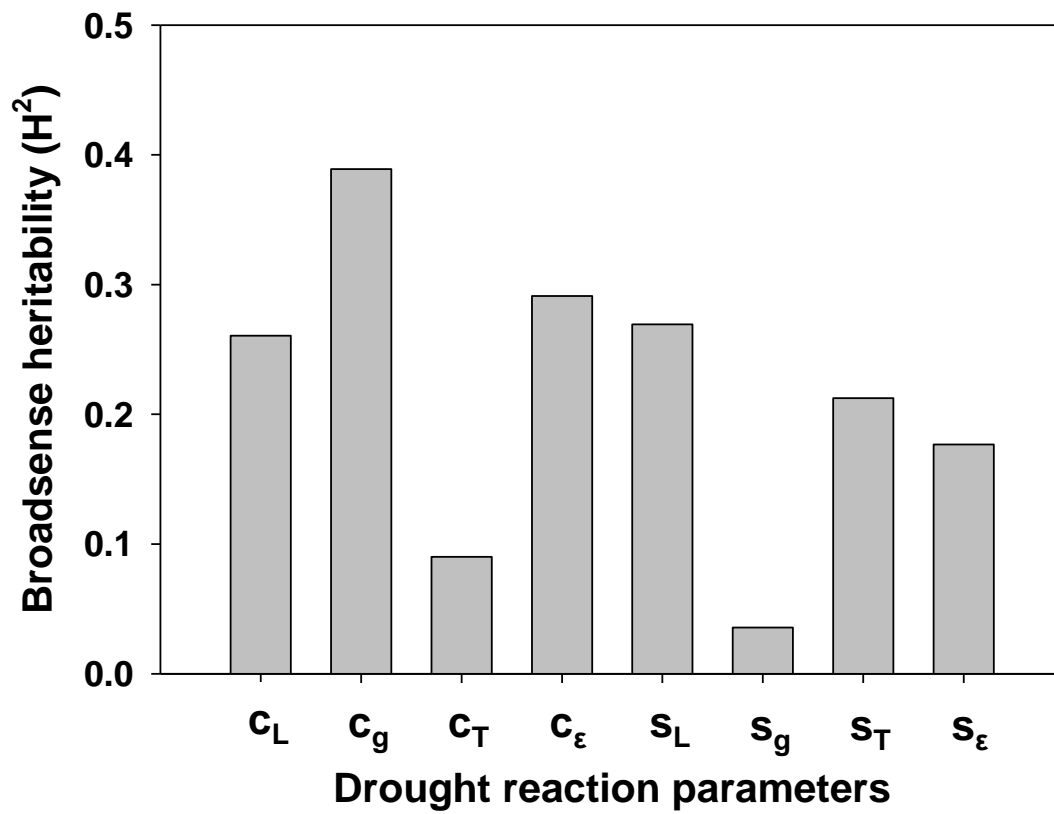
Fig. 3-4. Broad-sense heritability of W_{ts} thresholds and intensities of decline for r_L, r_g, r_T and r_ε.

QTL-trait associations for drought response parameters

For eight parameters of plant processes, there 16 regions were identified holding putative QTLs ($p < 0.05$, **Table 3-2, Fig. 3-5A**). Taking account of overlapping and non-overlapping regions, the bin of detected QTLs spanned around 7 to 55 cM. Among them, 31.3% (5 regions) exhibited decreased QTL effects (R) compared to recurrent M82, particularly for s_g (6.3%) and c_L (25%), and 68.7% (11 regions) of the genome library showed an increased effect. The majority of detections (62.5%) were mapped for soil water thresholds with R ranges of 17.3 - 48.7% regardless of increased or decreased allelic stage. The threshhold for leaf expansion, c_L, was associated with four regions from Chromosome 5, 7, 8 and 9 with similar QTL effects (R = 17.3 – 20.5%). Out of them, three regions (IL5-2, 8-3, 9-3) showed QTL co-localizations for s_L. Among the QTLs associated with c_g, two QTLs (IL4-3, 7-3) were co-localized with c_T and s_g. Seven ILs showed no QTL-co-localization. Since the s_x for the most traits were generally environmental and correlated well with c_x, only the R for c_x are depicted in **Fig. 3-5A**. The c_g showed the varying contribution in both directions on the genome-wide scale. A considerable number of Sp chromosome regions revealed major QTL effects for c_L. QTL co-localization was fairly well reflected by the results of the correlations (**Fig. 3-S6**). Pooling all studied traits, the heritability could explain 36% of the QTL abundance (**Fig. 3-S10**).

QTL effect on the slope of δe response curves of thresholds

An overlay heat map of the line- trait associations for parameter slopes of δe response curves of thresholds is depicted in **Fig. 3-5B**. Relative QTL effects (%M82) were mostly for s_{cT} and $s_{c\varepsilon}$, but in both positive and negative for s_{cL} and s_{cg}. For four relative traits, ILs showing the slopes greater than or equal to 50% relative difference (increase or decrease) accounted for 44.5% of the total chromosome regions with the most abundance regions for s_{cL} (19%, 18 increase, and 20 decrease), followed by s_{cg} (17.5%, 4 increase, and 31 decrease), s_{cT} (4.5%, 3 increase, and 4 decrease) and $s_{c\varepsilon}$ (3.5%, 2 increase, and 5 decrease).

Table 3-2. Line - trait associations for soil water thresholds c_x and intensities of decline s_x of introgression lines evaluated by Dunnett's post hoc test at $p < 0.05$. R indicates the increased (+) and decreased (-) relative QTL effect (%M82), Dif., absolute difference and Chr., chromosome. Symbols of traits are described in **Table 3-1**.

Trait	IL	Chr.	Bin (cM)	Lsmeans	Dif.	R	P-value
c_L	IL05-2	5S	21-62	0.51	-0.13	-20.33	0.01960
	IL07-5	7S	2-9	0.52	-0.12	-18.70	0.03170
	IL08-3	8S	67-87	0.51	-0.13	-20.48	0.01870
	IL09-3	9S	61-116	0.53	-0.11	-17.29	0.04710
c_g	IL04-3	4S	68-101	0.64	0.17	36.23	0.01932
	IL07-3	7S	43-64	0.70	0.23	48.73	0.00165
	IL12-4	12S	102-120	0.63	0.16	32.64	0.03508
c_T	IL04-3	4S	68-101	0.60	0.10	20.86	0.04750
c_ε	IL01-4	1S	140-165	0.64	0.17	34.59	0.01248
	IL08-1	8S	0-25	0.61	0.14	28.58	0.03899
s_L	IL05-2	5S	21-62	2.19	0.72	49.08	0.00082
	IL08-3	8S	67-87	2.08	0.61	41.74	0.00444
	IL09-3	9S	61-116	2.00	0.53	36.03	0.01406
s_g	IL07-3	7S	43-64	1.28	-0.84	-39.35	0.02770
s_T	IL01-3	1S	92-127	3.01	0.74	32.62	0.04855
	IL03-2	3S	32-71	3.56	1.29	56.87	0.00058
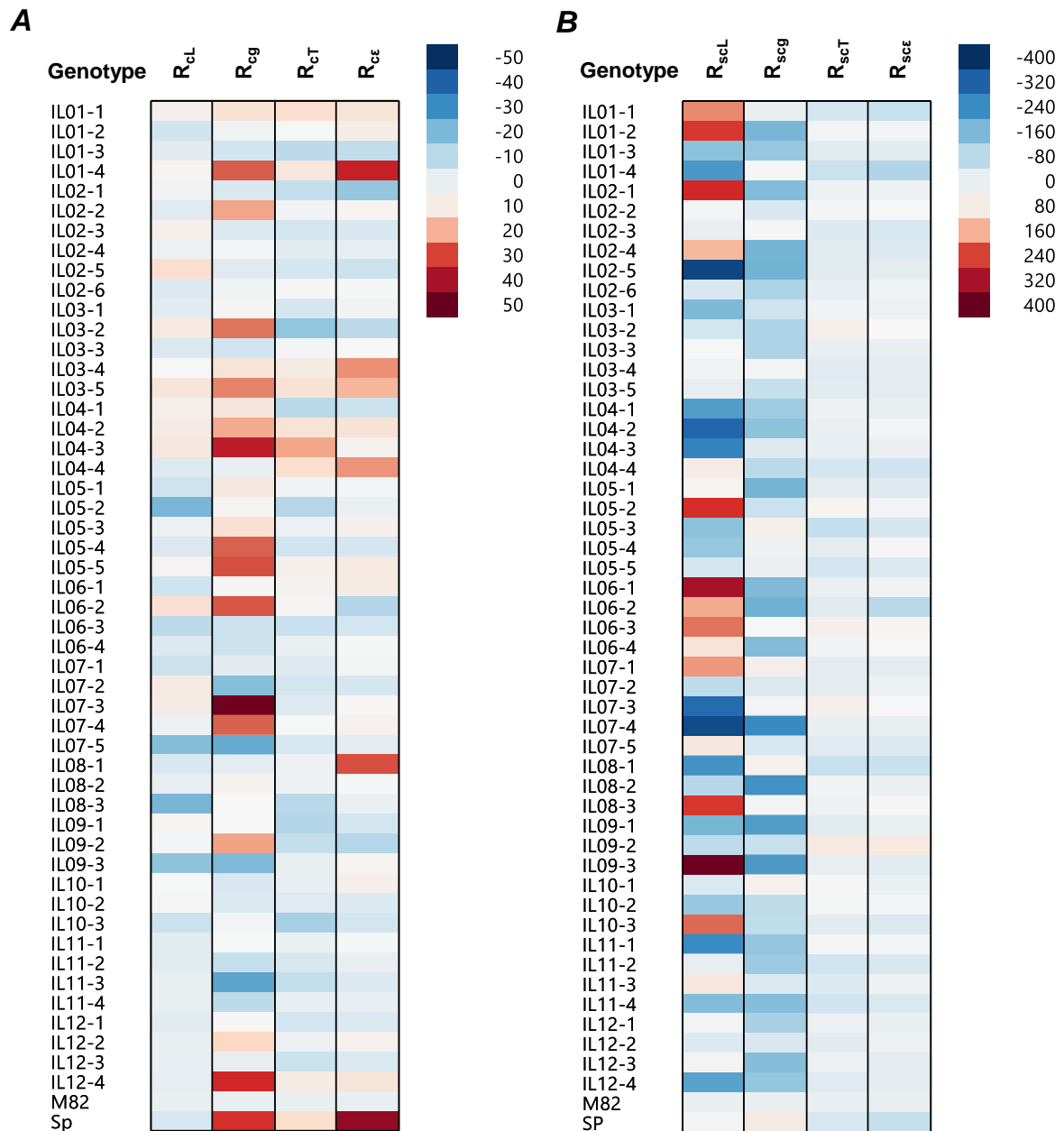
Fig. 3-5. Overlay heat maps of relative QTL effects on (A) soil water thresholds (R_{cL}, R_{cg}, R_{cT}, $R_{c\varepsilon}$) and (B) parameter slopes of δe response curves of thresholds (R_{scL}, R_{scg}, R_{scT}, $R_{sc\varepsilon}$) described as % dif. M82. Regions of red or blue indicate the allelic states (relative increase (+) or decrease (-)) of trait values after introgression of *Solanum pennellii* chromosome segments. Pale regions indicate that IL had no appreciable difference from M82 (normalized to zero). The ILs are presented in chromosomal order (from top of chromosome 1 to base of chromosome 12) from top to bottom.

Specific transpiration and leaf area growth of stressed tomatoes lines

Fig. 3-6A-B shows the specific transpiration ε_d during the stressed period which used c_g (M2-2) as the soil water threshold. Simulations were performed with or without the consideration of δe effects. The ε_d was predicted well across three independent environments. A goodness of fit for ε_d was high ($R^2 = 0.72$-0.74) in both conditions with or without the use of s_{cg}. With s_{cg} as input, the prediction did not show improvement. Regardless of the parameter s_{cg}, the results showed a good fit under 1.4 and 1.9 kPa δe conditions with the slopes close to 1 and intercepts close to zero. The final leaf area A_{ld} showed higher values with lower δe conditions, and was predicted with the R^2 values of 0.37 to 0.73 (**Fig. 3-6C-D**). Again the model better predicted the leaf area under 1.4 and 1.9 kPa δe conditions. With the input of δe effect, there was slight improvement in fittings especially for 2.3 kPa δe condition. Under 1.9 kPa δe condition, the simulation performed better than that in low or high δe conditions in terms of slopes and intercepts. The leaf expansion rate E_d over the stressed period (**Fig. 3-S11A, B)** showed high goodness of fit between simulated and observed values across environments ($R^2 = 0.5$-0.8), with the best correspondance under 1.4 kPa δe condition. With the parameter s_{cL}, the fitting became improved for both 1.4 and 2.3 kPa δe conditions. Under a high δe condition, the model showed a systematic deviation from the 1:1 line to both low and high directions. Prediction of leaf areas at different time points A_d showed a good fitting for different δe environments (**Fig. 3-S11C, D)**, regardless of the consideration of the δe effect on c_L.
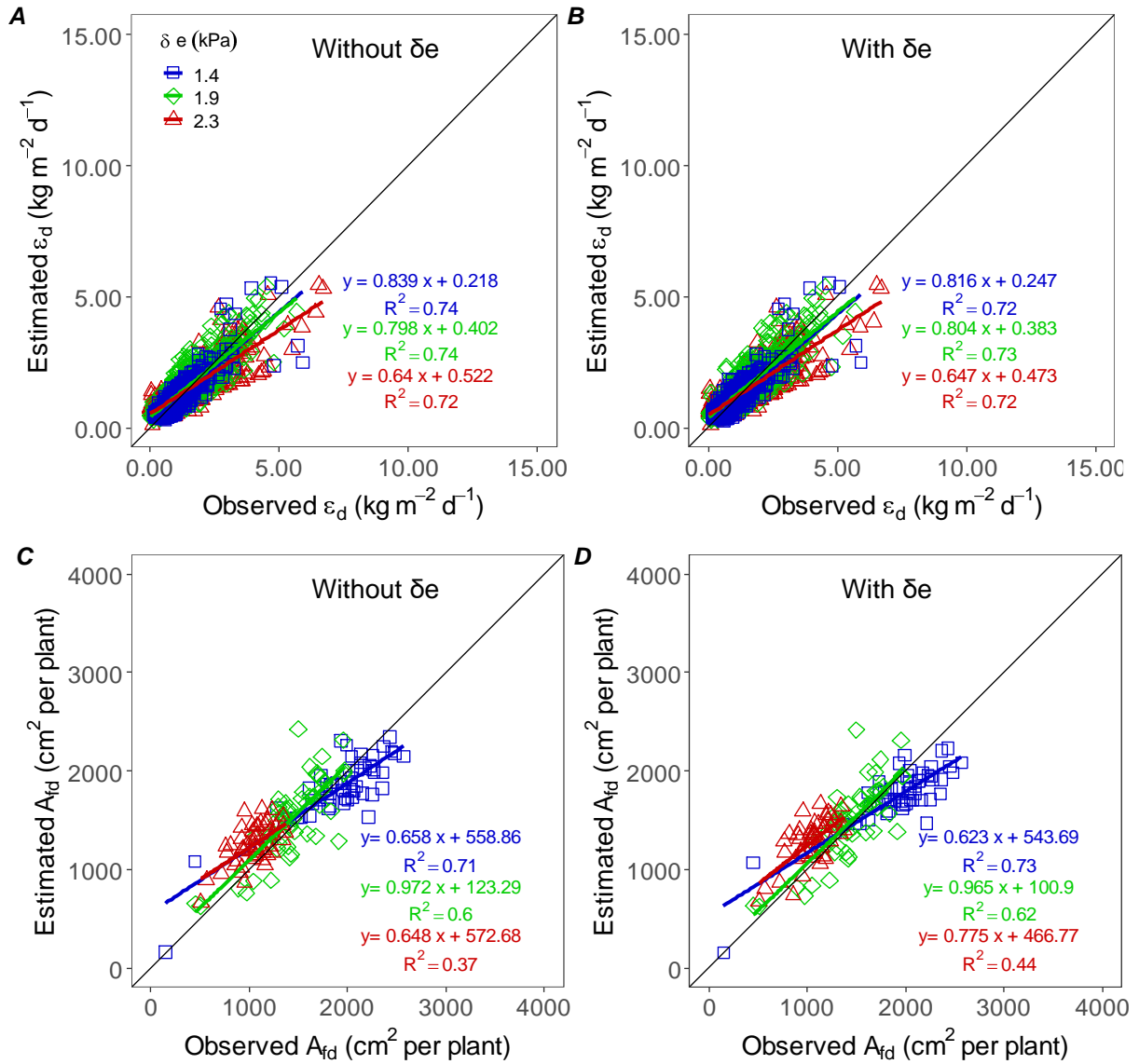
Fig. 3-6. Simulated versus observed (A, B) specific transpiration ε_d and (C, D) final leaf area (A_{fd}) of stressed tomato lines under three vapour pressure deficits δe conditions using QTL derived parameters without or with consideration of δe response functions, respectively. The ε_d is determined using the soil water thresholds of stomatal conductance c_g (M2-2). A_{fd} is the sum of the initial A_{ld} and integral of E_d (dA_{ld}/dt) for the drying period. The E_d and A_{ld} during the stress period are described in **Fig. 3-S11**.

Plant transpiration under drought stress condition

Using the QTL-based parameters in the M2-2 approach (c_L, c_g, s_{cL}, s_{cg}), canopy transpiration T_d along the stress period showed a good correspondance across environments (R^2 =0.5-0.64,) (**Fig. 3-7A, B**). Throughout the stress period, the model predicted the T_d better for 1.4 and 1.9 kPa conditions in terms of slopes. Under 2.3 kPa, there were over- and under-estimations for low and high values of T_d, which made a justification of total transpiration T_{td} as can be seen in **Fig. 3-7C, D**. With δe effects, the prediction showed improvement for 1.9 and 2.3 kPa δe conditions. Across experiments, the prediction could be improved through the addition of the s_{cL} and s_{cg} describing the δe response functions of c_L and c_g. A goodness of fit between simulated and observed values of T_{td} was observed under 1.9 kPa δe condition (R^2 = 0.61-0.63). With consideration of δe, T_{td} prediction was improved under 2.3 kPa δe condition. Simulations with M1 and M2-1 approaches resulted in transpiration T_d with more or less similar prediction powers as M2-2, especially for the values of T_d (**Fig. 3-S12**). Compared with M2-2, predictions of total transpiration T_{td} in both M1 and M2-1 approaches gave a lower fitting with larger magnitudes of errors especially when s_{cx} was incorporated in the model.

Since the model parameters of soil water thresholds and their slopes of δe response curves were generated from individual lines, the genome-wide prediction was performed primarily by using them as genotype-specific parameters (GSPs) in our crop model. The predictions using GSPs and QTL-based models are compared in terms of evaluation criteria (**Table 3-S1**). Simulations and evaluation with the use of outputs from QTL-based model in comparison to that of GSP based ones gave similar levels of predictability for T_{td}. The high level of aggrement was observed for T_d upon 2.3 kPa δe condition. With the consideration of δe effect on thresholds, T_{td} prediction turned out to improve for 1.9 and 2.3 kPa of δe conditions. In both ways, the use of s_{cL} and s_{cg} improved the model outputs in terms of the most evaluation criteria. Comparison between QTL- and GSP-based approaches for predicted transpiration values showed that both daily canopy transpiration and total transpiration showed more agreement with the consideration of δe responses of soil water thresholds (**Fig. 3-8**, **S13),** regardless of the modelling approaches used. Predicted total transpiration showed the high coefficient of determination in regression between GSP- and QTL-based approaches. Either using GSPs or QTL-based approaches, the model predictions could fit well with the observed variations.
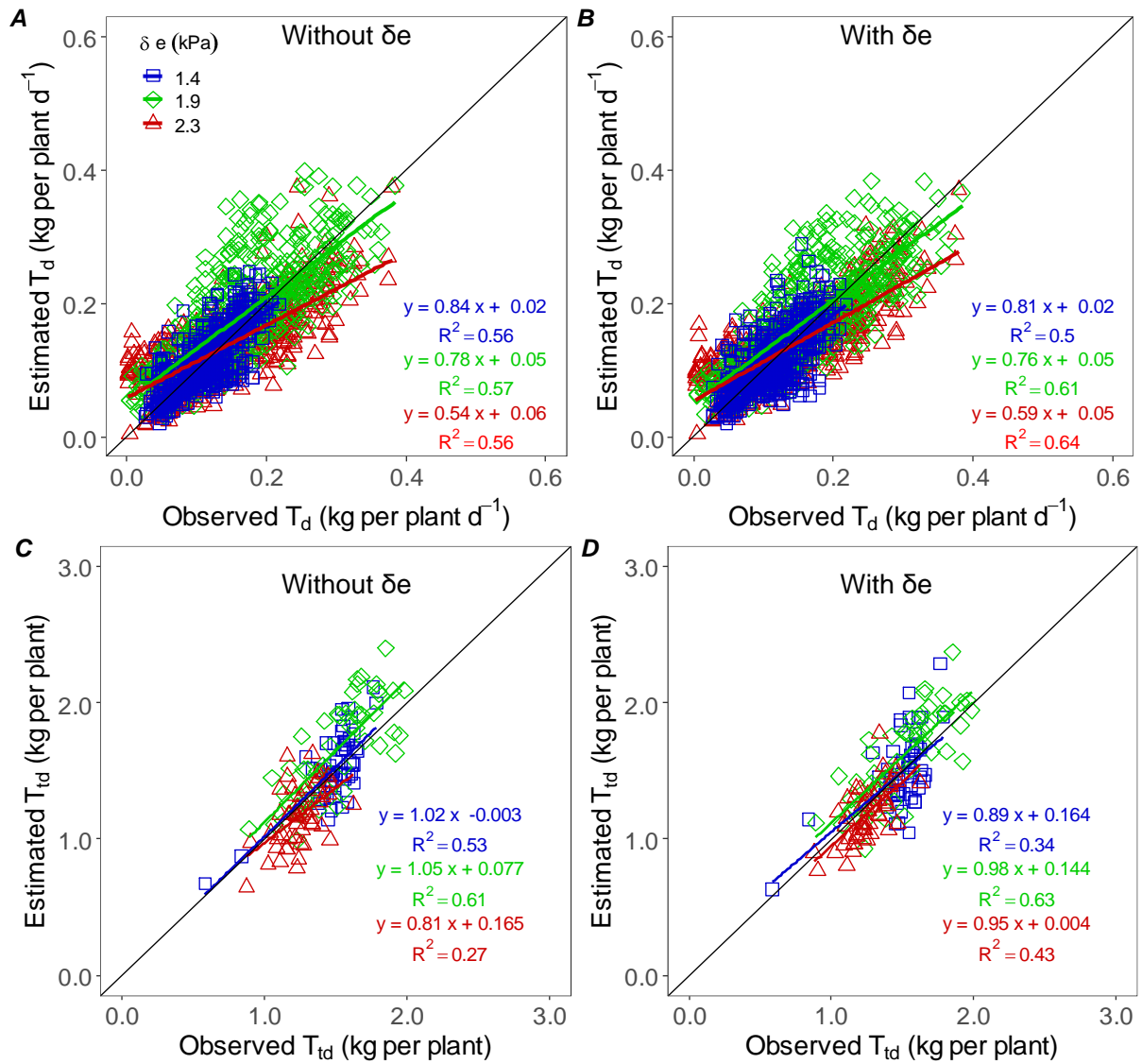
Fig. 3-7. Estimated versus observed transpiration (T_d) (A, B) and total transpiration (T_{td}) (C, D) of drought-stressed tomato lines under three *δe* conditions. The model uses QTL-derived parameters without or with consideration of *δe* response functions, respectively. T_d is determined by using c_L and c_g (M2-2). Outputs of M1 and M2-1 approaches for T_d are shown in **Fig. 3-S12**.
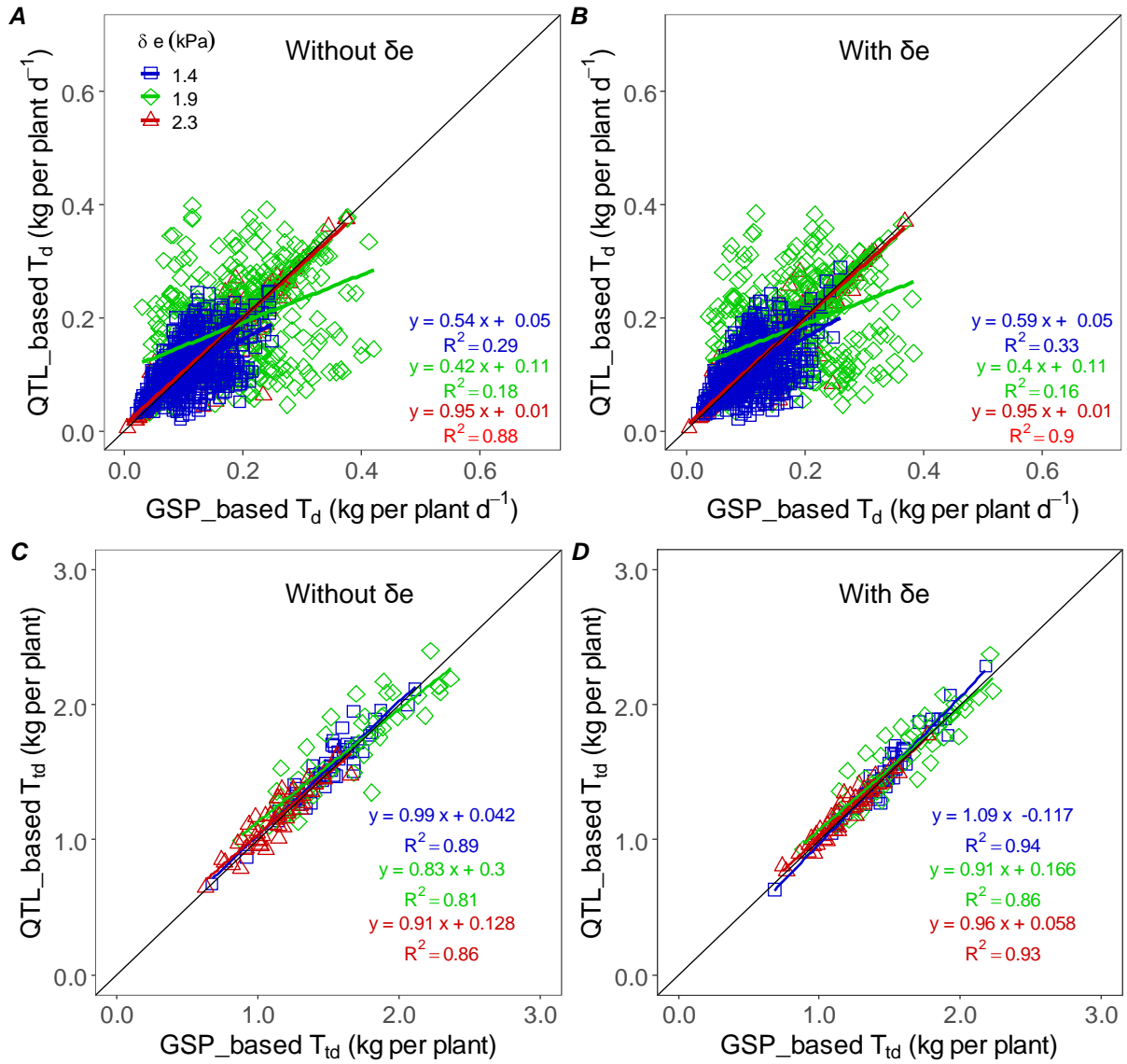
Fig. 3-8. Comparison between GSP-based and QTL-based plant transpiration (T_d) (A, B) and total transpiration (T_{td}) (C, D) of drought-stressed tomato lines under three δe conditions. The model uses QTL-based or GSP-based parameters without or with consideration of δe response functions, respectively. T_d is determined through the use of c_L and c_g (M2-2).

Discussion

This study is a first attempt to develop and evaluate a QTL-based model of growth and water use of tomatoes under drought stress across environments by using soil water thresholds of key traits relevant for drought adaptation. The genomic regions responsible for thresholds and their response coefficients to current air vapour pressure deficits (δe) were inputs of genetic factors controlling the variation in drought responses. Incorporation of the QTL parameters in a crop model gave a reasonable representation of water use dynamics under drought stress at the genome-wide scale.

Experimental conditions and model parameters

Since we performed the trials in different seasons, the calendaric ages of plants at the time of drought imposition ranged from 23 - 30 days after emergence (**Table 3-S3**), but their developmental stages were similar (ca. 7th leaf stage). Average daily temperature spanned around 22 to 28 °C for trials used for parameterization and 23 to 27 °C for evaluation. In trials 3 and 7, supplemental light was provided because of the low external radiation, resulting in a less fluctuating light condition throughout the stress period. We assumed that the response of thresholds c_x was dependent on seasonal δe averaged over the entire stress period, even though the actual c_x could be variable across or within environments. Moreover, the c_x response to δe was assumed to be linear, and the 50% relative difference in parameter s_{cx} from M82 was used as a critical point to declare the presence of specific QTL.

Drought responses of plant processes imply coping strategies

Responses of the IL library showed a decline in leaf expansion relatively earlier (i.e. at higher water contents) in the drought cycle than other traits (**Fig. 3-2**). Reduced leaf expansion is usually the first symptom of mild water deficits (Boyer, 1970; Hsiao, 1973; Saab and Sharp, 1989). Under drought stress, cell wall rheological properties can adapt rapidly, resulting in a decrease of leaf expansion rate, even before the turgor and leaf water potential begins to change (Spollen and Sharp, 1991; Pritchard et al., 1991; Tardieu, 1996). The average soil water threshold for leaf expansion of 0.64 is comparable to other findings in several crops (0.59-0.64 for African nightshade (Masinde et al., 2006); 0.51 - 0.83 for sunflower (Sadras et al., 1993; Casadebaig et al., 2008); 0.73-1.0 for potato (Jefferies, 1993a); 0.61 across species and growing conditions (Sadras and Milroy, 1996)). The wild type *S. pennellii* was slightly

less sensitive to soil drying compared to M82, possibility because of its leaf morphology (small, waxy and thick leaflets) fitted for survival under desert conditions.

The effect of drought stress on leaf expansion was often considered largely non-hydraulic (mainly through ABA) because of the sustained turgor maintenance in growing cells (Tang and Boyer, 2002). Enhancement of this chemical control could be part of a water-saving strategy, especially in isohydric species under severe drought (Blum, 2015). Stomatal conductance and specific transpiration of *S. pennellii* showed this type of reaction by 31% and 43% larger thresholds than M82 (**Fig. 3-3B, D**). Domesticated tomato cultivars like M82 have been categorized anisohydric (Sobeih et al., 2004) using a water spending strategy (Blum, 2015) with delayed stomatal closure. Stomatal conductance was less responsive (lower thresholds) to water deficits than tissue expansion (Hsiao et al., 1976; Passioura, 1988; Sadras et al., 1993). The reduction of leaf water potential under soil water deficit could have a role in the regulation of stomatal conductance via a modification of the stomatal sensitivity to ABA, originating from the mesophyll of the leaves or arriving from the roots in the xylem stream (Tardieu and Davies, 1992; Tardieu et al., 1993). The c_T value (0.50) was comparable to many findings described elsewhere (Sadras and Milroy, 1996; Masinde et al., 2006; Casadebaig et al., 2008; Kholová et al., 2010). The similar magnitudes of c_T, c_ε and c_g (**Fig. 3-3B-D**) and correlations among them (**Fig. 3-S6**) imply that the reduction of ε_d regulated by the stomatal closure reduced the T_d with soil drying. A significant correlation between c_T and c_L also suggests that transpiration was reduced partly due to the reduction of leaf expansion under moderate stress (Borrell et al., 2000). The negative relation of thresholds and growth traits illustrates the tradeoffs between water saving and carbon assimilation. The wide ranges of genotypic means for c_g and c_L indicate considerable genetic variation for these parameters (see also **Fig. 3-S5**).

Drought reactions of leaf expansion and stomatal conductance reflect the underlying QTLs

In some studies with tomato introgression lines, the a relative difference of 30% in phenotypic values of a particular IL was used for identification of QTLs (Frary et al., 2010; Frary et al., 2011; Rousseaux et al., 2005). A more common method for tomato introgression lines harbouring a single introgressed segment of the wild type is to use Dunnett's test which was used in this study.

We found 16 genomic regions for thresholds and intensity of decline for four relative traits. Eshed and Zamir (1995) observed 104 regions controlling six yield-related traits. This is understandable since yield is a more complex trait than the traits investigated in this paper. Since we identified the main QTL effects across environments, the genotype x environment (block) interaction could be encapsulated (Tardieu and Tuberosa, 2010), resulting in a lower number than the possible total QTLs if estimated in individual environments. The most abundant genome regions of varying QTL effects ($|R| = 17.29\text{-}48.73\%$) were observed for c_L and c_g, despite considerable environmental variation. This indicates a clear multigenic nature of these complex traits. All detections for c_L showed the determinism also for s_L (**Table 3-2**). It shows that intensity of deline of relative leaf expansion rate was simply dependent on the timing when it started to react to drought.

Among the ILs investigated, IL7-3 resembles *S. pennellii* in terms of growth habit with relatively small canopy size and its drought reaction strategy was similar to *S. pennellii*. Interestingly, Eshed and Zamir (1994) found over-dominance in an IL7-3 hybrid (IL7-3 x M82) associated with higher fruit yield than M82. Among the ILs harbouring QTLs for the reaction of leaf expansion, IL7-5 even in the homozygous (inbred) stage showed a higher horticultural yield than M82 (Eshed et al., 1996). IL12-4 with the early reaction for r_g was previously mapped as a promising line for a combination of fruit and biomass production while IL3-2 (s_T) and IL4-3 (c_g, c_T) were those with the agronomic performances inferior to M82 under unstressed conditions (Caruso et al., 2016). It indicates that some of the ILs detected for higher thresholds are holding both favourable and unfavourable wild alleles for plant performance (inevitable trade-offs between survival and performance).

QTL-based model using threshold for stomatal conductance could predict transpiration

The transpiration of tomato under drought stress can be predicted well by using the soil water thresholds at a genome-wide scale (**Fig. 3-7**; **Table 3-S1**). The virtue of using two thresholds at sub-level is that one can examine the drought reactions of the expansive and gas exchange processes, and adaptive mechanisms separately.

The prediction of transpiration using QTL-based parameters and genotype-specific parameters (GSPs) gave a similar level of fitness and accuracy (**Table 3-S1**). It showed the virtue of the QTL based model, which could largely avoid the tedious tasks including parameterization of

multiple genotypes. The low coefficient of determination for daily transpiration (≤ 0.46) and high coefficient of determination (> 0.88) of the regressions for total transpiration between two approaches (QTL and GSP) indicated that discrepancies between constitutive and adaptive nature of drought response traits. This also indicated that mean QTL information could be applied in crop model, with the consideration of their environmental dependence (**Fig. 3-8**, **S13**). Soltani et al. (2000) argued based on the simulations across years and locations that the differences (up to 20%) in c_L and c_T under water deficit conditions had little contribution to grain yield of chickpea genotypes. According to Reymond et al. (2003), dissection of a phenotype into elementary responses may be associated with several risks, including the inadequacy and generation of noise that may result in unstable traits (e.g. soil water thresholds) and hamper QTL detection. To deal with the potential instability of genetic parameters such as thresholds, we designed in our parameterization to estimate main QTLs effects first, and develop a regression function for its environmental sensitivities (here average vapour pressure deficit). Use of c_g in M2-2 approach gave a promising agreement between simulated and observed total water transpired, which was more evident in high δe condition (**Table 3-S1**). It indicates that the response function of c_g to δe condition is more reliable than that of c_L, c_T and c_ε for incorporation into the ecophysiological model as a QTL-based parameter.

Soil water thresholds vary with the average evaporative demand

In the unstressed treatment, leaf expansion was negatively affected by increasing evaporative demand (Shackel et al., 1987; Sadok et al., 2007), which could be linked to hydraulic processes (Welcker et al., 2011). Early drought responses of expansive growth and transpiration under low δe (**Fig. 3-S4**) implies the dominance of non-hydraulic signals regarding the changes in soil water potential when there was low atmospheric humidity mainly responsible for hydraulic control. Under low δe, delayed stomatal closure could have supported the continuation of specific transpiration. At the same time, there was a gradual soil water deficit leading to a decrease in cell expansion. In this situation, only those lines with a specific mechanism such as turgor maintenance (e.g. OA) or adjustment of cell wall properties could sustain the carbon assimilation and ameliorate the relative reduction of canopy dry matter production driven by the drought. The different reaction of transpiration under low and high δe supported the fact that c_T was largely environment-dependent (**Fig. 3-4**) and therefore should be described in connection to environmental factors. One reason for low c_T under above-optimum δe could be that increase in transpiration rates up to the certain

thresholds of δe caused the increased plant hydraulic conductance which can compensate the rapid limitation imposed by a decreased soil conductance (Ray et al., 2002; Ruggiero et al., 1999). We can conclude that under low δe, the early reaction of canopy transpiration was mainly regulated by reducing canopy expansion rate (Sadras et al., 1993), whereas the delayed reaction under high δe can be attributed to both decreased expansion rate and stomatal conductance (**Fig. 3-S2**). This result however is different from the consensus including the finding of Ray et al. (2002), who described that there was no apparent tendency in maize in response to varying δe, and that of Abdul-Jabbar et al. (1983) who found slightly increased c_T in soybean with increasing δe. This discrepancy could be brought about by different experimental conditions and calculation methods of LRP parameters. The proportion of the δe sensitive lines for drought reaction parameters revealed that the local response curve should be used for r_L and r_g (**Fig. 3-3, S3**). Compared to M82, the wild type *S. pennellii* showed its early sensitivities for most traits, except r_L, to drought, especially under high δe condition. High variability of soil water fraction under high δe indicates the more pronounced genotypic variation with increasing evaporative demand (**Fig. 3-S14**).

Practical implications of the model

Modelling stressed transpiration based on QTL-controlled parameters looks promising, as it is a general and semi-mechanistic approach, showing good agreement between measurements and simulation for a range of vapour pressure deficit conditions. The parameterization steps at the sub-levels are simple and straight forward, avoiding complex equations for water transport. Using inputs of unstressed performance for the tested environment allows simulations for varying climatic conditions. Although the parameters of soil water and δe responses are IL-specific, using QTLs ensures the versatility of the model for the genome-wide predictions. The average sizes of chromosome fragments are 33 cM, and the resolution of detected QTLs can be fine-tuned through suitable breeding schemes. Incorporation of our stressed response model in a more comprehensive ecophysiological growth model will allow performing sensitivity tests under greenhouse systems for further calibration and model improvement.

Conclusion

Using linear plateau regression models, we performed the genome-wide evaluation of drought response indicators in tomato introgression lines under a range of environments differing in

evaporative demand. We identified wildtype chromosome regions holding QTLs associated with drought reaction parameters. Using the QTL parameters in the crop model, we simulated leaf growth and transpiration under drought stress at a genome-wide scale. Canopy transpiration could be well predicted using QTL-based parameters in place of genotype specific parameters. Parameters of linear plateau regression models are suitable to predict the transpiration of tomato genotypes under soil water depletion.

Chapter 4

A genome-based eco-physiological model of leaf area, transpiration and dry matter production for vegetative growth stage of tomatoes under drought-stress

San Shwe Myint[1,2], Dany Moualeu-Ngangue[1], Hartmut Stützel[1]

[1]*Institute of Horticultural Production Systems, Leibniz Unversität, Hannover, Germany;* [2]*Department of Horticulture, Yezin Agricultural University, Naypyitaw, Myanmar*

Abstract

Eco-physiological models are useful tools to study the plant's functions in varying environments. Typically, these models include genotype or species-specific function parameters. In contrast, a QTL-based model can predict the plant performance through any combination of alleles information. Combining genetic information and eco-physiological models expected to better predict genotype x environment interactions than conventional models. Introducing the genotype-specific parameters or QTLs, we built an eco-physiological model for the vegetative growth stage of tomatoes, combining the established models after some structural adjustments. Four greenhouse experiments were conducted for parameterization and three for evaluation. The model was constructed in a JAVA platform to describe three major modules: 1) leaf growth 2) transpiration and 3) dry matter production. For well-watered or drought-stressed conditions, the growth processes were modelled with a stepwise input of leaf area and soil water fraction. Without inputs, the aggregated model predicted the leaf area, transpiration and shoot dry matter with accuracy of 69-84% for unstress conditions and 55-73% for stress conditions with 20-30% overestimation of leaf area under drought stress. With the leaf area input, the transpiration sum and soil water were predicted with more accuracies than the aggregate one. With the input of unstressed leaf area and using soil water thresholds for either of specific transpiration ratio or relative stomatal conductance, QTL-based model predicted the transpiration of stressed plants with fair accuracy. A considerable variation in model performance was observed between different environments. Function of soil water deficit on specific leaf area at different canopy layers should be implemented for improved prediction of leaf area under drought stress.

Keywords: Introgression lines, *Solanum pennellii*, QTL, eco-physiological model, transpiration, dry matter, leaf area, transpirable soil water

Introduction

Under drought stress, crops need to maintain a balance between processes keeping sustained production and processes minimising severe water stresses (Jones and Tardieu, 1998).

Leaf area determines the fraction of incident radiation absorbed by the canopy (Marcelis et al., 2009), and thus canopy photosynthesis, biomass production and transpiration. Leaf area development can be seen as a combination of leaf emergence rate, rate and duration of expansion of individual leaves and their lifetime (duration) (Marcelis et al., 1998). In crop models, leaf area is described either as a function of plant developmental stage (or accumulated temperature sum) (sink-driven) or calculated from simulated leaf dry weight and specific leaf area SLA (source-driven).

In tomato, the initiation rate of leaves is primarily determined by temperature, while leaf area per leaf is also affected by assimilate supply (Heuvelink and Marcelis, 1996).

In TOMGRO, Jones et al. (1991) simulated the daily dynamics of SLA depending on environmental factors within the boundary of minimum and maximum limits. Heuvelink (1999) used the minimum and maximum SLA in his tomato model TOMSIM, where minimum SLA was dependent on the day of the year as a forcing function. Introducing the concept of structural SLA and carbohydrate pool in TOMGRO was found to be more promising (Gary et al., 1993; Marcelis et al., 2009). All of the above models did not take account of drought stress and age effects.

Biomass accumulation and its dependence on water deficit are modelled in different ways through either i) the concept of radiation use efficiency (RUE) or ii) the simulation of photosynthesis and respiration at the leaf level, or iii) with the integration of a model of leaf photosynthesis (Farquhar et al., 1980). An effect of water deficit was simulated directly on RUE or its components, or indirectly as the minimum of light-limited and water-limited biomass accumulation, where transpiration efficiency and available water were taken account (Hammer et al., 2010).

In photosynthesis-based models, first, the interception of light by the leaf area is calculated to stimulate the production of photosynthates. Subsequently, the use of photosynthates for respiration, conversion into structural dry matter DM, the partitioning of assimilates or DM among the different plant organs is calculated (Marcelis et al., 1998). Many models simulate photosynthesis limitation under drought stress by merely reducing the slope of the

relationship between stomatal conductance and net carbon assimilation rate (Egea et al., 2011b), similarly for all plant function types (Zhou et al., 2018). Due to the shortage of model-oriented studies on stomatal and non-stomatal effects of the drought stress on photosynthesis, large discrepancies exist in how current ecosystem models represent (Powell et al., 2013; Medlyn et al., 2016). Moreover, there has been a scientific debate on how to represent stomatal closure as soil moisture declines (via leaf water potential or soil water potential) (Bonan et al., 2014), and what processes limit photosynthesis under drought (Chaves, 1991; Lawlor, 2002). According to some findings in plant ecophysiology, photosynthesis limitation by drought is mainly of diffusive (stomatal and mesophyll conductance) rather than of metabolic (biochemical) origin, especially under mild to moderate drought stress (Egea et al., 2011a; Galmés et al., 2007; Grassi and Magnani, 2005).

Marcelis (1993) distinguished three main approaches for simulation of DM partitioning: descriptive allometry, functional equilibrium and sink regulation, roughly representing an empirical, a teleonomic and a mechanistic respectively (Thornley and Johnson, 1990). Most of the applications of the modelling approach based on sink strengths (or potential demands) are found in reproductive crops, like sweet pepper, cucumber, tomato, peach, grapevine, kiwifruit, citrus, rose and bean (Marcelis, 1993). This approach has some mechanistic aspects and can be used to model DM partitioning between any plant parts. As discussed by Challa (1997), this approach could have a wider application in growth of vegetative organs and plant morphogenesis.

In most models, transpiration under unstressed condition is simulated in similar ways according to the study of Parent and Tardieu (2014). For example, many crop models such as STICS (Brisson et al., 2008), GECROS (Yin and van Laar, 2005), CROPGRO (Boote et al., 1998), CropSyst (Stockle et al., 1994), and CERES (Lizaso et al., 2005; Lizaso et al., 2003) simulate the transpiration demand via a Penman-Monteith-like equation (Allen et al., 1998; Priestley and Taylor, 1972; Penman, 1948) while in others like APSIM-maize (Hammer et al., 2010), it is simulated as the product of biomass accumulation by transpiration efficiency and air vapour pressure deficit.

For the water-stressed condition, plant water status and transpiration are simulated based on indices such as a supply/demand ratio in APSIM-maize, the ratio of actual vs potential transpiration in CERES, CSM-IXIM (Lizaso et al., 2011), SUCROS1&2 (van Laar et al., 1997; Goudriaan and van Laar, 1994), GECROS, and CropSyst, or directly via available water content in the root zone in STICS. These simplifications avoid complex equations of

water transfer in the plant (Tardieu and Davies, 1993; Caldeira et al., 2014) and in the soil (Janott et al., 2011).

From a functional standpoint, the drought response of plant transpiration is regulated via the regulation of stomatal behaviours (rate) and expansive growth (size). Although essential, modelling stomatal behaviour under drought stress is quite hard to achieve success, especially for horticultural crops (Jones and Tardieu, 1998). Many empirical models assume that different environmental variables act independently in determining stomatal conductance, leading to multiplicative form. However, there could still be a large component of the total variance that remains unexplained.

Prado et al. (2018) used the inversion of Penman-Monteith (P-M) model to calculate back the plant level g_s using the measured data of transpiration rate. This approach minimizes the risk of uncertainty regarding the aerodynamic conductance and provides the plant g_s averaged over 24 hours. However, it needs the data of measured transpiration as an input in experiments for model evaluation. Leuning (1995) modified and recommended a semi- mechanistic equation for g_s under the unstressed condition as an extension to FvCB model (Farquhar et al., 1980), in which g_s is dependent on net photosynthesis, leaf-to-air vapour pressure deficit and air carbon dioxide. Most attempts were made to introduce drought effects into this equation still at the leaf scale. However, to implement the causal relationship at the canopy level, it needs to develop a separate g_s model from which g_s value can be used as an input to FvCB model after adjusting the absorbed light per unit leaf area index as a daily average. Using the data set for parameterization, integrating the multiplicative function in inverse calculation can yield the maximum plant g_s, which could be used as an input in simulations.

Regarding the soil water status, because of the difficulty of getting the required information (e.g. soil hydraulic conductance, soil and root water potential) to model the soil moisture accurately, people in most horticultural systems commonly use the simplified models. These include a multilayer approach, water reservoir approach, and indirect estimation by predawn leaf water potential (Jones and Tardieu, 1998). In terms of accuracy and feasibility, water reservoir approach is more suitable than the other counterparts provided that the rooting volumes of the containers are known and great care in the measurement given. In this approach, changes in available water can be calculated using a water balance calculation, or through the regular measurement of the changes in pot weights. Although this approach has no real physical base, it can be beneficial and virtually all crop models use it in one form or another (Jones and Tardieu, 1998).

By the use of the linear plateau regression as a function of soil water status, one can estimate the parameters for drought responses (i.e. thresholds and slope) of both g_s and leaf expansion and use them as genotype-specific (or QTL) parameters that characterize the genotype. For each genotype, the model needs to run separately for different configurations of simulation with the regulation of major model inputs.

For transpiration of greenhouse-grown tomato under unstressed condition, the modified P-M model of Stanghellini (1987) has proven to be a promising one, but it was essentially developed for full-grown and unstressed indeterminate tomatoes with the maintenance of constant LAI. For tomato growth and yield, there are some well-validated mechanistic models, including TOMSIM and TOMGRO (Jones et al., 1991; Heuvelink, 1996b) again for unlimited water supply condition.

A key issue regarding the effects of water deficit is that individual processes have to be coordinated in the whole plant level. Drought stress responses are assumed to be coordinated (Tardieu et al., 2011) either (i) via "hubs" that control all processes simultaneously, (ii) in series, with one process governing the others, or (iii) in parallel, with all processes being affected independently with some feedbacks (**Fig. 4-1**). The last option better accounts for experimental results than the other two (Tardieu et al., 2011).

In 'in parallel' coordination, leaf area expansion and biomass accumulation are essentially independent processes with different response to water deficit. With the feedback control of leaf biomass supply, actual leaf growth can be source-limited if carbon resources available for leaves are insufficient to meet the sink strength (demand) of leaves. Leaf growth will be source-driven provided that there is an ample supply of carbon. The actual leaf expansion can be computed using the maximum SLA together with the consideration of environmental factors. Depending on the model structure, a given trait and the effect of the QTLs that determine it either has crucial importance in the overall plant response to water deficit or is one trait among others.

The drought responses of different species depend not only on drought duration and intensity but also on the species-specific degree of adaptation. Different degrees of drought tolerances could be identified between species of diverse origins through the model-orientated experiments (Zhou et al., 2018). The prediction of performances of multiple genotypes under any climatic scenario is possible provided that model parameters could be estimated at high throughput in phenotyping platforms (Reymond et al., 2003; Hammer et al., 2005; Tardieu, 2003).

The outputs of QTL analysis are useful for predicting the plant performances through any combination of alleles without extra experiments. However, a QTL model is an environment specific, not directly applicable to different environments (Tardieu, 2003). QTL and eco-physiological models can theoretically be combined if the QTL analysis is carried out on parameters of the eco-physiological model which was proven in a laboratory test for the response of maize leaf elongation rate to temperature and water deficit (Reymond et al., 2003; Tardieu, 2003). Therefore, incorporation of QTLs information for the parameters of drought responses (e.g soil water threshold) of leaf expansion or stomatal conductance could be possible in an eco-physiological model which included these parameters.

Observed genetic variability in a given trait is challenging to simulate if not explicitly present in the model. In this case, "in parallel" model class can simulate genetic variability in a trait or some traits as a consequence of associated QTLs in an independent manner (See **in Fig. 4-S5**). For instance, it is straightforward to simulate consequences of QTLs affecting leaf expansion (Reymond et al., 2003; Welcker et al., 2011) in an 'in parallel' type as in Chenu et al. (2009). Presenting the QTLs that affect soil water thresholds of leaf expansion and that of stomatal conductance, one can predict leaf area index, water transpired and accumulated biomass of multiple lines in different environments.

To predict the performances of multiple genotypes in different environments, there is a need of a system so-called genome-based eco-physiological model, which essentially includes the stable QTLs derived parameters describing the phenotypic variation in drought responses. Combining the sub-modules (models for growth and dry matter production, photosynthesis and transpiration) with the genetic inputs for drought responses could bring a useful platform to study the stressed and unstressed performances of multiple genotypes under varying environmental scenarios.
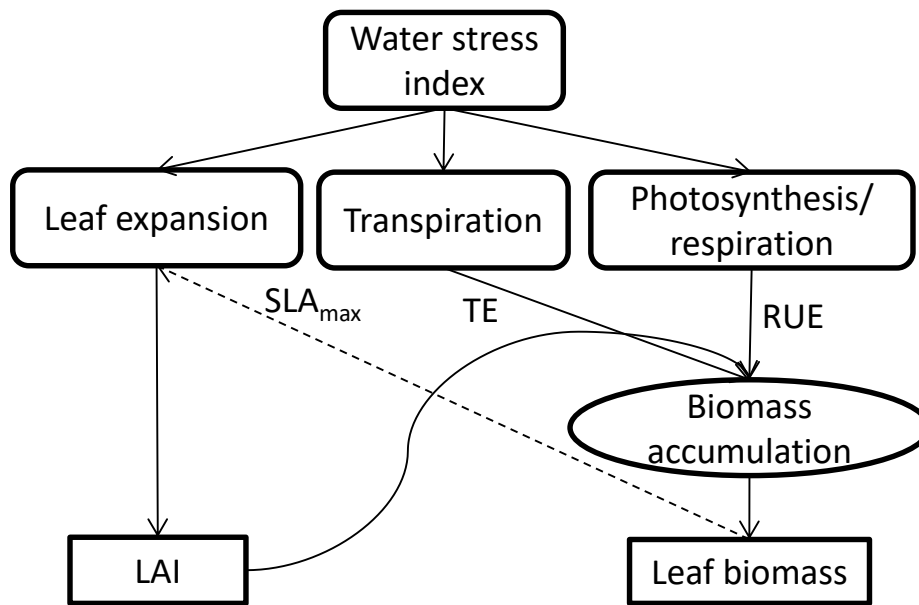
Fig. 4-1. A flow chart of drought stress effects on leaf area and leaf biomass of a *in parallel* type model (adapted from Parent and Tardieu (2014)). In this type leaf expansion is independent from biomass production while in the *in series* type model, leaf area index (LAI) solely depends on leaf biomass accumulation. With the use of maximum SLA (*SLA_max*), leaf expansion can be limited by leaf biomass accumulation. Biomass accumulation can either be the direct output of radiation use efficiency (RUE) or the minimum of RUE and transpiration efficiency (TE). The LAI has a feedback on both photosynthesis and plant transpiration through the limitation of light interception. Water stress index can be defined as the water available or as the transpiration ratio.

Accordingly, the following assumptions were made.

1) Leaf expansion rate is regulated by developmental stage and source-sink balance regardless of the water stress.

2) Genetic variations in soil water thresholds for leaf expansion rate and stomatal conductance determine the differing drought performances of transpiration and water uptake in tomatoes.

3) With the input of leaf area, the model can predict the plant transpiration and biomass accumulation more precisely than does the aggregated one.

4) QTL based eco-physiological model can predict the stressed transpiration of multiple genotypes similarly to the processed model which runs for each of genotype with specific parameters under varying environments.

Specific objectives of this work are, therefore:

1) to parameterize the generic and specific functions with respect to leaf area development, photosynthesis, dry matter production and partitioning of greenhouse tomatoes

2) to build an aggregated eco-physiological model with different modules for limited and unlimited water supply environments

3) to simulate and evaluate the sub-models of leaf area development, dry matter production, transpiration and water uptake through the manipulation of the major model inputs, and

4) to simulate and evaluate the QTL-based eco-physiological model for prediction of stressed transpiration of *Solanum pennellii* introgression library.

Materials and Methods

The Model

General description

A flow chart of the whole TILSIM model composed of different modules is described in **Fig. 4-S5**, which emphasizes source-sink regulation on growth and development with respect to transpiration, photosynthesis and dry matter production influenced by the genetic and environmental factors, especially for a water-limited condition. This mode was built on underlying three modules: 1) plant growth and development; 2) photosynthesis, dry matter production and partitioning; 3) transpiration and soil water uptake. TILSIM was constructed basically through the combination of other established models for different plant functions: TOMGRO (Jones et al., 1991) and TOMSIM (Heuvelink, 1996b) for growth, dry matter production and partitioning in tomato. Farquhar biochemical model for leaf photosynthesis of C3 plants (Farquhar et al., 1980) and Modified Penman-Monteith model for transpiration of greenhouse crops (Stanghellini, 1987), with some modifications and changes in model structure and functions to enable the incorporation of drought reactions and module of genotype. The simulations practices were performed in a way that the different modules can be evaluated for the traits at higher integration level, e.g. plant transpiration and shoot dry weight with or without the input of leaf area and/or soil water fraction. This model is the first version of that kind for multiple tomato genotypes, which needs to be evaluated separately at the lower levels, and calibration and even changes in model structure and functional relations of different components are required in terms of model concepts, assumptions and simulation purpose, and thereby sensitivity analysis and calibration can follow for model improvement and further silico experiments.

Plant growth and development

The development of total leaf area was dependent on thermal time (physiological leaf age) and a balance between assimilate supply and demand, regulated by leaf production, leaf expansion rate and leaf expansion duration of individual leaves. Minimum and maximum air temperature and relative humidity, soil water status, genotype-specific drought reaction parameters, assimilate supply for the total leaf area, maximum specific leaf area and maximum leaf expansion rate and thermal leaf appearance rate are inputs of this sub-module.

Leaf number

Leaf number per plant N_l (nr. per plant) was determined as the product of potential leaf appearance rate r_l (nr. °Cd^{-1}) and integral of thermal time TS (°Cd):

$$N_l = r_l \int_0^t (T_a - T_b)\, dt \qquad \text{(Eqn 4-1)}$$

where $(\int_0^t (T_a - T_b)\, dt)$ thermal time TS (°Cd), calculated from the 24h average air temperature T_a (°C) and the base temperature T_b (°C) starting from the date of emergence of the plant. The way to model non stressing temperatures was the use of thermal time (Chapman et al., 1993). It was assumed that there was no extreme T_a (i.e those causing chilling or heat shock) and that organogenesis during the vegetative period was not effected by drought stress.

Leaf area

Plant leaf area (A_l, cm^2 per plant) is the sum of the areas of individual leaves A_i (cm^2 per leaf), determined as the integral of actual leaf expansion rate E_i (cm^2 per leaf °Cd^{-1}):

$$A_i = \int_{t_{0i}}^t E_i(x)\, dx \qquad \text{(Eqn 4-2a)}$$

where E_i was a genotype specific expansion rate of ith leaf. The difference between the current time t and the time of leaf appearance t_{0i} was the thermal age Δt_i (°Cd) of the ith leaf. If r_l was the leaf appearance rate, then

$$t_{0i} = \frac{i}{r_l} \qquad \text{(Eqn 4-2b)}$$

Potential expansive growth of the plant

The actual leaf expansion rate E_i depends on potential expansion rate of the leaf at i^{th} rank $E_{pot,i}$ (cm^2 per leaf °Cd^{-1}). $E_{pot,i}$ is defined as the product of maximum leaf expansion rate $E_{i,max}$ (cm^2 per leaf °Cd^{-1}), and normalized effect of vapour pressure deficit δe, leaf physiological age Δt_i (°Cd) and fraction of transpirable soil water W_{ts} (unit-less):

$$\mathrm{E}_{pot,i}(t) = E_{i,max} \times E_{i,norm}(\delta e) \times E_{i,norm}(\Delta t_i) \times E_{i,norm}(W_{ts}) \qquad \text{(Eqn 4-3b)}$$

The normalized effects of δe and Δt_i are assumed to follow the linear and bell-shape functions, respectively:

$$E_{i,norm}(\delta e) = a_{ei} + b_{ei}\, \delta e\,(t), \qquad \text{(Eqn 4-3c)}$$

$$E_{i,norm}(\Delta t_i) = \begin{cases} exp\left\{-0.5 \times \left[(\Delta t_i(t) - \Delta t_{i,max})/h_l\right]^2\right\}, & TS\,(t) \geq t_{0i} \\ 0, & TS\,(t) < t_{0i} \end{cases} \qquad \text{(Eqn 4-3d)}$$

where a_{ei} and b_{ei} are empirical constants, Δt_i (°Cd) the thermal age of a given leaf determined as the difference between TS and t_{0i}, $\Delta t_{i,max}$ the leaf age (°Cd) when it reached the maximum expansion rate, and h_l the standard deviation of the age effect (**Fig. 4-S1**). The normalized effect of soil water deficit was described by a linear plateau model:

$$E_{i,norm}(W_{ts}) = \begin{cases} s_L(W_{ts}(t) - c_L) + 1, & W_{ts}(t) > c_L \\ 1, & W_{ts}(t) \leq c_L \end{cases} \qquad \text{(Eqn 4-3e)}$$

where s_L and c_L are genotype specific intensity of the slope and soil water threshold, respectively for leaf expansion rate.

Organ and plant level sink strength of leaf

The relative sink strength of a leaf f_i at a given time t was determined as the ratio between potential increase of individual leaf area $E_{pot,i}$ (cm^2 per leaf °Cd^{-1}) and that of total leaf area $E_{pot,l}$ (cm^2 per plant °Cd^{-1}), which is the integral of the individual expansion rates.

$$f_i(t) = \frac{E_{pot,i}}{E_{pot,l}}(t) \qquad \text{(Eqn 4-3f)}$$

Sink strength (or assimilate demand) of a leaf S_i (g DM per leaf °Cd^{-1}) was determined as the ratio between potential leaf area increase $E_{pot,i}$ (cm^2 per leaf °Cd^{-1}) and the minimum SLA, SLA_{min} (cm^2 g^{-1}).

$$S_i(t) = \frac{E_{pot,i}}{SLA_{min}}(t) \qquad \text{(Eqn 4-3g)}$$

Total sink strength of leaf portion S_l (g DM per plant °Cd^{-1}) at time t was the sum of the individual S_i at different layers.

Actual leaf growth and expansion rate

Actual growth rate of leaf i at time t, G_i (g DM per leaf °Cd^{-1}) was the product of its relative sink strength f_i (unit-less) and the minimum of the total leaf sink strength (or capacity) S_l (g DM per plant °Cd^{-1}) and assimilates (g DM) that can be allocated to leaves (or leaf mass supply), $M_{l,sup}$ (g DM per plant °Cd^{-1}):

$$G_i(t) = f_i(t) \times min(S_l, M_{l,sup})(t) \qquad \text{(Eqn 4-3h)}$$

where $M_{L,sup}$ was the dry matter input, and *SLA* and *SLA$_{min}$* were calculated in Eqn (4-4a) and (4-4d). If the supply was higher or equal to the sink strength, then the leaf would grow at its sink-driven full potential, otherwise assimilates supply would be distributed to different growing leaves according to their relative sink strengths f_i. The increase in total leaf dry weight at a given moment G_l (g DM per plant °Cd^{-1}) was the sum of G_i.

The actual leaf expansion rate E_i (cm^2 per leaf °Cd^{-1}) was estimated as the product of dry mass increase (actual leaf growth rate) G_i (g DM per leaf °Cd^{-1}) and specific leaf area (*SLA*, cm^2 g^{-1}).

$$E_i(t) = G_i(t) \times SLA(t) \qquad \text{(Eqn 4-3i)}$$

Specific leaf area

Specific leaf area *SLA* (cm^2 g^{-1}) was modelled as a function of the light intensity, the temperature, the sink-source ratio, and CO_2 concentration as reported in the literature (Enoch, 1990; Marcelis, 1993). Therefore, *SLA* was defined as the product of a function of aerial environments (i.e light, temperature, CO_2), plant age and soil water:

$$SLA(t) = SLA_p(t) \times SLA_{norm}(TS) \times SLA_{norm}(W_{ts}), \qquad \text{(Eqn 4-4a)}$$

where

$$SLA_p(t) = SLA_{min} + (SLA_{max} - SLA_{min}) \times SLA_{norm}(I_{id}, T_a, C_a); \qquad \text{(Eqn 4-4b)}$$

$$SLA_{norm}(I_{id}, T_a, C_a) = \frac{a_{sI} + b_{sI}I_{id}(t)}{[1 + \beta_{Ta}(24 - T_a(t))] \times [1 + \beta_{Ca}(C_a(t) - 350)]}, \qquad \text{(Eqn 4-4c)}$$

where $(a_{sI} + b_{sI}I_{id}(t))$ is a function of daily light integral (mol m^{-2} d^{-1}) on *SLA* (**Fig. 4-S2B**), $[1 + \beta_{Ta}(24 - T_a(t))]$ and $[1 + \beta_{Ca}(C_a(t) - 350)]$ functions of air temperature, T_a (°C) and air CO_2, *Ca* (µmol mol^{-1}) on specific leaf dry weight (*SLW=1/SLA*), respectively; β_{Ta}

and β_{Ca} are parameters describing the relative change in leaf dry mass per unit change in temperature and CO_2 from reference values of 24°C and 350 µmol mol^{-1} respectively. *SLA* was assumed to decrease under high light intensity, high CO_2 and low temperature, and vice versa. Parameters β_{Ta} and β_{Ca} are adjusted from the values of Jones et al. (1991) and Boote et al. (25-29 Nov 1991). *SLA* was constrained to vary between the minimum and maximum limits, which were calibrated for each introgression line. SLA_{min} was derived by fitting the minimum values of reference M82 measured in the different seasons to a simple sinusoidal function based on Heuvelink (1999) but using our empirical constants:

$$SLA_{min}(d_y) = a_{sdy} + b_{sdy}\sin\left[\left(\frac{2\pi\, d_y(t)}{365}\right) + c_{sdy}\right]$$

(Eqn 4-4d)

where a_{sdy}, b_{sdy} and c_{sdy} are the regression constants (**Fig. 4-S3**) and d_y day of the year. SLA_{max} was a genotype specific constant. Normalized plant age effect on *SLA* was described by a log-normal function:

$$SLA_{norm}(TS) = exp\left\{-0.5 \times \left[ln(\frac{TS}{TS_{s,max}})/h_s\right]^2\right\}$$

(Eqn 4-4e)

where $TS_{s,max}$ (°Cd) is the time at which *SLA* has the maximum (**Fig. 4-S2A**). The use of assimilates available for the leaf area growth was assumed to be increasing until the plant age of 250 °Cd, then it gradually decreased over time while dry matter increase in leaf continued. Normalized drought effect on *SLA* was assumed to follow a logistic-decay function:

$$SLA_{norm}(W_{ts}) = \begin{cases} 1/[(1 + a_{sw}\, exp\,(-b_{sw}\, W_{ts}(t))], & W_{ts}(t) < 0.8 \\ 1, & W_{ts}(t) \geq 0.8 \end{cases}$$

(Eqn 4-4f)

where a_{sw} and b_{sw} are constants, and W_{ts} the fraction of transpirable soil water.

Plant height

Plant height H_p (cm) at any time *t* is calculated as dependent on the increase of stem dry mass G_S (g DM per plant C°d^{-1}) and specific internode length L_{rin} (cm g^{-1}), calculated as the ratio between the stem length H_p and stem weight W_s:

$$H_p = L_{rin} \int_0^t G_s(t)\, dt$$

(Eqn 4-5)

where L_{rin} was a genotype specific constant for both drought treatments and G_s derived from dry matter production and partitioning module, model variables and coefficients are listed in **Tables 4–6** and **4-7**.

Photosynthesis, dry matter production and partitioning

This module includes light absorption, photosynthesis, maintenance and growth respiration and dry matter partitioning**.** The inputs of driving and state variables are daily global radiation, daily average air temperature, air CO_2, dynamics of soil water status, leaf area index, and stomatal conductance to water vapour.

Light absorption

The irradiance absorbed per unit leaf area (weighted by leaf area index) I_{abs} (µmol photon m^{-2} s^{-1}) was model using the Lambert-Beers law (Monsi and Saeki, 1953; Thornley, 2002; Marcelis et al., 1998):

$$I_{abs} = \frac{(1 - \alpha)\, I_0\, (1 - \exp\,(-k \times L))}{L} \qquad \text{Eqn (4-6a)}$$

where α denotes the reflection coefficient, k extinction coefficient, and L cumulative leaf area index, and I_o (µmol photon m^{-2} s^{-1}) the above canopy irradiance. A homogeneous canopy was assumed with leaves of the same photosynthetic characteristics and that the leaf angle distribution was random.

Net assimilation

For photosynthesis, the parameters of the FvC such as parameters of Rubisco kinetics and maximum electron transport rate (Farquhar et al. (1980)) for standard leaf temperature 25°C, and the mesophyll and stomatal conductance to CO_2 (g_m and g_s, mol CO_2 m^{-2} s^{-1}) are model inputs from measurements and calibrations, respectively.

The daily integral of canopy gross assimilation rate (P_{gd}, g CH_2O m^{-2} ground d^{-1}) was calculated by multiplying the instantaneous photosynthesis rate of the whole canopy P_t (µmol CO_2 m^{-2} ground s^{-1}) with a constant conversion factor 2.59.

P_t was determined as the product between the steady-state averaged leaf photosynthesis rate (P_n, µmol CO_2 m^{-2} leaf s^{-1}) and the cumulative leaf area index, L (m^2 leaf m^{-2} ground):

$$P_t = P_n \times L. \tag{Eqn 4-6b}$$

The leaf photosynthetic rate P_n was determined as the minimum of RuBP-carboxylation limited (P_c, µmol CO_2 $m^{-2}s^{-1}$) and RuBP-regeneration limited (P_j, µmol CO_2 $m^{-2}s^{-1}$) following the biochemical model developed by Farquhar et al. (1980):

$$P_n = \min (P_c, P_j), \tag{Eqn 4-6c}$$

with

$$P_c = \frac{V_{cmax} (C_c - \Gamma^*)}{C_c + K_c (1 + O/K_o)} - R_d \tag{Eqn 4-6d}$$

and

$$P_j = \frac{J(C_c - \Gamma^*)}{4C_c + 8\Gamma^*} - R_d \tag{Eqn 4-6e}$$

where (V_{cmax}, µmol CO_2 m^{-2} s^{-1}) is maximum rate of rubisco activity at the site of carboxylation, Cc (µmol CO_2 mol^{-1}) CO_2 partial pressure near Rubisco, C_i (µmol CO_2 mol^{-1}) intercellular carbon dioxide concentration, g_m and g_s mesophyll and stomatal conductance to CO_2, Γ^* (µmol CO_2 m^{-2} s^{-1}) carbon dioxide compensation point in the absence of mitochondrial (dark) respiration, K_c (µmol CO_2 mol^{-1}) and K_o (mmol O_2 mol^{-1}) the Michaelis-Menten constants of Rubisco for the carboxylation and oxygenation reactions, respectively; O (mmol O_2 mol^{-1}) the O_2 concentration at the site of the carboxylation, and R_d (µmol CO_2 m^{-2} s^{-1}) the daytime respiration rate.

CO_2 partial pressure near Rubisco C_c depends on steady-state stomatal conductance (g_{sc}, mol CO_2 m^{-2} s^{-1}) and mesophyll conductance (g_m, mol CO_2 m^{-2} s^{-1}) to CO_2.

$$C_c = C_a - P_n \times \left(\frac{g_s + g_m}{g_s \times g_m}\right) \tag{Eqn 4-6f}$$

where C_a (µmol CO_2 mol^{-1}) is atmospheric CO_2 concentration and g_m (mol CO_2 m^{-2} s^{-1}) an input constant.

Stomatal conductance to CO_2 g_s (mol CO_2 m^{-2} s^{-1}) was derived from stomatal conductance to water vapour g_{sw} (mol H_2O m^{-2} s^{-1}) (input from transpiration module) by using the ratio of the diffusivities of CO_2, and coupling the function of soil drying:

$$g_s(W_{ts}) = \frac{g_{sw}}{1.6} \times \begin{cases} s_g(W_{ts} - c_g) + 1, & W_{ts} > c_g \\ 1, & W_{ts} \leq c_g \end{cases} \qquad \text{(Eqn 4-6g)}$$

in which s_g and c_g are genotype-specific parameters describing the slope and soil water threshold at which g_s starts declining in response to drought stress. Here g_{sw} was separately calibrated (see Transpiration module) from the measured dataset of leaf g_{sw} and plant transpiration T_p (kg per plant d^{-1}) under unstressed condition (Eqn 4-9c).

The steady-state P_c under well-watered and drought-stressed condition was solved analytically with Eqn (4-6d) and (4-6f), and P$_j$ with Eqs (4-6e) and (4-6f) following Moualeu-Ngangue et al. (2016). Model variables and coefficients are listed in **Tables 4–6** and **4-7**.

Daytime respiration R_d was calculated as a function of leaf temperature:

$$R_d = R_{d,25} \, Q_{10,l}^{\,(0.1(T_l - 25))} \qquad \text{(Eqn 4-6h)}$$

in which $R_{d,25}$ is daytime respiration rate at reference leaf temperature T_l of 25°C and $Q_{10,l}$ the ratio between daytime respirations at T_l+10 and T_l. Leaf temperature is assumed to be equal to greenhouse air temperature T_a.

Photosystem II electron transport rate J (µmol e$^-$ m^{-2} s^{-1}) is determined depending on photosynthetic photon flux density absorbed per unit leaf area (big leaf approach) (I_{abs}, µmol photon m^{-2} s^{-1}) (Farquhar and Wong, 1984; Ögren and Evans, 1993; Buckley and Diaz-Espejo, 2015):

$$J = \frac{k_{2LL}\,I_{abs} + J_{max} - \sqrt{(k_{2LL}I_{abs} + J_{max})^2 - 4\,\theta_J\,k_{2LL}\,I_{abs}\,J_{max}}}{2\theta_J} \qquad \text{(Eqn 4-6i)}$$

where k_{2LL} (µmol e$^-$ µmol^{-1}photon) denotes conversion efficiency of I_{abs} to J at limiting light, J_{max} (µmol e$^-$ m^{-2} s^{-1}) maximum electron transport rate and θ_J (unit-less) a convexity factor for the response of J to I_{abs}.

J_{max} was calculated from the measured electron transport rate J_{high} at high irradiance I_{high} (1500 µmol photon m^{-2} s^{-1}) according to Buckley and Diaz-Espejo (2015):

$$J_{max} = J_{high}\left(1 + \frac{(1 - \theta_J)J_{high}}{k_{2LL}I_{high} - J_{high}}\right) \qquad \text{(Eqn 4-6j)}$$

An Arrhenius function of the form described the temperature dependence of the other Rubisco kinetic parameters and that of the J_{max} following Caemmerer et al. (2009).

Sensitivities of V_{cmax} and J_{max} upon soil water status were determined by using empirical logistic functions following the approaches of Zhou et al. (2013) and Tuzet et al. (2003), but substituting with W_{ts} instead of predawn leaf water potential:

$$f_c(W_{ts}) = \frac{1 + exp(-f_{cw}W_{tsc})}{1 + exp[-f_{cw}(W_{ts} - W_{tsc})]} \qquad \text{(Eqn 4-6k)}$$

and

$$f_j(W_{ts}) = \frac{1 + exp(-f_{jw}W_{tsj})}{1 + exp[-f_{jw}(W_{ts} - W_{tsj})]} \qquad \text{(Eqn 4-6l)}$$

where $f_c(W_{ts})$ accounts for the relative effect of W_{ts} on apparent V_{cmax}, f_{cw} the sensitivity parameter indicating the steepness of the decline and, W_{tsc} a reference value indicating the soil water at which $f_c(W_{ts})$ decreases to half of its maximum value. The function $f_j(W_{ts})$ and the parameters f_{jw} and W_{tsj} are those of J_{max}.

Dry matter production

For dry matter production, daily gross assimilation rate, air temperature, thermal time, maximum relative growth rate are inputs. Based on the dry matter production models described in SUKAM (Gijzen, 1992), SUCROS87 (Spitters et al., 1989), and TOMSIM (Heuvelink, 1996a), the potential growth rates of tomato introgression lines $G_{t,pot}$ are simulated, i.e dry matter accumulation under pest, disease and weed-free environment under the prevailing greenhouse conditions of well- watered and drought stressed scenarios:

$$G_{t,pot} = C_f \left\{ P_{gd} - R_m[1 - exp\ (-f \times rgr)] \right\} \qquad \text{(Eqn 4-7a)}$$

where $G_{t,pot}$ is potential dry matter accumulation rate (g DM m^{-2} ground d^{-1}), C_f the conversion efficiency from assimilates to dry matter, P_{gd} the canopy gross assimilation rate per unit ground area (g CH$_2$O m^{-2} ground d^{-1}), R_m the maximum maintenance respiration rate per unit ground area (g CH$_2$O m^{-2} ground d^{-1}), f the regression parameter estimated for greenhouse tomato (Heuvelink, 1995; 1996b) and rgr relative growth rate of the plant (g g^{-1}).

R_m is calculated from the weights of the plant parts (leaves, stems, roots, (fruits)) multiplied by their specific maintenance coefficients, which depend on temperature only:

$$R_m(T_a) = (k_{ml}W_l + k_{ms}W_s + k_{mr}W_r + k_{mf}W_f) \, Q_{10,c}^{(0.1(T_a-25))} \qquad \text{(Eqn 4-7b)}$$

where k_{mx} and W_x are maintenance coefficients (g CH_2O g^{-1} DM d^{-1}) and dry weights (g DM m^{-2} ground) of specific organs (i.e. subscripts: L, leaf, S, stem, R, root, F, fruit), and $Q_{10,c}$ the ratio between maintenance respirations at $T_a + 10$ and reference temperature 25°C (≈ 2.0). The R_m of fruit is also calculated although the fruit production is not yet considered in the model. *RGR* follows the logistic decay as a function of plant physiological age (°Cd):

$$rgr(t) = \frac{rgr_{max}}{1 + exp\left\{-(TS(t) - TS_{inf})/h_g\right\}} \qquad \text{(Eqn 4-7c)}$$

where rgr_{max} is maximum *rgr*, TS_{inf} and h_g inflexion point when rgr has reached the half of the maximum rate and standard deviation of *rgr* decay function.

Assimilate requirements (or growth respirations R_g) are computed for different plant parts and described in terms of a crop conversion efficiency (C_f) (equivalent to *1-R_g*) of assimilates to dry matter (g DM g^{-1} CH_2O).

$$C_f = 1/(f_l ASR_l + f_s ASR_s + f_r ASR_r + f_f ASR_f) \qquad \text{(Eqn 4-7d)}$$

where ASR_x and f_x are assimilate requirements (g CH_2O g^{-1} DM) and partitioning factors (or relative sink strength) of different plant organs: leaves, stem, root, fruit (subscripts *l, s, r, f*). Parameter values of R_m and ASR_x of C_f were taken from TOMSIM (1.0) (Bertin and Heuvelink, 1993; Heuvelink, 1995; Spitters et al., 1989), based on the calculation of Spitters et al. (1989), and f_r was empirically derived for different genotypes separately for stressed and unstressed conditions.

Dry mass fraction available for the leaf portion $M_{l,sup}$ (g DM m^{-2} ground d^{-1}) can be derived from total potential growth $G_{t,pot}$ (g DM m^{-2} ground d^{-1}) by multiplication with partitioning factor for leaf portion f_l.

$$M_{l,sup} = G_{t,pot} \times f_l \qquad \text{(Eqn 4-7e)}$$

Dry matter partitioning

For dry matter partitioning, sink capacity of leaf (from leaf growth and development module), partitioning factors are inputs and soil water status are inputs.

It is assumed that there was a common assimilate pool, and that dry matter partitioning was independent from dry matter production (Heuvelink, 1996a; Marcelis, 1994). It is further

assumed that the priority for each of vegetative organs (total leaf, stem, roots) for partitioning was equal under non-stressed conditions. The fraction of partitioning (relative sink strength) f_x was described by:

$$f_x = \frac{G_x}{\sum_{i=1}^{n} G_x}$$
(Eqn 4-8a)

where G_x (g DM m^{-2} ground d^{-1}) refers to growth rates (or sink capacity) of different organs: leaf G_l, stem G_s and root G_r, and $\sum_{i=1}^{n} G_x$ growth rate of the whole canopy (G_t, g DM m^{-2} ground d^{-1}). If f_x was assumed constant for a given genotype, G_x could be calculated depending on total dry matter increase G_t ($i.e. \sum_{i=1}^{n} G_x$) and f$_x$. Actual G_t at time t was computed back from actual leaf growth rate G_l (g DM m^{-2} ground d^{-1}) and partitioning fraction of total leaf component f_l:

$$G_t(t) = G_l(t) \times 1/f_l$$
(Eqn 4-8b)

where G_l is the state variable from leaf growth module and f_l is an input parameter set by 0.65 (74% of shoot dry matter increase G_{sh}) for both well-watered and drought-stressed conditions.

Drought effect on shoot/root ratio was described as a relative change in root partitioning. It was assumed a genotype-specific constant, without accounting the phenological development stage. The fraction of root partitioning for unstressed condition f_{rw} was a genotype-specific constant (e.g. 0.12 for reference variety M82). The sensitivity of f_r to soil water depletion was assumed to follow a logistic function:

$$f_r(W_{ts}) = f_{rw} \times \frac{1 + \exp(\alpha_{rw} W_{tsr})}{1 + \exp[\alpha_{rw}(W_{tsr} - W_{ts})]}$$
(Eqn 4-8c)

where the function $f_r(W_{ts})$ denotes the fraction of root partitioning (relative sink strength), α_{rw} the steepness parameter of relative sensitivity and w_{tsr} a reference value of W_{ts} at which the sensitivity increases to half of its maximum value (1.0). A shift of partitioning starts when the soil water reaches below the threshold point for leaf expansion rate c_L.

Root growth rate G_r (g DM m^{-2} ground d^{-1}) at any time t was described as a function of total growth rate and partitioning factor of root:

$$G_r(t) = f_r \times G_t(t).$$
(Eqn 4-8d)

The growth rate of above-ground matter (i.e. increase of shoot dry weight) G_{sh} (g DM m^{-2} ground d^{-1}) was described depending on the growth rate of the whole plant and relative sink strength (partitioning factor) of root portion f_r.

$$G_{sh}(t) = G_t(t) \times (1 - f_r) \qquad \text{(Eqn 4-8e)}$$

The growth rate of stem G_s (g DM m^{-2} ground d^{-1}) was, therefore, the difference between G_{sh} and G_l.

For individual plant, shoot dry weight (W_{sh}, g DM per plant) at time t was the integral of shoot growth rate per plant G_{sh} (g DM per plant d^{-1}), after taking account of the area occupied by a plant:

$$W_{sh}(t) = a_{gp} \int_0^t G_{sh}(x) \; dx \qquad \text{Eqn (4-8f)}$$

where the parameter a_{gp} is the ground area per plant (0.134 m^2 per plant). The dry weights of other organs (i.e. $W_l, W_s, W_r, (W_f)$) were computed in a similar way.

As mentioned in TOMSIM, when the assimilate supply exceeds the sink capacity, a reserve pool will be formed which will be added to assimilate pool of the next time step (day). Possible negative feedback of growth condition to photosynthesis was not considered.

Plant transpiration and soil water uptake

In this module, various environmental variables such as global radiation, temperature and relative and plant parameters such as leaf area index, plant height, genotype specific parameters for soil water responses were model inputs. The module used the daily time step t.

Plant transpiration

Canopy transpiration of tomatoes introgression lines was modelled using Penman-Monteith type equation, by assuming two surface layers in aerodynamic term according to Stanghellini model for greenhouse tomatoes (Stanghellini, 1987). Simulations were performed in a stepwise manner, first potential transpiration rate under unstressed condition was simulated, and then the drought effect introduced.

Potential transpiration rate per unit leaf area (ϵ, kg m^{-2} d^{-1}) was determined using the radiation level absorbed by the unit leaf area index of the crop:

$$\epsilon = \frac{s\,(Rn - G) + (2\,\rho_a\,C_p \delta e\,g_a k_t)}{\lambda[(s + \gamma\,(1 + g_a/g_{sw})]} \qquad \text{(Eqn 4-9a)}$$

where s was the slope of the saturation vapour pressure curve (kPa K^{-1}), R_n the net radiation intercepted by unit leaf area index (MJ m^{-2} d^{-1}), G the soil heat flux (MJ m^{-2} d^{-1}), 2 two

surface layers of unit (big) leaf exchanging heat with the air, ρ_a the mean atmospheric density (kg m^{-3}), C_p specific heat of moist air (= 0.001013 MJ kg^{-1} K^{-1}), δe the vapour pressure deficit (kPa), k_t the time unit conversion factor (86400 s d^{-1}), λ the latent heat for vaporization of water (≈ 2.45 MJ kg^{-1}), γ the psychrometric constant (≈ 0.0665 kPa K^{-1}), g_a the aerodynamic conductance (m s^{-1}), and g_{sw} the bulk (canopy) surface conductance to water vapour (m s^{-1}). Exact values of ρ, γ, λ, and s were computed at each time step, depending on the prevailing mean air temperature (Jones, 1992).

Net radiation absorbed by the unit leaf area of the crop per unit ground area was calculated based on Beer's law of exponential extinction down a homogeneous canopy following Katsoulas and Stanghellini (2019):

$$R_n = \frac{(1 - \alpha)\, R_0\, (1 - exp\, (-k \times L))}{L} \qquad \text{(Eqn 4-9b)}$$

where R_0 (MJ m^{-2} d^{-1}) is the radiation level at the top of the canopy, α canopy reflection coefficient, k extinction coefficient and L cumulative leaf area index. The default values for k and α were 0.7 and 0.07, respectively (Marcelis et al., 1998).

Plant transpiration rate T_p (kg per plant d^{-1}) was calculated as the product of plant leaf area (m^2 per plant) and ϵ which was subject to be effected by drought depending on the threshold for either normalized specific transpiration ratio r_ε or relative stomatal conductance r_g, and their corresponding slopes of the linear decline similarly to Eqn (4-3e):

$$T_p(t) = A_l(t) \times \epsilon(t) \times f_{\varepsilon\, or\, g}(W_{ts}), \qquad \text{(Eqn 4-9c)}$$

$$f_\varepsilon(W_{ts}) = \begin{cases} s_\varepsilon(W_{ts}(t) - c_\varepsilon) + 1, & W_{ts}(t) < c_\varepsilon\,, \\ 1, & W_{ts}(t) \geq c_\varepsilon \end{cases} \qquad \text{(Eqn 4-9d)}$$

$$f_g(W_{ts}) = \begin{cases} s_g(W_{ts}(t) - c_g) + 1, & W_{ts}(t) < c_g\,, \\ 1, & W_{ts}(t) \geq c_g \end{cases} \qquad \text{(Eqn 4-9e)}$$

in which the leaf area A_l is input from leaf growth and development module. Total water transpired during the stressed period ($T_{p,sum}$ kg per plant) was the integral of the daily plant transpiration during the stress period:

$$T_{p,sum} = \int_{t_{d0}}^{t} T_p(t)\, dt \qquad \text{(Eqn 4-9f)}$$

where t_{d0} is time of drought imposition. The difference between t and t_{d0} is the duration of drought stress Δt_d.

Potential stomatal conductance to water vapour

Based on the approaches of Jarvis (1976) and Noe and Giersch (2004), stomatal conductance to water vapour g_{sw} (mol H_2O m^{-2} s^{-1}) was determined as a function of genotype-specific maximum stomatal conductance g_{smax} (mol H_2O m^{-2} s^{-1}), the normalized effects of the absorbed light intensity I_{abs} (μmol photon m^{-2} s^{-1}) and air vapour pressure deficit δe (kPa).

$$g_{sw}(I_{abs}, \delta e) = g_{smax} \times \min\ \{f(I_{abs}), f(\delta e)\} \qquad \text{(Eqn 4-9g)}$$

The normalized effect of absorbed light intensity on g_{sw} was described by a saturation function of extended Michaelis-Menten form (non-rectangular hyperbola) (Thornley and Johnson, 1990; Noe and Giersch, 2004):

$$f(I_{abs}) = g_{smin} + \frac{\alpha_g I_{abs} + (1 - g_{smin}) - \sqrt{(\alpha_g I_{abs} + (1 - g_{smin}))^2 - 4\,\theta_g\,\alpha_g I_{abs}\,(1 - g_{smin})}}{2\theta_g} \qquad \text{(Eqn 4-9h)}$$

where, g_{smin} was minimum stomatal conductance to water vapour during the night (mol H_2O m^{-2} s^{-1}), α_g the slope at zero irradiance and θ_g a shape parameter for $f(I_{abs})$. Stomatal response to evaporative demand δe was described by a modified hyperbolic decay function, according to Lohammar et al. (1980) and Leuning (1995):

$$f(\delta e) = \begin{cases} 1/(1 + \delta e\,(t)/\delta e_0), & \delta e\,(t) > 0 \\ 1, & \delta e\,(t) \leq 0 \end{cases} \qquad \text{(Eqn 4-9i)}$$

where the parameter δe_0 regulates the effect of δe on g_{sw}, the smaller its magnitude, the more decrease in g_{sw}.

Fraction of transpirable soil water

Under drought stress, the fraction of transpirable soil water (W_{ts}) at time t was determined as the ratio between the current transpirable soil water ($W_n(t) - W_{fn}$) (kg H_2O dm^{-3} soil) and total transpirable soil water ($W_0 - W_{fn}$) (kg H_2O dm^{-3} soil):

$$W_{ts}(t) = \frac{W_n - W_{fn}}{W_0 - W_{fn}}, \qquad \text{(Eqn 4-10a)}$$

where W_n is the current soil water status (kg H_2O per pot) and W_0 and W_{fn} soil water contents at 100% WHC and at 10% transpiration of the controlled plants (kg H_2O per pot). Current weight of soil water W_n (kg H_2O per pot) is computed as the initial soil water content minus the integral of the dynamics of plant transpiration (kg H_2O per plant d^{-1}):

$$W_n = W_0 - \int_{t_{d0}}^{t} T_p(t)\, dt, \qquad \text{(Eqn 4-10b)}$$

$$W_0 = \rho_s \times \theta_s \times \beta_0 \qquad \text{(Eqn 4-10c)}$$

$$W_{fn} = \rho_s \times \theta_s \times \beta_f \qquad \text{(Eqn 4-10d)}$$

where θ_s is the volume of soil in the pot at 100% WHC (10 dm^3 soil per pot), t_{d0} the day zero of drought imposition (°Cd), ρ_s (1.25 kg dm^{-3}) soil bulk density, β_0 the water holding capacity (0.28 kg H_2O kg^{-1} soil), and β_f the endpoint of available soil water (0.06 kg H_2O kg^{-1} soil).

Simulation and model evaluation

For the simulation, the aggregated model was dissected into sub-cases namely i) leaf growth and development, ii) transpiration and water uptake, and iii) photosynthesis, dry mass production and partitioning. Under drought stress, major plant functions were assumed to be limited by the soil water (W_{ts}). Leaf area A_l was a key medium for a balance and transfer of energy, carbon and water (and nutrients), and both organ and canopy level expansive growth of a genotype was assumed to be dependent on thermal time, organogenesis, expansion duration and source-sink balance. For the modal validation of combined modules at the higher level of the hierarchy, the simulation scheme for both unstressed- and stressed-conditions was designed with five stepwise levels:

1) Simulating transpiration and shoot dry mass with the inputs of both W_{ts} and A_l.
2) Simulating leaf area, transpiration and shoot dry mass with the input of W_{ts},
3) Simulating transpiration, shoot dry mass and soil water with the input of A_l,
4) Simulating leaf area, transpiration, shoot dry mass and soil water with no inputs of W_{ts} and A$_l$ (aggregated model),
5) Simulating stressed-transpiration with or without the inputs of unstressed A_l, using the QTLs for thresholds of leaf expansion rate, specific transpiration rate and stomatal conductance.

The simulations were run from step 1 to 4 for all 52 tomatoes lines using a genome-based mechanistic growth model of tomato introgression lines (called TILSIM, **T**omato **I**ntrogression **L**ines **SIM**ulator), developed on a Java platform (Apache NetBeans IDE). The last simulation was performed in a Microsoft excel program using the required outputs of simulation in TILSIM and integrating them in the QTL-based model, where drought reaction parameters controlled the stressed performances. The detailed procedure of this part is described in Chapter 3.

The simulations and model evaluation were performed for three independent greenhouse conditions (Expt. (5), (6) and (7) (May - October 2017)), which can be characterized by the averaged daytime vapour pressure deficit of 2.3 (±0.24), 1.9 (±0.22) and 1.4 (±0.07) kPa, respectively. Dynamic and static data of targeted output variables and measured data were drawn in 1:1 line regressions. As the dynamic data, leaf areas, plant transpiration, and fraction of transpirable soil water were evaluated. As the static data, the simulated total leaf area and total water transpired and shoot dry weight were evaluated. Statistics of the evaluation of model outputs were slope and intercept of the linear function, coefficient of regression, root mean square error (RMSE), bias, and accuracy (Kahlen and Stützel, 2011; Kobayashi and Salam, 2000).

Plant materials for model parameterization and evaluation

The tomato genome library of *Solanum pennellii* (Sp) LA0716 comprising 50 introgression lines (ILs)) in the genetic background of the recurrent domesticated parent (*Solanum lycopersicum* cv. M82 LA3475) was used in this experiment. The seeds were kindly provided by C.M. Rick Tomato Genetics Resource Center (TGRC), University of California, Davis, USA. Each of the ILs contained a single RFLP marker defined chromosome segment of Sp genome**.** The introgression lines contained an average of 33 cM from a total genome size of 1200 cM (2.75%) with overlapping regions between neighbouring lines, covering the complete Sp genome (Eshed and Zamir, 1995).

Plant cultivations and setup of experimental trials

Pot experiments were conducted in a greenhouse of the Institute for Horticultural Production Systems, Leibniz Universität Hannover (52.5° N, 9.7° E). 10L plastic pots (25 cm height and 24 cm diameter) were filled with loess soil obtained from the Ruthe research station, south of Hannover, soil bulk density of 1.25 g cm^{-3}. The pot's water holding capacity (WHC) was

measured to be 0.28 (w/w) (0.35 (v/v)). The pots were filled with water until ca. 100% of WHC, and the whole block was covered with plastic sheets to prevent evaporative loss before the onset of the experiment. The experiment was laid out in RCBD using seven different periods from June 2016 and October 2017, from which the first four trials were used as blocks for parameterization, and the last three for model evaluation. Temperature sum (GDD) and air vapour pressure deficits (δe, kPa) were calculated by using the daily maximum and minimum air temperature and humidity. The averaged δe conditions ranged from 1.2 to 2.6 kPa for the first four trials and 1.4 and 2.3 kPa for the three trials of evaluation.

For the establishment, eight seeds of each introgression line and 16 seeds of each parent line were sown in separate cells (50 cm^3) of plastic trays using peat-based growing media (>90% organic matter, pH 5.5-6.5, EC 0.7-1.2, bulk density 330-430 kg m^{-3}, Potgrond H, Klasmann-Delimann, Germany). Emergence started in most lines about four days after sowing (DAS). When two leaves were fully unfolded (153°Cd, ca.10 DAS at 25°C), the four most uniform seedlings were transplanted, two to the main experimental pots, and two to 2L pots to take initial data. During the experimental period, the average daily temperature was 25.0°C (17.0–37.7 °C), and relative humidity in the glasshouse was 63.4% (50.6–87.8%). Fertilizers (Ferty$^®$ 2 Special, Planta, GMBH, Germany) were applied with the irrigation water before the drying cycle at a rate corresponding to 160 kg N ha^{-1}, 60 kg P$_2$O$_5$ ha^{-1} and 260 kg K$_2$O ha^{-1}.

During the first 2-3 weeks (until 6–8 leaves emerged) all the pots were irrigated daily. At drought stress imposition (7th leaf initiation stage of most lines, ca. 350°Cd), initial data on morphological and dry matter traits were recorded from plants grown in the 2L pots. Then half of the rest of the pots were irrigated daily to replenish into the initial well-watered conditions and the remaining half were subject to drought stress by withholding water supply until the transpiration rate of the stressed plants reached below 10% of the control. The soil surface was covered to a depth of ca. 4 cm with quartz gravels to minimize soil evaporation. Moreover, to take account of any evaporation, two pots without plants were allocated with similar conditions as treated pots. The pots were moved and rearranged every measurement day to have a random distribution in each set of the greenhouse. When necessary particularly in the morning and evening, we provided the supplementary light (400 W High-Pressure Sodium Lamp (HPS)) to ensure 14 hours of daylight with the required PPFD (average ca. 200 μmol m^2 s^{-1}). Throughout the experiment, the plants were kept single stand by removing the side shoots.

Measurements and parameter estimations

Leaf growth and development

Measurements of leaf length (cm) from the insertion point of petiole to the tip of the terminal leaflet were made for all growing leaves at the two-day interval for each genotype. The leaves of 1 cm length were considered for counting and measuring. The base temperature (7.7 °C) for leaf elongation estimated previously for M82 was used for all lines. The leaf appearance rate R_l (no. °Cd^{-1}) was computed from the linear regression of leaf number over temperature sum (*TS*). The leaf length data measured along the course of time was fitted to a simple logistic function to reproduce the daily data points. Allometric relationship between length and area of individual leaves was performed for each line by using an empirical power function (see in chapter 3), and dynamics of plant leaf area A_l (cm^2 per plant) estimated. Total A_l at harvest was measured by using the leaf area meter (LI3100; LICOR, Lincoln, NE, USA). The leaf expansion rate (E_i, cm^2 per leaf °Cd^{-1}) was computed as the ratio between the change in leaf area A_i (cm^2 per leaf) and the change in thermal time. Based on data of E_i for all leaves at different time, the maximum potential leaf expansion rate ($E_{i,max}$, cm^2 per leaf °Cd) was further recorded as a genotype coefficient.

Soil water uptake and transpiration

Daily measurement of soil water level was performed by taking the pot weight around 16:00 h every day. W_{ts} is was calculated as the ratio between the amount of transpirable soil water remaining in the pot and the total transpirable soil water according to Sinclair and Ludlow (1986). The detailed procedure is described in Chapter 3. Daily plant transpiration T_p (kg H$_2$O per plant d^{-1}) was determined as the difference in pot weights between two consecutive days. Canopy specific transpiration ϵ (kg H$_2$O m^{-2}leaf d^{-1}) was calculated as the ratio between T_p and A_l.

Stomatal conductance

In experiment 1 to 4, g_{sw} was measured daily on a fully expanded upper leaf per plant between 10:00– 13:00 h during the stressed period by using a steady-state porometer (LAI-1600, LI-COR Inc., Lincoln, NE, USA).

For using canopy conductance in transpiration module, velocity unit was converted into mole unit depending on the current air temperature and pressure:

$$g_s = (g_s' \, V_0) \times (T_a/T_0) \times (P_0/P) \qquad \text{(Eqn 4-11)}$$

where g_s is the canopy conductance in velocity unit (m s^{-1}), g_s' the canopy conductance in mole unit (mol m^{-2} s^{-1}), V_0 the molar volume of air (22.7 x 10^{-3} m^3 mol^{-1}) at T_0 (273 K) and P_0 (100 kPa).

Daily average plant stomatal conductance

The values of maximum stomatal conductance g_{smax} and the parameters in normalized effects of δe and light averaged for the whole day and canopy were estimated from the g_{sw} (called g_{sw}') derived from the inversion of Eqn 4-9a, using the net radiation R_n per unit canopy leaf area (MJ m^{-2} day^{-1}), vapour pressure deficit δe (kPa), measured values of specific transpiration ϵ (kg H$_2$O m^{-2} day^{-1}) and optimized value of aerodynamic conductance g_a (ms^{-1}) following Prado et al. (2018).

$$g_{sw}' = \frac{g_a \epsilon \lambda \gamma}{s\,(Rn - G) + \left(2\,\rho_a\,C_p \delta e\,g_a k_t\right) - \epsilon \lambda (s + \gamma)} \qquad \text{(Eqn 4-12)}$$

This calibration was performed for reference variety M82 in all trials conducted for parameter estimation under unstressed condition. The respected values of other lines were computed based on their average relative differences from M82 based on porometer data, and the distribution of g_{smax} is given in **Fig. 4-2**.

Aerodynamic conductance

Under the greenhouse condition, aerodynamic conductance g_a (m s^{-1}) is lower than field condition because of light wind speed if there is no force ventilation. Using the 24h average wind speed adjusted from inverse Penman (Eqn 4-12) and substituting the input of plant height in a place of reference grass height, g_a was calculated:

$$g_a = (U_z K)/\{ln\,(z_m - d\,)/z_{0m} \times ln\,(z_h - d)/z_{0h}\} \qquad \text{(Eqn 4-13)}$$

where U_z is the measured wind speed at $z = 2$m height (m s^{-1}), K the von Karman's constant (0.41), z_m and z_h the height of wind and humidity measurements (m), d the zero plane

displacement height (m), z_{0m} and z_{0h} roughness lengths governing the transfer of momentum (m) and that of heat and vapour (m).

Photosynthesis parameters

In experiment 5 to 7, the light-saturated net photosynthetic rate under PPFD of 1500 µmol photons m^{-2} s^{-1} (A_{1500}, µmol CO_2 m^{-2} s^{-1}) and short light response curves were measured weekly for all tomatoes lines using a portable photosynthesis system (LI-6800; Li-Cor Inc., Lincoln, NE, USA). Based on the light response curve, daytime respiration R_d was estimated following Yin method (Yin et al., 2011). All measurements were carried out under-sample CO_2 400 µmol mol^{-1}, leaf temperature 25 °C and relative humidity 55–65%. V_{cmax} was estimated using the one-point method (De Kauwe M. G. et al., 2016). Chlorophyll fluorescence was measured using the multiphase flash following Moualeu-Ngangue et al. (2017). Using the dataset of a standard A-C_i curve developed for recurrent line M82, simultaneous estimation of photosynthetic parameters J (J_{high}), V_{cmax} and g_m was done according to a new method of Moualeu-Ngangue et al. (2017). The estimated mesophyll conductance g_m was averaged and used as a constant for all tomato lines. The parameters estimated for well-watered condition only were used in the model as inputs.

Parameters of drought responses and associated QTLs

Relative leaf expansion rate r_L and relative stomatal conductance r_g were calculated as the ratios between stressed and control values. Normalized specific transpiration ratio r_ε was calculated according to Ray and Sinclair (1998) and Masinde et al. (2006). The detailed procedure is described in Chapter 3. Parameters of drought reactions in plant processes (r_L, r_g, r_ε) were estimated by using a linear-plateau regression model in nonlinear function PROC NLIN of SAS (SAS Institute Inc., Cary, NC, USA) as a function of W_{ts}:

$$r_\times = \begin{cases} s_\times \times (W_{ts} - c_\times) + 1, & W_{ts} < c_\times \\ 1, & elsewhere \end{cases} \qquad \text{(Eqn 4-14)}$$

where r_x is the magnitude of the relative trait in question, s_x the slope of the linear decline, and c_x the soil water threshold at which the relative trait began to decline.

After one- way ANOVA step, QTLs detection for drought reaction parameters was performed using the two-sided Dunnett test (Dunnett, 1955), based on the assumptions of Eshed and Zamir (1995). The detailed procedure of QTL detection for ILs was described in Chapter 3.

Results

Distribution of genotype specific parameters

The data set describes the mean of four trials for each of 52 tomatoes lines (**Fig. 4-2**). Between lines variation in parameter values is described by CV%, where the highest variation was exhibited by maximum leaf expansion rate $E_{i,max}$ and the lowest by maximum stomatal conductance $g_{sw,max}$. The recurrent M82 revealed a similar magnitude to average values for leaf appearance rate R_l and $g_{s,max}$. R_l, $g_{s,max}$ and maximum specific leaf area SLA_{max} somewhat followed the normal distribution, while the rest were skewed to the left (the side of mother line M82). The extreme values observed elsewhere were those of donor parent *Solanum pennellii* and IL6-2, which were characterized by relatively smaller plant sizes than the rest of lines. About 60% of lines showed the R_l ranging from 0.017 to 0.019 nr. $°Cd^{-1}$ and $E_{i,max}$ from 3 to 4cm^2 per leaf $°Cd^{-1}$. About 75% of lines showed the SLA_{max} by the range of 320 to 380 cm^2 g^{-1} and $g_{s,max}$ of 0.21 to 0.23 mol H_2O m^{-2}s^{-1}. Distribution in photosynthesis parameters $V_{c,max}$ and J_{max} indicate that about 75% of lines were characterized by J_{max} value of 210 - 230 μmol e$^-$m^{-2}s^{-1} while about 60% of lines exhibited the $V_{c,max}$ of 140 - 150 μmol CO_2 m^{-2}s^{-1} at estimated 25°C leaf temperature.
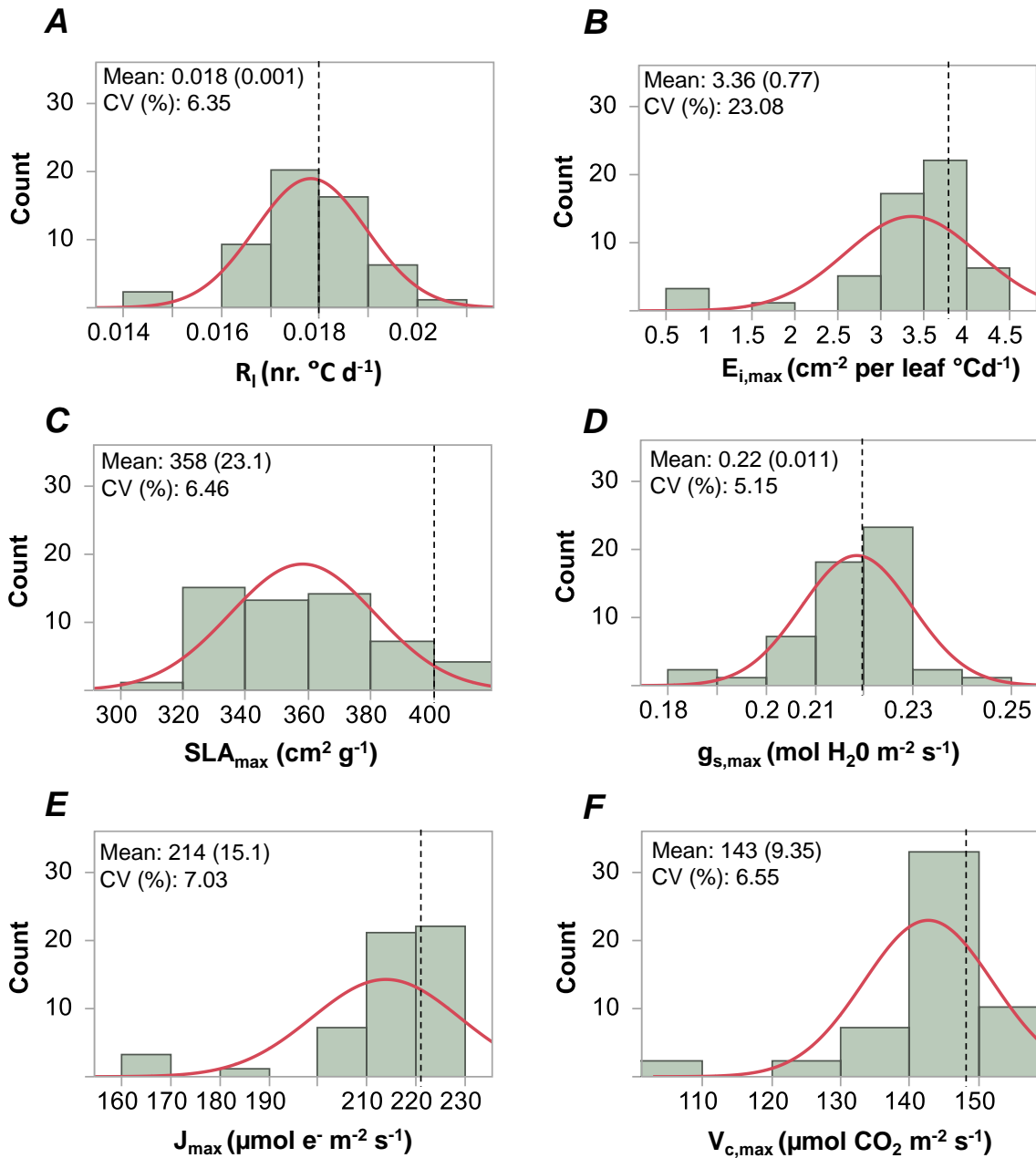
Fig. 4-2. Distribution of the genotype specific parameters of tomato lines. (A) leaf appearance rate, (B) leaf expansion rate, (C) maximum specific leaf area of plant, (D) maximum stomatal (canopy) conductance to water vapour, (E) maximum electron transport rate, (F) maximum Rubisco carboxylation rate. Dotted line describes the value of the recurrent parent cv. M82. Mean (SD) and CV (%) are provided in each figure. The bars are fitted by red solid normal curve. N = 52.

Leaf area

Without the input of the fraction of transpirable soil water W_{ts}, stressed leaf area A_l was simulated in the aggregated model. The predicted total plant leaf area A_l (cm^2 per plant) showed higher accuracy for well-watered (WW) plants than for drought-stressed (DS) ones (**Fig. 4-3**). Under DS, most lines with larger A_l were under-estimated and those of smaller ones over-estimated, whereas the regression was close to 1:1 line under WW condition. Predicted A_l during the stressed period showed a better fitting with higher and lower magnitudes of regression coefficients and intercepts, respectively than the total A_l at harvest time in both water supply treatments, resulting in higher coefficients of determination. For different trials, the accuracy of predictions under DS with the inputs of W_{ts} ranged from 0.60 to 0.66 during vegetative growth and 0.62 to 0.77 at final harvest, being the highest in trial with the lowest prevailing vapour pressure deficit (1.4 kPa in Expt.7) (**Table 4-1**). Predictions with and without the inputs of W_{ts} showed no clear trend of differences in A_l. Most of the under-estimations occurred in Expt. 6 (positive values of bias), and over-estimation in Expt. 7 especially under DS with W_{ts} input (**Fig. 4-4**).
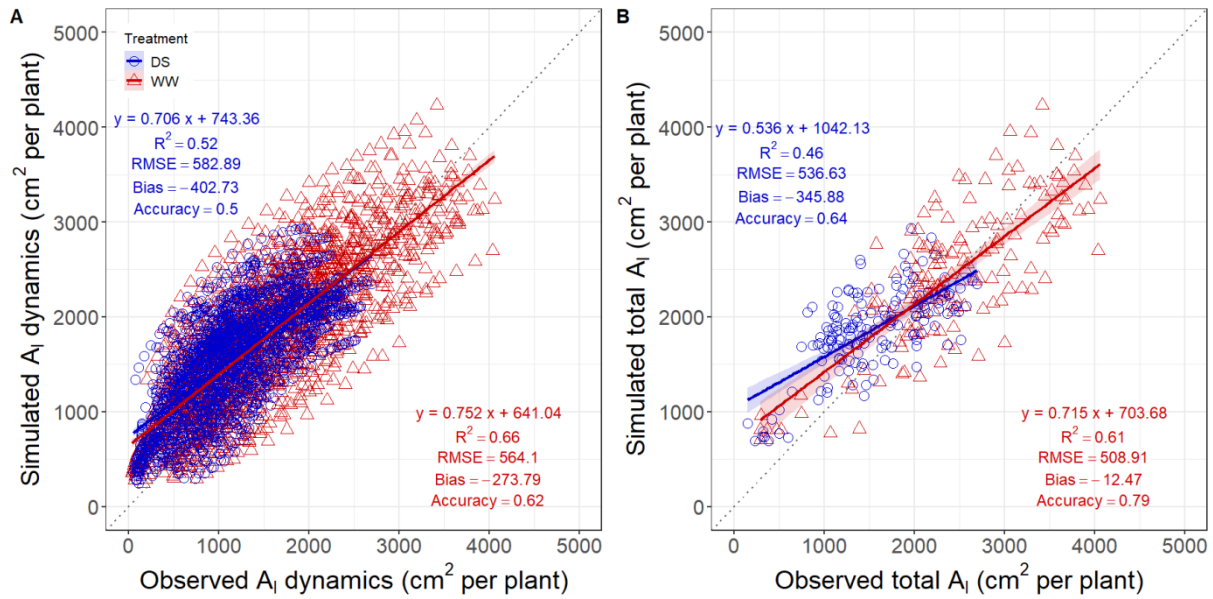
Fig. 4-3. Comparison of simulated and observed plant leaf area A_l (cm^2 per plant) of tomato lines under drought-stressed (DS) and well-watered (WW) conditions using aggregated model: (A) A_l during the treatment period; (B) total A_l at harvest Model evaluation was performed using the independent datasets of three greenhouse trials (May-Oct 2017).
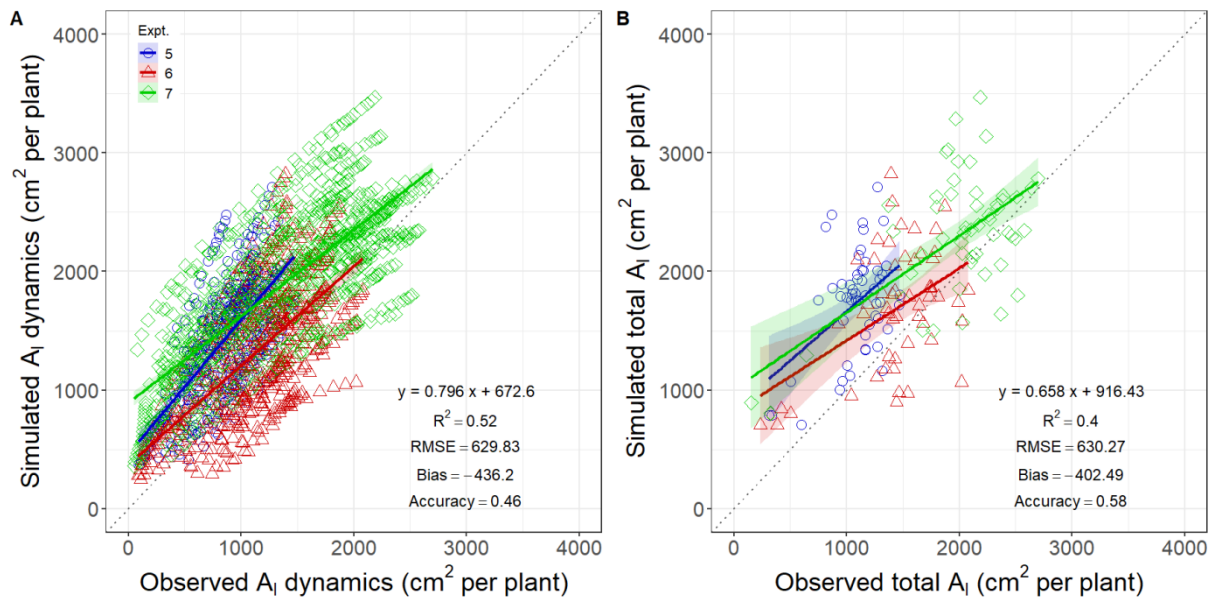
Fig. 4-4. Comparison of simulated and observed leaf area A_l (cm^2 per plant) of tomato lines under drought stress (DS) for three experiments with the input of W_{ts}: (A) A_l during the treatment period; (B) total A_l at harvest. Experiments (Expt. 5 - Expt.7) were characterized by the average day-time vapour pressure deficits of 2.3 ($\pm$0.24), 1.9 ($\pm$0.22), and 1.4 ($\pm$0.07) kPa, respectively.

Table 4-1. Statistical analysis of the comparison between simulated and observed data for A_l during the treatment (cm^2 per plant) and total A_l at harvest (cm^2 per plant) in two ways of simulation: with and without the input of fraction of transpirable soil water W_{ts}. Model evaluations were performed by using the independent datasets of three greenhouse trials (Apr-Oct 2017). WW, well-watered, DS, drought-stressed.

Trait	Treat.	Expt.	Without W_{ts} input					With W_{ts} input				
			Slope	R^2	RMSE	Bias	Accuracy	Slope	R^2	RMSE	Bias	Accuracy
A_l												
	WW	5	0.70	0.68	341	122	0.72	0.70	0.68	341	122	0.72
	WW	6	0.93	0.73	569	370	0.62	0.93	0.73	569	370	0.62
	WW	7	0.74	0.85	453	-109	0.72	0.74	0.85	453	-109	0.72
	DS	5	0.94	0.50	315	-143	0.63	0.87	0.41	334	-122	0.60
	DS	6	0.74	0.49	378	146	0.67	0.63	0.42	423	214	0.63
	DS	7	0.59	0.64	425	-111	0.68	0.70	0.65	451	-194	0.66
Total A_l												
	WW	5	0.63	0.41	456	241	0.76	0.63	0.41	456	241	0.76
	WW	6	0.67	0.34	656	394	0.72	0.67	0.34	656	394	0.72
	WW	7	0.97	0.65	558	264	0.82	0.97	0.65	558	264	0.82
	DS	5	0.65	0.29	344	-228	0.68	0.22	0.11	408	-189	0.62
	DS	6	0.47	0.33	327	-17.9	0.77	0.40	0.16	448	161	0.69
	DS	7	0.45	0.47	448	188	0.77	0.70	0.39	459	-0.25	0.77

Plant transpiration

Without the input of A_l, transpiration module used the simulated A_l of aggregated model and could have predicted the dynamics of plant transpiration T_p and total water transpired $T_{p,sum}$ of WW plants, with the accuracies of 0.58 and 0.69, respectively for the whole panel (50 lines) of genome library and two parent lines (**Fig. 4-5**). For DS condition, the accuracy was lower for T_p than for $T_{p,sum}$ as expected. The regression lines in both WW and DS conditions were almost parallel to 1:1 lines in $T_{p,sum}$, and regression coefficients (slope) were close to 1 (0.931 and 0.836) but with the high magnitudes of intercept, resulting in a slight over-estimations. With the input of A_l, the validity of the T_p module especially for $T_{p,sum}$ was much improved for both WW and DS conditions, exhibited by the most statistical figures: the 20% higher accuracy (0.83 vs 0.69), 39% higher coefficients of determination ($R^2 = 0.78$ vs 0.56), much less bias (0.012 vs -0.66 kg) and RMSE (0.729 vs 1.326 kg) than the ones run in aggregated mode (**Fig. 4-5B, D**). With the input of A_l, predicted values under DS condition showed the slope values greater than 1 (1.1) and low values of intercept being close to zero (0.279), indicating that the larger the plant size of lines the higher the risk of over-estimation. For WW condition, the regression line of simulated points showed an almost perfect fit with the 1:1 line between observed and simulated ones. Evaluations for different traits revealed that the improvement of prediction with the input of A_l occurred in all environmental conditions for both dynamic and sum data in both water supply treatments, being more evident in Expt. 5 and 7 than Expt. 6 (**Table 4-2**). Without the input of A_l, the model in aggregated mode predicted the $T_{p,sum}$ with a fairly high accuracy for both WW (0.70 to 82) and DS (0.57 to 0.68) conditions after taking account of the variability of prevailing environments under study. With the A_l input, the higher R^2 and higher magnitude of slope (close to 1) were exhibited only in Expt. 7 (1.4 kPa).
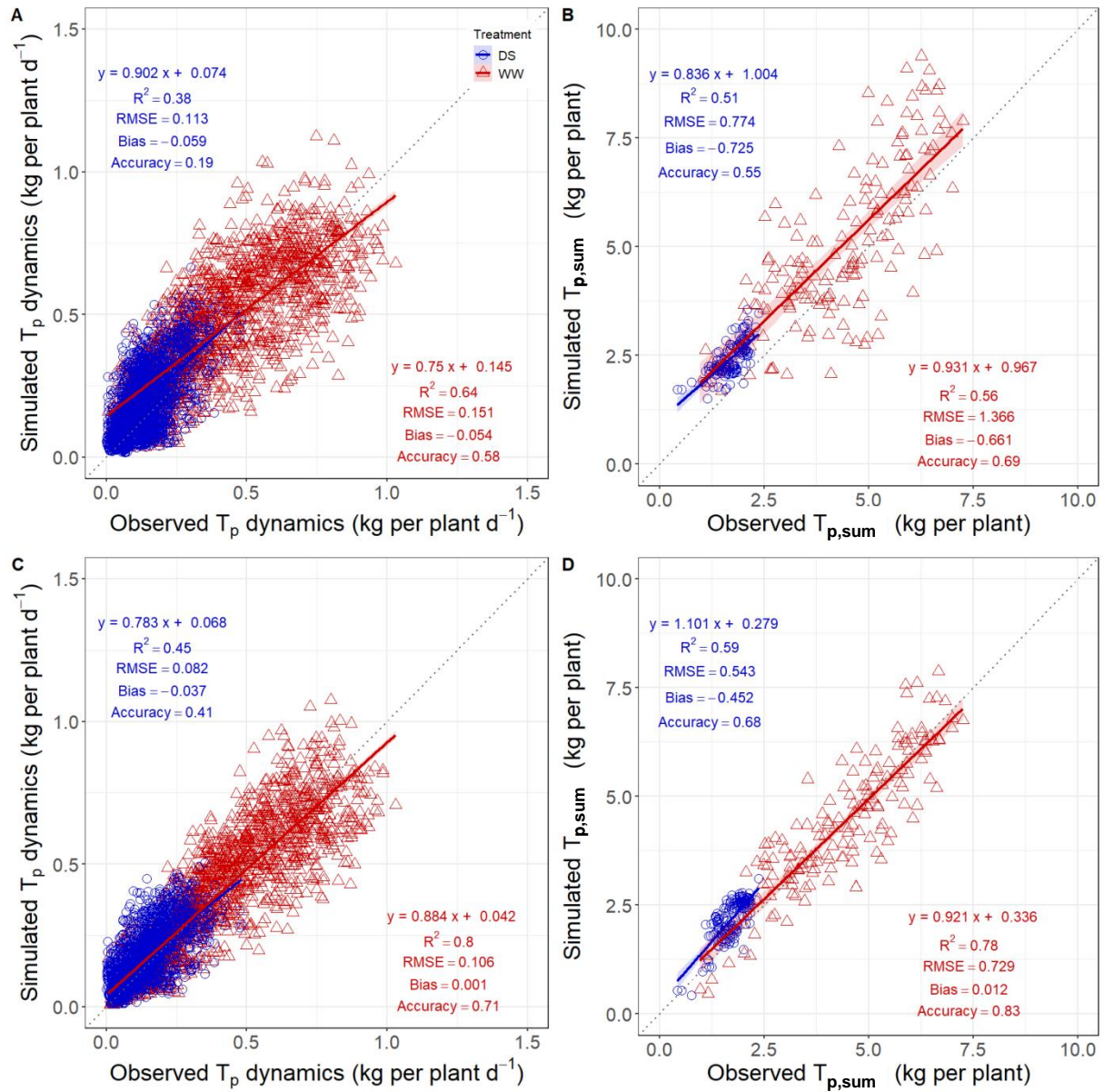
Fig. 4-5. Comparison of simulated and observed dynamics of plant transpiration T_p and total water transpired $T_{p,sum}$ of tomato lines under drought-stressed (DS) and well-watered (WW) conditions in two ways of simulation: (A-B) without and (C-D) with leaf area input. Model evaluations were done using the independent datasets of three greenhouse trials (Apr – Oct 2017). N = 1980 (T_p), 162 ($T_{p,sum}$).

Table 4-2. Statistical analysis of the comparison between simulated and observed data for T_p (kg per plant d^{-1}) and $T_{p,sum}$ (kg per plant) for the stress period in two ways of simulation: with and without the input of leaf area. Model evaluations were done using the independent datasets of three greenhouse trials (Apr – Oct 2017). WW, well-watered, DS, drought –stressed.

Trait	Treat.	Expt.	Without leaf area input					With leaf area input				
			Slope	R^2	RMSE	Bias	Accuracy	Slope	R^2	RMSE	Bias	Accuracy
T_p												
	WW	5	0.61	0.58	0.138	-0.006	0.62	0.70	0.68	0.126	-0.041	0.65
	WW	6	0.76	0.66	0.145	0.053	0.63	0.93	0.73	0.133	-0.031	0.66
	WW	7	0.55	0.71	0.139	-0.026	0.59	0.74	0.85	0.099	-0.004	0.71
	DS	5	0.73	0.51	0.096	-0.052	0.46	0.72	0.65	0.076	-0.042	0.57
	DS	6	0.51	0.16	0.124	-0.060	0.14	1.04	0.57	0.102	-0.064	0.28
	DS	7	0.94	0.23	0.102	-0.049	0.14	1.35	0.62	0.068	-0.036	0.42
$T_{p,sum}$												
	WW	5	0.40	0.17	0.940	-0.050	0.70	0.52	0.33	0.864	-0.380	0.73
	WW	6	0.50	0.22	1.155	0.608	0.74	0.94	0.62	0.769	-0.354	0.83
	WW	7	0.87	0.62	1.021	-0.431	0.82	1.03	0.83	0.636	-0.062	0.89
	DS	5	0.48	0.17	0.510	-0.455	0.68	0.93	0.47	0.415	-0.368	0.74
	DS	6	0.41	0.20	0.732	-0.677	0.55	0.64	0.26	0.805	-0.742	0.50
	DS	7	0.84	0.69	0.823	-0.795	0.57	1.40	0.89	0.626	-0.582	0.68

QTL-based plant transpiration

Using QTLs for soil water thresholds of leaf expansion rate c_L, stomatal conductance c_g and specific transpiration rate c_ε, predicted outputs of the stressed transpiration T_p with or without the input of unstressed A_l is described in **Fig. 4-6**. Without the input of A_l, outputs of the aggregated model such as unstressed T_p, leaf area and W_{ts} were simultaneously incorporated in QTL-based model for the prediction of the stressed T_p as mentioned in Chapter 3. The accuracy of predicted T_p revealed the over-estimation particularly in Expt. 6 (1.9 kPa), and high density of the occurrence with zero T_p. The overall accuracy was relatively low (0.35 with c_ε and 0.36 with c_g), although the global fitting was close to 1:1 line. With the input of unstressed A_l, the newly predicted outputs of unstressed T_p and W_{ts} were used in the scheme of QTL-based simulation procedure. The prediction was improved in terms of the most statistical figures, except bias. The use of QTLs for c_L and c_ε gave a slightly promising prediction as compared to that for c_L and c_g (**Fig. 4-6B, D**).

Table 4-3 describes the breakdown of the model evaluations into three different environments for both daily T_p along the stressed period and $T_{p,sum}$ without or with the inputs of unstressed A_l. Improvement of prediction accuracy with the input of A_l was mainly observed in Expt. 5 (2.3 kPa) and 7 (1.4 kPa) for both T_p and $T_{p,sum}$. With the use of QTLs for c_L and c_ε, the accuracies of prediction for $T_{p,sum}$ ranged from 0.65 to 0.75 without the input of A_l and 0.55 to 0.84 with the input of A_l. The incorporation of QTLs for c_L and c_ε in the model gave the outputs with the accuracy ranges of 0.64 to 0.75 and of 0.44 to 0.76 without and with A_l inputs, respectively. The most noticeable improvement was observed in Expt. 7, also in terms of the slope and R^2 no matter either pair of QTLs linked traits was applied.
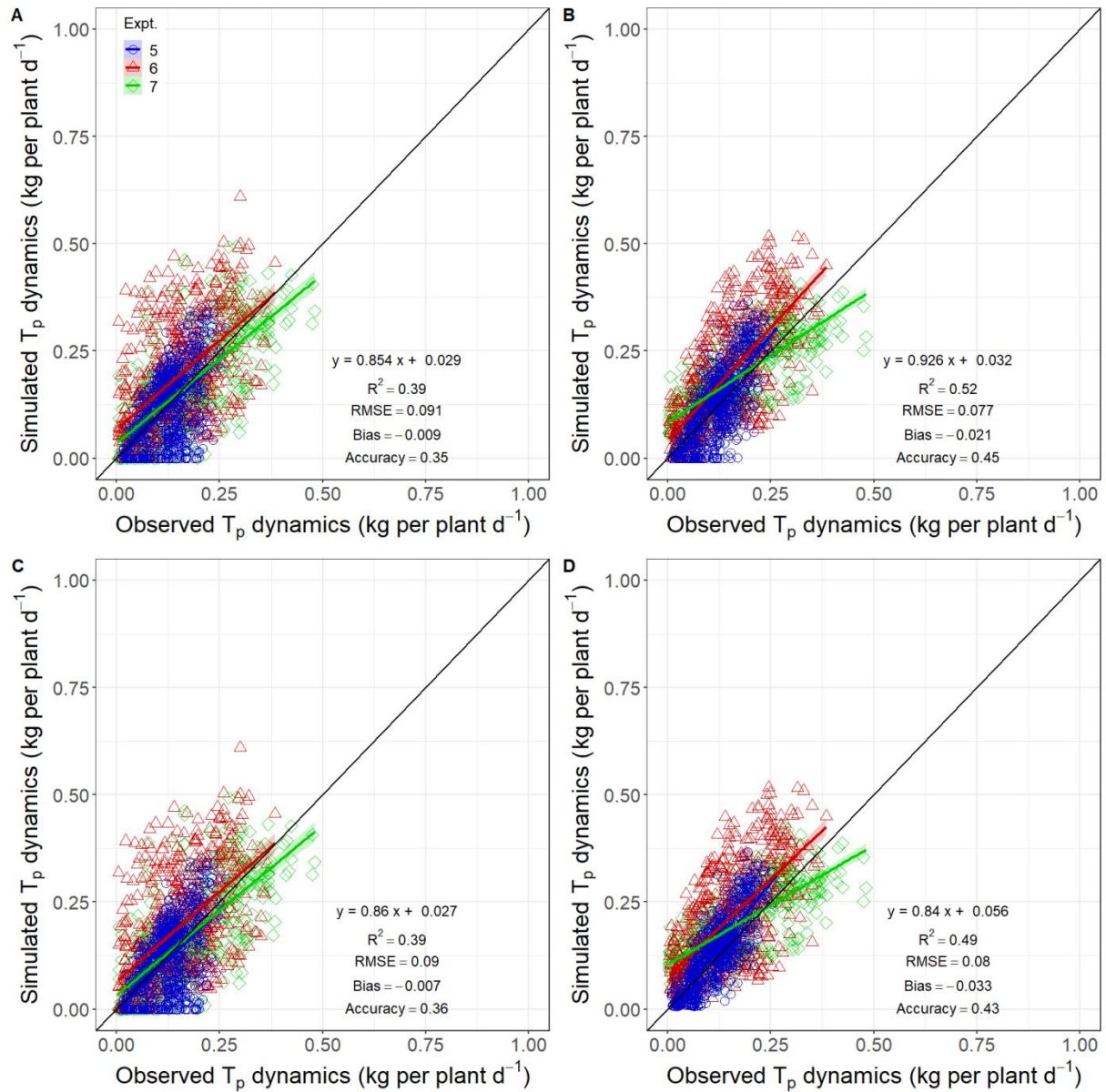
Fig. 4-6. Comparison of simulated and observed dynamics of plant transpiration T_p of tomato lines under drought-stressed condition using QTLs controlling soil water thresholds for leaf expansion c_L and that for (A-B) specific transpiration c_ε and (C-D) stomatal conductance c_g without and with unstressed A_l inputs, respectively. Experiments (Expt. 5 - Expt.7) were characterized by the average day-time vapour pressure deficits of 2.3 (±0.24), 1.9 (±0.22), and 1.4 (±0.07) kPa, respectively.

Table 4-3. Statistical analysis of the comparison between simulated and observed data for T_p (kg per plant d^{-1}) and $T_{p,sum}$ (kg per plant) in the integrated model using QTLs controlling soil water thresholds for leaf expansion c_L and that for specific transpiration c_ε and stomatal conductance c_g of the stressed plants relative to unstressed ones in two ways of simulation: with and without the input of unstressed leaf area. Model evaluations were performed using the independent datasets of three greenhouse trials (Apr-Oct 2017). WW, well-watered, DS, drought-stressed.

Trait	Threshold	Expt.	Without leaf area input					With leaf area input				
			Slope	R^2	RMSE	Bias	Accuracy	Slope	R^2	RMSE	Bias	Accuracy
T_p												
	c_L, c_ε	5	0.88	0.53	0.092	-0.027	0.49	0.80	0.66	0.070	-0.029	0.61
	c_L, c_ε	6	0.79	0.32	0.111	-0.043	0.21	1.31	0.61	0.110	-0.054	0.22
	c_L, c_ε	7	0.83	0.23	0.082	0.013	0.31	1.25	0.43	0.077	-0.008	0.35
	c_L, c_g	5	0.88	0.54	0.091	-0.025	0.50	0.71	0.62	0.078	-0.042	0.56
	c_L, c_g	6	0.80	0.32	0.111	-0.041	0.21	1.16	0.55	0.118	-0.073	0.16
	c_L, c_g	7	0.83	0.23	0.082	0.014	0.31	1.29	0.55	0.067	-0.023	0.43
$T_{p,sum}$												
	c_L, c_ε	5	0.67	0.09	0.480	-0.233	0.70	0.25	0.05	0.360	-0.252	0.77
	c_L, c_ε	6	0.39	0.20	1.000	-0.496	0.65	0.72	0.23	1.000	-0.624	0.55
	c_L, c_ε	7	0.55	0.19	0.489	0.210	0.75	0.85	0.56	0.311	-0.135	0.84
	c_L, c_g	5	0.84	0.14	0.460	-0.217	0.71	0.46	0.15	0.430	-0.364	0.72
	c_L, c_g	6	0.30	0.09	1.000	-0.476	0.64	0.70	0.22	1.000	-0.836	0.44
	c_L, c_g	7	0.63	0.25	0.480	0.224	0.75	1.05	0.67	0.456	-0.367	0.76

Shoot dry matter production

For simulation of shoot dry matter production without the A_l input, all the sub-modules of aggregated model are incorporated for leaf growth, transpiration, soil water, and photosynthesis. **Fig. 4-7** shows the comparison of simulated and observed shoot dry matter produced W_{sh} (g DM per pant) under DS and WW conditions without and with the input of A_l. Both approaches could have predicted the W_{sh} with high accuracy in both water supply treatments (0.66 - 0.84). With the input of A_l, the magnitude of the regression coefficients (slope) (0.763 vs 0.768; 0.646 vs 0.752) and intercepts (5.251 vs 4.838; 5.023 vs 4.695) were slightly improved as compared to the case of the simulation without the input of A_l under both WW and DS conditions. However, the accuracy and coefficient of determination (R^2) were decreased, and the bias and RMSE increased under DS condition. Under WW condition, the prediction with the input of A_l showed a slight improvement with the decrease of RMSE (2.65 vs 2.60 g) and bias (-1.429 vs -1.092), and the high value of accuracy (0.84) was unchanged.

With the input of W_{ts}, the prediction of W_{sh} under DS condition improved the slope and intercept being more fitted to 1:1 line as compared to the aggregated one, but with the less accuracy and higher errors (**Fig. 4-8**). With the input of both W_{ts} and A_l, stressed performance of simulated W_{sh} was more improved in terms of most evaluation criteria, except R^2 as compared to the results of simulations with either input of W_{ts} or A_l,

In each case of evaluation trials, the improvement in accuracy of prediction for W_{sh} was visualized in Expt. 6 with the A_l input as compared to aggregated one in both WW (0.57 vs 0.71) and DS (0.50 vs 0.72) conditions (**Table 4-5**). The slope and RMSE also showed the improvement with A_l inputs, especially in Expt. 6, whereas other experiments did not show any improvement in evaluation criteria as compared to that observed with the aggregated model.
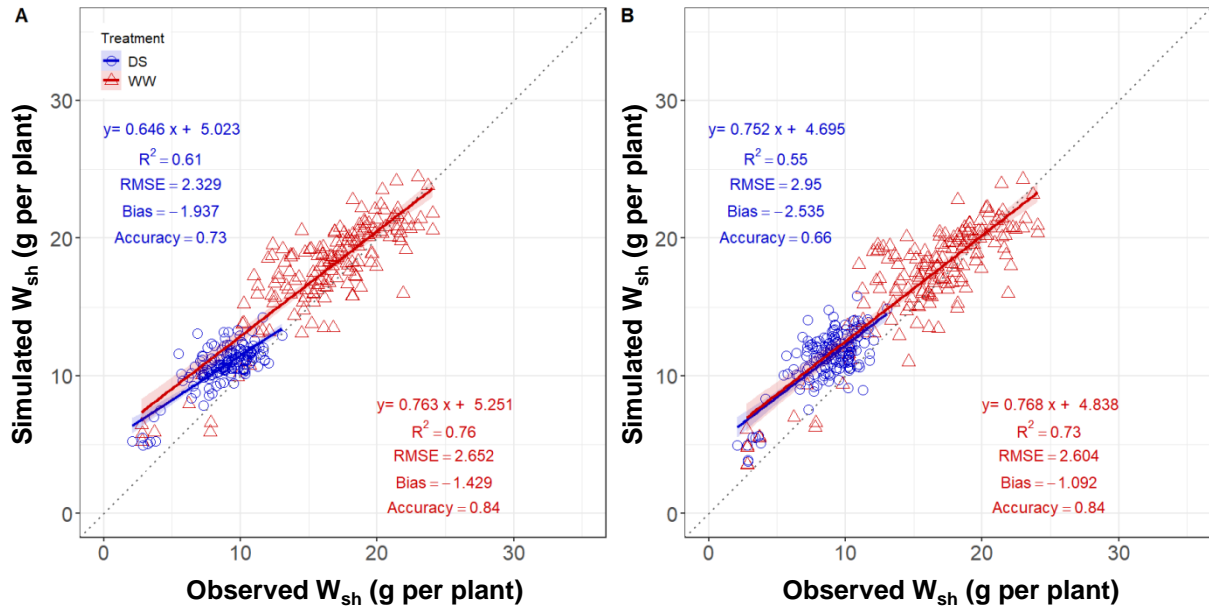
Fig. 4-7. Comparison of simulated and observed shoot dry weight (W_{sh}) of tomato lines under drought-stressed (DS) and well-watered (WW) conditions in two ways of simulation: (A) without and (B) with leaf area input. Model evaluations were done using the independent datasets of three greenhouse trials (Apr – Oct 2017). N = 162.
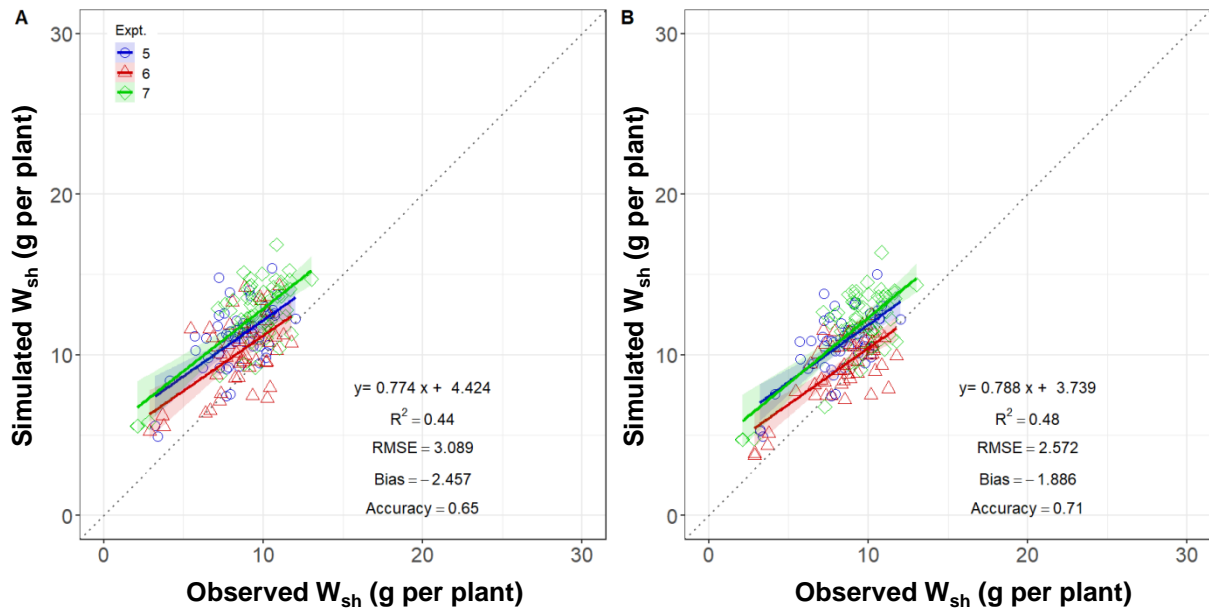
Fig. 4-8. Comparison of simulated and observed shoot dry weight (W_{sh}) of tomato lines under drought-stressed (DS) condition for three experiments: with (A) W_{ts}, and (B) W_{ts} and A_l inputs. Experiments (Expt. 5 - Expt.7) were characterized by the average day-time vapour pressure deficits of 2.3 (±0.24), 1.9 (±0.22), and 1.4 (±0.07) kPa, respectively.

Table 4-4. Statistical analysis of the comparison between simulated and observed data for shoot dry weight W_{sh} (kg per plant) at harvest and fraction of transpirable soil water W_{ts} during the stressed period in two ways of simulation: without and with the inputs of leaf area. Model evaluations were done using the independent datasets of three greenhouse trials (Apr-Oct 2017). WW, well-watered, DS, drought-stressed.

Trait	Treat.	Expt.	Without leaf area input					With leaf area input				
			Slope	R^2	RMSE	Bias	Accuracy	Slope	R^2	RMSE	Bias	Accuracy
W_{sh}												
	WW	5	0.80	0.74	2.518	-1.026	0.86	0.80	0.70	2.881	-1.430	0.85
	WW	6	0.82	0.70	6.587	-1.574	0.57	0.90	0.61	4.027	-3.083	0.71
	WW	7	0.83	0.78	3.095	-2.272	0.82	0.81	0.75	2.988	-1.957	0.83
	DS	5	0.61	0.64	1.939	-1.555	0.77	0.65	0.52	2.441	-2.008	0.70
	DS	6	0.62	0.55	4.260	-1.553	0.50	0.64	0.46	2.417	-1.833	0.72
	DS	7	0.72	0.62	2.538	-2.173	0.73	0.84	0.60	2.910	-2.498	0.69
W_{ts}												
	DS	5	1.08	0.84	0.129	-0.056	0.72	1.06	0.93	0.109	-0.083	0.76
	DS	6	0.90	0.85	0.164	-0.101	0.65	0.97	0.92	0.109	-0.051	0.77
	DS	7	1.09	0.93	0.105	0.041	0.77	1.13	0.94	0.100	-0.023	0.78

Fraction of transpirable soil water

Without A_l input, the aggregated model predicted the fraction of transpirable soil water W_{ts} with the overall accuracy of 0.66, the high level of goodness of fit ($R^2 = 0.87$, RMSE = 0.1198) and small magnitude of bias (0.0535) (**Fig. 4-9**). The overall regression line was highly matched to 1:1 line characterized by the slope and intercept values of 1.041 and -0.07. However, the spread of individual data points indicated some uncertainties of water uptake along with the drought duration of some lines revealed by over- (Expt. 6) and under-estimation (Expt. 7). With the A_l input, the validity of the model was more visualized in all evaluation statistics, with 5% and 8% improvement in coefficient of determination (R^2) and accuracy, respectively. Moreover, RMSE and bias showed much lower errors in prediction with A_l input than the aggregated one. In all of three trials with A_l input, a slight over-estimation of W_{ts} (low water uptake) was observed especially for Expt. 6 as characterized by the large value of regression coefficient (1.126), but with the almost zero (-0.018) of the intercept. Among the predictions for different environments, W_{ts} values for Expt. 6 showed the least accuracy and highest RMSE when simulated without A_l input (**Table 4-5**).
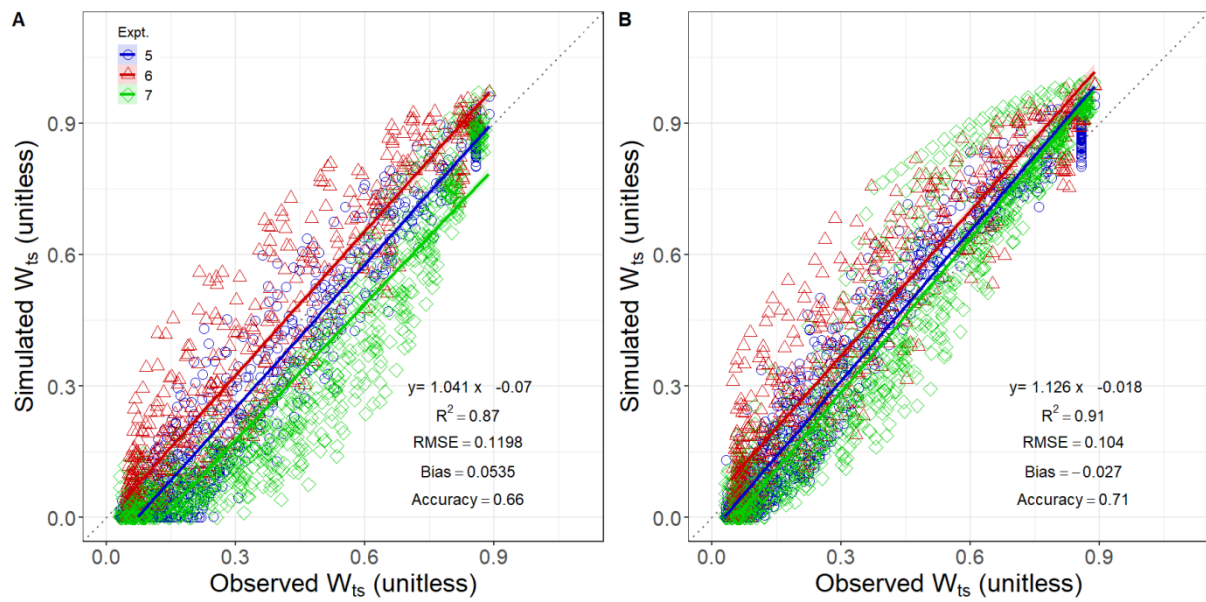
Fig. 4-9. Comparison of simulated and observed fractions of transpirable soil water (W_{ts}) of tomato introgression lines under terminal drought stress in two ways of simulation: (A) without and (B) with leaf area inputs. Model evaluations were performed using the independent datasets of three greenhouse trials (Apr-Oct 2017). Experiments (Expt. 5 - Expt.7) were characterized by the average day-time vapour pressure deficits of 2.3 (±0.24), 1.9 (±0.22), and 1.4 (±0.07) kPa, respectively. N =1954.

Table 4-5. Input and output variables of the TILSIM model

Variable	Description	Unit	Equation	Type
A_i	Area of the leaf i	cm^2 per leaf	(4-2a)	Output
A_l	Total leaf area of the plant	cm^2 per plant	(4-2a)	Output
C_c	CO_2 partial pressure near Rubisco	$\mu mol\ CO_2\ m^{-2}\ s^{-1}$	(4-6f)	Output
C_f	Conversion efficiency from assimilates to dry mass	-	(4-7d)	Output
C_a	Atmospheric CO_2 concentration	$\mu mol\ CO_2\ m^{-2}\ s^{-1}$	-	Input
$C_\times$	Soil water threshold describing a function of soil water deficit on a relative trait	-	-	Output
δe	Air vapour pressure deficit	kPa	-	Input
d	Zero plane displacement height	m	(4-13)	Output
d_y	Day of the year	day	(4-4d)	Input
Δt_i	Physiological age of leaf i	°Cd	(4-3d)	Output
E_i	Expansion rate of leaf i	cm^2 per leaf °Cd^{-1}	(4-3i)	Output
ϵ	Potential canopy specific transpiration rate	$kg\ H_2O\ m^{-2}$ leaf d^{-1}	(4-9a)	Output
$E_{pot,i}$	Potential expansion rate of leaf i	cm^2 per leaf °Cd^{-1}	(4-3b)	Output
$E_{pot,l}$	Potential plant leaf area increase	cm^2 per plant °Cd^{-1}	(4-3f)	Output
$E_{i,max}$	Maximum leaf expansion rate of leaf i (M82)	cm^2 per leaf °Cd^{-1}	-	Input
$E_{i,norm}$	Normalized leaf expansion rate of leaf i	-	(4-3c-e)	Output
$f_\varepsilon(W_{ts})$	Relative effect of soil water deficit on specific transpiration through c_ε	-	(4-9d)	Output
$f_g(W_{ts})$	Relative effect of soil water deficit on specific transpiration through c_g	-	(4-9e)	Output
$f_c(W_{ts})$	Relative drought effect on apparent V_{cmax}	-	(4-6k)	Output
$f_j(W_{ts})$	Relative drought effect on apparent J_{max}	-	(4-6l)	Output
$f(\delta e)$	Relative effect of vapour pressure deficit on g_{sw}	-	(4-9i)	Output
$f(I_{abs})$	Relative effect of light on g_{sw}	-	(4-9h)	Output
$f(W_{ts})$	Relative drought effect on g_{sw}	-	(4-9h)	Output
f_i	Relative sink strength of leaf i	-	(4-3f)	Output
f_l	Relative sink strength of leaf portion	-	(4-8a)	Output
f_r	Relative sink strength of root portion	-	(4-8c)	Output
f_s	Relative sink strength of stem portion	-	(4-8a)	Output
$f_\times$	Relative sink strength of a given organ	-	(4-8a)	Output
g_m	Mesophyll conductance to CO_2	$mol\ CO_2\ m^{-2}\ s^{-1}$	-	Input
$g_s{'}$	Stomatal conductance in velocity unit	$m\ s^{-1}$	(4-11)	Output
g_{smax}	Maximum stomatal conductance to water vapour	$mol\ H_2O\ m^{-2}\ s^{-1}$	-	Input
g_{sw}	Stomatal conductance to water vapour	$mol\ H_2O\ m^{-2}\ s^{-1}$	(4-9g)	Output
$g_{sw}{'}$	Plant (stomatal) conductance to water vapour derived from inversion of Penman equation	$m\ s^{-1}$	(4-12)	Output
$g_s(W_{ts})$	Relative drought effect on g_s	$mol\ CO_2\ m^{-2}\ s^{-1}$	(4-6g)	Output
g_s	Stomatal conductance to CO_2	$mol\ CO_2\ m^{-2}\ s^{-1}$	(4-11)	Output
g_a	Aerodynamic conductance to water vapour	$mol\ H_2O\ m^{-2}\ s^{-1}$	(4-13)	Output
G_i	Actual growth rate of leaf i	g DM per leaf °Cd^{-1}	(4-3h)	Output
$G_\times$	Actual growth rate of a given organ	g DM °Cd^{-1}	(4-8a)	Output

G_r	Actual growth rate of root	g DM °Cd^{-1}	(4-8c)	Output
G_s	Actual growth rate of stem	g DM °Cd^{-1}	(4-8d)	Output
G_{sh}	Actual growth rate of shoot	g DM °Cd^{-1}	(4-8e)	Output
G_t	Actual growth rate of the crop	g DM per plant °Cd^{-1}	(4-8b)	Output
$G_{t,pot}$	Potential growth rate of the crop	g DM per plant °Cd^{-1}	(4-7a)	Output
γ	Psychrometric constant	kPa K^{-1}	-	Output
λ	Latent heat for vaporization of water	MJ kg^{-1}	-	Output
H_p	Plant height	m	(4-5)	Output
I_{id}	Daily PPED integral	mol photon m^{-2} d^{-1}	-	Input
I_{abs}	Absorbed light intensity	mol photon m^{-2} s^{-1}	(4-6a)	Output
I_0	Incident PAR at the top of the canopy	µmol photon m^{-2} s^{-1}	-	Input
			(4-6j)	Output
J	Electron transport rate	µmol e$^-$ m^{-2} s^{-1}	(4-6i)	Output
L	Leaf area index	-	-	Output
$M_{l,sup}$	Assimilate supply available for leaf portion	g DM °Cd^{-1}	(4-7e)	Output
N_l	Number of leaf	# per plant	(4-1)	Output
P_{gd}	Daily integral of canopy gross assimilation rate	g CH$_2$O m^{-2} ground d^{-1}	(4-6b)	Output
P_t	Photosynthesis of the whole canopy	µmol CO$_2$ m^{-2} ground s^{-1}	(4-6b)	Output
P_n	Steady-state net photosynthetic rate	µmol CO$_2$ m^{-2} s^{-1}	(4-6c)	Output
P_c	RuBP-carboxylation limited photosynthetic rate	µmol CO$_2$ m^{-2} s^{-1}	(4-6d)	Output
P_j	RuBP-regeneration limited photosynthetic rate	µmol CO$_2$ m^{-2} s^{-1}	(4-6e)	Output
r_L	Relative leaf expansion rate	-		Output
r_g	Relative stomatal conductance	-		Output
r_ε	Normalized specific transpiration ratio	-		Output
$r_\times$	Relative performance of a given trait	-	(4-14)	Output
$R_{d,25}$	Daytime respiration at leaf temperature 25 °C	µmol CO$_2$ m^{-2} s^{-1}	-	Input
R_d	Daytime respiration rate	µmol CO$_2$ m^{-2} s^{-1}	(4-6h)	Output
rgr	Relative growth rate	g g^{-1} d^{-1}	(4-7c)	Input
R_m	Canopy maintenance respiration rate	g CH$_2$O m^{-2} d^{-1}	(4-7b)	Output
R_n	Net radiation absorbed by unit leaf area	mol photon m^{-2} s^{-1}	(4-9b)	Output
R_0	Global radiation incident at the top of the canopy	µmol photon m^{-2} s^{-1}	(4-9b)	Input
ρ_a	Mean atmospheric density	kg m^{-3}	-	Output
s	Slope of the saturation vapour pressure curve	kPa K^{-1}	-	Output
SLA	Specific leaf area	cm^2 g^{-1}	(4-4a)	Output
SLA_{min}	Minimum specific leaf area	cm^2 g^{-1}	(4-4d)	Output
SLA_p	Plant specific leaf area as a function of light, temperature and CO$_2$	cm^2 g^{-1}	(4-4b)	Output
S_i	Sink strength of ith leaf	g DM per leaf d^{-1}	(4-3g)	Output
S_l	Sink strength of total leaf area	g DM per plant d^{-1}	(4-3g)	Output
T_a	Air temperature	°C	-	Input
t_{d0}	The plant age at the time of drought imposition	°Cd	(4-9e)	Input
T_l	Leaf temperature	°C	-	Input
t_{0i}	Time of leaf appearance	°Cd	(4-2b)	Output
T_p	Plant transpiration rate	kg H$_2$O per plant d^{-1}	(4-9c)	Output

$T_{p,sum}$	Total water transpired by the plant	kg H_2O per plant	(4-9f)	Output
TS	Temperature sum starting from time of emergence	°Cd	-	Output
W_{ts}	Fraction of transpirable soil water	-	(4-10a)	Output
W_l	Dry weight of total leaf	g DM per plant	(4-8e)	Output
W_s	Dry weight of stem	g DM per plant	(4-8e)	Output
W_r	Dry weight of root	g DM per plant	(4-8e)	Output
W_f	Dry weight of fruit	g DM per plant	(4-8e)	Output
W_{sh}	Dry weight of shoot	g DM per plant	(4-8f)	Output
W_n	Current weight of soil water	kg H_2O per pot	(4-10b)	Output
W_{fn}	Final weight of soil water at 10% transpiration of the well-watered plant	kg H_2O per pot	(4-10d)	Input
W_0	Initial weight of soil water at 100% WHC	kg H_2O per pot	(4-10c)	Input
z_{0m}	Roughness length governing the transfer of momentum	m	(4-13)	Output
z_{0h}	Roughness length governing the transfer of heat and vapour	m	(4-13)	Output

Table 4-6. Parameters and coefficients used in the TILSIM model

Parameter	Description	Value	Unit
ASR_l	Assimilate requirements for formation of leaf DM	1.39	g CH_2O g^{-1}DM d^{-1}
ASR_s	Assimilate requirements for formation of stem DM	1.45	g CH_2O g^{-1}DM d^{-1}
ASR_r	Assimilate requirements for formation of root DM	1.39	g CH_2O g^{-1}DM d^{-1}
ASR_f	Assimilate requirements for formation of fruit DM	1.37	g CH_2O g^{-1}DM d^{-1}
a_{ei}	Constant relating normalized E_i to vapour pressure deficit	-0.1418	-
a_{sw}	Constant relating normalized SLA to the soil water deficit	25.0	-
a_{gp}	Ground area per plant	0.134	m^2
a_{sI}	Constant relating normalized SLA to the light	-0.011	-
a_{sdy}	Constant relating SLA_{min} to the day of the year (Hannover)	218	cm^2 g^{-1}
α	Reflection coefficient of tomato canopy	0.07	-
α_g	Slope of stomatal conductance at zero irradiance	0.04	mol H_2O mol^{-1}photon
b_{sI}	Constant relating normalized SLA to the irradiance	0.93	-
b_{sw}	Constant relating normalized SLA to the drought	5.0	-
b_{ei}	Constant relating normalized E_i to vapour pressure deficit	1.0	-
b_{sdy}	Constant relating SLA_{min} to the day of the year (Hannover)	35	cm^2 g^{-1}
β_{Ca}	Relative change in leaf mass per unit change of CO_2 with respect to reference value 350 ppm	0.00085	-
β_{Ta}	Relative change in leaf mass per unit change of temperature with respect to reference value 24°C	0.0085	-
β_f	Endpoint of transpirable soil water	0.06	kg H_2O kg^{-1}soil
β_0	Water holding capacity of the soil (Ruthe, South Hannover)	0.28	kg H_2O kg^{-1}soil
c_L	Soil water threshold for leaf expansion rate	variable	-
c_g	Soil water threshold for stomatal conductance	variable	-
C_p	Specific heat of moist air	0.001013	MJ kg^{-1} K^{-1}
$C_\times$	Soil water threshold for a given relative trait	variable	-
c_{sdy}	Constant relating SLA_{min} to the day of the year (Hannover)	1.85	-
$\Delta t_{i,max}$	Leaf age when it has attained the maximum expansion rate	152	°Cd
δe_0	Constant relating stomatal conductance to vapour pressure deficit	3.5	-
f	Parameter relating maintenance respiration to relative growth rate	33	-
f_{cw}	Sensitivity parameter describing the steepness of decline in V_{cmax}	10	-
f_{jw}	Sensitivity parameter describing the steepness of decline in J_{max}	10	-
f_f	Relative sink strength of fruit	0.0	-
f_{rd}	Relative sink strength of root under drought stress condition	0.14	-
f_{rw}	Relative sink strength of root under well-watered condition	0.12	-
G	Latent heat flux	0.0	MJ m^{-2} d^{-1}
g_{smin}	Minimum stomatal conductance	0.009	mol H_2O m^{-2} s^{-1}
h_g	Standard deviation relating relative growth rate to plant age	-39.99	-
h_s	Standard deviation relating normalized SLA to plant age	1.35	-
h_l	Standard deviation relating leaf expansion rate to leaf age	57.9	-
θ_g	Convexity factor relating light to the stomatal conductance	0.75	-

Symbol	Description	Value	Unit
θ_J	A constant convexity factor describing the response of J to I_{abs}	0.75	-
θ_s	Initial volume of soil filled in the pot	10.0	m^3
J_{high}	Light saturated electron transport rate	variable	$\mu mol\ e^-\ m^{-2}\ s^{-1}$
J_{max}	Maximum electron transport rate at 25°C	variable	$\mu mol\ e^-\ m^{-2}\ s^{-1}$
k	Light extinction coefficient	0.7	-
k_{ml}	Maintenance respiration for leaves of tomato at 25°C	0.03	$g\ CH_2O\ g^{-2}\ DM\ d^{-1}$
k_{ms}	Maintenance respiration for stem of tomato at 25°C	0.015	$g\ CH_2O\ g^{-2}\ DM\ d^{-1}$
k_{mr}	Maintenance respiration for root of tomato at 25°C	0.1	$g\ CH_2O\ g^{-2}\ DM\ d^{-1}$
k_{mf}	Maintenance respiration for fruit of tomato at 25°C	0.1	$g\ CH_2O\ g^{-2}\ DM\ d^{-1}$
k_{2LL}	Conversion efficiency of photons to J at limiting light	0.425	$\mu mol\ e^-\ \mu mol^{-1}photon\ s^{-1}$
K	von Karman's constant	0.41	-
K_c	Michaelis-Menten constant of Rubisco for carboxylation reaction	404	$\mu mol\ CO_2\ mol^{-1}$
K_o	Michaelis-Menten constant of Rubisco for oxygenation reaction	278	$mmol\ O_2\ mol^{-1}$
k_t	Time unit conversion factor from day to second	86400	$s\ d^{-1}$
L_{rin}	Specific internode length	9.0	$cm\ g^{-1}\ DM$
Γ^*	CO_2 compensation point in the absence of mitochondrial respiration	43.02	$\mu mol\ CO_2\ m^{-2}\ s^{-1}$
O	O_2 concentration at the site of the carboxylation	210	$mmol\ O_2\ mol^{-1}$
P	Atmospheric pressure at a given altitude	101.3	kPa
ρ_s	Soil bulk density (Ruthe, South Hannover)	1.25	$g\ cm^{-3}$
P_0	Atmospheric pressure at the sea level	101.3	kPa
$Q_{10,l}$	Q10 value for temperature effect on leaf daytime respiration	2.0	-
$Q_{10,c}$	Q10 value for temperature effect on maintenance respiration	2.0	-
r_l	thermal leaf appearance rate	variable	$nr.\ °Cd^{-1}$
rgr_{max}	Maximum relative growth rate of the crop over the preceding 5 days	0.11	$g\ g^{-1}\ d^{-1}$
s_g	Slope relating relative stomatal conductance to drought stress	variable	-
s_L	Slope relating leaf expansion rate to drought stress	variable	-
$s_\times$	Slope relating a relative trait to drought stress	variable	-
SLA_{max}	Maximum specific leaf area	400	$cm^2\ g^{-1}$
$\mathbf{T}_0$	Air temperature in Kelvin scale at 0°C	273.0	K
T_b	Base temperature for the expansive growth	7.7	°C
$TS_{s,max}$	Thermal time when the plant has attained the maximum SLA	250.0	°Cd
TS_{inf}	Inflexion point when the relative growth rate has decreased to half of the maximum value	679.02	°Cd
U_z	Estimated wind speed inside the greenhouse at 2 m height	0.5	m
V_0	Molar volume of soil water	22.7 x 10^{-3}	$m^3\ mol^{-1}$
V_{cmax}	Maximum carboxylation rate at 25°C	variable	$\mu mol\ CO_2\ m^{-2}\ s^{-1}$
W_{tsc}	Reference soil water status at which apparent V_{cmax} decreases to half of its maximum value	0.4	-
W_{tsj}	Reference soil water status at which apparent J_{max} decreases to half of its maximum value	0.4	-
z_m	Height of wind measurement	2.0	m
z_h	Height of humidity measurement	2.0	m

Discussion

Parameterization and simulation schemes

This work is an attempt to implement the integration between eco-physiological model and QTL-derived parameters of 50 tomato introgression lines together with parental lines - the threshold for leaf expansion rate and that for stomatal conductance. By using these two traits as drivers of differing plant reactions, drought performance of all lines was simulated in parallel with the unstressed performances. For visualization of the absolute variability between lines, the maximum limit of each line for specific traits (e.g. maximum leaf expansion rate) was provided. Aside from specific coefficients, the general parameters and global functions were applied equally for all lines and all experiments, without any empirical adjustment. With some empirical fixing in parameter values for different experimental conditions, the modelling performance would have been better, but this would degrade the generality of model equations and diminish the model transparency. Therefore, we avoided doing such kind of correction; instead, we tried to understand what would be the underlying causes of those errors and inaccuracies and how the model can be improved from the perspectives of biological meaning and physical principles.

Model evaluation was done separately for outputs of different configurations in different simulation schemes. For instance, prediction of leaf area was performed in two modelling schemes –in an aggregated form and with the input of soil water, yielding the same outputs for unstressed condition. Simulations of transpiration, shoot dry mass, and soil water (under stressed condition) were executed without or with the input of leaf area. Finally, the outputs were incorporated in the QTLs based model, constructed in a spread sheet (detail in Chapter 3). On this interface, QTLs information for target thresholds was used instead of genotype-specific values. With the inputs of unstressed values for leaf area, plant transpiration and soil water, the simulation work was performed again for stressed transpiration. From the input of leaf area and plant transpiration, specific transpiration ratio and relative leaf expansion rate at the plant level were calculated for unstressed condition. QTL information on thresholds of relative leaf expansion rate was used to impose the drought performance of leaf expansion rate and leaf area. For the performance of stressed specific transpiration ratio, either threshold for specific transpiration ratio or that of relative stomatal conductance was used. Although the model predicted the important traits such as stomatal conductance and photosynthesis the evaluation was done only on more relevant traits at the upper scales. There is a possibility to

perform sensitivity tests to make the model integrity better and hypothesis testing for a better understanding of the systems and acquire the quantitative knowledge of the mechanistic connection between different components.

Phenotypic variability is the highest in maximum leaf expansion rate and the lowest in maximum stomatal conductance

All introgression lines are nearly isogenic to the recurrent line and each other with the only difference in one introgressed segment ($\approx$ 3% of the total genome size). CV% indicates both the environmental and genetic variation, which shows the highest for maximum expansion rate and the lowest for maximum stomatal conductance. The similarity between grand mean and mean of recurrent parent M82 as observed in leaf appearance rate and maximum stomatal conductance indicates the extent of genetic relatedness between all lines and common genetic determinism for these traits. Accordingly, the values of these traits in recurrent M82 can be regarded as the average of the total population. At the same time, the maximum SLA showed a strong influence of wild type, which was observed to have the leaves much thicker than the recurrent line.

Predicting leaf area -with or without the input of soil water?

The model in aggregated mode predicted the total leaf area A_l (cm^2 per plant) with more agreement between measured and simulated data under WW as compared to DS condition (**Fig. 4-3**). It should be noted that the parameters of regression and criteria of evaluation shown in the figures were computed at the global level by taking account of three experiments together. For A_l, the parameters of a linear function (i.e. slope and intercept) and coefficient of regression in both cases of water supply revealed a better fit in dynamic data than in total A_l while the RMSE, bias and accuracy showed the more errors of prediction in A_l (**Fig. 4-3**). These errors could be attributed to a higher number of data points for A_l, which encompassed the performances over the time course of stressed period and seasons simulated for each line. By adding the soil water W_{ts} as an input in DS condition, there was no improvement in most evaluation criteria, except the regression coefficient (slope) and intercept for both dynamic and total A_l (**Fig. 4-4**). The input of W_{ts} resulted in a more over-estimation than the case without its input, particularly in Expt. 7 where vapour pressure deficit was lower than other experiments (**Table 4-2**). This can be attributed to either inaccuracy in prediction of W_{ts} or different sensitivities of drought reaction parameter of leaf expansion rate (i.e. soil water

threshold) to environmental condition, on which the model did not take account. However, with the inputs of both W_{ts} Regardless of the input of W_{ts}, the higher errors in predicted A_l under DS as compared to WW case, could also be attributed to the larger errors in SLA prediction (**Fig. 4-S6**), where the range of predicted SLA at harvest time was much narrower (120-165 cm^2 g^{-1}) than the measured range (140-300 cm^2 g^{-1}). The shallow slope of predicted SLA could explain why the predicted total leaf areas of larger plants were mostly underestimated and that of the smaller plants over-estimated. Canopy profile of SLA at a specific growth stage and soil water status need to be quantified in order to find out the the possible causes of discrepancies and reduce the errors of under and over estimation inrelation to plant size. Many factors, including light intensity, temperature, sink –source ratio and CO_2 concentration, are known to affect SLA (Enoch, 1990; Marcelis, 1993). However, quantitative knowledge of the underlying principles of this area is limited and therefore it is difficult to predict SLA (Marcelis et al., 1998). Improvement in SLA prediction by using the funtion of leaf age and soil water condition would possibly result in a more precise prediction of A_l under the drought stress scenarios.

The input of leaf area improves the model performance for plant transpiration

The model in aggregated mode predicted the total water transpired $T_{p,sum}$ with the accuracies of 0.69 and 0.55 for WW and DS condition, respectively. With the measured A_l used as an input, the model could have predicted the $T_{p,sum}$ for both DS and WW conditions with the higher accuracy than the aggregated form (**Fig. 4-5B, 4-5D**). A great deal of improvement in prediction was observed even for the daily dynamics of transpiration T_p by the input of A_l in both cases of water supply environments (**Fig. 4-5A, 4-5C**). Under DS, a large spread of data points observed in prediction of dynamic T_p with aggregated mode showed a high sensitivity of transpiration to environmental factors, resulting in very low accuracy. With the input of A_l, model performance for the stressed condition began much improved, reflecting that the accuracy in predicting leaf areas over the course of stressed period played a major role in controlling the transpiration dynamics. Evaluation of model performance for T_p in each environment showed that the regression coefficient in Expt. 7 became higher when simulated with the input of A_l particularly under DS condition (**Table 4-3**). Since the total leaf area in Expt. 7 was slightly over estimated, over-estimation of plant T_p could be attributed to the errors in prediction of both leaf area and specific transpiration rate. For the part of specific transpiration rate, the possible errors would reside on plant stomatal conductance and

aerodynamic conductance because we adjusted the values of M82 only and the values of other lines were computed based on their mean relative difference from M82.

For the tomato plant with the LAI of 3, the typical values for minimum stomatal resistance at canopy level is assumed to be 200 s m^{-1} (Stanghellini, 1987), which is equivalent to 0.20 mol m^{-2}s^{-1} of g_s at 25°C and 100 kPa. However, Heuvelink (1995) used the fixed value of 50 and 100 s m^{-1} (0.81 and 0.4 mol m^{-2}s^{-1} in conductance units) for leaf stomatal resistance and boundary layer resistance in TOMSIM (1.0). As observed in the data of Prado et al. (2018), the light-saturated plant g_{sw} was approximately half the leaf g_{sw} (ca. 0.1 vs 0.2 mol m^{-2} s^{-1}). Prado *et al.* (2018) mentioned that they performed the inversed calculation of P-M for plant stomatal conductance for each genotype and each experiment. In our case, we used the data from the first four experiments while that from the last three were used only for model evaluation. Stanghellini and Taeke (1995) showed that, besides the well-known thermal feed-back, the hydraulic feed-back in greenhouses further decreases the sensitivity of the transpiration of greenhouse crops to variations (or inaccurate estimates) of the aerodynamic resistance. Katsoulas and Stanghellini (2019) suggested that when looking for simplifications, a constant (but accurate) value for the aerodynamic resistance and simple (empirical) model relating stomatal resistance only to light would be required. Therefore uncertainty in estimating these two variables would not be a serious issue if the values are in the reasonable range.

Role of QTL-based parameters for predicting transpiration under drought stress scenario

A crop model with genetic inputs potentially indicates where and when a given combination of alleles confers a positive or negative effect on plant performance (Tardieu and Tuberosa, 2010; Messina et al., 2011). With the use of QTL-linked thresholds for soil water thresholds of leaf expansion rate c_L, stomatal conductance c_g and specific transpiration rate c_ε, the model could predict fairly the stressed transpiration (**Fig. 4-6**). It is noteworthy that we first performed the simulation with or without (in aggregated form) the input of A_l in a complete genome-based model as mentioned above. Then, using the outputs of unstressed transpiration and A_l, we computed the leaf expansion rate and specific leaf area at the plant level for WW condition. Together with simulated soil water under DS, we replaced the simulated data in the place of formerly measured input data in the QTLs-based model where QTLs controlled parameters (i.e. c_L, c_g and c_ε) were nested. It was not surprising that the performance of

stressed transpiration in this approach was less accurate as compared to predicted outputs using the input of all measured data for WW condition (see Chapter 3). However, it showed quantitative information regarding which combination of QTLs parameters would fit in a genome based eco-physiological model for prediction of stressed transpiration. According to the outputs, stressed transpiration could reasonably be predicted if the measured unstressed leaf area is provided just by using QTLs for two traits of drought reaction. It should also be noted that dynamics of measured leaf area itself was also calculated from empirical relationships with a measured leaf length of individual leaves, and described as non-destructive leaf areas. Therefore, the prediction of stressed transpiration with QTLs based model primarily used the measured data of leaf lengths and QTLs for soil water thresholds of leaf expansion rate, specific transpiration rate and stomatal conductance.

Interactions between the sub systems play a role for shoot dry matter accumulation

The model in full simulation mode allows the interactions between the individual modules, which may result in poor performance (Heuvelink, 1995). This expectation holds fairly true in our validation tests, especially under DS where more interactions might have occurred along with the integration of drought response parameters into the compartments. Such kind of interaction can bring either positive or negative influence in the model performance. This situation was observed in the prediction of higher level trait such as W_{sh}, for which more number of modules including that of photosynthesis were involved in interactions (**Fig. 4-7**). Coefficient of determination (R^2) and the magnitude of accuracy indicated that the model performance for the prediction of W_{sh} in the aggregated mode tended to be even more promising than that with the input of A_l. During the simulation in aggregated mode, the possible several errors in the values of sub-level traits could have compensated each other, resulting in a good performance at the upper level component. However, with the inputs of both A_l and W_{st}, global evaluation for all trials revealed that the prediction of W_{sh} was improved with respect to accuracy (+8 and +7%), bias (-30 and -34%), RMSE (-17 and -13%) and parameters of regression as compared to the either case with the input of W_{st} or A_l, respectively (**Fig. 4-7B, 4-8**). Lower magnitude of R^2 reflects the inconsistency in model performance between and within experiments.

Soil water status under drought - a feedback control of transpiration and leaf area

Accuracy in predicting soil water status W_{ts} is very important in our model framework for DS condition because all major plant functional processes such as leaf growth, photosynthesis and transpiration were affected by drought via the soil water thresholds as a function of W_{ts}. Since the feedback controls were included for system stability, W_{ts} status directly depends on soil water uptake through the plant transpiration T_p which was under the controls of soil water thresholds. Therefore in Chapter 3, we have evaluated the validity of soil water thresholds using the measured data of W_{ts} and respected unstressed traits (e.g plant leaf area). The magnitude of errors in prediction of T_p is also ascribed to errors in the prediction of A_l. This feedback control of A_l on W_{ts} can be seen in the difference between values of W_{ts} predicted with and without the input of A_l (**Fig. 4-9**). With the input of A_l, prediction of W_{ts} became more accurate as compared to outputs of prediction in aggregated mode (without A_l input). Despite a large spread of point clouds along the course of stressed duration, global regression line revealed a good fit to 1:1 line even without the input of A_l. Therefore it should be sufficient to use the predicted values of W_{ts} for incorporation with QTLs derived parameters that we used (above) for prediction of stressed transpiration.

Conclusion

Crop models are powerful tools to identify of the optima in the expression of adaptive traits to abiotic stresses (e.g. soil water deficits), to provide useful guidance for management, and to investigate the physiological controls involved. This study aimed at developing an integrated model which requires only the genotype specific parameters or QTL information for specific target traits, enabling the simulation of plant growth, transpiration and biomass production simultaneously in one framework allowing the interaction between components. In this modelling work for tomato intrgression lines, environment dependent traits were first dissected from the genotype-specific ones. The genome regions (or QTLs) for selected model parameters were detected, and later with the inputs of environmental and/or management data, a stepwise simulation was made in different schemes for the performance of multi-genotypes characterized genotype-specific parameters (GSPs) or QTL- derived parameters under a set of environmental conditions. The model performed with a fairly high accuracy for the prediction of major canopy traits namely plant leaf area, transpiration and shoot dry mass for both well-watered and drought stressed condition, and for fraction of transpirable soil water under drought stress. Consistant overestimation of stressed leaf area linked to errors in predicted

SLA could be resolved by using leaf area input for better prediction of other traits such as transpiration and soil water. After detailed evaluation and fine-tuning of different sub-modules with the constraints of other components through sensitivity analysis, model improvement can be made in order to minimize the parameterization requirement while maintaining the level of model complexity depending on the purpose of tests.

Chapter 5

General Discussion

There are two broad reasons for incorporating the genetic information into crop models. The first reason is to enable one to predict the crop phenotype from genetic information in specific conditions. The second reason is to improve scientific understanding of genetic control of plant processes (Wallach et al., 2018). This study aimed at making predictions about the growth behaviour of tomato genotypes under drought stressed conditions in different environments through the incorporation of genotype specific parameters (GSPs) as well as QTL-derived parameters into the eco-physiological crop model. Using the genome-based dynamic model, individual plant reaction to stressful environments can be evaluated in the context of the genetic background and interaction with environmental factors. This knowledge can be used both when defining breeding goals, when choosing a variety and when designing an ideotype relevant for drought adaptation.

The genotypes set of tomatoes used in this study are interspecific near isogenic lines (NILs), the genetic information regarding the location and length of chromosome segment introgressed in each line, and corresponding genetic markers are available (https://tgrc.ucdavis.edu/). Moreover, the complete genome of donor parent *Solanum pennellii* has been sequenced (Bolger et al., 2014a).

Making assumption is inevitable, but essential step in modelling practices no matter what statistical or processed based models were going to be built. Three main assumptions had to be made for the implementation of this model. Firstly, it was assumed that the plant growth was developmental and source-sink balance dependent, which meant (leaf) growth and photosynthesis (or dry matter production) were in parallel with feedback control. Secondly, it was assumed that the stressed performances of the growth processes were under the control of soil water thresholds for leaf expansion, stomatal conductance and transpiration. The final assumption was that GSPs (e.g. maximum leaf expansion, maximum stomatal conductance) were stable genetic traits, largely independent from environment or with encapsulated environmental effect.

White and Hoogenboom (2003) categorized the six levels of genetic detail for simulations to elucidate differences in plant growth and development among cultivars. These are 1) generic model with no reference to species, 2) species-specific model with no reference to genotypes,

3) genetic differences represented by cultivar-specific parameters, 4) genetic differences represented by specific alleles, with gene action and gene effects represented through linear effects on model parameters, 5) genetic differences represented by genotypes, with gene action explicitly simulated based on knowledge of regulation of gene expression and effects of gene products, and 6) genetic differences represented by genotypes, with gene action simulated at the level of interactions of regulators, gene-products, and other metabolites. Most modelling practices are at level 3 (e.g. CROPGRO, CERES), and the last three levels are the continuum of approaches involving a more significant levels of genetic and biochemical detail. The model developed in this study is essentially a level 3 category.

The first setup of experimental work (four trials) was designed with dual purposes (chapter 2). The first purpose was an analysis of static (harvest) data which exhibited the plastic responses after a moderate and short term terminal drought stress, and the second purpose was an analysis of dynamic data which showed the genetic determinism on drought reactions for expansion and apparent gas exchange. In these trials, the adaptation strategies were shown by differing plastic responses of the morphological (drought avoidance), water relation (drought tolerance) and dry matter (negative drought effect) traits. Less magnitude of plasticity in dry matter produced in comparison to morphological traits (e.g. leaf area), indicated the merit of water-saving strategy as a generic feature of the IL population. High magnitude of plasticity in turgid osmotic potential was addressed alternatively by osmotic adjustment (OA). It turned out that most leaf traits such as water potential, osmotic potential, nitrate-nitrogen content were more sensitive than most canopy traits (**Fig. 2-1, 2- S1**).

Moreover, QTLs analysis on the trait values and plasticity revealed a strong linkage between heritability and abundance of associated regions (**Fig. 2-S10**). QTL analysis was also based on three assumptions: 1) each associated IL carries only a single QTL, 2) two overlapping introgressions with a significant effect in the same direction carry the same QTL and 3) a QTL is counted only if the IL is significantly different from the control M82 at $p < 0.05$ (Eshed and Zamir, 1995). Although the ILs are the "first generation" set, comprising 50 introgression lines, the whole genome of donor parent *Solanum pennellii* was covered. The chromosome segment was rather long with the average of length of 33 cM. Fine tuning of ILs could be done by using the currently available 76 ILs, including 26 more sub-ILs with shorter segments to improve mapping resolution. The advantage of using ILs is that any difference in target phenotype from recurrent M82 can be attributed to the introgressed segment.

For the second purpose (chapter 3), the dynamics of genotype-specific raw data were acquired along the course of soil drying to be used for parameter estimation. Since there was only one replication in each trial, the terminal drought imposition was done for only one cycle, and the plants were harvested when the stress plants showed less than 10% transpiration of the control. The time when the plant processes began to react to soil drying and intensity of the following decline was estimated using a linear plateau regression model. For parameterization of soil water reaction, this empirical model was applied based on the four assumptions: 1) the behaviours of plant physiological processes such as leaf expansion, stomatal behaviour and transpiration were driven by current volumetric soil water status under terminal drought stress; 2) there was a threshold point at which a particular plant process began to react to soil drying; 3) the subsequent decline of a plant process in response to soil water deprivation followed a linear function; and 4) the average soil water threshold derived from the environmental ranges was a genotype-specific trait, with a linear dependence on conditional evaporative demand. In practical implication, this threshold was far from a constant depending on the interplays of ontogeny, intensity and speed of soil water decline in reaction to confounding factors aside from evaporative demand. However, these assumptions were required to make use of soil water threshold as a drought reaction parameter in a crop model.

There is a possibility to get stable QTLs of sensitivity to environmental variables. For example, leaf elongation rate which varies with time according to environmental conditions reaches its maximum value during the night, and therefore its response to evaporative demand or soil water deficit is common to different experiments for each genotype of a mapping population (Tardieu and Tuberosa, 2010; Reymond et al., 2003). This dissection approach sounds useful, however, practically was not feasible in our system.

Identification of QTLs was performed on the drought reaction parameters (i.e. thresholds and slopes) for leaf expansion, stomatal conductance and transpiration. To avoid the interaction between thresholds and slopes, QTL-derived thresholds only were used, while the slopes were described as a function of thresholds. For the validation of QTLs derived parameters, a semi-empirical model for plant transpiration under stressed was built based on unstressed values which took account of the environmental and genetic variation for absolute trait values (chapter 3). Here drought effect was introduced either directly on plant transpiration or indirectly on two components- specific transpiration rate and transpiring area. It was assumed that stressed values of specific transpiration could be driven via thresholds of either stomatal conductance or specific transpiration itself. Because of that, three modelling approaches were

designed for separate simulations. Stressed value of specific transpiration relative to unstressed one was assumed to be controlled by genotype-specific parameters, particularly soil water threshold, which in turn depended on soil water status for the timing of its expression. The empirical function of vapour pressure deficit (VPD) on thresholds was also introduced into the model. Two intermediate variables, specific transpiration rate and leaf expansion rate under drought stress were determined as the product of unstressed values and function of soil water status by using the previously estimated thresholds as model inputs.

The model performed quite well for plant transpiration in both cases of direct (via the threshold of transpiration) and indirect approach (via thresholds of specific transpiration and leaf expansion), regardless of the effect of VPD on thresholds in each case of simulation using QTL-derived parameters or GSPs. This indicated that the use of soil water threshold as an input of genetic parameter could be possible in a gene-based crop model. Less precise prediction under high VPD condition was reflected in the accuracies of predicted leaf expansion rate (Fig. 3-S11). This could be either because of error in threshold values or that in unstressed leaf expansion rate itself. The more precise prediction could be made for total transpiration with the introduction of VPD effect on threshold of stomatal conductance, especially under high VPD condition. However confounding factors involved in this aspect could bring a more complication, although it was well known that evaporative demand was the central indicator of atmospheric drought.

In the next step of incorporation between the genetic information and eco-physiological model (chapter 4), mean thresholds only were introduced to represent the stable genetic trait for drought reactions for leaf expansion, stomatal conductance and specific transpiration. It needs to clarify that there were two data types of the genetic parameters, namely the parameters which characterize the specific genotypes for unstressed conditions and those for the stressed condition. The later could be GSPs or QTL-derived ones, particularly soil water thresholds for expansive growth and gases exchange processes.

The model for the unstressed condition was first built in a modular structure comprising three modules: i) (leaf) growth and development; ii) photosynthesis, dry matter production and partitioning; and iii) transpiration and soil water uptake. The whole model was basically *in parallel* type with feedback loops of leaf biomass to leaf area, leaf area to transpiration and photosynthesis, transpiration to soil water uptake, and soil water to leaf expansion and stomatal conductance, and stomatal conductance to transpiration and photosynthesis (**Fig. 4-1**, more detail in **Fig. 4-S5**). These feedback loops formed the interdependence between modules

and ensured the stability of the model in aggregated form. One peculiarity of this model is the role of stomatal conductance and SLA. Stomatal conductance was modelled separately from photosynthesis being dependent on genetic and current environmental factors and used as a causal factor for the behaviour of photosynthesis and transpiration. Similarly, SLA was modelled depending on genetic and environmental factors and used to regulate the source-sink balance. For calculation of potential sink capacity, minimum SLA was used, and for calculation of actual leaf expansion, maximum SLA was used while taking account of the environments. The model overestimated considerably the lower values of SLA (< 200 cm^2 g^{-1}) and underestimated the higher values, being more pronouned under drought stress. This inaccuracy in SLA prediction could have led to a weak prediction (over estimation) of leaf area of stressed plants. Taking account of the canopy profile of SLA depending on leaf age and soil water status could possibly improve the model performance in future works.

Each module was constructed based on one or two of established models in such a way that it satisfied the incorporation of genetic inputs and crop model to fulfil the model purpose for predicting the performances of multiple genotypes under water-limited environments. Model performances were evaluated at a higher integration level of agronomic interest. Since the main purpose of building this model was to construct a virtual system in which the genetic, environment, and management factors (e.g. regulation of irrigation, light supplement) and their interactions in a real system were incorporated, on the basis of physiological knowledge on the growth, transpiration, and dry matter production and drought reactions. The reference models applied and/or adapted into the current model are TOMSIM (Heuvelink, 1996b) and TOMGRO (Jones et al., 1991) for leaf growth, respiration, dry matter production and partitioning, Farquhar model for photosynthesis (Farquhar et al., 1980) and Penman-Monteith (Penman, 1948) and Stanghellini (Stanghellini, 1987) models for transpiration. The model performance was evaluated with or without the inputs of measured leaf area and soil water. The state variables of one module would be inputs of other modules. At this stage, the evaluated canopy traits were leaf areas, shoot dry matter and plant transpiration for both stressed and well-watered conditions, and soil water status under stressed conditions in three environmental conditions, differing mainly in vapour pressure deficits.

The model predicted the target traits in a good agreement with observed data even in aggregated mode and performed with high accuracy if the measured leaf area was used as input. Soil water input did not play a much role, meaning that the model had a functional balance on the flow of simulated soil water status. It turned out that the use of two genetic

parameters- thresholds for leaf expansion and stomatal conductance could address the genetic variations for higher-level complex traits such as shoot mass production, canopy leaf area under a stressed condition. With the manipulation in the levels of one factor (genetic or environment), the model sensitivity can easily be tested at different hierarchical states. For example, one can manipulate the magnitude of genetic factors such as soil water threshold and maximum leaf expansion or environmental factors such as light levels, CO_2 temperature etc., by making hypotheses which cannot be easily answered in a real system.

Although the whole model was constructed on the basis of plausible concepts and assumptions, it is just a first version of such kind, and there are many black boxes and may have issues with the structural part. After different steps of improvements in functional relation and even structural adjustment, the model would be useful for hypothesis testing in virtual experiments for better understanding of the real systems, and could be extended to other modules and increased in model complexity for particular compartments (e.g. photosynthesis, soil water relation).

Future research

The current model has a module for individual leaf growth, but the photosynthesis was estimated based on a big-leaf approach. With some adjustment, photosynthesis module can be changed to sun-shade or multilayer one if measured data of light condition at the crop level are available. The further step should be to conduct the plausible evaluations on some basic components such as sub-modules of stomatal conductance and specific leaf area. The model could be used for better understanding of the sensitivities of plant reactions to changes in environmental components, such as light, VPD and temperature or that of plant performances in response to changes in some state variables such as stomatal conductance, leaf expansion or in SLA. Moreover, it could also be possible to study the influence of changes in characteristics of virtual ILs on their drought reactions such as leaf expansion process or the performance of traits at upper integration level such as water use or dry matter accumulation. Since, components and processes shaping the canopy architecture (such as leaf width, internode length) are mainly under the genetic influence and highly heritable (Wu and Stettler, 1994; Wu, 1998; De Wit et al., 2002; Perez et al., 2016), integration of architectural traits in breeding programs is a new perspective (Wu, 1998; Rötter et al., 2015). If the genetic inputs or QTL information on heritable architectural traits are available, properly defined and incorporated in functional structural plant modelling (FSPM) framework, the hypothesis regarding the effects of G x E interaction on these traits and consequences on physiological processes multiple genotypes could be answered.

Previously, studies on genetic variability in FSPMs have included the estimation of the physiological or morphological parameters by using QTL information (Letort et al., 2007; Xu et al., 2011). QTL effects were used to predict the values of some FSPM input parameters such as those determining organ sink strength on virtual recombinant populations (Letort et al., 2007). Since the current model has already built the virtual ILs which are characterized by specific parameters for varying growth, water relation, dry matter production and drought reactions, it is possible to integrate this information into a FSPM platform. Moreover, there is enough information for all lines regarding the architectural traits such as leaf geometry and leaf angle, and therefore to build a virtual IL library in FSPM is possible. Implementing the genetic module in FSPM platform could bring a new dimension of research in genome-based modelling.

Supplementary Materials
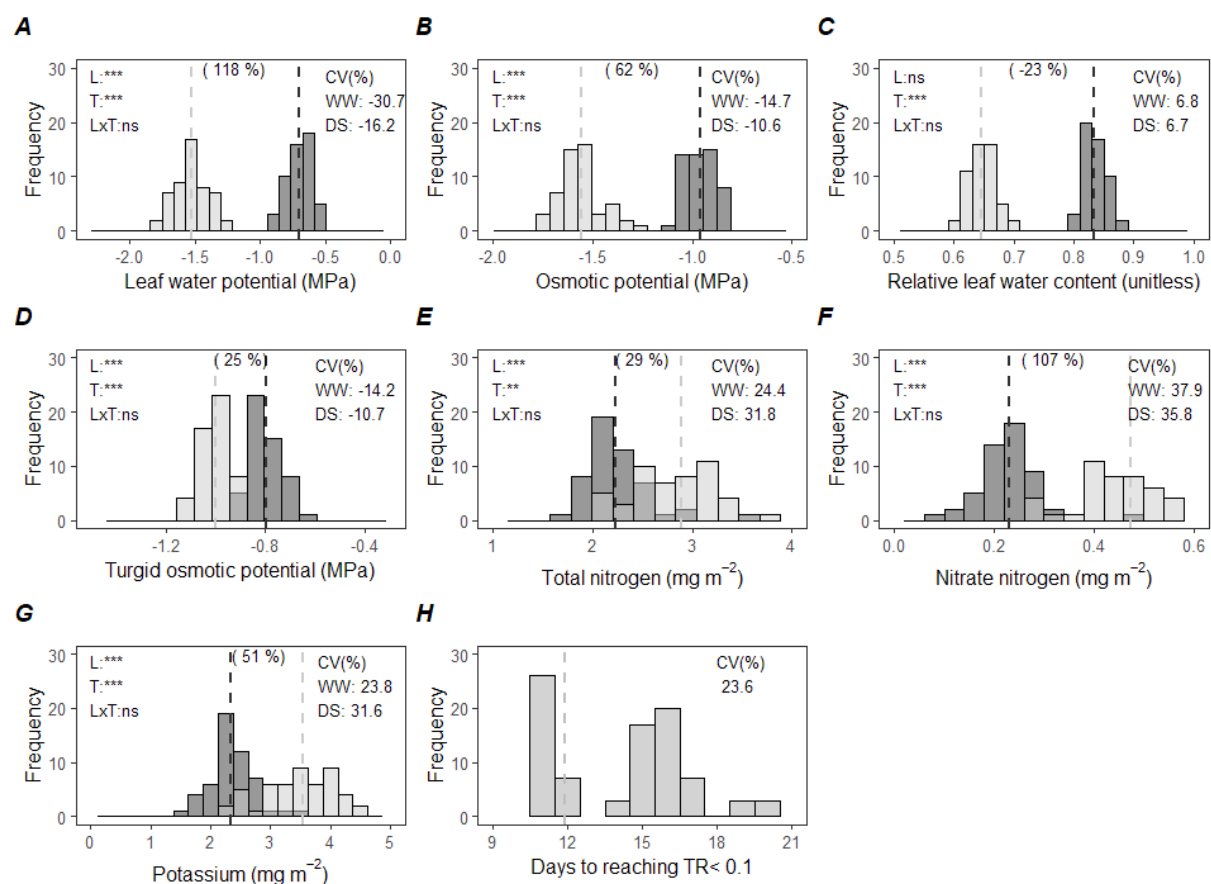
Fig. 2-S1. Frequency distribution of physiological traits under well-watered (WW, dark grey) and drought stressed (DS, light grey) conditions and days to reaching transpiration ratio (TR) < 0.1. Dashed lines indicate the trait means for each water supply environment. Mean phenotypic plasticity is described in parentheses as a relative change (percent increase (+) or decrease (-)) upon stress. F-test shows line (L), treatment (T) and interaction (L x T) effects. CV (%) are given for each WW and DS conditions. *, *** and ns denote significance at p<0.05, 0.001 and non-significance.

Fig. 2-S2. Overlay heat map of the phenotypic values of ILs compared with M82 for well-watered (A) and drought stressed (B) conditions, and phenotypic plasticity upon drought stress, osmotic adjustment and drought survival (C). Regions of red or blue indicate relative increase or decrease of trait values, after introgression of *Solanum pennellii* segments. Pale regions indicate that IL had no appreciable wild allelic effect. The ILs are presented in chromosomal order from top of chromosome 1 to base of chromosome 12 from top to bottom. A total of 50 ILs and 18 traits overlapped in four blocks (replications).

.

Fig. 2-S3. Regression of the phenotypic plasticity of shoot dry weight and cumulative transpiration plotted against that of turgid osmotic potential (A, C) and osmotic adjustment (B, D), respectively. Dashed and dotted lines indicate the values of M82 and Sp lines respectively. Regression is done from LSMEANS of individual lines. For trait acronyms, trait and classes see the **Table 2-1.**

Table 2-S1. Summary of ANOVA for trait classes describing the F-value and P-value using linear mixed model for the main effects of line (L) and drought treatment (T) and interaction between them (L x T) as fixed factors. ns denotes non-significance; *, ** and *** denote significant at P< 0.05, 0.01, and 0.001, respectively.

Attribute	Line (L)		Treatment (T)		L x T effect	
	F	*P*	*F*	*P*	*F*	*P*
(A) Morphological trait						
SL (cm plant^{-1})	6.0081	<2E-16	420.7313	<2E-16	0.9636	0.5483
LN (nr. plant^{-1})	4.5555	<2E-16	119.4261	<2E-16	0.5122	0.9977
INL (cm)	1.7857	0.00153	66.7381	6.97E-15	0.691	0.9456
LA$_t$ (cm^2 plant^{-1})	5.2194	**<2E-16**	1535.38	<2E-16	1.4453	0.0318
SLA$_t$ (cm^2 g^{-1})	3.54	2.95E-12	227.9853	<2E-16	0.6776	0.9542
(B) Dry matter trait						
DW$_{le}$ (g plant^{-1})	4.1379	2.25E-15	1116.416	<2E-16	1.1248	0.2707
DW$_{st}$ (g plant^{-1})	3.5331	3.21E-12	420.9059	<2E-16	0.7997	0.8333
DW$_{sh}$ (g plant^{-1})	3.3934	1.73E-11	981.4388	<2E-16	0.9968	0.4854
(C) Physiological trait						
CT (kg plant^{-1})	2.8113	1.82E-08	2483.599	<2E-16	1.4044	0.0437
TE (g kg^{-1})	2.1079	5.52E-05	850.6993	<2E-16	0.4751	0.9991
ST (kg m^{-2}day^{-1})	2.6299	1.53E-07	620.7938	<2E-16	0.5312	0.9965
WP (MPa)	1.849	0.00082	1670.303	<2E-16	0.5085	0.9979
OP (MPa)	2.2597	1.05E-05	1936.94	<2E-16	1.1911	0.1871
RWC	1.2028	0.1745	2123.786	<2E-16	0.8287	0.7906
OP$_{100}$ (MPa)	1.8405	0.00089	417.6939	<2E-16	0.6538	0.9670
TN (mg cm^{-2})	3.272	7.44E-11	111.4961	<2E-16	0.6981	0.9406
NN (mg cm^{-2})	3.6447	8.37E-13	497.6214	<2E-16	0.8042	0.8271
K (mg cm^{-2})	3.4931	5.19E-12	269.1744	<2E-16	0.9681	0.5397

Table 2-S2. Summary of ANOVA for phenotypic plasticity of traits and of OA and drought survival (SUR) with Satterthwaite's method using linear mixed model for the main effects of line (L) as fixed factors. ns denotes non-significance; ., * and *** denote significant at $P<$ 0.1, 0.05, and 0.001, respectively. SSE, sum of squared errors, MSE, mean squared errors, NumDF, numerator degree of fredom, DenDF, denominator degree of fredom, Sig., significance. Acronyms are described in **Table 2-1**.

Trait	SSE	MSE	NumDF	DenDF	F-value	Pr (>F)	Sig.
pSL	25901	507.85	51	161	1.024	0.444	ns
pLN	26644	522.43	51	161	0.956	0.563	ns
pINL	61913	1214	51	161	1.100	0.323	ns
pLAt	6110	119.8	51	161	1.070	0.368	ns
pSLAt	16770	328.82	51	161	1.056	0.390	ns
pDWle	5777.2	113.28	51	161	0.996	0.491	ns
pDWst	11953	234.38	51	161	1.097	0.326	ns
pDWsh	6127	120.14	51	161	0.989	0.504	ns
pCT	2359.7	46.268	51	161	1.212	0.185	ns
pTE	39599	776.45	51	161	1.403	0.059	.
pST	7470.2	146.47	51	161	1.477	0.036	*
pWP	173261	3397.3	51	161	0.962	0.552	ns
pOP	43201	847.07	51	161	1.631	0.012	*
pRWC	1857.9	36.429	51	161	1.271	0.133	ns
pOP100	16396	321.48	51	161	1.371	0.072	.
pTN	55497	1088.2	51	161	1.052	0.396	ns
pNN	513800	10074	51	161	0.780	0.847	ns
pK	103968	2038.6	51	161	1.105	0.315	ns
OA	0.6959	0.0136	51	161	1.557	0.020	*
SUR	394.21	7.7296	51	161	3.227	<0.001	***

Table 2-S3. Summary of phenotypic variations among parent lines (*Solanum pennellii* (Sp) x *Solanum lycopersicum* cv. M82) and introgression lines (ILs) for 19 traits upon water supply conditions. WW, well-watered; DS drought-stressed. Acronyms are described in **Table 2-1**.

Trait and treat.	M82 (n=12)				SP (n=4)				IL (n=200)			
	Mean	Min	Max	CV(%)	Mean	Min	Max	CV(%)	Mean	Min	Max	CV(%)
(A) Morphological trait												
SL (cm plant^{-1})												
WW	17.68	12.00	24.50	25.69	32.38	23.00	42.00	28.01	19.40	4.00	34.50	30.40
DS	11.06	4.50	17.00	36.47	23.63	12.00	32.00	35.56	11.37	2.00	26.00	37.24
Across	14.37	4.50	24.50	37.53	28.00	12.00	42.00	33.38	15.38	2.00	34.50	42.34
LN (nr. plant^{-1})												
WW	4.17	2.00	6.00	30.42	7.50	5.00	10.00	31.74	4.67	2.00	10.00	38.83
DS	3.75	2.00	5.00	28.14	5.75	5.00	7.00	16.65	3.53	2.00	7.00	37.56
Across	3.96	2.00	6.00	29.31	6.63	5.00	10.00	29.02	4.10	2.00	10.00	41.12
INL (cm)												
WW	4.44	3.00	6.50	24.77	4.40	3.80	5.30	16.40	4.59	1.75	10.59	39.22
DS	3.01	1.50	4.50	33.24	4.11	2.40	5.33	34.37	3.42	0.86	9.33	40.73
Across	3.73	1.50	6.50	33.87	4.25	2.40	5.33	24.67	4.01	0.86	10.59	42.70
LA$_t$ (cm plant^{-1})												
WW	2030.6	1357.7	3230.4	29.3	627.1	459.6	867.3	31.2	1816.0	260.2	3260.1	27.6
DS	750.8	420.6	1384.3	42.9	314.5	113.3	421.2	44.0	716.9	86.7	1542.7	39.7
Across	1390.7	420.6	3230.4	57.8	470.8	113.3	867.3	48.7	1266.5	86.7	3260.1	54.0
SLA$_t$ (cm^2 g^{-1})												
WW	216.7	172.4	302.2	20.4	189.9	167.7	224.2	14.1	204.3	85.7	320.4	20.0
DS	161.1	103.1	236.2	23.3	148.3	115.6	183.7	18.8	155.5	54.2	257.2	25.4
Across	188.9	103.1	302.2	26.0	169.1	115.6	224.2	19.9	179.9	54.2	320.4	26.1
(B) Dry matter trait												
DW$_{le}$ (g plant^{-1})												
WW	9.42	6.36	13.58	23.67	3.39	2.05	5.11	38.41	8.94	2.70	14.32	23.71
DS	4.58	3.27	7.21	27.87	2.06	0.98	2.90	38.76	4.54	1.60	7.86	27.16
Across	7.00	3.27	13.58	43.49	2.73	0.98	5.11	44.98	6.74	1.60	14.32	41.60
DW$_{st}$ (g plant^{-1})												
WW	2.48	1.57	4.14	26.82	2.05	0.76	3.09	51.80	2.62	1.06	4.51	25.53
DS	1.54	1.14	2.10	22.38	1.34	0.34	1.89	52.15	1.70	0.65	3.16	26.83
Across	2.01	1.14	4.14	35.11	1.69	0.34	3.09	53.90	2.16	0.65	4.51	34.02
DW$_{sh}$ (g plant^{-1})												
WW	11.90	8.12	17.72	23.75	5.44	2.81	8.20	42.73	11.55	3.91	18.83	22.98
DS	6.12	4.56	9.25	26.15	3.40	1.32	4.64	43.09	6.23	2.25	10.41	25.62
Across	9.01	4.56	17.72	41.16	4.42	1.32	8.20	47.54	8.89	2.25	18.83	38.77
(C) Physiological trait												
CT (kg plant^{-1})												
WW	4.44	2.99	6.38	25.01	1.99	1.02	3.93	67.10	4.08	1.04	6.74	21.79
DS	1.32	0.84	1.82	22.72	0.80	0.34	1.14	45.09	1.30	0.41	2.29	19.19
Across	2.88	0.84	6.38	61.89	1.39	0.34	3.93	79.38	2.69	0.41	6.74	57.18
TE (g kg^{-1})												
WW	2.78	1.57	3.50	24.36	3.00	2.09	3.70	24.27	2.91	1.45	4.49	22.08
DS	4.80	2.87	6.73	26.80	4.27	3.94	4.99	11.31	4.91	1.96	7.71	26.03
Across	3.79	1.57	6.73	38.02	3.64	2.09	4.99	24.35	3.91	1.45	7.71	36.40
ST (kg m^{-2} day^{-1})												
WW	2.62	1.65	3.86	28.50	3.84	1.83	5.47	41.12	2.57	1.04	6.43	41.13

DS	1.07	0.69	1.47	23.01	2.10	1.34	3.17	36.56	1.12	0.52	4.02	42.57
Across	1.84	0.69	3.86	52.05	2.97	1.34	5.47	49.78	1.84	0.52	6.43	59.34
WP (MPa)												
WW	-0.78	-1.20	-0.40	-33.90	-0.70	-1.00	-0.40	-45.55	-0.70	-1.24	-0.30	-30.26
DS	-1.57	-1.90	-1.15	-16.28	-1.50	-1.70	-1.30	-10.89	-1.53	-1.95	-1.10	-16.34
Across	-1.18	-1.90	-0.40	-40.73	-1.10	-1.70	-0.40	-44.34	-1.11	-1.95	-0.30	-42.72
OP (MPa)												
WW	-1.02	-1.14	-0.85	-10.01	-0.86	-0.98	-0.59	-21.02	-0.96	-1.30	-0.51	-14.74
DS	-1.49	-1.61	-1.24	-6.99	-1.26	-1.46	-1.08	-12.35	-1.56	-1.95	-1.08	-10.37
Across	-1.25	-1.61	-0.85	-20.77	-1.06	-1.46	-0.59	-25.21	-1.26	-1.95	-0.51	-26.76
RWC												
WW	0.82	0.77	0.87	3.84	0.82	0.76	0.87	5.83	0.84	0.69	0.93	6.96
DS	0.63	0.55	0.72	6.60	0.70	0.65	0.72	4.92	0.64	0.53	0.73	6.60
Across	0.73	0.55	0.87	14.24	0.76	0.65	0.87	10.03	0.74	0.53	0.93	14.61
OP_{100} (MPa)												
WW	-0.84	-0.91	-0.70	-8.70	-0.70	-0.80	-0.50	-19.62	-0.80	-1.06	-0.46	-14.28
DS	-0.94	-1.09	-0.81	-7.93	-0.88	-0.95	-0.77	-8.93	-1.01	-1.27	-0.78	-10.58
Across	-0.89	-1.09	-0.70	-10.07	-0.79	-0.95	-0.50	-17.80	-0.90	-1.27	-0.46	-16.71
TN (mg m^{-2})												
WW	2.08	1.27	2.65	21.49	2.11	1.76	2.36	14.06	2.24	1.24	4.81	24.66
DS	2.73	1.86	4.30	26.31	2.92	2.33	3.80	21.73	2.89	1.64	8.15	32.27
Across	2.41	1.27	4.30	27.94	2.51	1.76	3.80	25.20	2.57	1.24	8.15	32.45
NN (mg m^{-2})												
WW	0.24	0.14	0.40	32.83	0.25	0.12	0.32	35.44	0.23	0.08	0.53	38.44
DS	0.46	0.25	0.68	32.03	0.39	0.28	0.55	30.80	0.48	0.17	1.16	36.01
Across	0.35	0.14	0.68	46.19	0.32	0.12	0.55	38.10	0.35	0.08	1.16	52.23
K (mg m^{-2})												
WW	2.16	1.49	2.70	17.88	1.66	1.51	1.94	11.82	2.36	1.23	5.21	23.71
DS	3.26	2.21	5.10	26.02	2.40	1.64	3.02	24.56	3.58	1.43	9.49	31.53
Across	2.71	1.49	5.10	31.50	2.03	1.51	3.02	27.93	2.97	1.23	9.49	36.25
OA (MPa)												
DS	0.10	0.04	0.19	53.18	0.18	0.10	0.27	37.46	0.21	0.02	0.48	49.88
SUR (dpi)												
DS	11.50	9.00	16.00	21.14	16.00	13.00	19.00	16.14	11.85	9.00	20.00	23.52

Table 2-S4. List of line x phenotype associations for morphological, dry matter and physiological traits of introgression lines in WW and/or DS treatments and phenotypic plasticity (pX in %). Bold RD (LSMEAN$_{ILs}$- LSMEAN$_{M82}$)/LSMEANS$_{M82}$*100) values indicate significant wild allelic effects at FDR < 0.05. L, line main effects; L+I, line main effects and line x treatment interactions; I, line x treatment interactions only. WW, well-watered; DS, drought-stressed

Trait	ILs	Chr.	Position (cM)		Effect	LSMEANS				RD (% M82)			
						Across	WW	DS	pX	Across	WW	DS	pX
(A) Morphological traits													
SL	IL 01-4	1S	127.5	165	L	19.1	24.4	13.8	-42.1	**32.7**	38.0	24.4	9.9
(cm plant^{-1})	IL 03-3	3S	71.5	85	L + I	7.3	9.8	4.8	-53.3	**-49.6**	**-44.9**	**-57.1**	39.2
	IL 07-3	7S	40.8	64	L + I	27.1	31.4	22.9	-27.8	**88.8**	**77.5**	**106.8**	-27.5
	IL 07-4	7S	2	45.5	L + I	19.2	25.3	13.1	-48.1	**33.4**	**42.9**	18.3	25.6
	IL 11-4	11S	84	103	L + I	19.2	25.1	13.4	-46.3	**33.9**	**41.8**	21.3	20.8
	IL 12-1	12S	0	21	I	17.9	25.0	10.9	-56.9	24.8	**41.4**	-1.7	48.6
	IL 12-4	12S	103	120	L + I	20.1	26.4	13.8	-48.2	**39.8**	**49.4**	24.4	25.8
LN	IL 04-3	4S	46	110	L	5.5	6.3	4.8	-19.2	**39.0**	50.0	26.7	142.5
(nr. plant^{-1})	IL 07-3	7S	40.8	64	L + I	7.4	8.3	6.5	-19.1	**86.3**	**98.0**	**73.3**	141.6
LA$_t$	IL 02-3	2S	18	68	L + I	896.7	1290.7	502.8	-59.5	**-35.5**	**-36.4**	-33.0	-6.1
(cm^2 plant^{-1})	IL 03-1	3S	0	32	I	1023.6	1470.9	576.3	-52.3	-26.4	**-27.6**	-23.2	-17.5
	IL 03-2	3S	32	76.5	I	1047.8	1414.0	681.6	-50.6	-24.7	**-30.4**	-9.2	-20.1
	IL 03-3	3S	71.5	85	L + I	838.7	1245.7	431.8	-64.7	**-39.7**	**-38.7**	**-42.5**	2.1
	IL 03-5	3S	141	171	I	1004.0	1391.6	616.4	-55.2	-27.8	**-31.5**	-17.9	-12.9
	IL 06-2	6S	33.5	80	L + I	534.3	759.4	309.2	-54.8	**-61.6**	**-62.6**	**-58.8**	-13.4
	IL 07-3	7S	40.8	64	I	987.5	1273.4	701.6	-47.1	-29.0	**-37.3**	-6.6	-25.7
SLA$_t$	IL 02-3	2S	18	68	L	148.5	168.3	128.8	-23.3	**-21.4**	-22.3	-20.1	-3.9
(cm^2 g^{-1})	IL 03-1	3S	0	32	L + I	136.0	151.5	120.5	-6.9	**-28.0**	**-30.1**	-25.2	-71.6
	IL 03-3	3S	71.5	85	L + I	135.7	157.9	113.5	-27.6	**-28.2**	**-27.1**	**-29.5**	13.6
	IL 03-5	3S	141	171	L + I	150.9	161.4	140.3	-8.7	**-20.1**	**-25.5**	-12.9	-64.1
	IL 06-2	6S	33.5	80	L + I	116.5	134.5	98.4	-27.7	**-38.4**	**-37.9**	**-38.9**	14.4
	IL 09-2	9S	32	61.7	L	230.1	260.3	199.9	-22.6	**21.8**	20.1	24.1	-6.8
(B) Drymatter traits													
DW$_{le}$	IL 06-2	6S	33.5	80	L + I	3.91	5.02	2.81	-36.8	**-44.1**	**-46.7**	**-38.7**	-27.1
(g plant^{-1})	IL 07-3	7S	40.8	64	L + I	4.76	6.11	3.41	-45.1	**-32.0**	**-35.1**	**-25.6**	-10.7
DW$_{st}$	IL 01-1	1S	0	58	L	2.62	3.27	1.97	-39.3	**29.9**	31.5	27.3	12.3
(g plant^{-1})	IL 02-3	2S	18	68	L + I	2.63	2.90	2.35	-17.5	**30.3**	16.7	**52.2**	-50.1
	IL 05-4	5S	102	112.5	L + I	2.66	3.35	1.97	-40.0	**32.0**	**34.9**	27.4	14.4
	IL 06-1	6S	4	34	L + I	2.74	3.36	2.12	-36.3	**36.1**	**35.4**	**37.3**	3.7
	IL 07-3	7S	40.8	64	L + I	2.88	3.46	2.31	-32.6	**43.1**	**39.2**	**49.4**	-6.6
	IL 11-1	11S	0.5	29	L + I	2.69	3.64	1.73	-52.5	**33.4**	**46.6**	12.2	50.2
DW$_{sh}$	IL 06-2	6S	33.5	80	L + I	5.48	6.85	4.11	-33.6	**-39.2**	**-42.5**	**-32.9**	-29.2
(g plant^{-1})													
(C) Physiological traits													
CT	IL 06-2	6S	33.5	80	L + I	1.50	2.20	0.81	-59.0	**-47.7**	**-50.4**	**-38.8**	-15.5
(kg plant^{-1})	IL 07-3	7S	40.8	64	L + I	1.90	2.84	0.95	-65.3	**-34.1**	**-36.0**	**-27.7**	-6.5
TE	IL 02-5	2S	68	136	I	4.56	3.60	5.51	52.1	20.3	**29.6**	14.9	-30.0
(g kg^{-1})	IL 03-3	3S	71.5	85	L + I	2.82	2.22	3.42	53.2	**-25.5**	-19.9	**-28.8**	-28.4

	IL 07-3	7S	40.8	64	L + I	4.72	3.46	5.98	76.5	**24.6**	24.6	**24.6**	2.8
	IL 11-1	11S	0.5	29	L + I	4.62	3.65	5.59	52.3	**21.9**	**31.3**	16.5	-29.7
ST	IL 01-1	1S	0	58	L + I	2.57	3.37	1.76	-42.3	39.2	28.9	64.4	-27.5
(kg m^{-2} day^{-1})	IL 03-5	3S	141	171	I	2.23	2.74	1.72	-43.5	21.1	4.8	**61.2**	-25.4
	IL 05-2	5S	13.5	62.3	I	2.30	3.01	1.60	-43.9	25.0	14.9	**49.7**	-24.7
	IL 06-2	6S	33.5	80	I	2.44	3.16	1.73	-46.8	32.4	20.6	**61.5**	-19.7
	IL 08-2	8S	30	67	L + I	2.73	3.86	1.61	-56.1	**48.2**	47.4	**50.2**	-3.8
WP (MPa)	IL 12-1	12S	0	21	L	-0.90	-0.53	-1.28	161.2	**-23.5**	-32.6	-19.0	32.8
OP	IL 01-1	1S	0	58	I	-1.33	-0.94	-1.73	90.1	6.2	-8.2	16.1	**92.3**
(MPa)	IL 02-2	2S	12.5	20	I	-1.26	-0.88	-1.63	89.4	0.1	-13.8	9.7	**90.8**
	IL 04-2	4S	46	68	I	-1.21	-0.83	-1.60	94.0	-3.5	-19.0	7.2	**100.6**
	IL 08-3	8S	57	87	I	-1.24	-0.87	-1.62	91.1	-0.9	-14.6	8.5	**94.3**
	IL 09-2	9S	32	61.7	I	-1.16	-0.81	-1.52	88.4	-7.2	-20.7	2.0	**88.5**
RWC	IL 07-3	7S	40.8	64	I	0.77	0.84	0.70	-16.5	5.8	2.0	**10.7**	-28.6
OP$_{100}$	IL 01-1	1S	0	58	I	-0.93	-0.76	-1.10	44.8	4.8	-8.7	16.8	**252.4**
(MPa)	IL 02-2	2S	12.5	20	I	-0.87	-0.73	-1.01	40.3	-2.4	-12.9	7.0	**217.3**
	IL 03-4	3S	85	141	I	-0.85	-0.72	-0.97	36.3	-4.8	-14.3	3.6	**185.3**
	IL 04-2	4S	46	68	I	-0.84	-0.69	-0.99	41.8	-5.5	-17.1	4.8	**228.6**
	IL 05-1	5S	0	21	I	-1.02	-0.90	-1.14	28.0	15.1	7.9	21.5	120.2
	IL 05-2	5S	13.5	62.3	I	-0.95	-0.81	-1.09	36.9	7.0	-3.2	16.1	**190.5**
	IL 07-5	7S	2	9	I	-0.83	-0.69	-0.96	42.0	-6.8	-17.2	2.5	**230.3**
	IL 08-3	8S	57	87	I	-0.87	-0.72	-1.02	43.5	-2.3	-14.4	8.4	**242.1**
	IL 09-2	9S	32	61.7	I	-0.80	-0.66	-0.94	43.5	-9.8	-21.3	0.4	**242.2**
	IL 10-1	10S	0	43	I	-0.84	-0.71	-0.96	38.7	-5.5	-14.6	2.5	**204.2**
TN	IL 03-1	3S	0	32	L + I	3.23	3.02	3.44	30.1	**34.2**	**44.9**	26.1	-11.0
(mg m^{-2})	IL 03-3	3S	71.5	85	L + I	3.36	2.72	4.00	48.4	**39.7**	30.7	**46.6**	42.9
	IL 03-5	3S	141	171	I	2.99	2.85	3.13	14.1	24.3	**36.8**	14.7	-58.5
	IL 06-2	6S	33.5	80	L + I	4.43	3.65	5.21	42.9	**84.0**	**75.1**	90.8	26.6
NN	IL 01-4	1S	127.5	165	I	0.23	0.11	0.35	236.2	-34.3	**-54.4**	-23.9	114.2
(mg m^{-2})	IL 02-5	2S	68	136	L	0.48	0.28	0.68	161.2	**38.3**	18.1	48.8	46.1
	IL 03-3	3S	71.5	85	L + I	0.60	0.47	0.72	53.8	**70.9**	**96.7**	57.5	-51.2
	IL 05-3	5S	62.3	102	L	0.22	0.14	0.30	137.9	**-36.9**	-41.4	-34.6	25.0
	IL 06-1	6S	4	34	L	0.48	0.33	0.64	96.2	**38.6**	36.9	39.4	-12.8
	IL 08-1	8S	0	36.7	L + I	0.19	0.10	0.28	213.2	**-45.9**	**-59.3**	-39.0	93.3
	IL 09-3	9S	57.5	116	L	0.48	0.30	0.67	120.7	**38.8**	25.2	45.9	9.4
	IL 12-4	12S	103	120	L	0.22	0.14	0.29	102.9	**-38.2**	-39.5	-37.5	-6.7
K	IL 03-1	3S	0	32	L + I	3.73	3.33	4.14	43.2	**37.7**	**53.8**	27.1	-21.0
(mg m^{-2})	IL 03-3	3S	71.5	85	L + I	4.06	2.90	5.22	80.2	**49.8**	34.0	**60.3**	46.8
	IL 06-2	6S	33.5	80	L + I	4.59	3.49	5.70	57.9	**69.4**	**61.3**	74.8	6.0
OA (MPa)	IL 01-1	1S	0	58					0.33			**222.7**	
	IL 01-3	1S	92.7	140.5					0.26			**145.8**	
	IL 02-2	2S	12.5	20					0.28			**168.0**	
	IL 03-4	3S	85	141					0.26			**148.0**	
	IL 03-5	3S	141	171					0.27			**158.1**	
	IL 04-2	4S	46	68					0.29			**181.4**	
	IL 05-1	5S	0	21					0.24			**131.1**	

	IL 05-2	5S	13.5	62.3	0.28	**171.8**
	IL 07-5	7S	2	9	0.27	**161.2**
	IL 08-3	8S	57	87	0.30	**192.3**
	IL 09-2	9S	32	61.7	0.29	**175.7**
	IL 09-3	9S	57.5	116	0.25	**141.0**
	IL 10-1	10S	0	43	0.25	**140.0**
	IL 11-2	11S	20.5	57	0.24	**132.8**
	IL 11-4	11S	84	103	0.25	**140.5**
	IL 12-1	12S	0	21	0.25	**138.8**
SUR (dpi)	IL 04-3	4S	46	110	14.3	**23.9**
	IL 06-2	6S	33.5	80	15.3	**32.6**
	IL 07-3	7S	40.8	64	16.5	**43.5**
	IL 11-1	11S	0.5	29	14.3	**23.9**
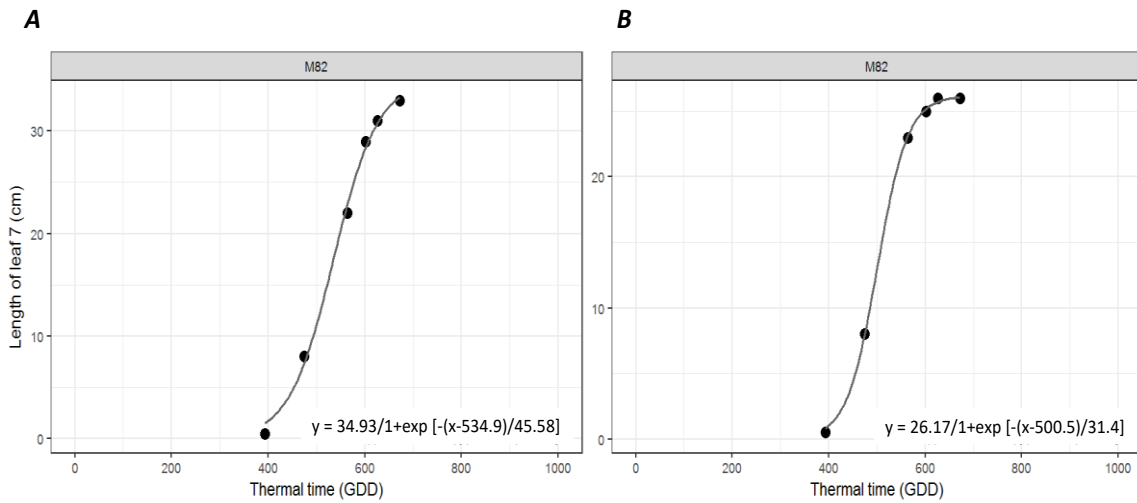
Fig. 3-S1. Dependency of leaf length growth (leaf 7) on thermal time (GDD) for M82 under (A) well-watered and (B) drought-stressed conditions. Three parameter logistic function was used for all leaves. Time of leaf appearance was estimated as initial point based on phyllochron (55°Cd per leaf) averaged for all lines. LAR was calculated through the linear fitting of leaf number per plant on GDD.
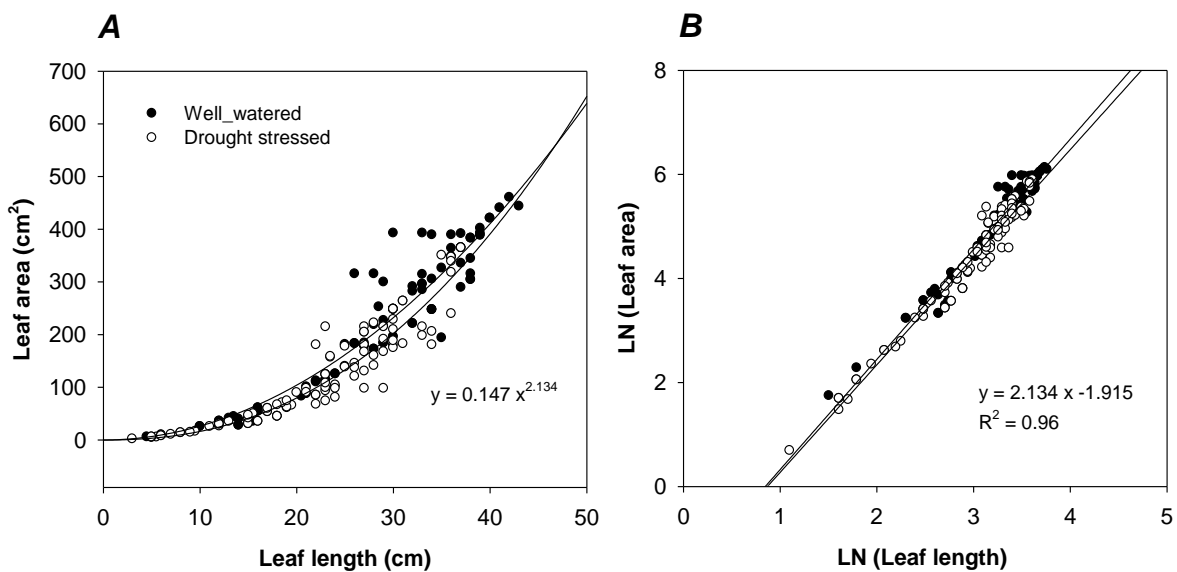
Fig. 3-S2. Allometric relationship between leaf length and leaf area of the recurrent line, M82 measured at the harvest times from three trials. (A) Absolute values, (B) Log-transformed values. Genotype-specific relationship was performed for all leaves across the drought treatments.
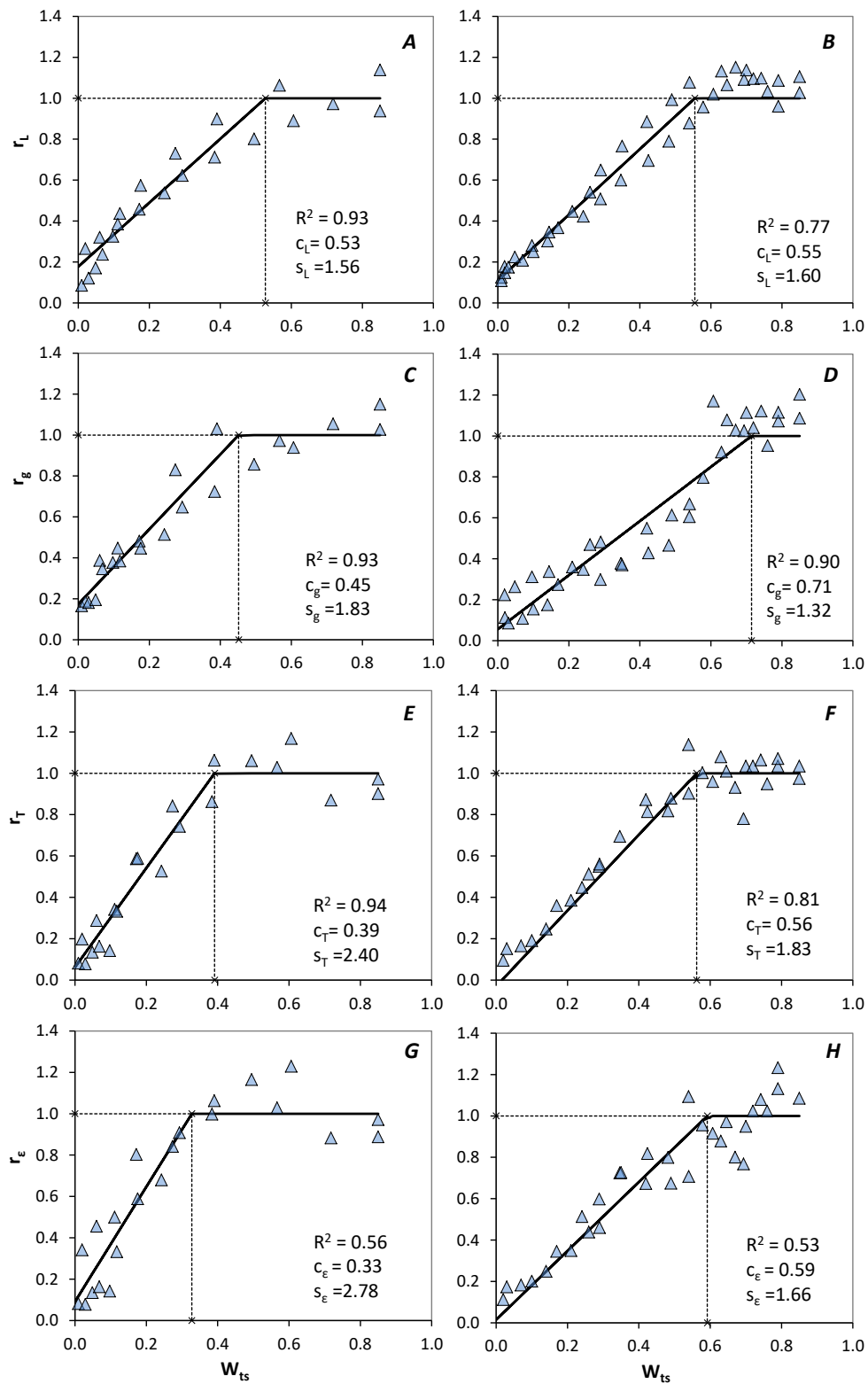
Fig. 3-S3. Linear plateau model fitted drought reactions of r_L, r_g, r_T and r_ε as a function of W_{ts} under high δe (2.62 ±0.64 kPa) observed in two parent lines: (A, C, E, G) recurrent M82 and (B, D, F, H) donor Sp.
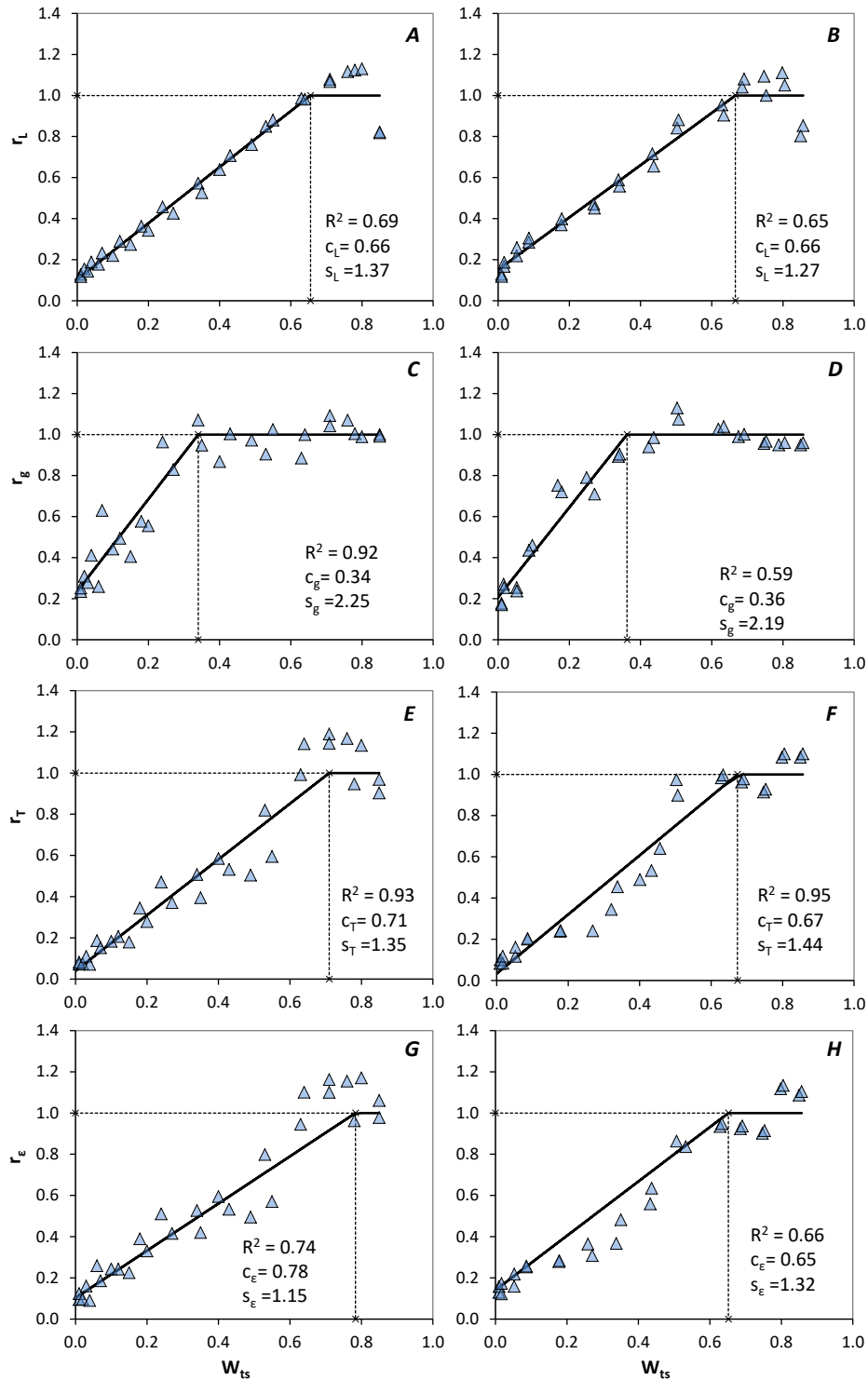
Fig. 3-S4. Linear plateau model fitted drought reactions of r_L, r_g, r_T and r_ε as a function of W_{ts} under low δe (1.20 ±0.18 kPa) observed in two parent lines: (A, C, E, G) recurrent M82, (B, D, F, H) donor Sp.
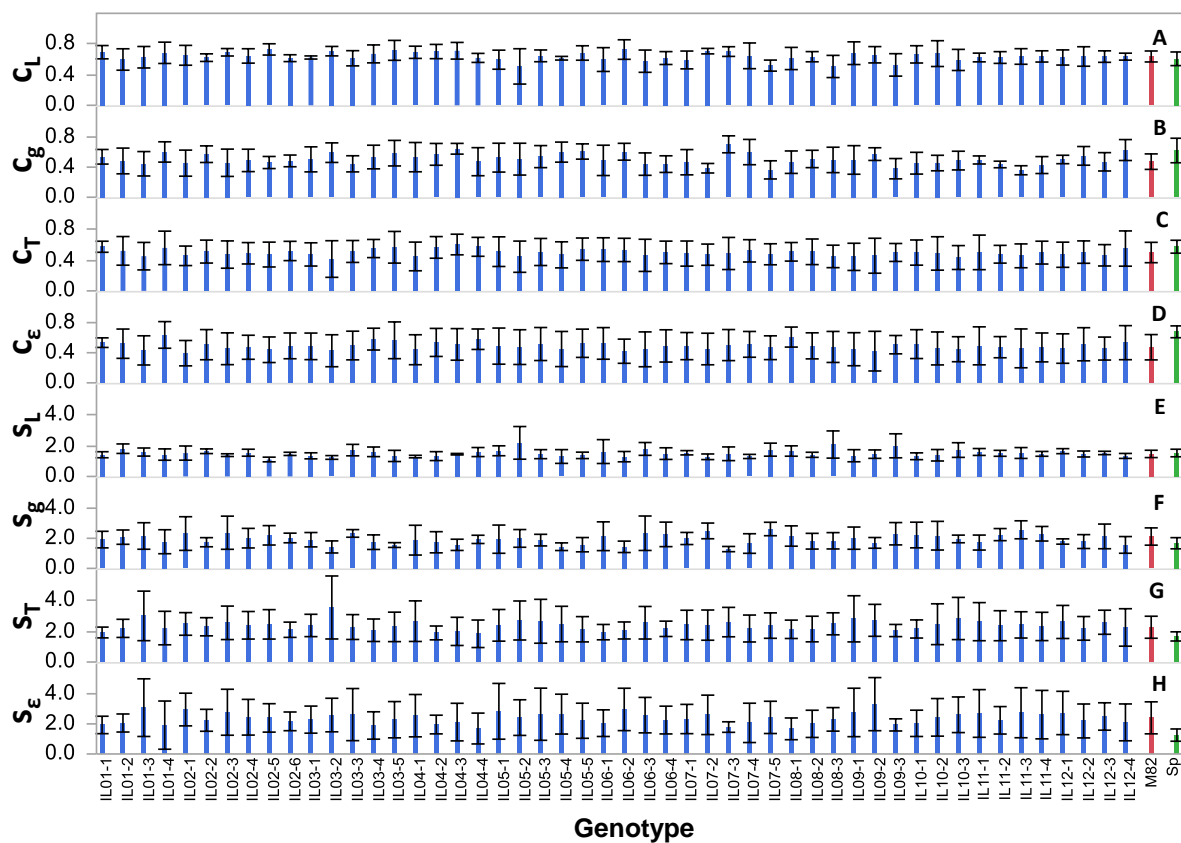
Fig. 3-S5. Mean (±SD) of (A - D) soil water thresholds and (E - H) and slope of the linear decline of 52 tomato lines for r_L, r_g, r_T and r_ε estimated by linear plateau model. There were 4, 12 and 8 replications for each IL, M82 and Sp, respectively.
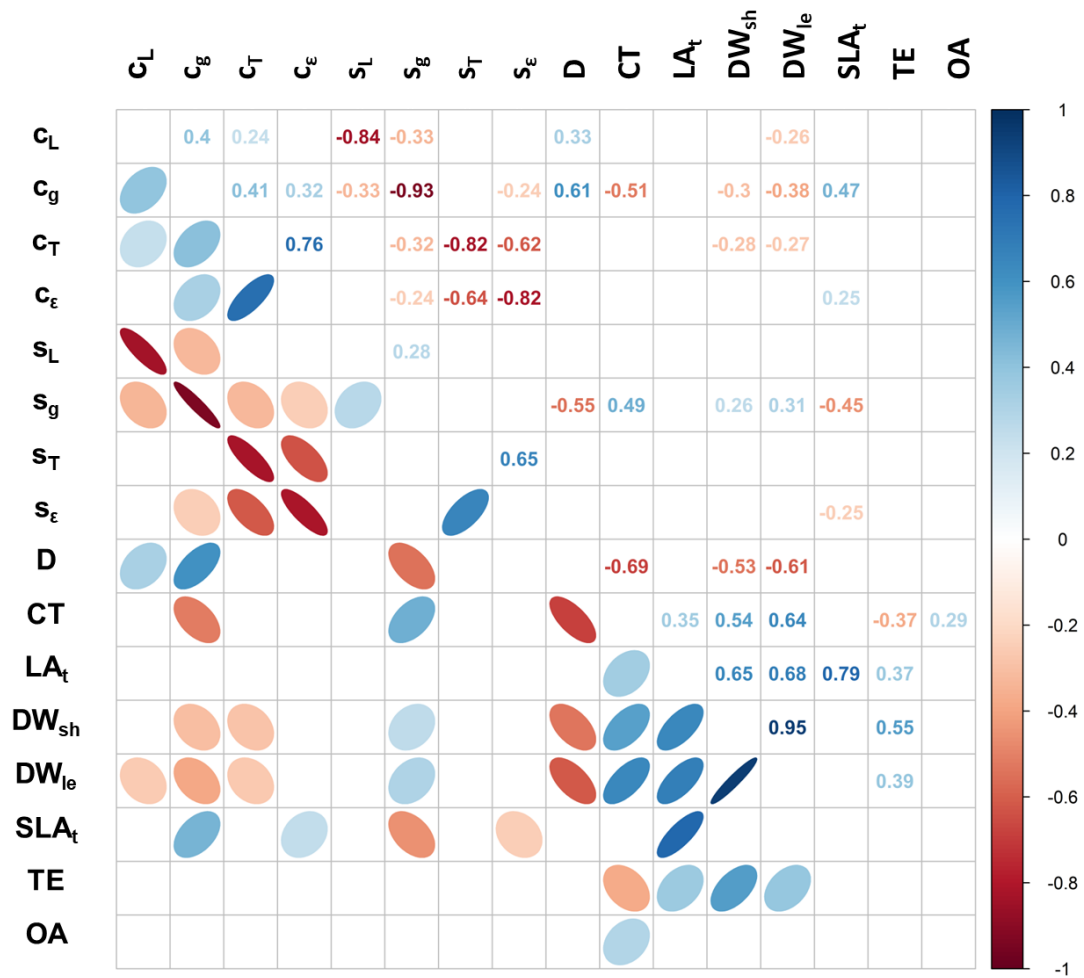
Fig. 3-S6. Pearson's correlations among the drought response parameters and agronomic traits. Significant correlation coefficients ($p < 0.05$) only are shown. Positive correlations are displayed in blue (right oblique) and negative correlations in red (left oblique) colour. Colour intensity and the size of the ellipses are proportional to the correlation coefficients.

A

$$y = 0.836\ x^{-1.297}$$
$$R^2 = 0.72$$

B

$$y = 0.953x^{-1.027}$$
$$R^2 = 0.87$$

C

$$y = 0.920\ x^{-1.345}$$
$$R^2 = 0.72$$

D

$$y = 0.845\ x^{-1.412}$$
$$R^2 = 0.73$$
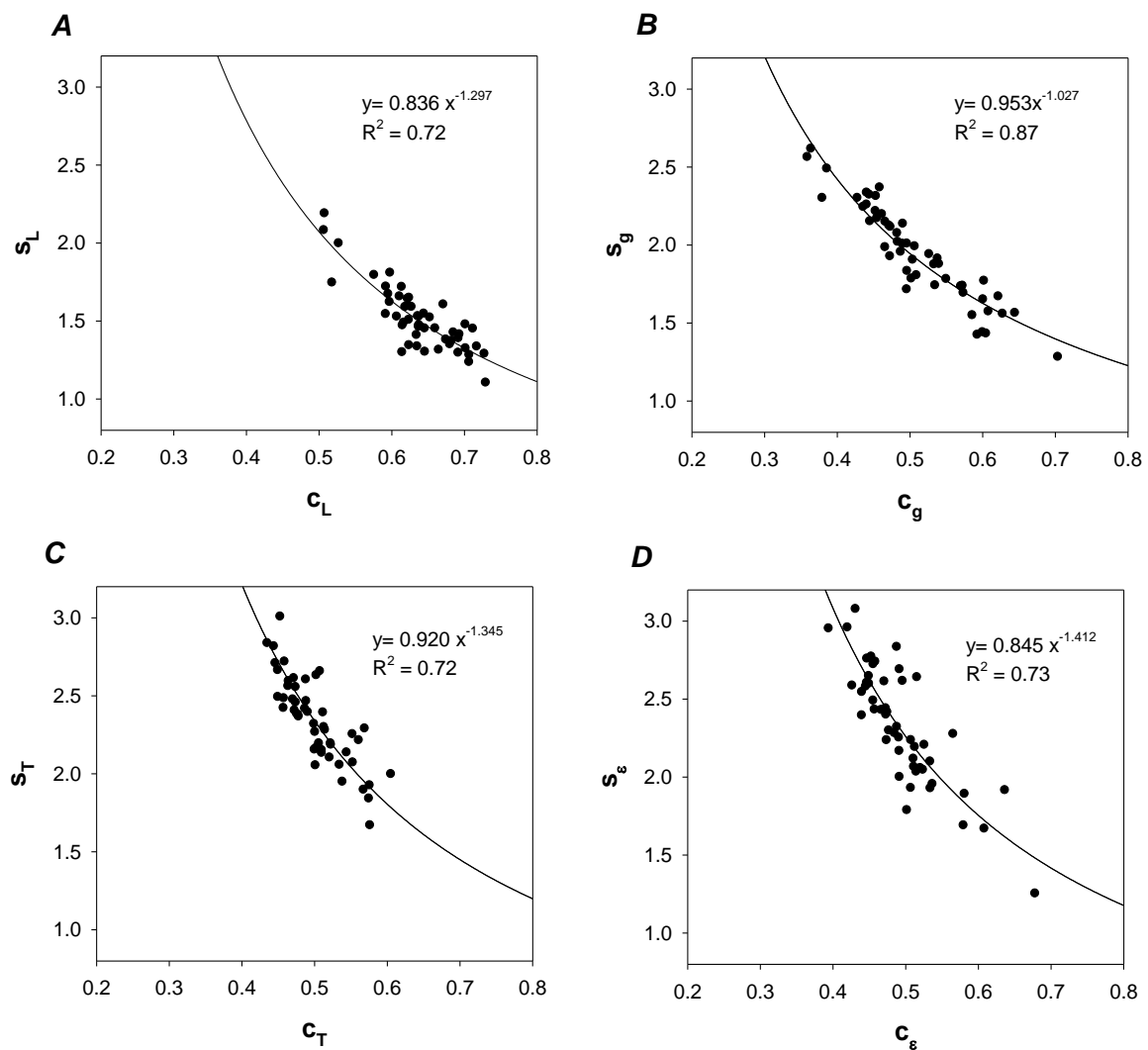
Fig. 3-S7. Relationships between genotype-specific (n = 4) W_{ts} thresholds, c_x, and slope of the linar decline, s_x, of 52 tomato lines under drought stress for four relative traits: (A) r_L, (B) r_g, (C) r_T and (D) r_ε.
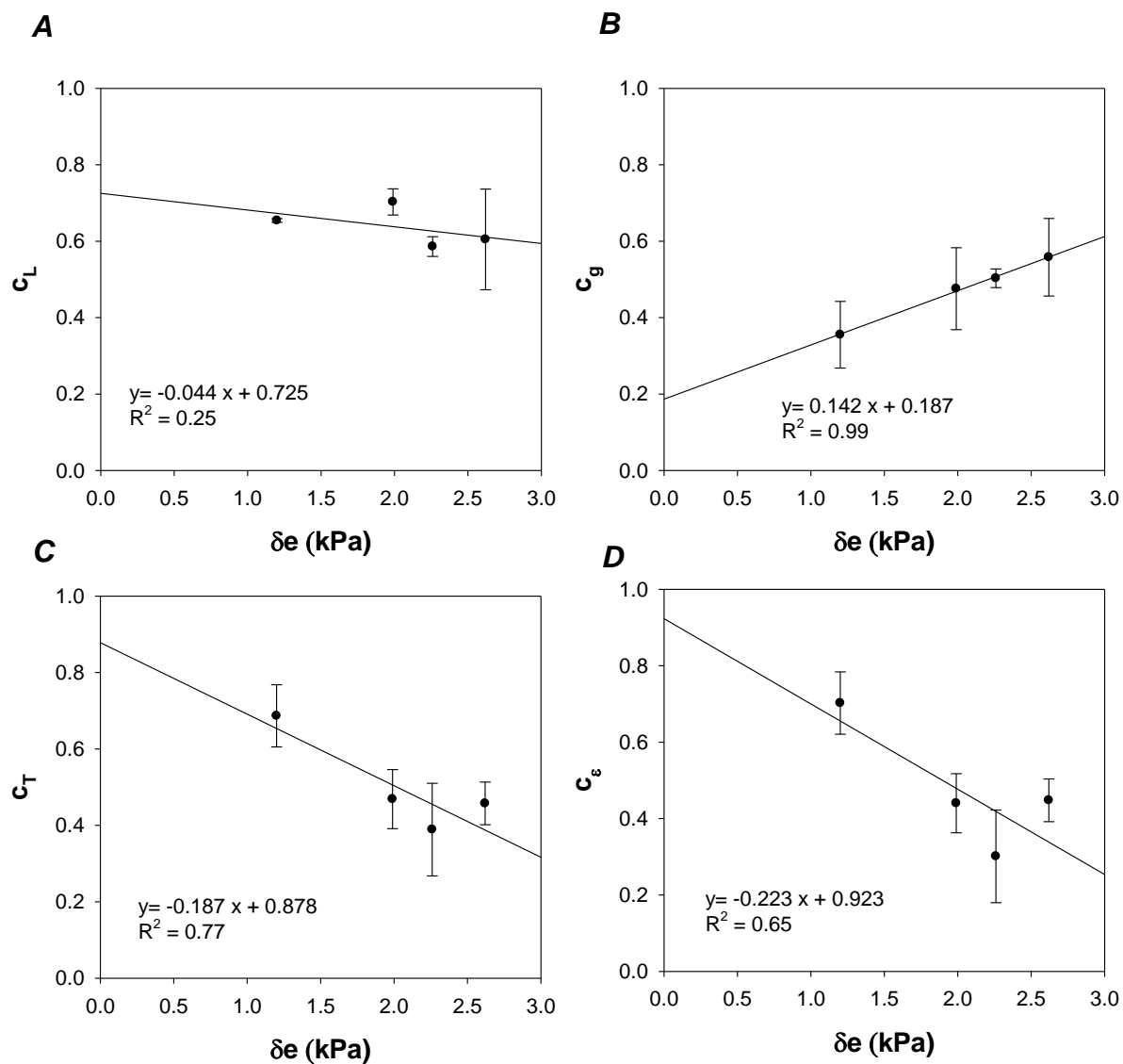
Fig. 3-S8. Responses of W_{ts} to daytime vapour pressure deficit δe for relative physiological traits observed in recurrent line M82: (A) c_L, (B) c_g, (C) c_T and (D) c_ε. Each point represents the mean (±SD) of three replications.
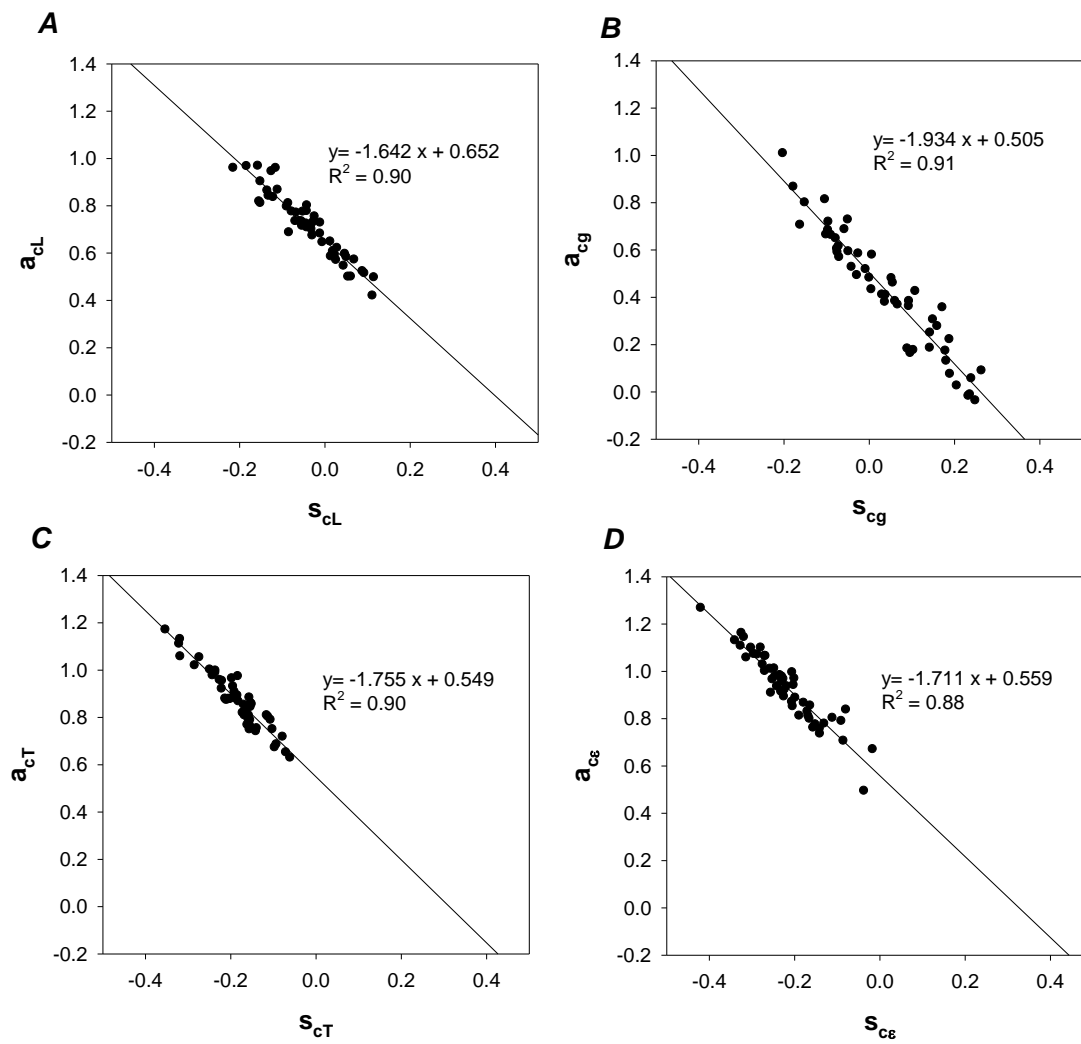
Fig. 3-S9. Trait specific relationships between the parameters slope s_c and intercept a_c of δe response curves for (A) c_L, (B) c_g (C) c_T and (D) c_ε of all tested lines under drought stress.
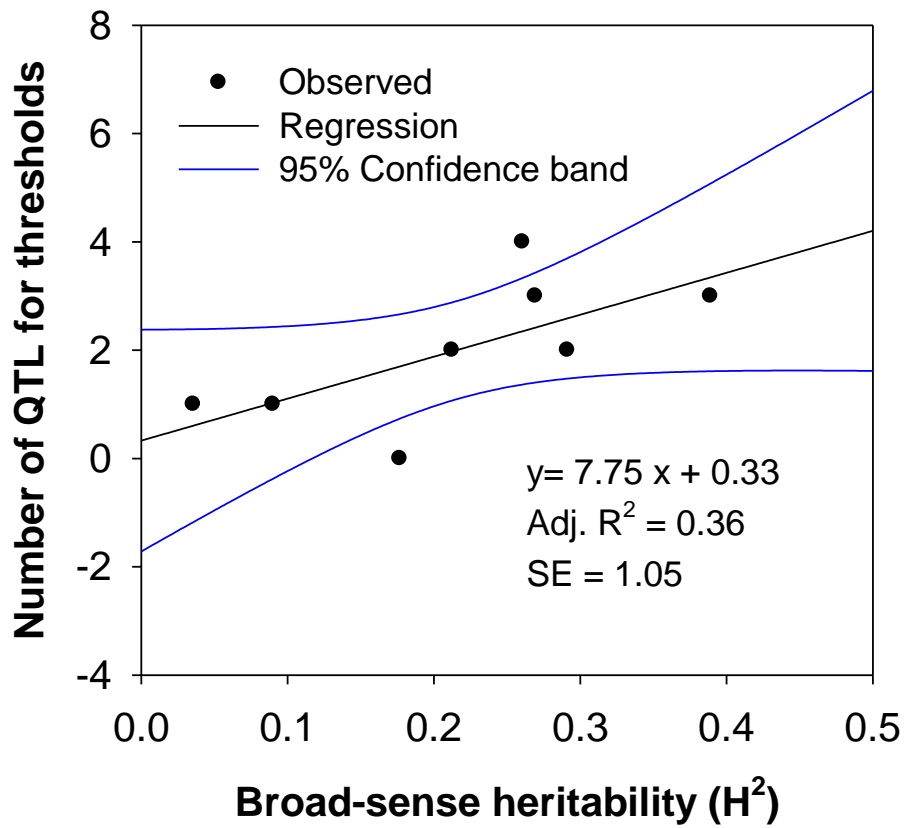
Fig. 3-S10. Dependence of QTL count on broad-sense heritability of drought reaction parameters (thresholds and intensity of decline) of four relative traits. QTL detection was performed by using Dunnett test at $p < 0.05$.
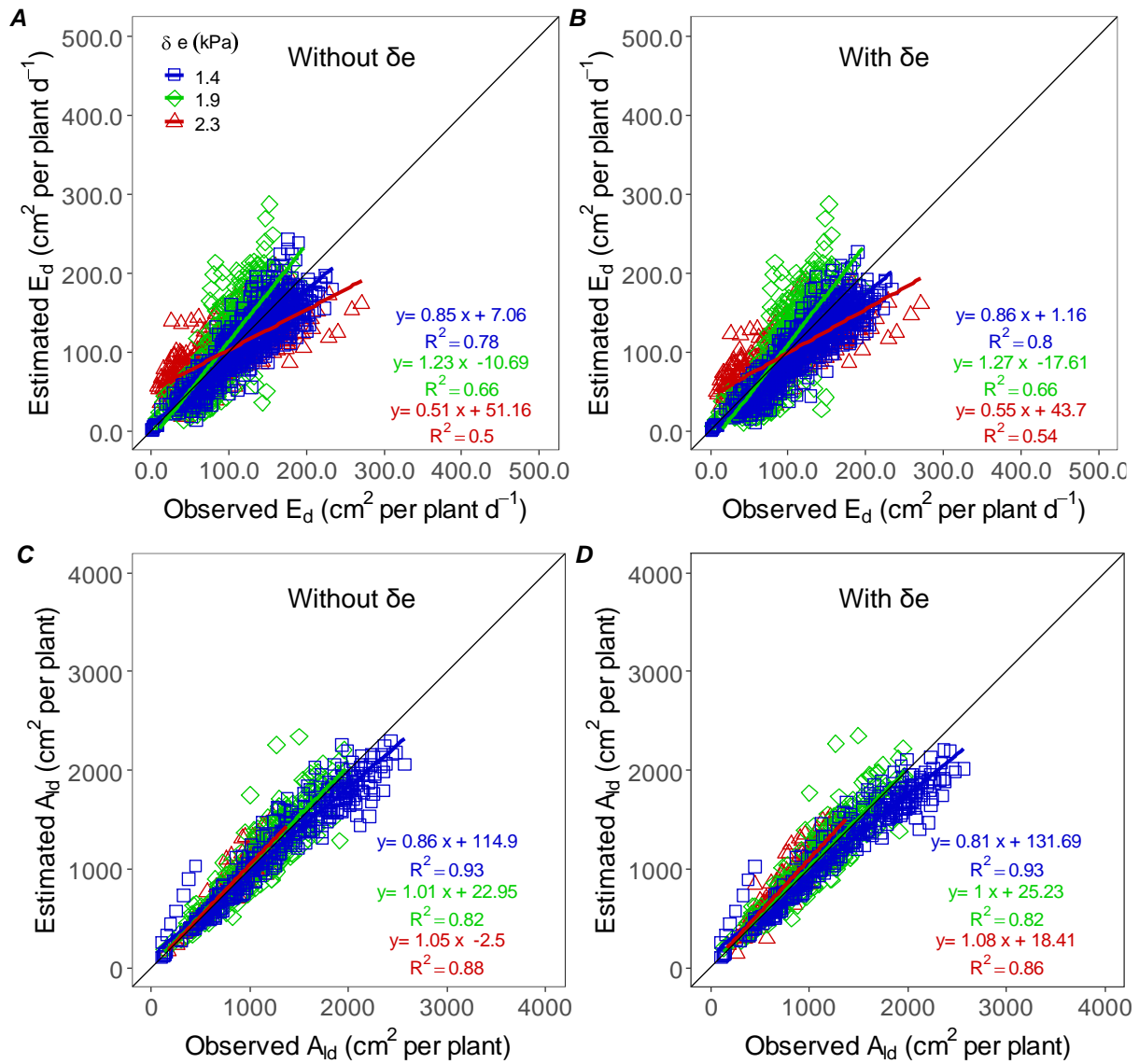
Fig. 3-S11. Simulated versus observed (A, B) leaf expansion rate E_d and (C, D) canopy leaf area A_{ld} of tomato lines over the stress period under three vapour pressure deficits δe conditions without (-) or with (+) parameter slopes of δe response curves of soil water thresholds. E_d is the change of leaf area between two successive days (dA_{ld}/dt).
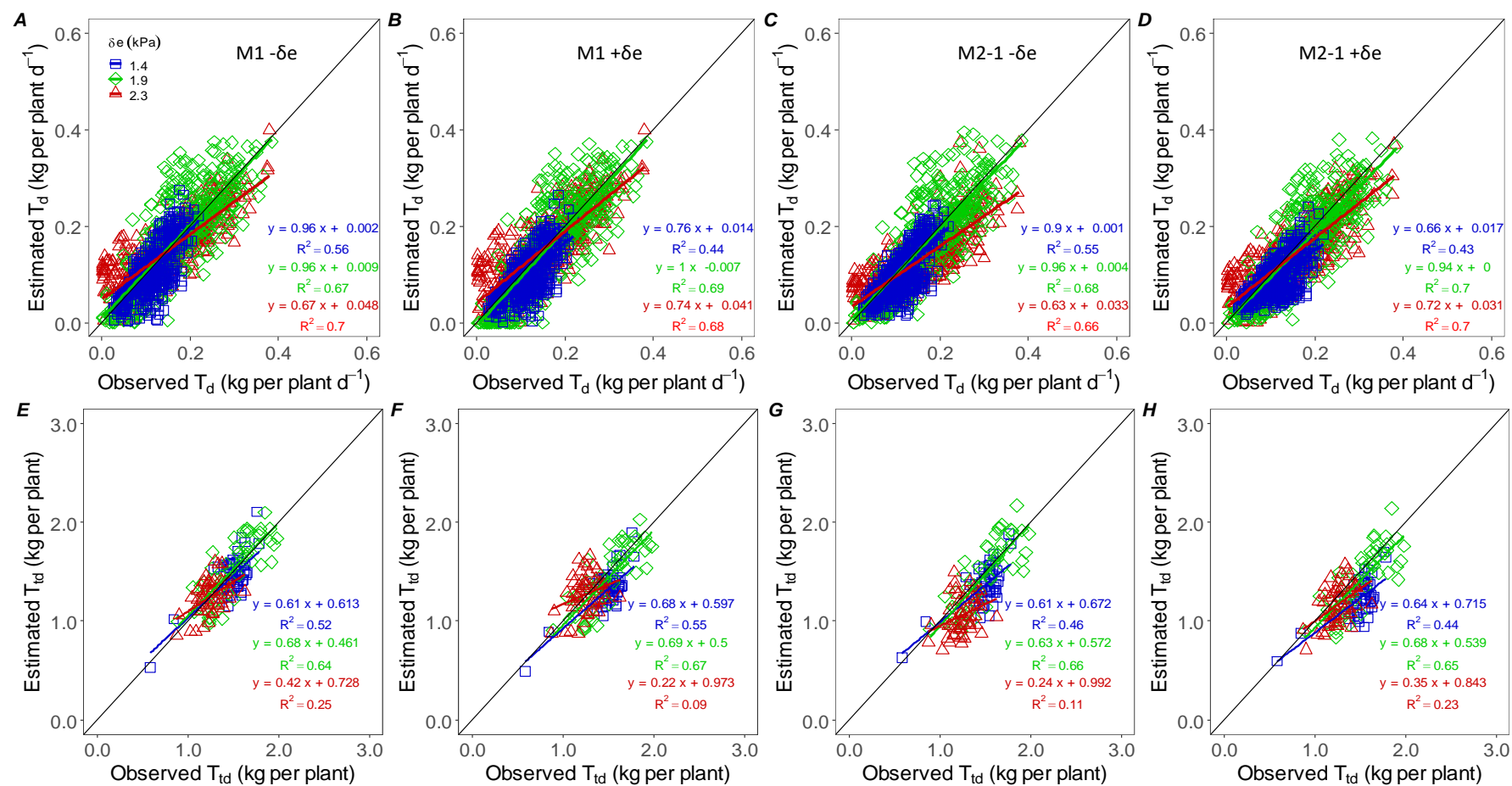
Fig. 3-S12. Simulated versus observed (A-D) transpiration T_d over time and (E-H) total transpiration T_{td} of drought stressed tomato lines under three δe conditions. T_d was estimated by using QTL-based parameters either in M1 or M2-1 approach without (-) or with (+) parameter slopes of δe responses curves of soil water thresholds. Local evaluations for each δe condition are described in **Table 3-S2**. M1: c_T; M2-1: c_L and c_ε.
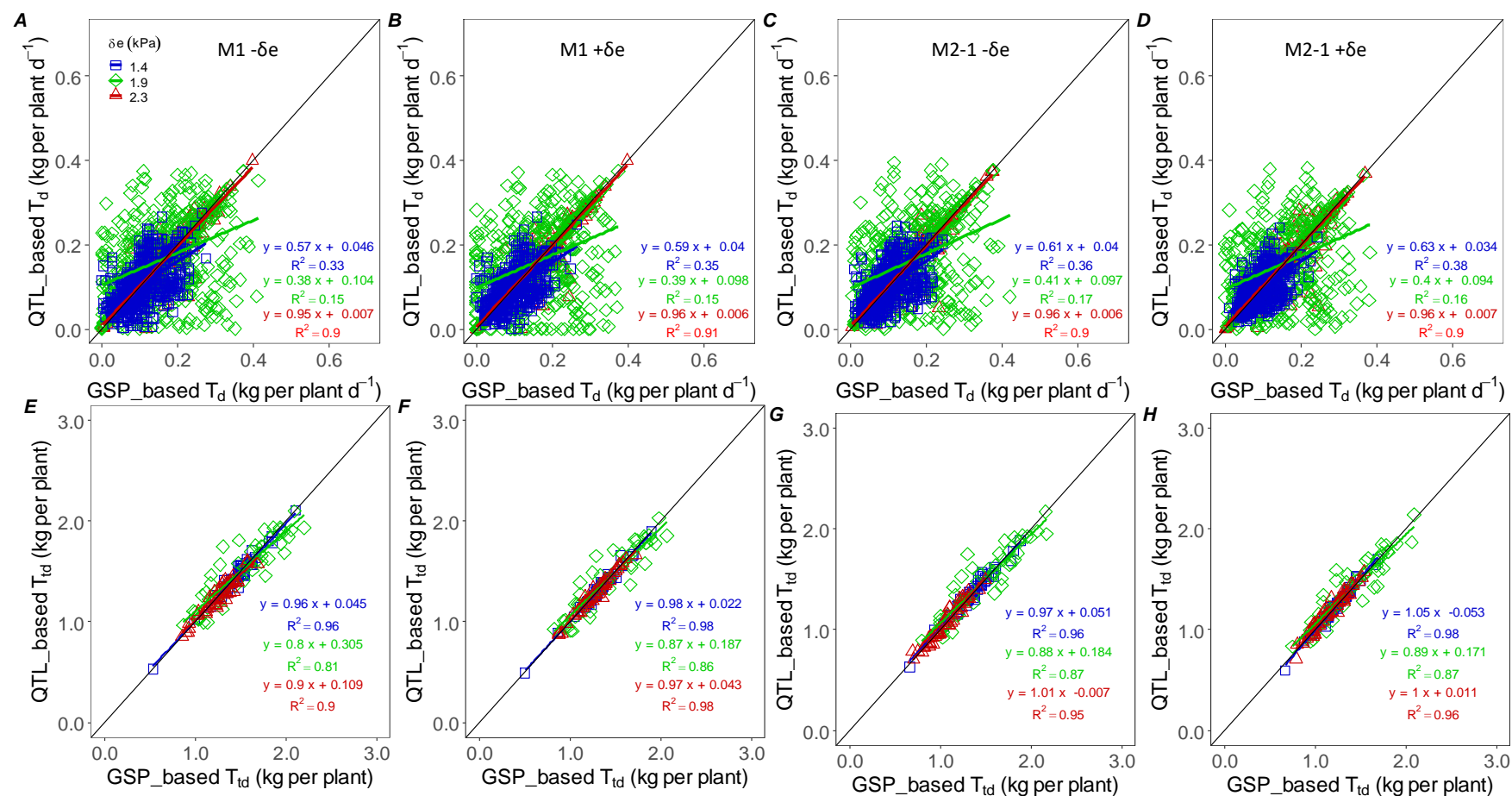
Fig. 3-S13. GSP- versus QTL-based (A-D) transpiration T_d over time and (E-H) total transpiration T_{td} of drought stressed tomato lines under three δe conditions. T_d was estimated either in M1 or M2-1 approach without (-) or with (+) parameter slopes of δe responses curves of soil water thresholds.

Table 3-S1. Local and across environments evaluations of total transpiration (T_{td}) predicted by using genotype specific parameters and QTL-based parameters without (-) or with (+) consideration of vapour pressure deficit δe responses curve of soil water thresholds. The environments were characterized by three average δe ($\pm$SD) conditions. The modelling approaches are designed depending on which thresholds were used to determine the time of drought reactions, M1: c_T, M2-1: c_L and c_ε, M2-2: c_L and c_g.

| Trial	Approach	Without δe response				With δe response			
		R^2	RMSE	Bias	Accuracy	R^2	RMSE	Bias	Accuracy
GSP-based									
Across									
	M1	0.61	0.197	0.054	0.87	0.48	0.249	0.126	0.83
	M2-1	0.63	0.270	0.179	0.82	0.52	0.294	0.207	0.80
	M2-2	0.67	0.250	-0.025	0.83	0.67	0.217	-0.012	0.85
1.4									
	M1	0.48	0.215	0.137	0.87	0.52	0.312	0.274	0.81
	M2-1	0.37	0.302	0.243	0.81	0.39	0.394	0.357	0.76
	M2-2	0.46	0.199	0.004	0.88	0.34	0.229	0.030	0.86
1.9									
	M1	0.65	0.207	0.026	0.87	0.70	0.219	0.120	0.86
	M2-1	0.68	0.227	0.088	0.86	0.69	0.247	0.160	0.85
	M2-2	0.61	0.324	-0.184	0.80	0.69	0.243	-0.144	0.85
2.3									
	M1	0.22	0.165	-0.001	0.87	0.09	0.201	-0.013	0.84
	M2-1	0.15	0.276	0.205	0.78	0.21	0.208	0.107	0.83
	M2-2	0.38	0.208	0.102	0.83	0.44	0.172	0.076	0.86
QTL-based									
Across									
	M1	0.63	0.191	0.062	0.87	0.48	0.249	0.126	0.83
	M2-1	0.63	0.265	0.172	0.82	0.50	0.291	0.199	0.81
	M2-2	0.68	0.239	-0.053	0.84	0.66	0.223	-0.029	0.85
1.4									
	M1	0.50	0.215	0.143	0.87	0.53	0.313	0.276	0.81
	M2-1	0.39	0.295	0.237	0.82	0.40	0.391	0.354	0.76
	M2-2	0.49	0.191	-0.025	0.88	0.33	0.241	0.013	0.85
1.9									
	M1	0.68	0.194	0.036	0.88	0.71	0.219	0.121	0.86
	M2-1	0.68	0.222	0.084	0.86	0.67	0.247	0.153	0.85
	M2-2	0.66	0.310	-0.214	0.81	0.69	0.253	-0.163	0.84
2.3									
	M1	0.24	0.158	0.007	0.87	0.08	0.201	-0.016	0.84
	M2-1	0.14	0.271	0.194	0.78	0.21	0.201	0.091	0.84
	M2-2	0.32	0.199	0.076	0.84	0.43	0.165	0.062	0.87

Table 3-S2. Summary of predicted soil water thresholds for different relative traits across three environments as genotype specific paramaters and QTL-based parameters with or without taking account of vapour pressure deficit conditions. Min, Minimum; Max, Maximum; SD, standard error; SE, standard deveration; CV, coefficient of variation. The symbols for thresholds of relative traits are described in **Table 3-1**. N = 159.

|		Without δe response				With δe response			
		c_L	c_g	c_T	c_ε	c_L	c_g	c_T	c_ε
GSP-based									
	Mean	0.637	0.505	0.499	0.489	0.647	0.504	0.528	0.523
	Min	0.506	0.359	0.415	0.394	0.511	0.372	0.356	0.312
	Max	0.729	0.703	0.605	0.636	0.728	0.627	0.674	0.690
	SD	0.055	0.073	0.041	0.048	0.041	0.055	0.073	0.089
	SE	0.032	0.042	0.023	0.027	0.024	0.032	0.042	0.051
	CV (%)	8.60	14.52	8.12	9.74	6.30	10.99	13.79	16.96
QTL-based									
	Mean	0.628	0.484	0.502	0.479	0.644	0.494	0.528	0.512
	Min	0.506	0.473	0.500	0.473	0.511	0.372	0.356	0.312
	Max	0.637	0.703	0.605	0.636	0.728	0.613	0.674	0.690
	SD	0.033	0.044	0.014	0.029	0.036	0.051	0.073	0.086
	SE	0.019	0.025	0.008	0.017	0.021	0.029	0.042	0.050
	CV (%)	5.21	9.09	2.85	6.03	5.67	10.28	13.84	16.80
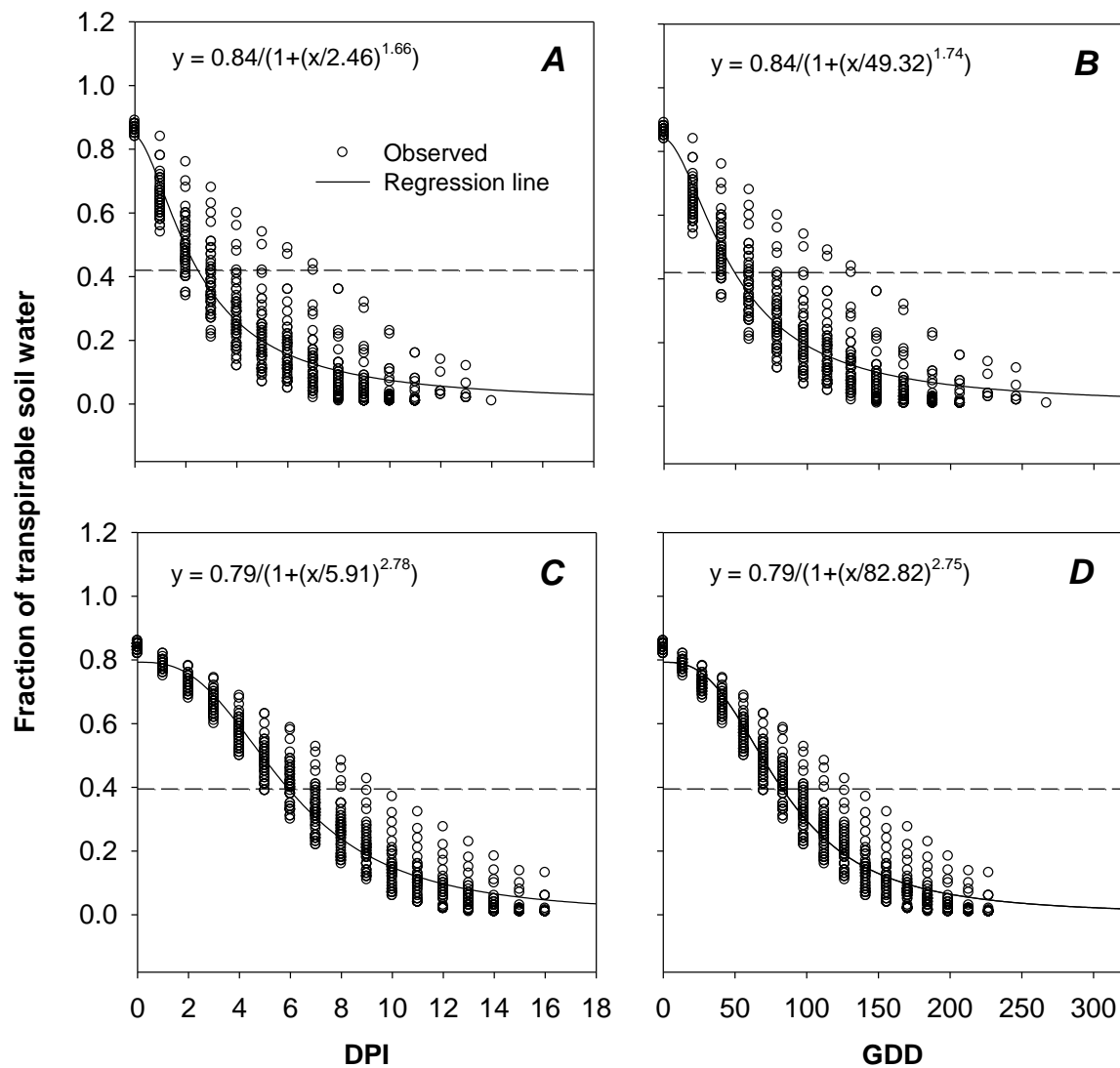
Fig. 3-S14. Soil water depletion of tomatoes lines as a function of time under two vapour pressure deficit conditions: (A, B) 2.6 kPa, (C, D) 1.2 kPa. Time course is described in days post drought imposition (DPI) and growing degree days (GDD). Dashed lines are fraction of transpirable soil water at inflection points.

Table 3-S3. Details of greenhouse trials used for model parameterization (1-4) and evaluation (5-7). The δe values are average of the post drought imposition period. In trial 3 and 7, supplemental lights (14/10) were provided by using HPS lamps to ensure the proper growth of plants.

Trial	Year	Sowing date	Drought onset	Drought duration (days)	Average 24 h temperature (°C)	Average daytime δe (kPa)	Average global radiation outside (MJ m^{-2} d^{-1})
1	2016	13 Jun	11 Jul	9-20	27.7	2.2	16.1
2	2016	26 Jul	29 Aug	9-14	26.5	2.6	12.8
3	2016	13 Sep	18 Oct	13-16	21.9	1.2	3.1
4	2017	12 Feb	18 Mar	11-20	24.2	1.9	9.4
5	2017	13 Apr	15 May	11-16	26.5	2.3	16.4
6	2017	10 Jun	10 Jul	8-18	26.0	1.9	12.5
7	2017	29 Aug	2 Oct	12-15	22.9	1.4	5.3
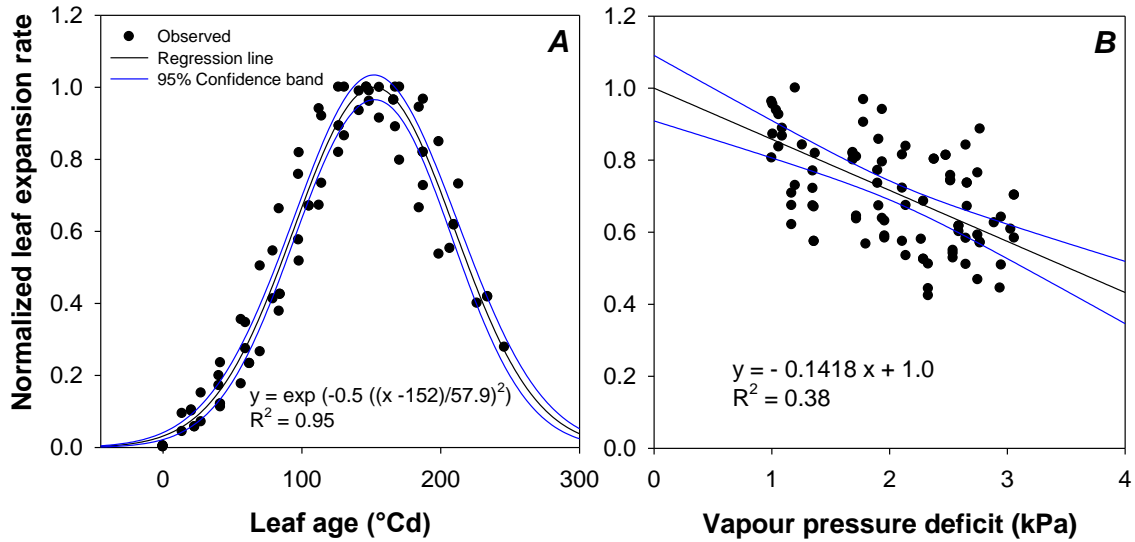
Fig. 4-S1. Normalized leaf expansion rate of recurrent tomato cv. M82 as a function of (A) leaf age and (B) air vapour pressure deficit. N = 80.
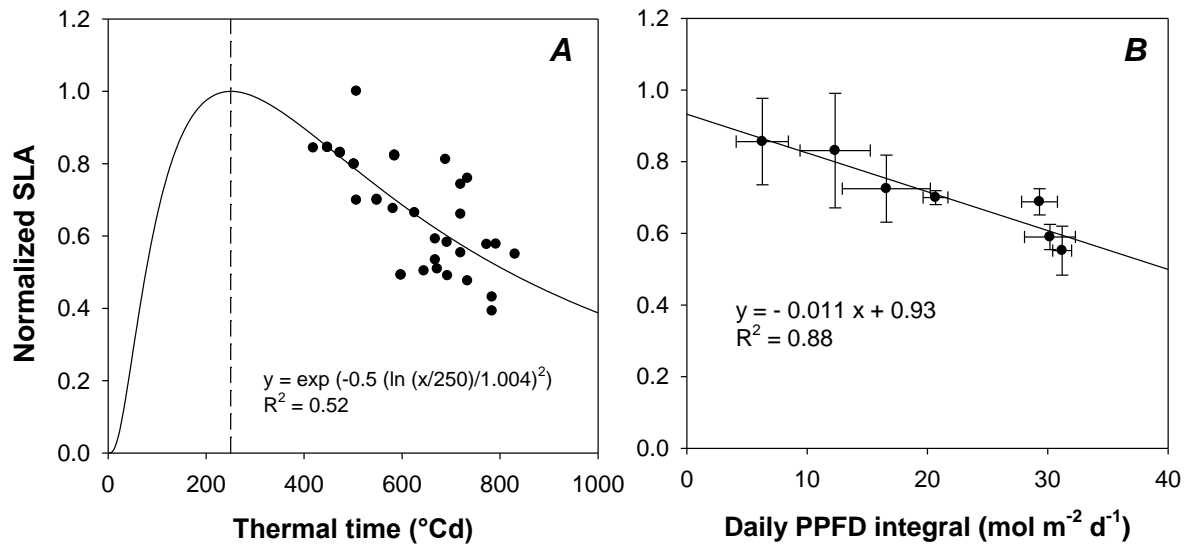
Fig. 4-S2. Normalized specific leaf area of tomatoes as a function of (A) thermal age, and (B) daily light integral. Extrapolation was made for age effect to fit the available data points to log-normal function by assuming that the SLA increases till 250 °Cd (dished line) to invest more assimilates for leaf area expansion than for dry matter, then decreases gradually with age. N = 37. For normalized effect of light, data from seven experiments were used with three replications. For both cases, recurrent M82 was used.
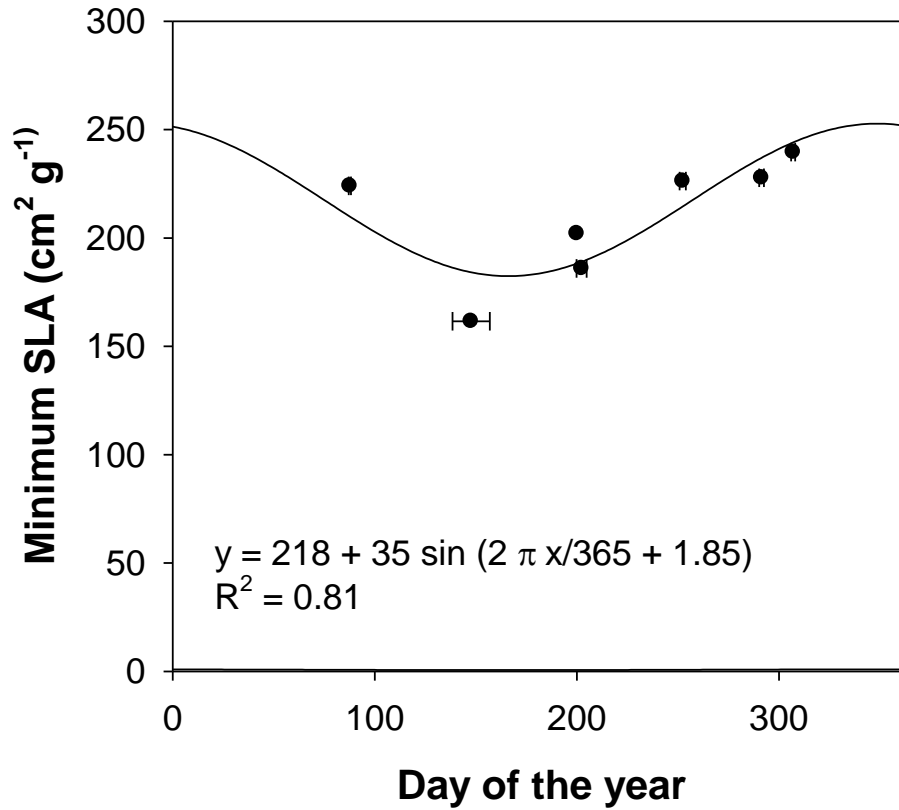
Fig. 4-S3. Minimum specific leaf area of recurrent tomato cv. M82 as a function of day of the year in Hannover (52.2°N, 2016 -17). The minimum value out of three replications from seven experiments was used.
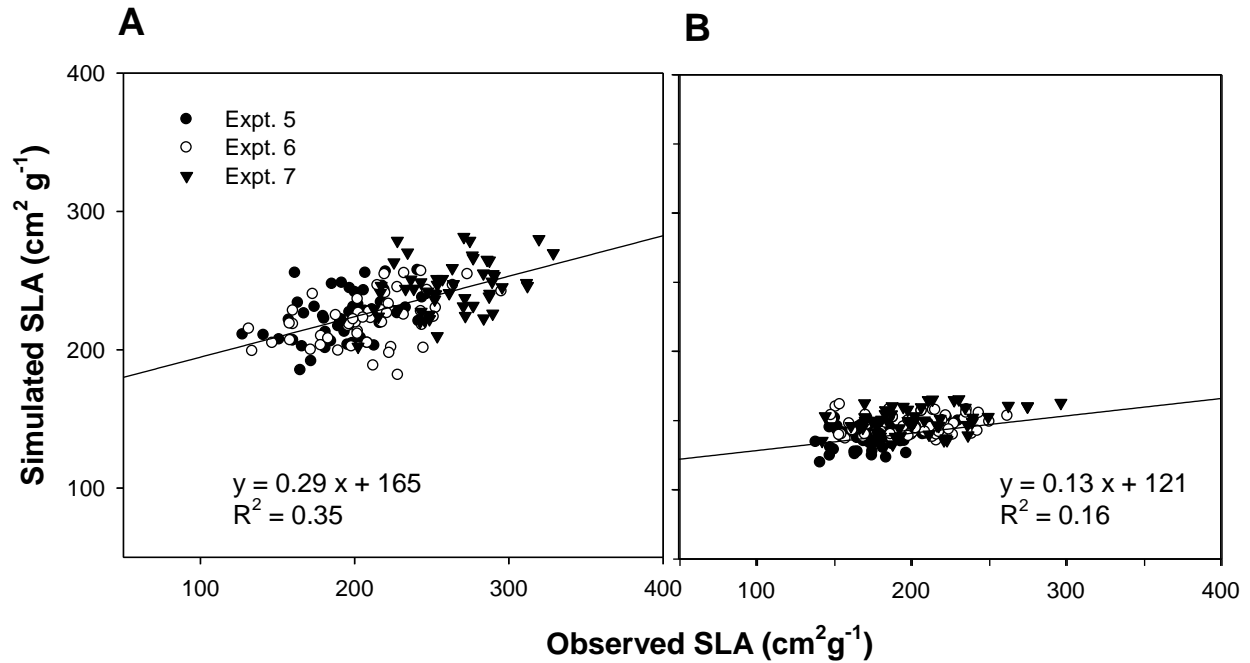
Fig. 4-S4. Comparison of simulated and observed SLA of tomato introgression lines under (A) well-watered and (B) drought stressed condition using the outputs of aggregated model and harvest data of three independent greenhouse trials.
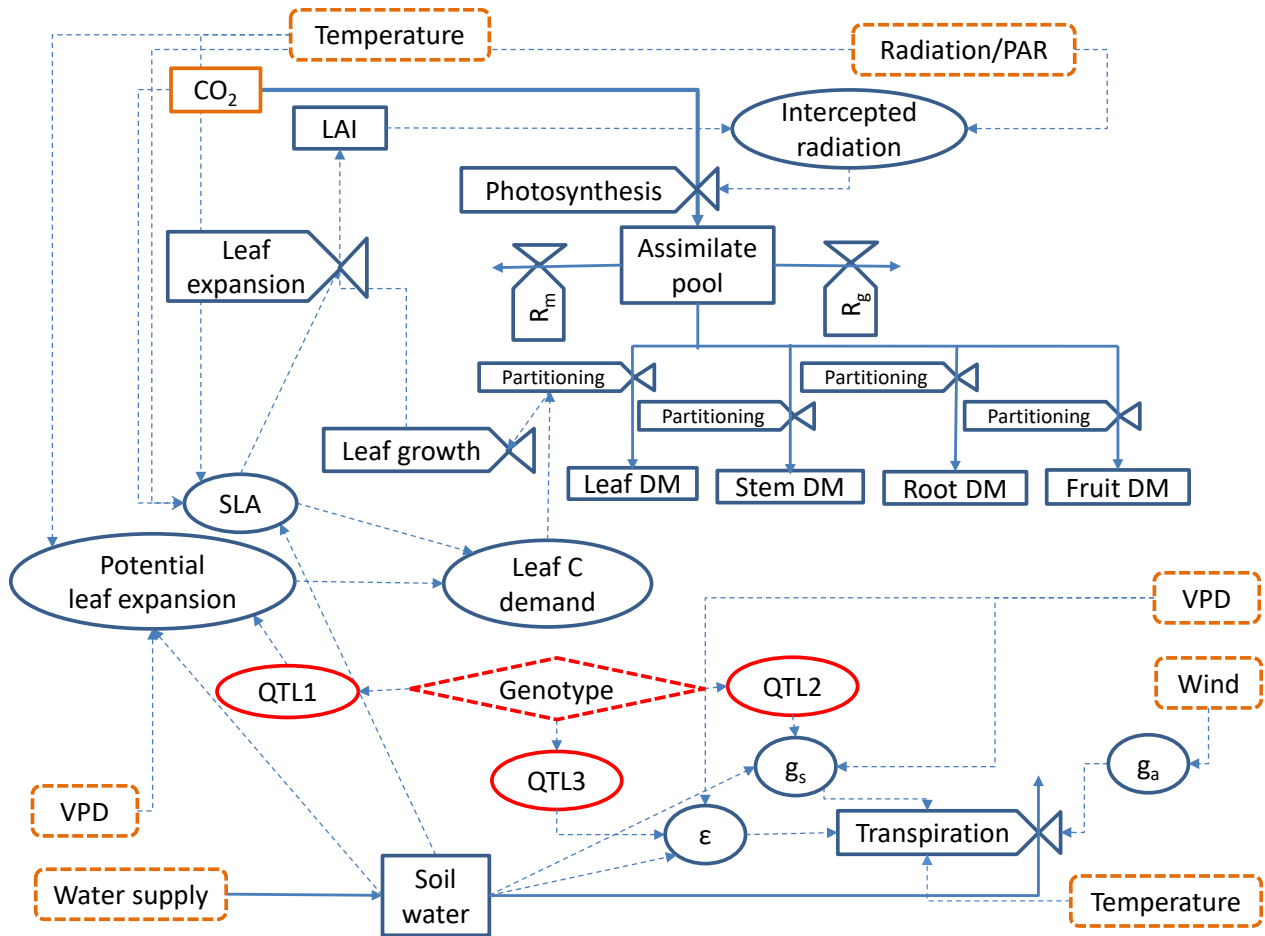
Fig. 4-S5. A flow chart of TILSIM describing the major plant functions (leaf growth, transpiration, photosynthesis) in connection to environmental and genetic inputs. The environmental variables (orange) are described in dashed boxes without corners. The genetic module (red) is incorporated through six GSPs (for unstressed condition, not shown here) and three QTL-derived parameters (for stressed condition, QTL1-3). Rectangular boxes are pools and outputs. Elliptic circles and valves show parameters and processes, respectively. R_m and R_g are maintenance and growth respirations, g_s, g_a and ε stomatal conductance, aerodynamic conductance and specific transpiration. SLA regulates the leaf carbon demand and expansion, and stomatal conductance regulates the photosynthesis and transpiration. Solid lines refer to mass flow and dotted lines denote information flow.
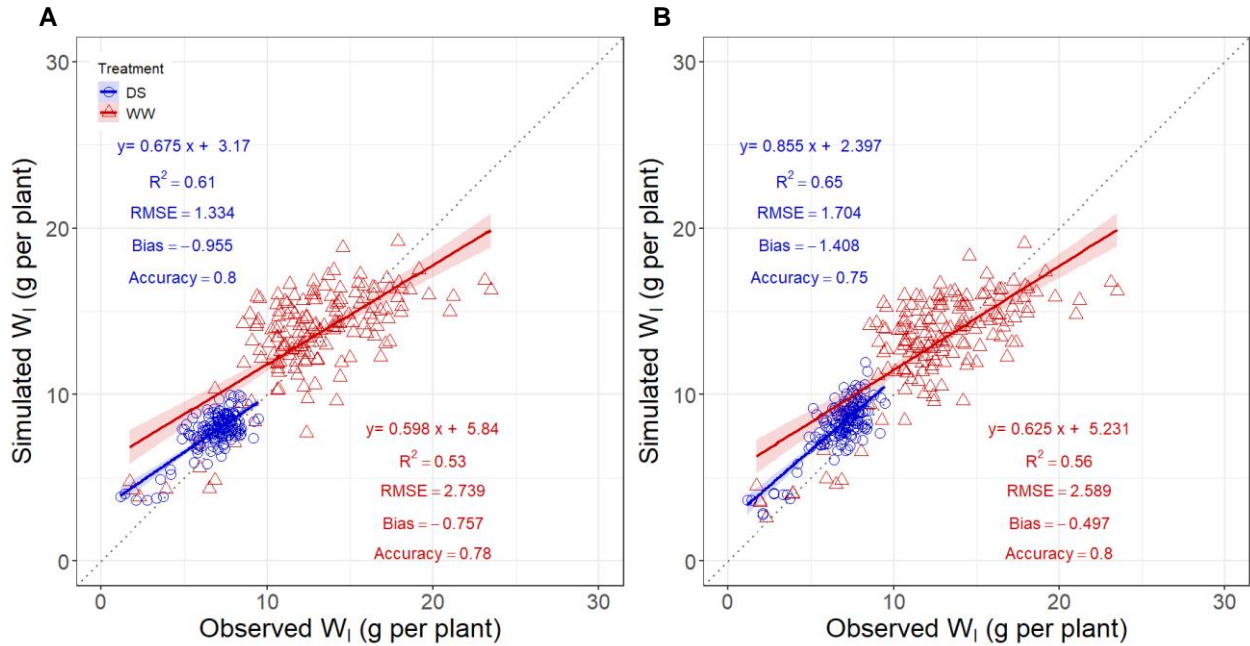
Fig. 4-S6. Comparison of simulated and observed leaf dry weight (W_l) of tomato lines under drought-stressed (DS) and well-watered (WW) conditions in two ways of simulation: (A) without and (B) with leaf area input. Model evaluations were done using the independent datasets of three greenhouse trials (Apr – Oct 2017). N = 162.
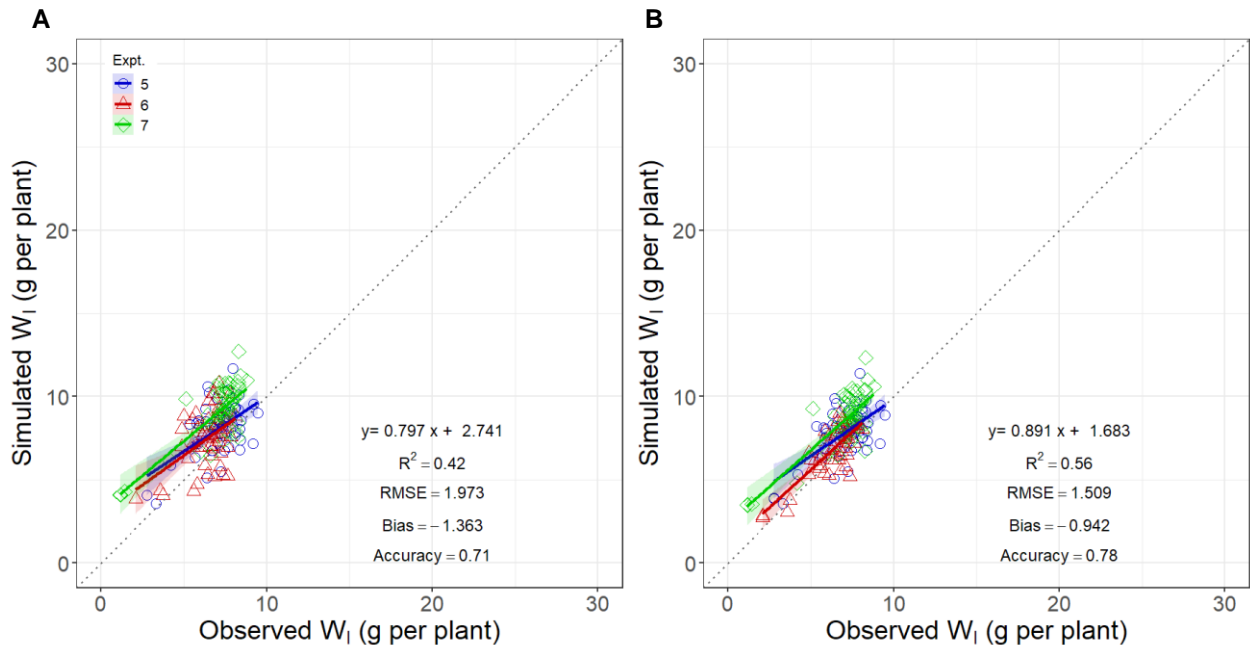
Fig. 4-S7. Comparison of simulated and observed leaf dry weight (W_l) of tomato lines under drought-stressed condition for three experiments: with (A) W_{ts}, and (B) W_{ts} and A_l inputs. Experiments (Expt. 5 - Expt.7) were characterized by the average day-time vapour pressure deficits of 2.3 (±0.24), 1.9 (±0.22), and 1.4 (±0.07) kPa, respectively.
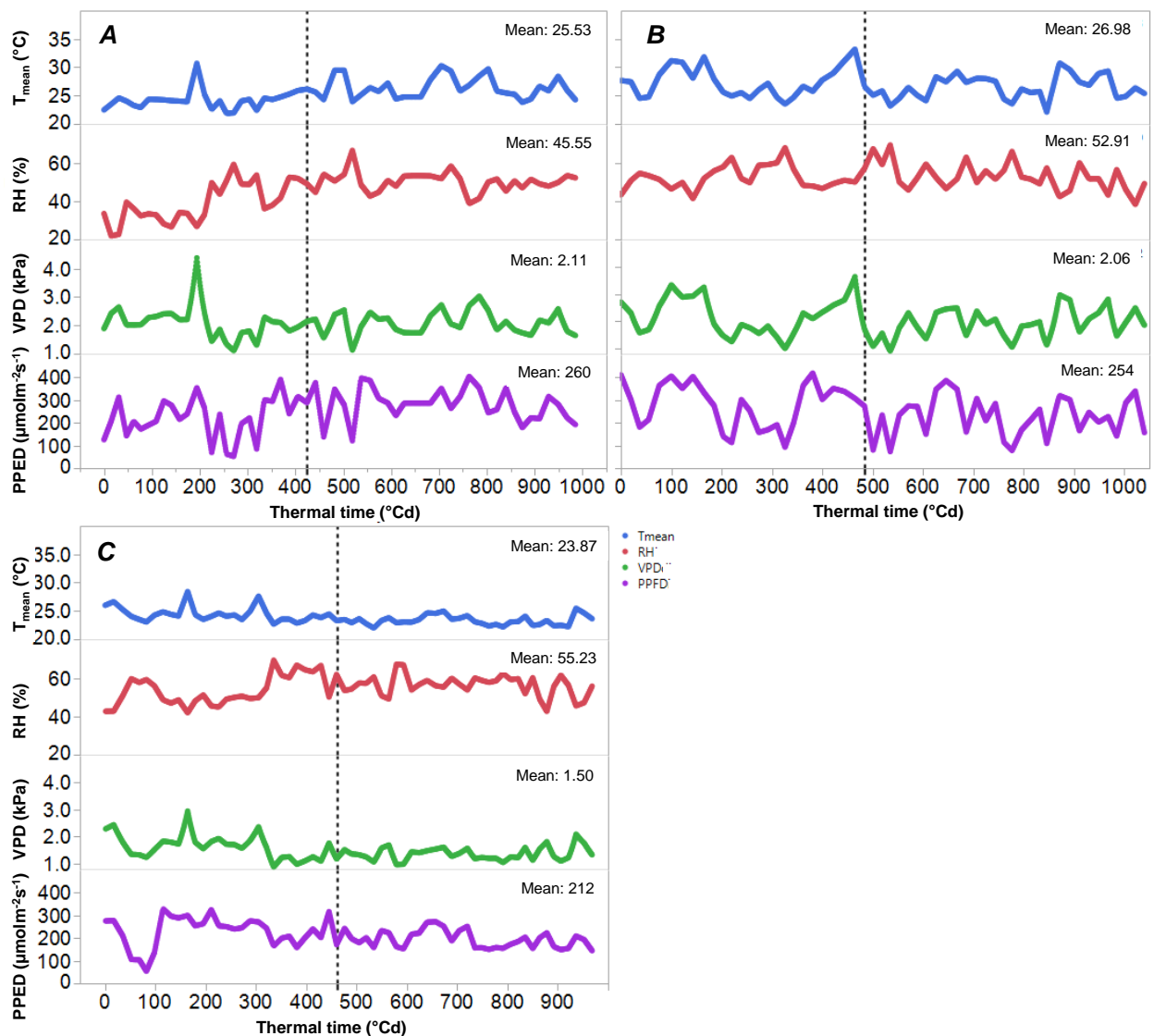
Fig. 4-S8. Greenhouse climatic conditions of three experiments evaluated in TILSIM: (A) Expt. 5; (B) Expt. 6; (C) Expt. (7), describing daily mean temperature (T_{mean}) (blue), relative humidity (RH) (red), vapour pressure deficit (VPD) (green) and photosynthetic photon flux density (PPFD) (purple). Mean of the whole growing period is provided. Dotted line in each sub-figure indicates the time of drought imposition.

References

Abdul-Jabbar, A. S., Sammis, T. W., Lugg, D. G., Kallsen, C. E. and Smeal, D. (1983). Water use by alfalfa, maize, and barley as influenced by available soil water. *Agricultural Water Management* **6**, 351–363.

Allen, R., Pereira, L. S., Raes, D. and Smith, M. (1998). Crop evapotranspiration: guidelines for computing crop water requirements. Rome (Italy): Agriculture Organization of the United Nations.

Alseekh, S., Tohge, T., Wendenberg, R., Scossa, F., Omranian, N., Li, J., Kleessen, S., Giavalisco, P., Pleban, T., Mueller-Roeber, B. et al. (2015). Identification and mode of inheritance of quantitative trait loci for secondary metabolite abundance in tomato. *The Plant Cell* **27**, 485–512.

Andersen, M. N., Asch, F., Wu, Y., Jensen, C. R., Naested, H., Mogensen, V. O. and Koch, K. E. (2002). Soluble invertase expression is an early target of drought stress during the critical, abortion-sensitive phase of young ovary development in maize. *Plant Physiology* **130**, 591–604.

Arms, E. M., Yan, Z. and St Clair, D. A. (2017). Differential transcriptional regulation in roots of tomato near-isogenic lines in response to rapid-onset water stress. *Frontiers in Plant Science* **8**, 166.

Aroca, R., ed. (2012). *Plant responses to drought stress*: Springer Berlin Heidelberg. Berlin, Heidelberg.

Atarés, A., Moyano, E., Morales, B., Schleicher, P., García-Abellán, J. O., Antón, T., García-Sogo, B., Perez-Martin, F., Lozano, R., Flores, F. B. et al. (2011). An insertional mutagenesis programme with an enhancer trap for the identification and tagging of genes involved in abiotic stress tolerance in the tomato wild-related species *Solanum pennellii*. *Plant Cell Reports* **30**, 1865–1879.

Bertin, N. and Heuvelink, E. (1993). Dry-matter production in a tomato crop: comparison of two simulation models. *Journal of Horticultural Science* **68**, 995–1011.

Blum, A. (1996). Crop responses to drought and the interpretation of adaptation. *Plant Growth Regulation* **20**, 135–148.

Blum, A. (1999). Towards standard assays of drought resistance in crop plants. In *Molecular approaches for the genetic improvement of cereals for stable production in water-limited environments. A Strategic Planning Workshop* (ed. J. M. Ribaut and D. Poland), pp. 29–34. El Batan, Mexico: A Strategic Planning Workshop held at CIMMYT.

Blum, A. (2005). Drought resistance, water-use efficiency, and yield potential—are they compatible, dissonant, or mutually exclusive? *Australian Journal of Agricultural Research* **56**, 1159.

Blum, A., ed. (2011). *Plant breeding for water-limited environments*: Springer New York. New York, NY.

Blum, A. (2015). Towards a conceptual ABA ideotype in plant breeding for water limited environments. *Functional Plant Biology* **42**, 502.

Blum, A. (2017). Osmotic adjustment is a prime drought stress adaptive engine in support of plant production. *Plant, Cell & Environment* **40**, 4–10.

Bolger, A., Scossa, F., Bolger, M. E., Lanz, C., Maumus, F., Tohge, T., Quesneville, H., Alseekh, S., Sørensen, I., Lichtenstein, G. et al. (2014a). The genome of the stress-tolerant wild tomato species *Solanum pennellii*. *Nature Genetics* **46**, 1034–1038.

Bolger, A., Scossa, F., Bolger, M. E., Lanz, C., Maumus, F., Tohge, T., Quesneville, H., Alseekh, S., Sørensen, I., Lichtenstein, G. et al. (2014b). The genome of the stress-tolerant wild tomato species Solanum pennellii. *Nature Genetics* **46**, 1034–1038.

Bonan, G. B., Williams, M., Fisher, R. A. and Oleson, K. W. (2014). Modeling stomatal conductance in the earth system: linking leaf water-use efficiency and water transport along the soil–plant–atmosphere continuum. *Geoscientific Model Development* **7**, 2193–2222.

Boote, K. J., Jones, J. W. and Singh, P. (1991). Modeling growth and yield of groundnut. In *Groundnut-a global perspective. Proceedings of an international workshop* (ed. S. N. Nigam), pp. 331–343. Patancheru, Andhra Pradesh, India: ICRISAT Asia Centre.

Boote, K. J., Jones, J. W. and Hoogenboom, G., eds. (1998). *Simulation of crop growth: CROPGRO model*. New York: Marcel Dekker Inc.

Borrell, A. K., Hammer, G. L. and Henzell, R. G. (2000). Does maintaining green leaf area in sorghum improve yield under drought? II. Dry matter production and yield. *Crop Science* **40**, 1037.

Boyer, J. S. (1970). Leaf enlargement and metabolic rates in corn, soybean, and sunflower at various Leaf water potentials. *Plant Physiology* **46**, 233–235.

Brisson, N., Launay, M., Mary, B. and Beaudoin, N., eds. (2008). *Conceptual basis, formalisations and parameterization of the STICS crop model*. Versailles, France.

Brown, T. B., Cheng, R., Sirault, X. R. R., Rungrat, T., Murray, K. D., Trtilek, M., Furbank, R. T., Badger, M., Pogson, B. J. and Borevitz, J. O. (2014). TraitCapture: genomic and environment modelling of plant phenomic data. *Current Opinion in Plant Biology* **18**, 73–79.

Buckley, T. N. and Diaz-Espejo, A. (2015). Reporting estimates of maximum potential electron transport rate. *New Phytologist* **205**, 14–17.

Bunce, J. A. (1986). Volume and osmotic potential changes in relation to inhibition of photosynthesis by water stress in intact leaves. *Canadian Journal of Botany* **64**, 557–560.

Caemmerer, S. von, Farquhar, G. and Berry, J. (2009). Biochemical model of C_3 photosynthesis. In *Photosynthesis in silico* (ed. Govindjee, A. Laisk and L. Nedbal), pp. 209–230. Dordrecht: Springer Netherlands.

Caldeira, C. F., Bosio, M., Parent, B., Jeanguenin, L., Chaumont, F. and Tardieu, F. (2014). A hydraulic model is compatible with rapid changes in leaf elongation under fluctuating evaporative demand and soil water status. *Plant Physiology* **164**, 1718–1730.

Caruso, G., Gomez, L. D., Ferriello, F., Andolfi, A., Borgonuovo, C., Evidente, A., Simister, R., McQueen-Mason, S. J., Carputo, D., Frusciante, L. et al. (2016). Exploring tomato *Solanum pennellii* introgression lines for residual biomass and enzymatic digestibility traits. *BMC Genetics* **17**, 56.

Casadebaig, P., Debaeke, P. and Lecoeur, J. (2008). Thresholds for leaf expansion and transpiration response to soil water deficit in a range of sunflower genotypes. *European Journal of Agronomy* **28**, 646–654.

Cataldo, D. A., Haroon, M., Schrader, L. E. and Youngs, V. L. (1975). Rapid colorimetric determination of nitrate in plant tissue by nitration of salicylic acid. *Communications in Soil Science and Plant Analysis* **6**, 71–80.

Challa, H. (1997). Growth of vegetative plant organs; the result of interacting ontogenetic patterns. *Acta Horticulturae*, 183–192.

Chapman, S. C., Hammer, G. L. and Palta, J. A. (1993). Predicting leaf area development of sunflower. *Field Crops Research* **34**, 101–112.

Chaves, M. M. (1991). Effects of water deficits on carbon assimilation. *Journal of Experimental Botany* **42**, 1–16.

Chaves, M. M., Pereira, J. S., Maroco, J., Rodrigues, M. L., Ricardo, C. P., Osorio, M. L., Carvalho, I., Faria, T., Pinheiro and Pinheiro, C. (2002). How plants cope with water stress in the field? Photosynthesis and growth. *Annals of Botany* **89**, 907–916.

Chaves, M. M. and Oliveira, M. M. (2004). Mechanisms underlying plant resilience to water deficits: prospects for water-saving agriculture. *Journal of Experimental Botany* **55**, 2365–2384.

Chaves, M. M., Flexas, J. and Pinheiro, C. (2009). Photosynthesis under drought and salt stress: regulation mechanisms from whole plant to cell. *Annals of Botany* **103**, 551–560.

Chenu, K., Chapman, S. C., Hammer, G. L., McLean, G., Salah, H. B. H. and Tardieu, F. (2008). Short-term responses of leaf growth rate to water deficit scale up to whole-plant and crop levels: an integrated modelling approach in maize. *Plant, Cell & Environment* **31**, 378–391.

Chenu, K., Chapman, S. C., Tardieu, F., McLean, G., Welcker, C. and Hammer, G. L. (2009). Simulating the yield impacts of organ-level quantitative trait loci associated with drought response in maize: a "gene-to-phenotype" modeling approach. *Genetics* **183**, 1507–1523.

Claeys, H. and Inzé, D. (2013). The agony of choice: how plants balance growth and survival under water-limiting conditions. *Plant Physiology* **162**, 1768–1779.

Condon, A. G., Richards, R. A., Rebetzke, G. J. and Farquhar, G. D. (2004). Breeding for high water-use efficiency. *Journal of Experimental Botany* **55**, 2447–2460.

Cooper, M., Podlich, D., Micallef, K. P., Smith, O. S., Jensen, N. M., Chapman, S. C. and Kruger, N. L. (2002). Complexity, quantitative traits and plant breeding: a role for simulation modelling in the genetic improvement of crops. In *Quantitative genetics, genomics, and plant breeding* (ed. M. S. Kang), pp. 143–166. Wallingford: CABI.

Davies, W. J., and and Zhang, J. (1991). Root signals and the regulation of growth and development of plants in drying Soil. *Annu. Rev. Plant Physiol. Plant Mol. Bioi.* **42**, 55–76.

Davies, W. J., Tardieu, F. and Trejo, C. L. (1994). How do chemical signals work in plants that grow in drying soil?'. *Plant Physiology* **104**, 309–314.

Davies, W. J., Wilkinson, S. and Loveys, B. (2002). Stomatal control by chemical signalling and the exploitation of this mechanism to increase water use efficiency in agriculture. *New Phytologist* **153**, 449–460.

De Kauwe M. G., Lin, Y.-S., Wright, I. J., Medlyn, B. E., Crous, K. Y., Ellsworth, D. S., Maire, V., Prentice, I. C., Atkin, O. K., Rogers, A. et al. (2016). A test of the 'one-point method' for estimating maximum carboxylation capacity from field-measured, light-saturated photosynthesis. *New Phytologist* **210**, 1130–1144.

De Wit, I., Keulemans, J. and Cook, N. C. (2002). Architectural analysis of 1-year-old apple seedlings according to main shoot growth and sylleptic branching characteristics. *Trees* **16**, 473–478.

Denmead, O. T. and Shaw, R. H. (1962). Availability of soil water to plants as affected by soil moisture content and meteorological conditions1. *Agronomy Journal* **54**, 385.

Devi, J. M., Sinclair, T. R., Vadez, V. and Krishnamurthy, L. (2009). Peanut genotypic variation in transpiration efficiency and decreased transpiration during progressive soil drying. *Field Crops Research* **114**, 280–285.

Dodd, I. C., Munns, R. and Passioura, J. B. (2002). Does shoot water status limit leaf expansion of nitrogen-deprived barley? *Journal of Experimental Botany* **53**, 1765–1770.

Dong, Q., Louarn, G., Wang, Y., Barczi, J.-F. and Reffye, P. de (2008). Does the structure-function model GREENLAB deal with crop phenotypic plasticity induced by plant spacing? A case study on tomato. *Annals of Botany* **101**, 1195–1206.

Dunnett, C. W. (1955). A multiple comparison procedure for comparing several treatments with a control. *Journal of the American Statistical Association* **50**, 1096–1121.

Easlon, H. M. and Richards, J. H. (2009). Drought response in self-compatible species of tomato (Solanaceae). *American Journal of Botany* **96**, 605–611.

Egea, G., González-Real, M. M., Baille, A., Nortes, P. A. and Diaz-Espejo, A. (2011a). Disentangling the contributions of ontogeny and water stress to photosynthetic limitations in almond trees. *Plant, Cell & Environment* **34**, 962–979.

Egea, G., Verhoef, A. and Vidale, P. L. (2011b). Towards an improved and more flexible representation of water stress in coupled photosynthesis–stomatal conductance models. *Agricultural and Forest Meteorology* **151**, 1370–1384.

Egea, I., Albaladejo, I., Meco, V., Morales, B., Sevilla, A., Bolarin, M. C. and Flores, F. B. (2018). The drought-tolerant *Solanum pennellii* regulates leaf water loss and induces genes involved in amino acid and ethylene/jasmonate metabolism under dehydration. *Scientific Reports* **8**, 2791.

Elliott, J., Deryng, D., Müller, C., Frieler, K., Konzmann, M., Gerten, D., Glotter, M., Flörke, M., Wada, Y., Best, N. et al. (2014). Constraints and potentials of future irrigation water availability on agricultural production under climate change. *Proceedings of the National Academy of Sciences of the United States of America* **111**, 3239–3244.

Enoch, H. Z. (1990). Crop responses to aerial carbon dioxide. *Acta Horticulturae* **268**, 17–32.

Eshed, Y., Abu-Abied, M., Saranga, Y. and Zamir, D. (1992). *Lycopersicon esculentum* lines containing small overlapping introgressions from *L. pennellii. Theoretical and Applied Genetics* **83**, 1027–1034.

Eshed, Y. and Zamir, D. (1994). A genomic library of *Lycopersicon pennellii* in *L. esculentum.* A tool for fine mapping of genes. *Euphytica* **79**, 175–179.

Eshed, Y. and Zamir, D. (1995). An introgression line population of *Lycopersicon pennellii* in the cultivated tomato enables the identification and fine mapping of yield-associated QTL. *Genetics* **141**, 1147–1162.

Eshed, Y., Gera, G. and Zamir, D. (1996). A genome-wide search for wild-species alleles that increase horticultural yield of processing tomatoes. *Theoretical and Applied Genetics* **93**, 877–886.

Esmaeilzade-Moridani, M., Ghaderi_Far, F., A. Da Silva, Teixeira, J., Kamkar, B. and Galeshi, S. (2015). Leaf expansion and transpiration responses of millet species to soil water deficit. *Pedosphere* **25**, 834–843.

Farquhar, G. D., Caemmerer, S. von and Berry, J. A. (1980). A biochemical model of photosynthetic CO_2 assimilation in leaves of C_3 species. *Planta* **149**, 78–90.

Farquhar, G. D. and Wong, S. C. (1984). An empirical model of stomatal conductance. *Australian Journal of Plant Physiology* **11**, 191–210.

Fernandez-Moreno, J.-P., Levy-Samoha, D., Malitsky, S., Monforte, A. J., Orzaez, D., Aharoni, A. and Granell, A. (2017). Uncovering tomato quantitative trait loci and candidate genes for fruit cuticular lipid composition using the *Solanum pennellii* introgression line population. *Journal of Experimental Botany* **68**, 2703–2716.

Flexas, J., Bota, J., Galmés, J., Medrano, H. and Ribas-Carbó, M. (2006). Keeping a positive carbon balance under adverse conditions: responses of photosynthesis and respiration to water stress. *Physiologia Plantarum, 127(3), 343-352*. https://doi.org/10.1111/J.1399-3054.2006.00621.X.

Frary, A., Göl, D., Keleş, D., Okmen, B., Pinar, H., Siğva, H. O., Yemenicioğlu, A. and Doğanlar, S. (2010). Salt tolerance in *Solanum pennellii*: antioxidant response and related QTL. *BMC Plant Biology* **10**, 58.

Frary, A., Keleş, D., Pinar, H., Göl, D. and Doğanlar, S. (2011). NaCl tolerance in *Lycopersicon pennellii* introgression lines. QTL related to physiological responses. *Biologia Plantarum* **55**, 461–468.

Galmés, J., Medrano, H. and Flexas, J. (2007). Photosynthetic limitations in response to water stress and recovery in Mediterranean plants with different growth forms. *New Phytologist* **175**, 81–93.

Gary, C., Jones, J. W. and Longuenesse, J. J. (1993). Modelling daily changes in specific leaf area of tomato: the contribultion of the leaf assimilate pool. *Acta Horticulturae* **328**.

Gary, C., Barczi, J. F., Bertin, N. and Tchamitchian, M. (1995). Simulation of individual organ growth and development on a tomato plant: a model and a user-friendly interface. *Acta Horticulturae*, 199–206.

Gaudin, A. C. M., McClymont, S. A., Holmes, B. M., Lyons, E. and Raizada, M. N. (2011). Novel temporal, fine-scale and growth variation phenotypes in roots of adult-stage maize (Zea mays L.) in response to low nitrogen stress. *Plant, Cell & Environment* **34**, 2122–2137.

Gholipoor, M., Sinclair, T. R. and Prasad, P. V. V. (2012). Genotypic variation within sorghum for transpiration response to drying soil. *Plant Soil* **357**, 35–40.

Gijzen, H. (1992). *Simulation of photosynthesis and dry matter production of greenhouse crops. Simulation Report CABO-TT, 28, AB-DLO*. Wageningen, The Netherlands.

Godfray, H. C. J., Beddington, J. R., Crute, I. R., Haddad, L., Lawrence, D., Muir, J. F., Pretty, J., Robinson, S., Thomas, S. M. and Toulmin, C. (2010). Food Security: The Challenge of Feeding 9 Billion People. *Science* **327**.

Goudriaan, J. and van Laar, H. H. (1994). *Modelling potential crop growth processes. Textbook with exercises / by J. Goudriaan and H.H. Van Laar*. Dordrecht, London: Kluwer.

Grassi, G. and Magnani, F. (2005). Stomatal, mesophyll conductance and biochemical limitations to photosynthesis as affected by drought and leaf ontogeny in ash and oak trees. *Plant, Cell & Environment* **28**, 834–849.

Gratani, L. (2014). Plant Phenotypic Plasticity in Response to Environmental Factors. *Advances in Botany* **2014**, 1–17.

Hammer, G. L., Butler, D. G. and Muchow, R. C. (1996). Integrating physiological understanding and plant breeding via crop modelling and optimization. In *Plant Adaptation and Crop Improvement* (ed. M. Cooper and G. L. Hammer), pp. 419–441. Wallingford: CAB International.

Hammer, G. L., Chapman, S., van Oosterom, E. and Podlich, D. W. (2005). Trait physiology and crop modelling as a framework to link phenotypic complexity to underlying genetic systems. *Aust. J. Agric. Res.* **56**, 947.

Hammer, G. L., van Oosterom, E., McLean, G., Chapman, S. C., Broad, I., Harland, P. and Muchow, R. C. (2010). Adapting APSIM to model the physiology and genetics of complex adaptive traits in field crops. *Journal of Experimental Botany* **61**, 2185–2202.

Heuvelink, E. and Marcelis, L. (1989). Dry matter distribution in tomato and cucumber. *Acta Horticulturae* **260**, 149–157.

Heuvelink, E. (1995). Dry matter production in tomato crop: measurements and simulation. *Annals of Botany* **75**, 369–379.

Heuvelink, E. (1996a). Dry matter partitioning in tomato: validation of a dynamic simulation model. *Annals of Botany* **77**, 71–80.

Heuvelink, E. and Marcelis, L. F. M. (1996). Influence of assimilate supply on leaf formation in sweet pepper and tomato. *Journal of Horticultural Science* **71**, 405–414.

Heuvelink, E. (1996b). *Tomato growth and yield: quantitative analysis and synthesis. PhD Dissertation,* Wageningen Agricultural University. Wageningen, The Netherlands.

Heuvelink, E. (1999). Evaluation of a dynamic simulation model for tomato crop growth and development. *Annals of Botany* **83**, 413–422.

Hill, C. B., Taylor, J. D., Edwards, J., Mather, D., Bacic, A., Langridge, P. and Roessner, U. (2013). Whole-genome mapping of agronomic and metabolic traits to identify novel quantitative trait loci in bread wheat grown in a water-limited environment. *Plant Physiology* **162**, 1266–1281.

Holland, J. B., Nyquist, W. E. and Cervantes-Martínez, C. T. (2010). Estimating and interpreting heritability for plant breeding: an update. In *Plant breeding reviews* (ed. J. Janick). Oxford: John Wiley & Sons Inc.

Hsiao, T. C. (1973). Plant responses to water stress. *Annual Review of Plant Physiology* **24**, 519–570.

Hsiao, T. C., Acevedo, E., Fereres, E. and Henderson, D. W. (1976). Water stress, growth, and osmotic adjustment. *Philosophical Transactions of the Royal Society B: Biological Sciences* **273**, 479–500.

Hsiao, T. C., Silk, W. K. and Jing, J. (1985). Leaf growth and water deficits: biophysical effects. In *Control of leaf growth* (ed. N.R., Baker, W.J. Davies and C.K. Ong), pp. 239–266. Cambridge: Cambridge University Press,

Iovieno, P., Punzo, P., Guida, G., Mistretta, C., van Oosten, M. J., Nurcato, R., Bostan, H., Colantuono, C., Costa, A., Bagnaresi, P. et al. (2016). Transcriptomic changes drive physiological responses to progressive drought stress and rehydration in tomato. *Frontiers in Plant Science* **7**, 371.

Itoh, K., Yamada, T., Ishikawa, H., Ohta, E. and Sakata, M. (1986). Role of K^+ and Cl^- in osmotic adjustment in roots and hypocotyls of intact mung bean seedlings. *Plant and Cell Physiology* **27**, 1445–1450.

Itoh, K., Nakahara, K., Ishikawa, H., Ohta, E. and Sakata, M. (1987). Osmotic adjustment and osmotic constituents in roots of mung bean seedlings. *Plant and Cell Physiology*. https://doi.org/10.1093/oxfordjournals.pcp.a077309.

Jackson, R. B., Sperry, J. S. and Dawson, T. E. (2000). Root water uptake and transport: using physiological processes in global predictions. *Trends in Plant Science* **5**, 482–488.

Janott, M., Gayler, S., Gessler, A., Javaux, M., Klier, C. and Priesack, E. (2011). A one-dimensional model of water flow in soil-plant systems based on plant architecture. *Plant Soil* **341**, 233–256.

Jarvis, P. G. (1976). The interpretation of the variations in leaf water potential and stomatal conductance found in canopies in the field. *Phil. Trans. R. Soc. Lond. B.* **273**, 593–610.

Jefferies, R. A. (1993a). Responses of potato genotypes to drought. I. Expansion of individual leaves and osmotic adjustment. *Annals of Applied Biology* **122**, 93–104.

Jefferies, R. A. (1993b). Responses of potato genotypes to drought. I. Expansion of individual leaves and osmotic adjustment. *Ann Applied Biology* **122**, 93–104.

Jogaiah, S., Govind, S. R. and Tran, L.-S. P. (2013). Systems biology-based approaches toward understanding drought tolerance in food crops. *Critical Reviews in Biotechnology* **33**, 23–39.

Jones, H. G. (1992). *Plants and microclimate. a quantitative approach to environmental plant physiology.*

Jones, H. G. and Tardieu, F. (1998). Modelling water relations of horticultural crops: a review. *Scientia Horticulturae* **74**, 21–46.

Jones, H. G. (2007). Monitoring plant and soil water status: established and novel methods revisited and their relevance to studies of drought tolerance. *Journal of Experimental Botany* **58**, 119–130.

Jones, H. G. (2013). *Plants and Microclimate*. Cambridge: Cambridge University Press.

Jones, J. W., Dayan, E., Allen, L. H., van Keulen, H. and Challa, H. (1991). A dynamic tomato growth and yield model (TOMGRO). *Transactions of the ASAE* **34**, 663–672.

Juenger, T. E. (2013). Natural variation and genetic constraints on drought tolerance. *Current Opinion in Plant Biology* **16**, 274–281.

Kadam, N. N., Tamilselvan, A., Lawas, L. M. F., Quinones, C., Bahuguna, R. N., Thomson, M. J., Dingkuhn, M., Muthurajan, R., Struik, P. C., Yin, X. et al. (2017). Genetic control of plasticity in root morphology and anatomy of rice in response to water deficit. *Plant Physiology* **174**, 2302–2315.

Kahlen, K. and Stützel, H. (2011). Modelling photo-modulated internode elongation in growing glasshouse cucumber canopies. *New Phytologist* **190**, 697–708.

Katsoulas, N. and Stanghellini, C. (2019). Modelling crop transpiration in greenhouses: Different models for different applications. *Agronomy* **9**, 392.

Keurentjes, J. J. B., Bentsink, L., Alonso-Blanco, C., Hanhart, C. J., Blankestijn-De Vries, H., Effgen, S., Vreugdenhil, D. and Koornneef, M. (2007). Development of a near-isogenic line population of Arabidopsis thaliana and comparison of mapping power with a recombinant inbred line population. *Genetics* **175**, 891–905.

Kholová, J., Hash, C. T., Kakkera, A., Kocová, M. and Vadez, V. (2010). Constitutive water-conserving mechanisms are correlated with the terminal drought tolerance of pearl millet *Pennisetum glaucum* (L.) R. Br. *Journal of Experimental Botany* **61**, 369–377.

Klamkowski, K. and Treder, W. (2006). Morphological and physiological responses of strawberry plants to water stress. *Agriculturae Conspectus Scientificus* **71**, 159–165.

Kobayashi, K. and Salam, M. U. (2000). Comparing simulated and measured values using mean squared deviation and its components. *Agron. J.* **92**, 345.

Koenig, D., Jimenez-Gomez, J. M., Kimura, S., Fulop, D., Chitwood, D. H., Headland, L. R., Kumar, R., Covington, M. F., Devisetty, U. K., Tat, A. V. et al. (2013). Comparative transcriptomics reveals patterns of selection in domesticated and wild tomato. *Proceedings of the National Academy of Sciences* **110**, E2655-E2662.

Kooke, R., Johannes, F., Wardenaar, R., Becker, F., Etcheverry, M., Colot, V., Vreugdenhil, D. and Keurentjes, J. J. B. (2015). Epigenetic basis of morphological variation and phenotypic plasticity in Arabidopsis thaliana. *The Plant Cell* **27**, 337–348.

Kropff, M. J. and Struik, P. C. (2002). Developments in crop ecology. *NJAS* **50**, 223–237.

Lambers, H. and Oliveira, R. S. (2019). *Plant physiological ecology*. New York: Springer.

Langridge, P. and Reynolds, M. P. (2015). Genomic tools to assist breeding for drought tolerance. *Current Opinion in Biotechnology* **32**, 130–135.

Lawlor, D. W. (2002). Limitation to photosynthesis in water-stressed leaves: stomata vs. metabolism and the role of ATP. *Annals of Botany* **89 Spec No**, 871–885.

Lecoeur, J. and Sinclair, T. R. (1996). Field pea transpiration and leaf growth in response to soil water deficits. *Crop Science* **36**, 331.

Letort, V., Mahe, P., Cournede, P.-H., Reffye, P. de and Courtois, B. (2007). Quantitative genetics and functional-structural plant growth models: Simulation of quantitative trait loci detection for model parameters and application to potential yield optimization. *Annals of Botany* **101**, 1243–1254.

Leuning, R. (1995). A critical appraisal of a combined stomatal-photosynthesis model for C_3 plants. *Plant, Cell & Environment* **18**, 339–355.

Levitt, J. (1972). *Responses of plants to environmental stresses*. New York: Academic Press.

Levitt, J. (1980). *Responses of plants to environmental stresses. v. 1. Chilling, freezing, and high temperature stresses. v. 2. Water, radiation, salt, and other stresses.* New York: Academic Press.

Lippman, Z. B., Semel, Y. and Zamir, D. (2007). An integrated view of quantitative trait variation using tomato interspecific introgression lines. *Current opinion in genetics & development* **17**, 545–552.

Liu, F. and Stützel, H. (2002). Leaf water relations of vegetable amaranth (*Amaranthus spp.*) in response to soil drying. *European Journal of Agronomy* **16**, 137–150.

Lizaso, J., Batchelor, W., Westgate, M. and Echarte, L. (2003). Enhancing the ability of CERES-Maize to compute light capture. *Agricultural Systems* **76**, 293–311.

Lizaso, J. I., Batchelor, W. D., Boote, K. J. and Westgate, M. E. (2005). Development of a leaf-level canopy assimilation model for CERES-Maize. *Agron. J.* **97**, 722–733.

Lizaso, J. I., Boote, K. J., Jones, J. W., Porter, C. H., Echarte, L., Westgate, M. E. and Sonohat, G. (2011). CSM-IXIM: A new maize simulation model for DSSAT version 4.5. *Agron. J.* **103**, 766–779.

Lohammar, T., Larsson, S., Linder, S. and Falk, S. O. (1980). FAST: Simulation models of gaseous exchange in scots pine. *Ecological bulletins* **32**, 505–523.

Ludlow, M. M., Chu, A., Clements, R. J. and Kerslake, R. G. (1983). Adaptation of species of *Centrosema* to water stress. *Aust. J. Plant Phys.* **10**, 119–130.

Ludlow, M. M., ed. (1989). *Strategies of response to water stress. Structural and Functional Responses to Environmental Stresses*: SPB Academic Publishing,. The Hague.

Ludlow, M. M. and Much, R. C. (1990). A critical evaluation of traits for improving crop yields in water-limited environments. *Advances in Agronomy* **43**, 107–153.

Luo, L. J. (2010). Breeding for water-saving and drought-resistance rice (WDR) in China. *Journal of Experimental Botany* **61**, 3509–3517.

Mahajan, S. and Tuteja, N. (2005). Cold, salinity and drought stresses: an overview. *Archives of biochemistry and biophysics* **444**, 139–158.

Makino, A., Sakuma, H., Sudo, E. and Mae, T. (2003). Differences between maize and rice in N-use efficiency for photosynthesis and protein allocation. *Plant & Cell Physiology* **44**, 952–956.

Marcelis, L., Elings, A., Visser, P. de and Heuvelink, E. (2009). Simulating growth and development of tomato crop. In *Proc. IS on Tomato in the Tropics Acta Hort. 821, 2009* (ed. G. e. a. Fischer), pp. 101–110: ISHS.

Marcelis, L. F. (1994). A simulation model for dry matter partitioning in cucumber. *Annals of Botany* **74**, 43–52.

Marcelis, L. F. M. (1993). Fruit growth and biomass allocation to the fruits in cucumber. 1. Effect of fruit load and temperature. *Scientia Horticulturae* **54**, 107–121.

Marcelis, L. F. M., Heuvelink, E. and Goudriaan, J. (1998). Modelling biomass production and yield of horticultural crops: a review. *Scientia Horticulturae* **74**, 83–111.

Marchiori, P. E. R., Machado, E. C., Sales, C. R. G., Espinoza-Núñez, E., Magalhães Filho, J. R., Souza, G. M., Pires, R. C. M. and Ribeiro, R. V. (2017). Physiological plasticity is important for maintaining sugarcane growth under water deficit. *Frontiers in Plant Science* **8**, 2148.

Masinde, P. W., Stützel, H., Agong, S. G. and Fricke, A. (2005). Plant growth, water relations, and transpiration of Spiderplant [*Gynandropsis gynandra* (L.) Briq. under water-limited conditions. *J. Amer. Soc. Hort. Sci.* **130**, 469–477.

Masinde, P. W., Stützel, H., Agong, S. G. and Fricke, A. (2006). Plant growth, water relations and transpiration of two species of African nightshade (*Solanum villosum* Mill. ssp. miniatum (Bernh. ex Willd.) Edmonds and S. sarrachoides Sendtn.) under water-limited conditions. *Scientia Horticulturae* **110**, 7–15.

Matesanz, S., Gianoli, E. and Valladares, F. (2010). Global change and the evolution of phenotypic plasticity in plants. *Annals of Botany*, 35–55.

Ma, X., He, Q. and Zhou, G. (2018). Sequence of changes in maize responding to soil water deficit and related critical thresholds. *Frontiers in Plant Science* **9**, 511.

Medlyn, B. E., Kauwe, M. G. de, Zaehle, S., Walker, A. P., Duursma, R. A., Luus, K., Mishurov, M., Pak, B., Smith, B., Wang, Y.-P. et al. (2016). Using models to guide field experiments: a priori predictions for the CO_2 response of a nutrient- and water-limited native Eucalypt woodland. *Global Change Biology* **22**, 2834–2851.

Meier, I. C. and Leuschner, C. (2008). Genotypic variation and phenotypic plasticity in the drought response of fine roots of European beech. *Tree Physiology* **28**, 297–309.

Meir, P., Wood, T. E., Galbraith, D. R., Brando, P. M., Da Costa, A. C. L., Rowland, L. and Ferreira, L. V. (2015). Threshold responses to soil moisture deficit by trees and soil in tropical rain forests: insights from field experiments. *BioScience* **65**, 882–892.

Merilo, E., Yarmolinsky, D., Jalakas, P., Parik, H., Tulva, I., Rasulov, B., Kilk, K. and Kollist, H. (2018). Stomatal VPD response: There is more to the Story than ABA. *Plant Physiology* **176**, 851–864.

Messina, C. D., Podlich, D., Dong, Z., Samples, M. and Cooper, M. (2011). Yield-trait performance landscapes: from theory to application in breeding maize for drought tolerance. *Journal of Experimental Botany* **62**, 855–868.

Messina, C. D., Boote, K. J., Löffler, C. M., Jones, J. W. and Vallejos, C. E. (2014). Model-assisted genetic improvement of crops. In *Working with dynamic crop models. Method, tools, and examples for agriculture and environment* (ed. D. Wallach, D. Makowski, J. W. Jones and F. Brun). Amsterdam, Boston, Heidelberg: Elsevier AP.

Milroy, S. P. and Goyne, P. J. (1995). Leaf area development in barley—model construction and response to soil moisture status. *Australian Journal of Agricultural Research* **46**, 845.

Monsi, M. and Saeki, T. (1953). Über den Lichtfaktor in den Pflanzengesellschaften und seine Bedeutung für die Stoffproduktion. *Japanese Journal of Botany* **14**, 22–52.

Morgan, J. M. (1992). Osmotic components and properties associated with genotypic differences in osmoregulation in wheat. *Australian Journal of Plant Physiology* **19**, 67.

Moualeu-Ngangue, D. P., Chen, T.-W. and Stützel, H. (2016). A modeling approach to quantify the effects of stomatal behavior and mesophyll conductance on leaf water use efficiency. *Frontiers in Plant Science* **7**, 875.

Moualeu-Ngangue, D. P., Chen, T.-W. and Stützel, H. (2017). A new method to estimate photosynthetic parameters through net assimilation rate-intercellular space CO_2 concentration (A-C_i) curve and chlorophyll fluorescence measurements. *New Phytologist* **213**, 1543–1554.

Muchow, R. C. and Sinclair, T. R. (1991). Water deficit effects on maize yields modeled under current and greenhouse climates. *Agronomy Journal* **83**, 1052–1059.

Muller, B., Pantin, F., Génard, M., Turc, O., Freixes, S., Piques, M. and Gibon, Y. (2011). Water deficits uncouple growth from photosynthesis, increase C content, and modify the relationships between C and growth in sink organs. *Journal of Experimental Botany* **62**, 1715–1729.

Nable, R. O., Robertson, M. J. and Berthelsen, S. (1999). Response of shoot growth and transpiration to soil drying in sugarcane. *Plant and Soil* **207**, 59–65.

Naz, A. A., Arifuzzaman, M., Muzammil, S., Pillen, K. and Léon, J. (2014). Wild barley introgression lines revealed novel QTL alleles for root and related shoot traits in the cultivated barley (*Hordeum vulgare* L.). *BMC Genetics* **15**, 107.

Nelson, D. W. and Sommers, L. E. (1973). Determination of total nitrogen in plant material. *Agronomy Journal* **65**, 109–112.

Nicotra, A. B. and Davidson, A. (2010). Adaptive phenotypic plasticity and plant water use. *Functional Plant Biology* **37**, 117.

Noe, S. M. and Giersch, C. (2004). A simple dynamic model of photosynthesis in oak leaves: coupling leaf conductance and photosynthetic carbon fixation by a variable intracellular CO_2 pool. *Functional Plant Biology* **31**, 1195.

Novák, V. (2009). Physiological drought – how to quantify it? In *Bioclimatology and Natural Hazards* (ed. K. Střelcová, C. Mátyás, A. Kleidon, M. Lapin, F. Matejka, M. Blaženec, J. Škvarenina and J. Holécy), pp. 89–95. Dordrecht: Springer Netherlands.

Ofner, I., Lashbrooke, J., Pleban, T., Aharoni, A. and Zamir, D. (2016). *Solanum pennellii* backcross inbred lines (BILs) link small genomic bins with tomato traits. *The Plant Journal* **87**, 151–160.

Ögren, E. and Evans, J. R. (1993). Photosynthetic light-response curves. *Planta* **189**, 182–190.

Parent, B. and Tardieu, F. (2014). Can current crop models be used in the phenotyping era for predicting the genetic variability of yield of plants subjected to drought or high temperature? *Journal of Experimental Botany* **65**, 6179–6189.

Passioura, J. B. (1988). Root signals control leaf expansion in wheat seedlings growing in drying soil. *Functional Plant Biology* **15**, 687.

Penman, H. L. (1948). Natural evaporation from open water, bare soil and grass. *Proceedings of the Royal Society of London. Series A, Mathematical and Physical* **193**, 120–145.

Perez, R. P., Pallas, B., Le Moguédec, G., Rey, H., Griffon, S., Caliman, J.-P., Costes, E. and Dauzat, J. (2016). Integrating mixed-effect models into an architectural plant model to simulate inter- and intra-progeny variability: a case study on oil palm (Elaeis guineensisJacq.). *Journal of Experimental Botany* **67**, 4507–4521.

Pliura, A., Zhang, S. Y., MacKay, J. and Bousquet, J. (2007). Genotypic variation in wood density and growth traits of poplar hybrids at four clonal trials. *Forest Ecology and Management* **238**, 92–106.

Porporato, A., Laio, F., Ridolfi, L. and Rodriguez-Iturbe, I. (2001). Plants in water-controlled ecosystems: active role in hydrologic processes and response to water stress. *Advances in Water Resources* **24**, 725–744.

Powell, T. L., Galbraith, D. R., Christoffersen, B. O., Harper, A., Imbuzeiro, H. M. A., Rowland, L., Almeida, S., Brando, P. M., da Costa, A. C. L., Costa, M. H. et al. (2013). Confronting model predictions of carbon fluxes with measurements of Amazon forests subjected to experimental drought. *New Phytologist* **200**, 350–365.

Prado, S. A., Cabrera-Bosquet, L., Grau, A., Coupel-Ledru, A., Millet, E. J., Welcker, C. and Tardieu, F. (2018). Phenomics allows identification of genomic regions affecting maize stomatal conductance with conditional effects of water deficit and evaporative demand. *Plant, Cell & Environment* **41**, 314–326.

Premachandra, G. S., Hahn, D. T., Rhodes, D. and Joly, R. J. (1995). Leaf water relations and solute accumulation in two grain sorghum lines exhibiting contrasting drought tolerance. *Journal of Experimental Botany* **46**, 1833–1841.

Priestley, C. H. B. and Taylor, R. J. (1972). On the assessment of surface heat flux and evaporation using large-scale parameters. *Monthly Weather Review* **100**, 81–92.

Pritchard, J., Win Jones, R. G. and Tomos, A. D. (1991). Turgor, growth and rheological gradients of cereal roots and the effect of osmotic stress. *Journal of Experimental Botany* **42**, 1043–1049.

Ramadas, M. and Govindaraju, R. S. (2015). Probabilistic assessment of agricultural droughts using graphical models. *Journal of Hydrology* **526**, 151–163.

Ray, J. D. and Sinclair, T. R. (1997). Stomatal closure of maize hybrids in response to drying soil. *Crop Science* **37**, 803.

Ray, J. D. and Sinclair, T. R. (1998). The effect of pot size on growth and transpiration of maize and soybean during water deficit stress. *Journal of Experimental Botany* **49**.

Ray, J. D., Sinclair, T. R., Gesch, R. W. and Allen, L. H. (2002). The effect of vapor pressure deficit on maize transpiration response to a drying soil. *Plant and Soil* **239**, 113–121.

Reymond, M., Muller, B., Leonardi, A., Charcosset, A. and Tardieu, F. (2003). Combining quantitative trait loci analysis and an ecophysiological model to analyze the genetic variability of the responses of maize leaf growth to temperature and water deficit. *Plant Physiology* **131**, 664–675.

Reymond, M., Muller, B. and Tardieu, F. (2004). Dealing with the genotype x environment interaction via a modelling approach: a comparison of QTLs of maize leaf length or width with QTLs of model parameters. *Journal of Experimental Botany* **55**, 2461–2472.

Richards, R. A., Rebetzke, G. J., Condon, A. G. and van Herwaarden, A. F. (2002). Breeding opportunities for increasing the efficiency of water use and crop yield in temperate cereals. *Crop Science* **42**, 111.

Rosenthal, W. D., Arkin, G. F., Shouse, P. J. and Jordan, W. R. (1987). Water deficit effects on transpiration and leaf growth. *Agronomy Journal* **79**, 1019.

Rötter, R. P., Tao, F., Höhn, J. G. and Palosuo, T. (2015). Use of crop simulation modelling to aid ideotype design of future cereal cultivars. *Journal of Experimental Botany* **66**, 3463–3476.

Rousseaux, M. C., Jones, C. M., Adams, D., Chetelat, R., Bennett, A. and Powell, A. (2005). QTL analysis of fruit antioxidants in tomato using Lycopersicon pennellii introgression lines. *Theoretical and Applied Genetics* **111**, 1396–1408.

Ruggiero, C., Pascale, S. D. and Fagnano, M. (1999). Plant and soil resistance to water flow in faba bean (Vicia faba L. major Harz.). *Plant and Soil* **210**, 219–231.

Saab, I. N. and Sharp, R. E. (1989). Non-hydraulic signals from maize roots in drying soil: inhibition of leaf elongation but not stomatal conductance. *Planta* **179**, 466–474.

Sade, N., Gebremedhin, A. and Moshelion, M. (2012). Risk-taking plants: anisohydric behavior as a stress-resistance trait. *Plant signaling & behavior* **7**, 767–770.

Sadok, W., Naudin, P., Boussuge, B., Muller, B., Welcker, C. and Tardieu, F. (2007). Leaf growth rate per unit thermal time follows QTL-dependent daily patterns in hundreds of maize lines under naturally fluctuating conditions. *Plant, Cell & Environment* **30**, 135–146.

Sadras, V. O., Villalovos, F. J., Fereres, E. and Wolfe, D. W. (1993). Leaf responses to soil water deficits: Comparative sensitivity of leaf expansion rate and leaf conductance in field-grown sunflower (*Helianthus annuus* L.). *Plant and Soil* **153**, 189–194.

Sadras, V. O. and Milroy, S. (1996). Soil-water thresholds for the responses of leaf expansion and gas exchange: A review. *Field Crops Research* **47**, 253–266.

Sandhu, N., Raman, K. A., Torres, R. O., Audebert, A., Dardou, A., Kumar, A. and Henry, A. (2016). Rice root architectural plasticity traits and genetic regions for adaptability to variable cultivation and stress conditions. *Plant Physiology* **171**, 2562–2576.

Santakumari, M. and Berkowitz, G. A. (1991). Chloroplast volume:cell water potential relationships and acclimation of photosynthesis to leaf water deficits. *Photosynthesis Research* **28**, 9–20.

Sawkins, M. C., DeMeyer, J. and Ribaut, J. M. (2006). Drought adaptation in maize. In *Drought Adaptation in Cereals* (ed. J.M. Ribaut), pp. 259–299. New York: Haworth Press.

Scheiner, S. M. and Lyman, R. F. (1989). The genetics of phenotypic plasticity. I. Heritability. *Journal of Evolutionary Biology* **2**, 95–107.

Schmalenbach, I., Léon, J. and Pillen, K. (2009). Identification and verification of QTLs for agronomic traits using wild barley introgression lines. *Theoretical and Applied Genetics* **118**, 483–497.

Schmidt, J. J., Blankenship, E. E. and Lindquist, J. L. (2011). Corn and velvetleaf (*Abutilon theophrasti*) transpiration in response to drying soil. *Weed Science* **59**, 50–54.

Scholander, P. F., Hammel, H. T., Bradstreet, E. D. and Hemingeen, E. A. (1965). Sap pressure in vascular plants. *Science* **148**, 339–346.

Schulze, E.-D. (1986). Carbon dioxide and water vapor exchange in response to drought in the atmosphere and in the soil. *Annual Review of Plant Physiology* **37**, 247–274.

Shackel, K. A., Matthews, M. A. and Morrison, J. C. (1987). Dynamic relation between expansion and cellular turgor in growing grape (*Vitis vinifera* L.) leaves. *Plant Physiology* **84**, 1166–1171.

Sinclair, T. R. and Ludlow, M. M. (1986). Influence of soil water supply on the plant water balance of four tropical grain legumes. *Functional Plant Biology* **13**, 329.

Sinclair, T. R. and Muchow, R. C. (2001). System analysis of plant traits to increase grain yield on limited water supplies. *Agronomy Journal* **93**, 263.

Smith, M. A. L., Spomer, L. A. and Skiles, E. S. (1989). Cell osmolarity adjustment in *Lycopersicon* in response to stress pretreatments. *Journal of Plant Nutrition* **12**, 233–244.

Sobeih, W. Y., Dodd, I. C., Bacon, M. A., Grierson, D. and Davies, W. J. (2004). Long-distance signals regulating stomatal conductance and leaf growth in tomato (*Lycopersicon esculentum*) plants subjected to partial root-zone drying. *Journal of Experimental Botany* **55**, 2353–2363.

Soltani, A., Khooie, F. R., Ghassemi-Golezani, K. and Moghaddam, M. (2000). Thresholds for chickpea leaf expansion and transpiration response to soil water deficit. *Field Crops Research* **68**, 205–210.

Spitters, C., Keulen, H. and Kraalingen, D. (1989). A simple and universal crop growth simulator: SUCROS87. In *Simulation and system management in crop protection* (ed. R. Rabbinge, S. A. Ward and H. H. van Laar), pp. 147–181. Wageningen, The Netherlands: PUDOC.

Spollen, W. G. and Sharp, R. E. (1991). Spacial distrubution of turgor and root growth at low water potentials. *Plant Physiology* **96**, 438–443.

Stagnari, F., Galieni, A. and Pisante, M. (2016). Drought stress effects on crop quality. Chapter 23. In *Water stress and crop plants: a sustainable approach* (ed. P. Ahmad), pp. 375–392: John Wiley & Sons, Ltd.

Stanghellini, C. (1987). *Transpiration of greenhouse crops: an aid to climate management. Ph.D. Dissertation,* Instituut voor Mechanisatie, Arbeid en Gebouwen. Wageningen, The Netherlands.

Stanghellini, C. and Taeke, d. J. (1995). A model of humidity and its applications in a greenhouse. *Agrcultural and Forest Meteorology* **76**, 129–148.

Stockle, C. O., Martin, S. A. and Campbell, G. S. (1994). CropSyst, a cropping systems simulation model: Water/nitrogen budgets and crop yield. *Agricultural Systems* **46**, 335–359.

Streck, N. A. (2004). Do we know how plants sense a drying soil? *Plant, Cell & Environment* **34**, 581–584.

Tang, A.-C. and Boyer, J. S. (2002). Growth-induced water potentials and the growth of maize leaves. *Journal of Experimental Botany* **53**, 489–503.

Tardieu, F. and Davies, W. J. (1992). Stomatal response to abscisic acid is a function of current plant water status. *Plant Physiology* **98**, 540–545.

Tardieu, F. and Davies, W. J. (1993). Integration of hydraulic and chemical signalling in the control of stomatal conductance and water status of droughted plants. *Plant, Cell & Environment* **16**, 341–349.

Tardieu, F., Zhang, J. and GOWING, D. J. G. (1993). Stomatal control by both [ABA] in the xylem sap and leaf water status: a test of a model for draughted or ABA-fed field-grown maize. *Plant, Cell & Environment* **16**, 413–420.

Tardieu, F. (1996). Drought perception by plants. Do cells of droughted plants experience water stress? *Plant Growth Regulation* **20**, 93–104.

Tardieu, F. (2003). Virtual plants: modelling as a tool for the genomics of tolerance to water deficit. *Trends in Plant Science* **8**, 9–14.

Tardieu, F. and Tuberosa, R. (2010). Dissection and modelling of abiotic stress tolerance in plants. *Current Opinion in Plant Biology* **13**, 206–212.

Tardieu, F., Granier, C. and Muller, B. (2011). Water deficit and growth. Co-ordinating processes without an orchestrator? *Current Opinion in Plant Biology* **14**, 283–289.

Thornley, J. and Johnson, I. R. (1990). *Plant and crop modeling*: Oxford University Press, New York.

Thornley, J. H. M. (2002). Instantaneous canopy photosynthesis: analytical expressions for sun and shade leaves based on exponential light decay down the canopy and an acclimated non-rectangular hyperbola for leaf photosynthesis. *Annals of Botany* **89**, 451–458.

Toms, J. D. and Villard, M.-A. (2015). Threshold detection: matching statistical methodology to ecological questions and conservation planning objectives. *ACE*. https://doi.org/10.5751/ACE-00715-100102.

Tschaplinski, T. J. and Tuskan, G. A. (1994). Water-stress tolerance of black and eastern cottonwood clones and four hybrid progeny. II. Metabolites and inorganic ions that constitute osmotic adjustment. *Can. J. For. Res.* **24**, 681–687.

Tuberosa, R., Salvi, S., Sanguineti, M. C., Landi, P., Maccaferri, M. and Conti, S. (2002). Mapping QTLs regulating morpho-physiological traits and yield: case studies, shortcomings and perspectives in drought-stressed maize. *Annals of Botany* **89 Spec No**, 941–963.

Turner, N. C. and Jones, M. M. (1980). Turgor maintenance by osmotic adjustment. A review and evaluation. In *Adaptation of plants to water and high temperature stress* (ed. N. C. Turner and P. J. Kramer), pp. 87–103. New York: John Wiley & Sons, Inc.

Turner, N. C., Schulze, E.-D. and Gollan, T. (1985). The responses of stomata and leaf gas exchange to vapour pressure deficits and soil water content. II. In the Mesophytic Herbaceous Species Helianthus annuus. *Oecologia(Berlin)* **65**, 348–355.

Turner, N. C. (2017). Turgor maintenance by osmotic adjustment, an adaptive mechanism for coping with plant water deficits. *Plant, Cell & Environment* **40**, 1–3.

Tuzet, A., Perrier, A. and Leuning, R. (2003). A coupled model of stomatal conductance, photosynthesis and transpiration. *Plant, Cell & Environment* **26**, 1097–1116.

Valladares, F., Balaguer, L., Martinez-Ferri, E., Perez-Corona, E. and Manrique, E. (2002). Plasticity, instability and canalization: is the phenotypic variation in seedlings of sclerophyll oaks consistent with the environmental unpredictability of Mediterranean ecosystems? *New Phytologist* **156**, 457–467.

Valladares, F., Sanchez-Gomez, D. and Zavala, M. A. (2006). Quantitative estimation of phenotypic plasticity. bridging the gap between the evolutionary concept and its ecological applications. *J Ecology* **94**, 1103–1116.

van Laar, H. H., Goudriaan, J. and van Keulen, H., eds. (1997). *SUCROS97: simulation of crop growth for potential and water-limited production situations as applied to spring wheat*. Wageningen: Haren & PE.

Viger, M., Smith, H. K., Cohen, D., Dewoody, J., Trewin, H., Steenackers, M., Bastien, C. and Taylor, G. (2016). Adaptive mechanisms and genomic plasticity for drought tolerance identified in European black poplar (*Populus nigra* L.). *Tree Physiology* **36**, 909–928.

Volis, S., Mendlinger, S., Olsvig-Whittaker, L., Safriel, U. N. and Orlovsky, N. (1998). Phenotypic variation and stress resistance in core and peripheral populations of *Hordeum spontaneum*. *Biodiversity and Conservation* **7**, 799–813.

Wallach, D., Makowski, D., Jones, J. W. and Brun, F. (2018). *Working with dynamic crop models. Methods, tools and examples for agriculture and environment*. S.l.: ELSEVIER ACADEMIC PRESS.

Wang, J. P. and Bughrara, S. S. (2008). Evaluation of drought tolerance for *Atlas fescue*, perennial ryegrass, and their progeny. *Euphytica* **164**, 113–122.

Wang, Z.-Y., Li, F.-M., Xiong, Y.-C. and Xu, B.-C. (2008). Soil-water threshold range of chemical signals and drought tolerance was mediated by ROS homeostasis in winter wheat during progressive soil drying. *Journal of Plant Growth Regulation* **27**, 309–319.

Welcker, C., Boussuge, B., Bencivenni, C., Ribaut, J.-M. and Tardieu, F. (2007). Are source and sink strengths genetically linked in maize plants subjected to water deficit? A QTL study of the responses of leaf growth and of anthesis-silking interval to water deficit. *Journal of Experimental Botany* **58**, 339–349.

Welcker, C., Sadok, W., Dignat, G., Renault, M., Salvi, S., Charcosset, A. and Tardieu, F. (2011). A common genetic determinism for sensitivities to soil water deficit and evaporative demand: meta-analysis of quantitative trait loci and introgression lines of maize. *Plant Physiology* **157**, 718–729.

White, J. W. and Hoogenboom, G. (1996). Simulating effects of genes for physiological traits in a process-oriented crop model. *Agronomy Journal* **88**, 416–422.

White, J. W. and Hoogenboom, G. (2003). Gene-based approaches to crop simulation. Past experiences and future opportunities. *Agronomy Journal* **95**, 52.

Wu, R. and Stettler, R. F. (1994). Quantitative genetics of growth and development in Populus. I. A three-generation comparison of tree architecture during the first 2 years of growth. *Theoretical and Applied Genetics* **89-89**, 1046–1054.

Wu, R. L. (1998). Genetic mapping of QTLs affecting tree growth and architecture in Populus: implication for ideotype breeding. *Theoretical and Applied Genetics* **96**, 447–457.

Wu, Y. Z., Huang, M. B. and Warrington, D. N. (2011a). Growth and transpiration of maize and winter wheat in response to water deficits in pots and plots. *Environmental and Experimental Botany* **71**, 65–71.

Wu, Y. Z., Huang, M. B. and Warrington, D. N. (2011b). Responses of different physiological indices for maize (*Zea mays*) to soil water availability. *Pedosphere* **21**, 639–649.

Xu, B.-C., Deng, X.-P., Zhang, S.-Q. and Shan, L. (2010). Biomass partition, leaf gas exchange and water relations of alfalfa and milkvetch seedlings in response to soil drying. *Photosynthetica* **48**, 481–487.

Xu, L., Henke, M., Zhu, J., Kurth, W. and Buck-Sorlin, G. (2011). A functional–structural model of rice linking quantitative genetic information with morphological development and physiological processes. *Annals of Botany* **107**, 817–828.

Yan, M.-J., Yamanaka, N., Yamamoto, F. and Du, S. (2010). Responses of leaf gas exchange, water relations, and water consumption in seedlings of four semiarid tree species to soil drying. *Acta Physiol Plant* **32**, 183–189.

Yin, X., Stam, P., Dourleijn, C. J. and Kropff, M. J. (1999). AFLP mapping of quantitative trait loci for yield-determining physiological characters in spring barley. *Theoretical and Applied Genetics* **99**, 244–253.

Yin, X., Chasalow, S. D., Dourleijn, C. J., Stam, P. and Kropff, M. J. (2000). Coupling estimated effects of QTLs for physiological traits to a crop growth model: predicting yield variation among recombinant inbred lines in barley. *Heredity* **85**, 539–549.

Yin, X., Chasalow. S.D., Stam, P., Kropff, M. J., Dourlei jn, C. J., Bos, I. and Bindraban, P. S. (2002). Use of component analysis in QTL mapping of complex crop traits: a case study on yield in barley. *Plant Breeding* **121**, 314–319.

Yin, X., Struik, P. C. and Kropff, M. J. (2004). Role of crop physiology in predicting gene-to-phenotype relationships. *Trends in Plant Science* **9**, 426–432.

Yin, X. and van Laar, H. H. (2005). *Crop systems dynamics. An ecophysiological simulation model for genotype-by-environment interactions*. Netherland, Enfield NH: Wageningen Academic Publishers; Science Publishers.

Yin, X., Sun, Z., Struik, P. C. and Gu, J. (2011). Evaluating a new method to estimate the rate of leaf respiration in the light by analysis of combined gas exchange and chlorophyll fluorescence measurements. *Journal of Experimental Botany* **62**, 3489–3499.

Zamir, D. (2001). Improving plant breeding with exotic genetic libraries. *Nature Reviews. Genetics* **2**, 983–989.

Zamir, D. (2007). Sequencing *Solanum pennellii* - the wild parent of tomato introgression lines (ILs) that reveal a molecular and a system view of complex phenotypes. *Community Sequencing Program: Project Proposal*(CSP Letter of Intent ID: 'CSP_LOI_783890').

Zhang, Q. (2007). Strategies for developing Green Super Rice. *Proceedings of the National Academy of Sciences of the United States of America* **104**, 16402–16409.

Zhou, S., Duursma, R. A., Medlyn, B. E., Kelly, J. W. and Prentice, I. C. (2013). How should we model plant responses to drought? An analysis of stomatal and non-stomatal responses to water stress. *Agricultural and Forest Meteorology* **182-183**, 204–214.

Zhou, S.-X., Prentice, I. C. and Medlyn, B. E. (2018). Bridging drought experiment and modeling: representing the differential sensitivities of leaf gas exchange to drought. *Frontiers in Plant Science* **9**, 1965.

Zhu, M., Monroe, J. G., Suhail, Y., Villiers, F., Mullen, J., Pater, D., Hauser, F., Jeon, B. W., Bader, J. S., Kwak, J. M. et al. (2016). Molecular and systems approaches towards drought-tolerant canola crops. *New Phytologist* **210**, 1169–1189.

List of Publications

Papers in preparation

Myint, S.S., Moualeu-Ngangue, D.P, Stützel, H. (2022). Genetic variation in adaptive responses explains the growth performances of tomato introgression lines under drought (ready for submission)

Myint, S.S., Moualeu-Ngangue, D.P, Stützel, H. (2022). QTL-based prediction of water use in drought-stressed tomatoes (ready for submission)

Myint, S.S., Moualeu-Ngangue, D.P, Stützel, H. (2022). A genome-based eco-physiological model of leaf area, transpiration and dry matter production for vegetative growth stage of tomatoes under drought stress (in preparation)

Reviewed papers as co-author

Bollig, K., Specht, A., **Myint, S.S.**, Zahn, M., Horst, W.J. (2013). Sulphur supply impairs spread of *Verticillium dahiae* in tomato, *European Journal of Plant Pathology* 135 (1). 81-96

Klug, K., Hogekamp, C., Specht, A., **Myint, S.S.**, Blöink. D., Küster, H., Horst, W.J. (2015). Spatial gene expression analysis in tomato typocotyls suggests cysteine as key precursors of vascular sulfur accumulation implicated in *Verticillium dahlia* defense. *Phsiologia Plantarum*, 153 (2), 253-268

Conference papers

Myint, S.S., Moualeu-Ngangue, D.P., Fricke, A., Stützel, H. (2016) Functional and structural adaptations of tomato upon soil drying: plant growth, transpiration and water relations, *Mitteilungen der Gesellschaft für Pflanzenbauwissenschaften*, Band 28, pp 194-195

Myint, S.S., Moualeu-Ngangue, D.P., Fricke, A.; Stützel, H. (2017). Modelling leaf growth of tomato (*Solanum pennellii* x M82) introgression lines under varying vapor pressure deficits and soil drying, *Mitteilungen der Gesellschaft für Pflanzenbauwissenschaften*, Band 29, pp 34-35

Myint, S.S., Moualeu-Ngangue, D.P., Stützel, H. (2018). Genetic variance in the dynamics of architectural traits and photosynthesis responses of tomato (*Solanum pennellii* x M82) introgression lines under drought stress, *Mitteilungen der Gesellschaft für Pflanzenbauwissenschaften*, Band 30, pp 49-50

Myint, S.S., Moualeu-Ngangue, D.P., Stützel, H. (2018). Identification of favorable genomic regions associated to drought response traits of 50 tomato (*Solanum pennellii* x M82) introgression lines, *15th ESA Congress*. Geneva, Switzerland, 27 -31 August 2018

Myint, S.S., Moualeu-Ngangue, D.P., Stützel, H. (2019): Sensitivies of structural and functional drought reactions of tomatoes under varying vapour pressure deficits, *Mitteilungen der Gesellschaft für Pflanzenbauwissenschaften*, Band 31, pp 127-128

Acknowledgement

I would like to express my sincere gratitude to all the people who supported me in one way or another in this so long journey of my doctoral research.

Firstly, I would like to sincerely thank Prof. Dr. sc. agr. Hartmut Stützel for giving me an opportunity to join the institute as a PhD student. He is my supervisor, academic father in Germany. His unique way of guidance and supervision are incredible. Prof. Stützel led me a path to real science, gave me a chance to face challenges, and showed me his unequivocal patience to keep me stay on the track. I am also thankful to Prof. Dr. rer. nat. Thomas Debener, for being my co-advisor.

Secondly, I would like to show my heartfelt thanks to Dr. Dany Pascal Moualeu-Ngangue, my practical mentor of everything. He always spared time to lift me up whenever I was in need of his help, or in desperation. His enormous support and enthusiasm in my research work and progress of writing up could not be mentioned in words.

Furthermore, my special thanks go to Ilona Napp for her unwavering supports in all experiments. She very often looked like my mother and always made me feel at comfort with her warm heart. I am grateful to all members of IGPS, Gemüsebau. Special appreciations go to Dr. Andreas Fricke, Dr. Tsu-Wei Chen and Dr. Kunze for supports on academic stuff, Frau Bank, Frau Romey, Frau Leh mann, Herr Spillebeen, Herr Hering and Herr Vahrmeyer for their contribution in technical stuff, Herr Magnus Adler for his time and great effort in integrating my model into JAVA platform. My kind appreciations to Ms Yi-Chen Pao, Ms Mildred and Mr Samuel Kamau for sharing knowledge, our core values and fruitful discussion, Dr.Aung Myat San and Ko Myo Min Aung family for making me feel at home. Need not to say, my senior and junior country fellows and YAU comrades are ever in my mind.

Moreover, I am indebted to DAAD for financial support, TGRC for germplasms donation, Leibniz Universität Hannover, GRANAT for accepting me as a PhD student, those officials from Myanmar Embassy (Berlin), my ministry MoALI, and my respected teachers from my home university YAU for their permission, understanding, and sustained supports in many ways.

Last, but not least, I owe you my dear late mother, my lovely wife and my two daughters that you have been being so patient with daily struggles while waiting for the day I am back home.

Curriculum Vitae

Personal information

Name: San Shwe Myint
Date of birth   09.12.1975
Place of birth   Bogale
Nationality   Myanmar

Education background

Jun 1991 – Mar 1992   State High School, Bogale
Jun 1992 – Mar 1993   State High School, Mingaladon
May 1995 – Sep 2000   Yezin Agricultural University (YAU), Yezin (Naypyitaw)
                       B. Agr.Sc. (Specialization in Agronomy)
Jul 2005 – Sep 2007   Leibniz Universität Hannover (LUH)
                       M. Sc. International Horticulture (Major in Plant Nutrition)
Since Oct 2015   Ph.D. Candidate at the Institute of Horticultural Production Systems , LUH Vegetable Systems Modelling Section

Awards

Jul 2005 – Sep 2007   "Scholarship for Developing Countries", DAAD
Oct 2010   Workshop training for sub-tropical fruits production techniques, China
Apr 2011 – Jun 2011   "Re-invitation Program for former Scholarship Holders", DAAD
June 2015 – Sep 2019   " Research Grant for Doctoral Study", DAAD

Work experiences

2000 - 2007   Instructor, Department of Animal Science, YAU
2008 - 2013   Assistant Lecturer, Department of Horticulture, YAU
2013 -   Lecturer, Department of Horticulture and Agricultural Biotechnology, YAU

Research activities

2005 - 2007   Effect of sulphur nutrition on the resistance of tomato (*Solanum lycopersicum* L.) against *Pseudocercospora fuligena* (MSc. Thesis)

2011   Quantitative assessment on genomic DNA and spread of *Verticillium dahliae* on tomato hypocotyl as influenced by sulphur nutrition using real time PCR and 2D PAGE

2008 -2015   Supervisor and supervisory member in under-graduate and post-graduate research projects